Understanding the Proliferative and Self-renewal Potential of Different Leukaemic Stem Cell Populations

Elda Surhaida Latif

A thesis submitted in part requirement for the degree of Doctor of Philosophy from the Faculty of Medicine, Newcastle University, Newcastle upon Tyne, UK

July 2012

Northern Institute for Cancer Research
Paul O'Gorman Building, Medical School,
Framlington Place, Newcastle University,
Newcastle upon Tyne, NE2 4HH

DECLARATION

I hereby declare that this thesis presented my original research work and effort. Wherever contributions of others involved and other sources of information used have been specifically acknowledged.

20 July 2012 ELDA SURHAIDA LATIF

Abstract

Although contemporary treatment cures most children with ALL, with survival rates in the region of 90%, treatment outcomes in certain cytogenetic subgroups remain poor. Patients with such abnormalities have a greatly increased risk of relapse and re-treatment responses are poor. Understanding the mechanisms of resistance in these patients is therefore a priority in the search for improvements in chemotherapy.

The translocation t(17;19)(q22;p13) is a rare cytogenetic abnormality, which occurs in less than 1% of childhood ALL and is associated with a very poor prognosis and chemotherapy resistance. The translocation results in the fusion of *E2A* on chromosome 17 with *HLF* on chromosome 19. It has been commonly assumed that, following relapse, ALL cells will divide more rapidly than at presentation. To test this hypothesis, competitive transplantation studies were performed using paired presentation and relapse samples from a case of t(17;19)-positive ALL in a NSG xenograft mouse model. Surprisingly mice engrafted with the presentation cells survived significantly shorter ($p<0.05$, logrank test) than those with relapse cells, indicating the aggressiveness and rapid proliferation of presentation cells, while the survival curves of mice engrafted with various proportions of presentation and relapse cells had intermediate levels of survival. Administration of dexamethasone prolonged the survival of mice engrafted with the presentation cells and those with various proportions of cells, with no effect on survival of mice with relapse cells. Flow cytometry analysis showed that a high percentage (70%-95%) of human leukaemic cells engrafted in bone marrow and spleen across all groups tested. RT-PCR amplification identified this t(17;19) case to be a Type 1 E2A/HLF fusion.

In order to determine the genes responsible for chemo-insensitivity, whole genome SNP array analysis was performed on the matched presentation and relapse samples which demonstrated deletion of glucocorticoid receptor (*NR3C1*) gene in relapse cells which is not seen in presentation cells, confirmed by fluorescence *in situ* hybridisation. This deletion was used to identify the relapse cells (R) in mice engrafted with mixtures of presentation and relapse cells. FISH analysis showed the percentages of presentation cells (P) were higher than the ratios of the cell initially transplanted. In concordance, real-time PCR analysis showed high levels of NR3C1 in all mix cells ratios. These results indicated that presentation cells proliferate more rapidly and outgrow relapse cells in competitive

clonal repopulation experiments. Dexamethasone treatment reduced the percentages of presentation cells in all mix populations with high significance ($p<0.01$, t-test) in the 30%-P+70%-R ratio. Levels of NR3C1 in all mix cell populations were significantly depleted ($p<0.05$, t-test) by dexamethasone.

To be able to physically track the proliferation of leukemic cells populations *in vivo* and to follow progression of the disease, two lentiviruses pSLIEW (expressing firefly luciferase and green fluorescent protein) and pSRLICW (expressing *Renilla* luciferase and mCherry fluorescent protein) were generated. pSRLICW was just successfully generated but has not yet been tested. Lentivirus pSLIEW functionality was validated by transducing various leukaemic cell lines. By assessing the percentage of green fluorescence (gfp) cells, transduction efficiencies in SEM and RS4;11 (ALL cell lines) were 45% and 5% respectively, whereas transduction efficiencies in Kasumi-1 and SKNO-1 (AML cell lines) were 72% and 98% respectively, higher than the ALL cell lines. Transduced SEM and Kasumi-1 lines were sorted for higher gfp populations for xenograft purposes. Real time bioluminescence imaging on mice xenografted with sorted transduced SEM cells showed rapid progression of the disease in the systemic while Kasumi-1 cells xenografted in mice produced localised tumours and progressed much slower. These lentiviral-transduced cell lines xenografts have proven the *in vivo* monitoring capability by real time luminescence imaging.

The information gained from this project study provides novel insights into the mechanisms of relapse in childhood ALL. The growth characteristics of the leukaemic blasts should be considered in assigning patients to different therapeutic options.

Acknowledgement

This thesis would never have taken shape without the contribution and inspire of many. I would like to take this opportunity to thank the many people who make it possible.

I would like to thank The National University of Malaysia and Malaysian Ministry of Higher Education for awarding me the Academic Staff Training Scholarship and supporting my study here in Newcastle University. I would also like to acknowledge the NICR for giving me the opportunity to work in modernized and superb laboratories.

I am extremely grateful to my supervisors who are extraordinary wonderful and a pleasure to be supervised on – Dr. Olaf Heidenreich, for setting me on the right direction, guidance and technical support and for being patient with me, Prof. Andy Hall, for his guidance and persistent help in completing my study and preparing this thesis, and Prof. Josef Vormoor, thanks for recruiting me into the group and for trusting me with the challenging yet interesting project.

I am in debt to those who help me with the mouse work. Mike Batey, Klaus Rehe and Lars Buechler, the techniques and knowledge shared regarding xenograft and imaging are greatly appreciated.

I would also like to express my thanks and appreciation to Claire Schwab and Heather Morrison from the Leukaemia Research Cytogenetic Lab for helping me in completing the FISH analysis.

A big thank you is also due to all NICR staff especially the Leukaemia group members for their help and advice throughout my study in the institute.

I would like to thank Allah for giving me strength and courage to complete this study and thesis. With His blessing I embrace each day with confidence and faith to gain one of many knowledge yet to encounter.

For my family, with thanks.

To my parents, as promised.

List of Abbreviations

ACTH	adenocorticotropic hormone
AD	activation domain
AF	activation factor
ALL	acute lymphoblastic leukaemia
AML	acute myeloblastic leukaemia
AP	activation protein
bHLH	basic helix-loop-helix
bZIP	basic leucine zipper
CD	cluster of differentiation
cDNA	complementary deoxyribonucleic acid
CNS	central nervous system
CRH	corticotropin-releasing hormone
CSF	cerebrospinal fluid
DBD	DNA-binding domain
DNA	deoxyribonucleic acid
FACS	fluorescence-assisted cell sorting
FCS	fetal calf serum
FISH	fluorescence *in situ* hybridization
GC	glucocorticoid
gfp	green fluorescent protein
GR	glucocorticoid receptor
GRE	glucocorticoid response element

HLF	hepatic leukaemic factor
HPA	hypothalamus – pituitary – adrenal
HSC	hematopoietic stem cell
LBD	ligand-binding domain
LSC	leukaemic stem cell
MCS	multiple cloning site
MRD	minimal residual disease
NLS	nuclear localization signal
NR3C1	nuclear receptor subfamily 3 group C member 1
PAR	proline and acidic-rich
PB	peripheral blood
PCR	polymerase chain reaction
qPCR	quantitative polymerase chain reaction
RNA	ribonucleic acid
RT-PCR	reverse transcriptase-polymerase chain reaction
SNP	single-nucleotide polymorphism
TAD	transactivation domain
TCF3	transcription factor 3
TdT	terminal deoxynucleotidyl transferase
WBC	white blood cell

List of Figures

List of Tables

Table of Contents

CHAPTER 1

INTRODUCTION

CHAPTER 1

INTRODUCTION

1.1 General Introduction

Haematopoiesis is a highly orchestrated process producing mature blood cells in the bone marrow. It is a route by which blood cells are produced in a hierarchical line from a common ancestor, the hematopoietic stem cell (HSC) (Figure 1.1). HSCs have the ability to self-renew to maintain the undifferentiated stem cell pool, whilst producing progenitor cells – common myeloid progenitor and common lymphoid progenitor. The progenitors are cells restricted to differentiate into specific cell types and the subsequent differentiated cells show increasing proliferation potential and continuously providing blood cells to the cellular component. Disruption of a normal haematopoiesis can lead to uncontrolled proliferation and abnormal differentiation of blood cells. As such, mutation of cells or stem cells during haematopoiesis gives rise to abnormal regulation of cell growth as seen in many haematological disorders. Leukaemias are one of the results of such abnormalities.

1.2 Leukaemia

Leukaemia is a disease of the blood characterized by an increased proliferation of abnormal white blood cells (leukocytes) or their precursors. The disease can arise from affected stem cells as well as affected mature cells of lymphoid or myeloid lineages (Figure 1.2). As such, leukaemias are classified according to the types of hematological cells that form the malignant clone and by the maturity of the affected cells. Malignant clones formed from the immature undifferentiated cells are termed acute leukaemia (acute lymphoblastic leukaemia, ALL, and acute myeloid leukaemia, AML). Acute leukaemias present an excessive abnormal proliferation of immature leukocytes that rapidly accumulate in the bone marrow, spilling into the bloodstream leading to rapid onset of clinical symptoms and death, if untreated (Cancer Research UK, 2006). Conversely, in chronic leukaemia transformation occurs in a more mature cell (chronic lymphocytic leukaemia, CLL) or in the whole spectrum of myeloid precursors (chronic myeloid leukaemia, CML). Chronic leukaemias generally progress much more slowly with slower

accumulation of more mature blood cells over a long period of time, typically taking months or years to progress to symptomatic stages. In general, leukaemia can be viewed as a new form of an abnormal hematopoietic cell initiated by an aberrant and poor regulation process of leukaemic stem cells (LSC) (Passegué, Jamieson et al. 2003).

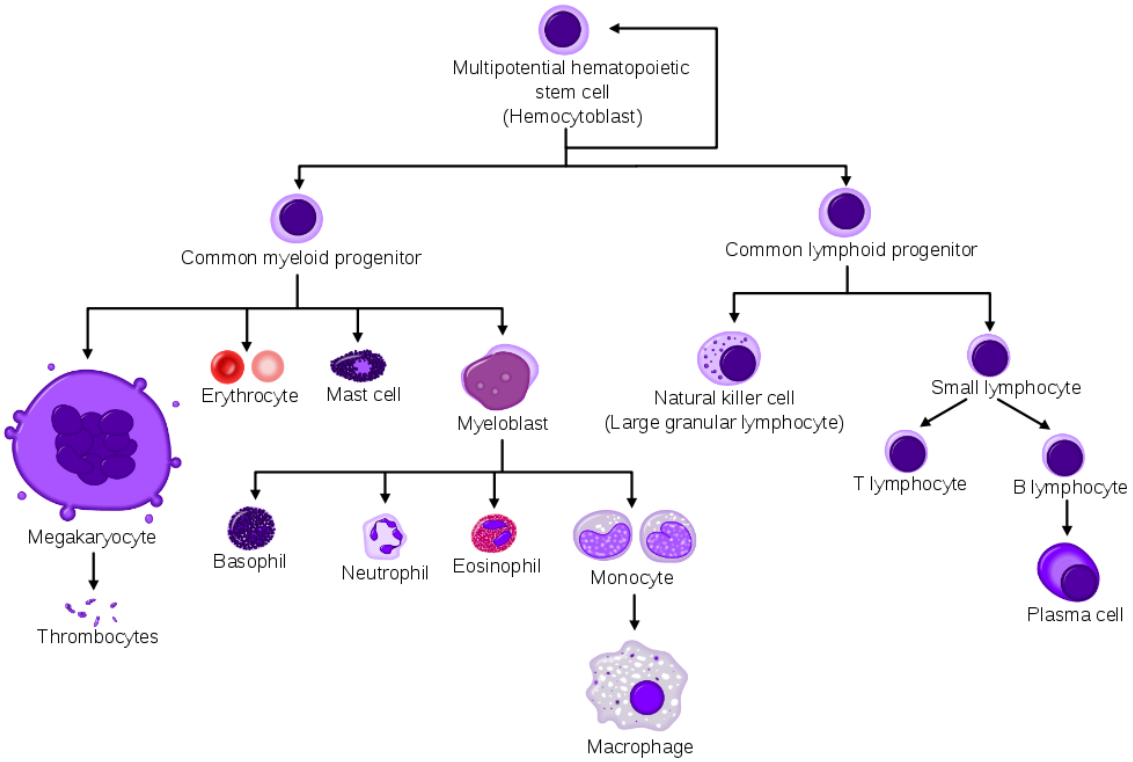

Figure 1.1 The hematopoietic hierarchy. Simple diagram showing development of a small pool of hematopoietic stem cell (HSC) into different mature blood cells of distinct lineages, in a hierarchical manner. (source: Stem Cell Network).

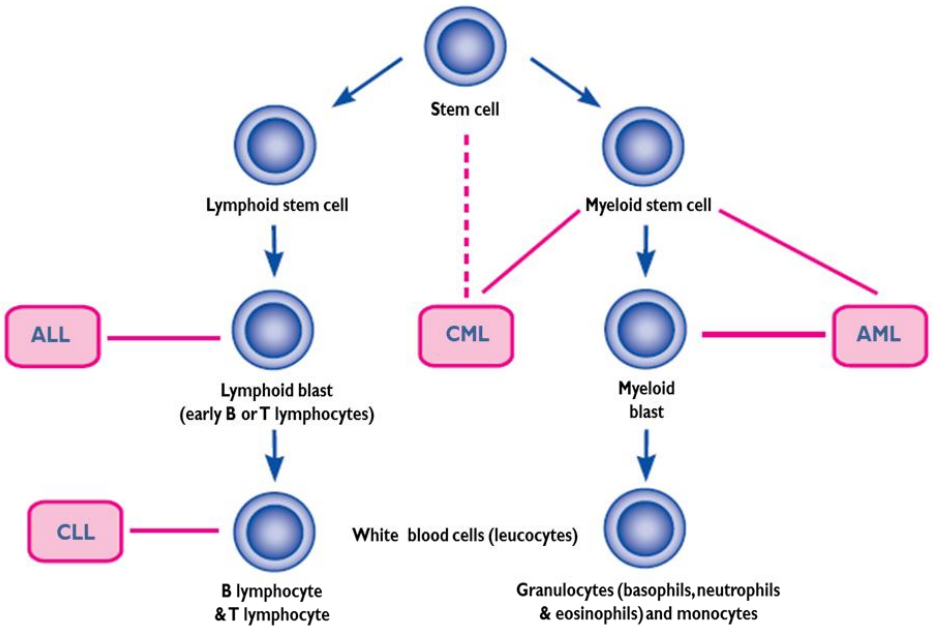

Figure 1.2 Simplified scheme of the origin of the major types of leukemia. Acute and chronic leukaemias arise from affected lymphoid and myeloid stem cells form the acute lymphoid leukaemia (ALL), chronic lymphoid leukaemia (CLL), acute myeloid leukaemia (AML) and chronic myeloid leukaemia (CML). (source: Cancer Research UK, 2006).

1.2.1 Leukaemic Stem Cell

Leukaemia generally can be viewed as a new form of abnormal haematopoietic cell initiated by leukaemic stem cells (LSCs) that undergo an aberrant and a poor regulation process which is analogous to that of HSCs (Passegué, Jamieson et al. 2003). Like other tumours, leukaemia arises from the clonal expansion of a single cell, and is sustained by a leukaemic stem cell (Warner, Wang et al. 2004).

In the concept of cancer, in principle, the notion of cancer biology that is widely acceptable is that most tumours arise from transformation of single cells due to genetic alteration (Hanahan and Weinberg 2000). Additionally, the relationship between tumour cell and stem cells is that cancer cells might contain some cancer stem cells (CSCs), which are rare cells with indefinite self-renewal potential that drive the formation and growth of the tumours (Bonnet 2005).

The cancer stem cell is defined as a cell within ‘a tumor that possesses the capacity to self-renew and to cause the heterogenous lineages of cancer cells that comprise the

tumour' (Clarke, Dick et al. 2006). In the general cancer stem cell (CSC) concept, CSCs are genetically identical to the rest of the malignant clone. However, this subset of CSCs or cancer-initiating cells is distinct from the bulk of the tumour and is responsible for long-term maintenance of tumour growth (Dick 2008). Due to their distinct property of stem cell-like character and functional similarities to that of normal stem cells, these definitive biological properties make the CSCs survive standard treatment (Dick 2008), show high resistance to chemotherapy (Essers and Trumpp 2010) and identify them as the prime candidates for initiation of relapse (Bomken, Fiser et al. 2010).

This concept of CSCs is supported by syngeneic murine assays for leukaemic stem cells. The first evidence proposing leukaemia-initiating cells (LICs) was when transplantation of primary AML cells into SCID mice showed that the LICs are rare malignant stem cells capable of initiating and sustaining growth of the leukaemic clone in serial transplantation, similar to the original disease. This rare malignant stem cell, which has the ability to engraft and repopulate in mice owing to the self-renew potential and the capacity to differentiate, was only found within the immature CD34+CD38- fraction but not the CD34+CD38+ subpopulation (Lapidot, Sirard 1994; Bonnet and Dick 1997). Subsequently, these findings show that AML is organized as a hierarchy of distinct, functionally heterogeneous classes of cells that is sustained by a small number of LSC (Bonnet 2005).

In childhood pre-B-cell ALL, the nature and frequencies of stem cells and leukaemia-initiating cells have been controversial and not easy to define. In proposing the LICs in ALL, NOD/SCID mice transplanted with B-cell ALL have shown that only primitive blasts with a CD34+CD38- immunophenotype were able to initiate overt ALL in mice (Cobaleda, Gutierrez-Sianca, et al. 2000). It has also been proposed that candidate leukaemic stem cell populations in ALL were represented by CD34+CD38lowCD19+ (Cox, Diamanti et al 2009), CD34+CD38+CD19+ and CD34+CD38-CD19+ leukaemic blasts (Kong, Yoshida et al. 2008) that were able to reinitiate and sustain leukaemic growth in NOD/SCID mice. A limiting dilution study has shown that preB-ALL blasts sorted into fractions: CD34+CD19-, CD34+CD19+ and CD34-CD19+, re-established the complete immunophenotype of the original leukaemia and were able to self-renew in NSG mice, thus showing that all populations contain leukaemic-initiating cells (Le Viseur, Hotfilder et al. 2008). Additionally, in lymphoblastic leukaemia, genetic diversity occurs in functionally defined leukaemia-initiating cells and many primary diagnostic

samples contain multiple genetically distinct leukaemia-initiating subclones (Notta, Mullighan et al. 2011). In general, it could be concluded that in ALL, the putative stem cells responsible for initiating and maintaining B-cell ALLs are not a fixed cell identity but are subject to evolution (Testa 2011).

Tumour heterogeneity can be shown morphologically as well as functionally, which can be explained by two models. The stochastic model proposes that all cells within a malignancy have the potential to act as cancer stem cells. Formation of tumours is initiated by intrinsic and extrinsic factors. The hierarchy model predicts that analogous to the normal tissue hierarchy, a malignancy is organized in a hierarchical manner with distinct cancer stem cells, which drive and maintain the malignancy (Dick 2008; Bomken, Fiser et al. 2010). Both the stochastic and hierarchy model support the functional LSCs in the formation and maintenance of leukaemia. To rule out which of the model fits the theory, John Dick proposed a functional LSC assay (perhaps by xenograft model) with isolated cell fractions followed by clonal analysis. If it is possible to fraction cells with LSCs activity from those that do not, the hierarchy model fits this theory. If the LSCs cannot be prospectively isolated in any fraction because all malignant cells have the same potential, then this theory fits the stochastic model. Thus, whereas AML fits the hierarchy model, ALL fits the stochastic model given credit to the discussion above.

1.3 Acute Lymphoblastic Leukaemia

Acute leukaemia is described as a fast progression of malignant disorder of white blood cells characterized by the clonal proliferation and successive division of progenitor cells with arrested maturation. The acute lymphoblastic leukaemia (ALL) is the main type of leukaemia in children which is also the most common childhood cancer overall. The majority of ALL cases are of B-cell origin, but it can also arise from T-cell precursors.

In ALL, abnormal gene expression occurring at an early differentiation stage arrests lymphoblast development. This is often a result of chromosomal translocations. The leukaemogenic event may occur in committed lymphoid cells of B-cell or T-cell lineages or in early lymphoid precursors. Defective lymphoid precursors proliferate and accumulate immature blast cells in the bone marrow, interfering with the production of normal blood cells. Over expression of the malignant clones in the marrow lead to blasts spilling into the peripheral circulation and organ infiltration.

1.3.1 Incidence of Childhood ALL

Acute leukaemia accounts for one third of all childhood cancers with approximately 450 new cases diagnosed a year in the United Kingdom (Greaves 2002) and about one child in 2000 develops leukaemia before the age of 15 (Dickinson 2005). ALL represents the biggest percentage of leukaemic cases which comprises 85% of childhood acute leukaemias in which it affects 59 of every 1 million children under the age of 5. Age-specific incidence patterns demonstrate a characteristic increase in children aged 2 to 5. Although ALL can affect all age groups, the peak incidence at age 4. In the United States almost 4000 cases of acute lymphoblastic leukaemia are diagnosed annually. Approximately two thirds of the cases are in children and adolescents, making ALL the most common cancer in these age groups (Pui and Evans 2006). In childhood ALL, males are more often affected than females, and an excess incidence occurs among whites than blacks (Greaves 1999; Pui 1999). Bigger babies have slightly increased risk of developing leukaemia (Hjalgrim, Rostgaard et al. 2004).

1.3.2 Aetiology and Epidemiology

There is no conclusive evidence linking environmental factors with the cause of ALL. Like many cancers, we only know potential triggers. It has been suggested that epidemiologically, paediatric leukaemia and common ALL in particular is more prevalent in more socio-economically advanced societies. Potentially offensive exposures to environmental factors such as pesticides, electromagnetic fields, ionizing radiation, vitamin K and chemically or genetically modified food may predispose a child to develop the disease (Greaves 2002).

There are several known risk factors of childhood leukaemia such as sex, age, race, exposure to ionizing radiation, and certain congenital diseases, such as Down syndrome, Li Fanconi's anemia, ataxia-telangiectasia and neurofibromatosis, which account for only 10% of the childhood leukaemia cases. Several lines of evidence suggest that childhood leukaemia may be more due to environmental rather than genetic factors, although genes may play modifying roles. The genetic abnormality is acquired rather than inherited, although certain inherited conditions such as Trisomy 21 predispose to ALL. Human and animal studies showed that the development of childhood leukaemia is a two-step process

that requires prenatal initiating events plus postnatal promoting events (Stiller 2004; Chang 2008).

A series of studies by Greaves and colleagues have demonstrated that some leukaemias originated in utero based on Guthrie cards test on children diagnosed with ALL at age below 2 (Greaves 1999). It is also suggested that children with identical twins who were diagnosed with the illness before age 6, have a 20% to 25% chance of developing ALL, whilst siblings or non-identical twins of leukaemic children have a risk of developing this illness only two to four times the average (Reynolds 1998; Greaves 1999).

Greaves also noted that ALL cases are much higher in industrialized countries than in developing countries and hypothesized that the chance of developing common ALL increases with better hygiene. This could be a pathological response to delayed exposure to some common infectious agents (Greaves 1999). Furthermore, pregnant women who are infected with any kind of virus could have passed the virus to the foetus and might be vulnerable to genetic damage (Smith 1997). Increased exposure to viruses or infectious organisms in high population areas also might have triggered the leukaemia particularly in genetically susceptible children (McNally and Eden 2004). Additionally, Kinlen found an increased incidence in childhood leukaemia in an extreme population mixing with new towns, commuter belts, major construction sites, country areas used for wartime evacuation or for military camps (Kinlen 2000).

1.3.3 Prognostic Factors

Predicting the prognosis of patients presenting with ALL is important for stratification into risk groups so that treatment can be tailored accordingly. In this way, patients which are likely to respond to standard chemotherapy are spared undue toxicity while a more intensified therapy is given to high-risk patients. Various factors have been found to have prognostic significance (Table 1.1) (Hoffbrand, Moss et al. 2006), however the most commonly used are presenting WBC, age and sex although haemoglobin level also have been reported to be important factor as well (Ng, Lin et al. 2000).

The white blood count (WBC) at presentation is one of the most reliable prognostic indicators of patient outcome. Patients with a high white blood cell count (>50 x 10^9/L) at diagnosis have a higher risk of treatment failure than patients with lower counts. Hence,

these patients receive a high risk treatment protocol. Another reliable prognostic indicator in ALL is the age of patients at presentation. This is partly because certain age groups have a high frequency of specific genetic abnormalities in the leukaemic blasts. In infant less than 12 months, 70-80% of cases present with rearrangements of the mixed lineage leukaemia (MLL) gene. These patients often also have a high WBC count, poor initial treatment response and absence of common ALL antigen (CD10) (Hilden, Dinndorf et al. 2006). Patient aged less than 10 years old with high risk cytogenetic features such as hypodiploidy, Philadelphia chromosome positive t(9;22)(q34;q11) or t(4;11)(q21;q23) are treated with the most intensive treatment. Patients with slow response to treatment as indicated by minimal residual disease (MRD) or assessed by the rate of clearance of leukemic cells from bone marrow, are most likely to be at high risk of treatment failure.

With these prognostic variables taken into account, patients can be identified who require more intensive therapy. At the same time the treatment is reduced to lessen the treatment toxicity as well as reducing short and long term side effects in patients less likely to relapse.

	Good	**Poor**
WBC	Low	High (>50x10^9/ L)
Sex	Girls	Boys
Immunophenotype	B-ALL	T-ALL (in children)
Age	Child	Adult (infant <2 years)
Cytogenetics	Hyperdiploidy (>50 chromosomes), TEL-AML fusion	Ph+ t(9;22), MLL rearrangement
Time to clear blast from blood	<1 week	>1 week
Time to remission	<4 week	>4 week
CNS disease at presentation	Absent	Present
Minimal residual disease	Negative at 1 – 3 months	Still positive at 3 – 6 months

Table 1.1 Prognosis in acute lymphoblastic leukaemia. Ph+, Philadelphia positive; WBC, white blood cell count. (Hoffbrand, Moss et al. 2006).

1.3.4 Clinical Characteristics

Children with ALL normally present with various forms of clinical presentations depending on the degree of severity of the disease. Many of the signs and symptoms of ALL result from the lack of normal and healthy blood cell production because of the malignant immature lymphoblast overcrowding the bone marrow cavity. Common signs and symptoms of ALL include paleness and lethargy caused by anaemia, pain in the bones or joints caused by overproduction of blast cells in the marrow, excessive and unexplained bruising, bleeding and/or petechiae due to low platelet levels. Patients may also present with painless lymphadenopathy, frequent infections and fevers or night sweats. A much more extensive condition due to extramedullary spread of patients with leukaemia include abdominal discomfort and swelling caused by splenomegaly or hepatomegaly which in turn leads to weight loss and/or loss of appetite due to the feeling of abdominal fullness.

Brain infiltration in acute leukaemia may present with headaches, vomiting, confusion, loss of muscle control and seizures. Other parts of the body may also be affected such as the digestive tract, kidneys, lungs, heart or testes.

1.3.5 Laboratory Features

Patients with leukaemia generally have abnormal leukocytes with a very low absolute neutrophil count. More than 50% of patients present with leukocytes count $>10x10^9$/L and 15% of patients come with $>50x10^9$/L leucocytes count. An increased WBC is commonly associated with anaemia. Almost 90% of patients have a haemoglobin $<11x10^9$g/dL with half of this group presenting with a haemoglobin $<7x10^9$g/dL. In 75% of leukaemia cases, blood tests show thrombocytopenia with a platelet count $<1x10^5/mm^3$.

1.3.6 Cell Identification

There are various subtypes of diseases in ALL which can be differentiated according to cell morphology, immunophenotype and genotyping analysis. Since the French American British (FAB) classification of ALL only describes the morphological aspects of the ALL

subtypes, to improve classification of biologically relevant ALL subsets and its prognostic value, other methods are applied.

In general, to achieve the treatment goal of eradicating leukaemia, immunophenotyping of leukaemic lymphoblasts is essential to establish the correct diagnosis and define cell lineage. Genotyping the leukaemic lymphoblasts with highly specific and sensitive techniques such as RT-PCR, fluorescence in-situ hybridization, cytogenetics and single nucleotide polymorphism array analysis are used to detect specific fusion transcript, gain or loss of cellular DNA content, or specific chromosomes with prognostic or therapeutic relevance (Pui, Robinson et al. 2008).

1.3.6.1 Cell Morphology

In 1976, a French, American and British (FAB) cooperative group proposed a morphological classification of acute leukaemia guidelines. This system is used to classify leukemic cells into three categories, L1, L2, and L3, based on the predominant morphology of leukaemic lymphoblasts and cytological features of the cells. The classification and details of the morphology for each type of leukaemic lymphoblast is summarized in Table 1.2 (Bain 1999). In general, type L1 is more frequent in childhood ALL whereas L2 is more frequent in adults. L3, however, is considered as a leukaemic form of Burkitt's lymphoma (Munker, Hiller et al. 2000; Szczepanski, van der Velden et al. 2003).

Cytological Features	L1	L2	L3
Cell size	Small cells predominate	Large, heterogeneous	Large, homogenous
Nuclear chromatin	Homogenous in any one case, maybe condensed in some cells	Variable, heterogenous in any one case	Finely stippled, homogenous
Nuclear shape	Mainly regular	Irregular; clefting and indentation common	Regular; oval or round
Nucleolus	Not visible or small and inconspicuous	Usually visible, often large	Usually prominent
Amount of cytoplasm	Scanty	Variable, often abundant	Moderately abundant
Cytoplasmic basophilia	Slight to moderate	Variable	Very strong
Cytoplasmic vacuolation	Variable	Variable	Often prominent

Table 1.2 Morphological features of ALL subtype. (adapted from Bain, 1999).

1.3.6.2 Immunophenotype

Leukaemic cells display characteristic patterns of surface antigen expression (CD antigens), which facilitate their identification and accurate classification. These markers play an important role in instituting appropriate treatment plans. During lymphocyte development, different antigens are expressed according to the stage of differentiation as well as cell type. Expression of specific antigens on leukaemic cell reflects the stage of differentiation at which the cell became malignant. Therefore, different subtypes of leukaemic cells can be identified based on these antigens.

Leukaemias of B-cell origin can be classified into four subtypes based on their surface marker. These are early pre-B cell, pre-B cell, transitional pre-B cell and mature B cell leukaemias. However, there has been a new proposed system for classifying B-cell ALL as described in Table 1.3 below (Szczepanski, van der Velden et al. 2003). Early precursor B-ALL is the most common subtype of which the phenotypes of the lymphoblast correspond to those of B-cell progenitors. Almost 70% of children with ALL are diagnosed with early pre-B cell ALL (EGIL B-I). Of these, only 20% of the patients have a better prognosis than those with pre-B cell ALL (EGIL B-III). Mature B-cell

leukaemia is treated differently to leukaemias arising from early progenitor blast cells. Patients with this subtype only receive short-term intensive chemotherapy.

Markers	Early Pre-B-ALL (EGIL B-I)	Common ALL (EGIL B-II)	Pre-B-ALL (EGIL B-III)	Transitional-pre-B-ALL (no EGIL code)
TdT	++	++	++	++
CD10	-	++	++	++
CD19	++	++	++	++
CD20	-	+	+	+
CD22	++	++	++	++
CyCD79	++	++	++	++
Cylgμ	-	-	++	++
SmVpre-B/λ5	-	-	-	++
SmIg-CD79	-	-	-	+
CD34	+	+	+	+
HLA-DR	++	++	++	++

Table 1.3 Immunological classification of childhood ALL. EGIL, European Group for the Immunological Characterization of Leukaemias. (adapted from Szczepanski, van der Velden et al. 2003).

1.3.6.3 Cytogenetics

ALL can be classified according to cytogenetics or chromosomal abnormalities within the leukaemic blasts. The abnormalities can be in form of chromosomal copy number (ploidy and aneuploidy) or chromosomal structure as in translocations. Cytogenetic abnormalities are now known to be important prognostic indicators of treatment outcome.

High hyperdiploidy (>50 chromosomes) is present in 30% cases of children with B-precursor ALL. This abnormality is associated with a favourable prognosis (Harrison and Foroni 2002) which is often coupled with a number of other positive prognostic factors such as low WBC at diagnosis and a favourable age (1-9 years). In contrast, hypodiploidy (<45 chromosomes) is associated with a high risk of treatment failure (Heerema, Nachman et al. 1999).

Abnormalities in the chromosome structure, commonly translocation, have an impact on the prognosis as well as ploidy. Translocation with poor prognosis such as t(9;22)(q34;q11), t(4;11)(q21;q23) and t(17;19)(q22;p13) (are discussed in more detail in section 3.1.1) are associated with high WBC at diagnosis and of age >10 and <1 years. In contrast t(12;21)(p13;q22) is associated with an excellent prognosis, independent of other prognostic factors. This translocation has a five-year event-free survival rate approaching 90% (Armstrong and Look 2005). Numerous other translocation have been identified, however the cases are not as significant as these four types.

1.3.7 Treatment

Leukaemias have traditionally been classified and treated on the basis of phenotypic characteristics such as morphology and cell surface markers and more recently, cytogenetic aberrations (Ravandi and Estrov 2006). Most leukaemias arise from acquired aberrations (changes) in the genes of growing blood cells. Because these errors occur randomly and unpredictably, there is currently no effective way to prevent most types of leukaemia. Nevertheless, treatment of acute leukaemias has progressed from earlier uniform strategies devised for large groups of patients to more refined protocols tailored for discrete subgroups with the risk of relapse (Look 1997). With current treatment regimens of combination chemotherapy used in ALL cases, the overall response has achieved an approximately 80% long-term event-free survival rate (Pui, Robinson et al. 2008), although this figure disguises success rates that vary from 10% to 90% with the different biological subtypes of the disease (Greaves 2002). Nonetheless, this success is led by careful stratification of patients at diagnosis in order to optimize risk-directed therapy with multi-agent chemotherapeutic drug regimens (Stankovic and Marston 2008). It has also been suggested that the success of treatment of childhood ALL is linked to the transformation of a B-cell progenitor prone to undergoing apoptosis (Greaves 1993) and B-cell precursor ALL (BCP-ALL) is commonly sensitive to chemotherapy (Pui, Robinson et al. 2008).

1.3.7.1 Treatment of Childhood ALL

The treatment used for patients diagnosed with ALL is administered in several phases with combinations of drugs. The treatment protocol is divided into chemotherapeutic blocks which include a first phase of remission induction therapy, followed by a second phase of consolidation therapy and the last phase is continuation/maintenance therapy. Outline of the principle of therapy in managing children with leukaemia is as shown in Figure 1.3 (Hoffbrand, Moss et al. 2006).

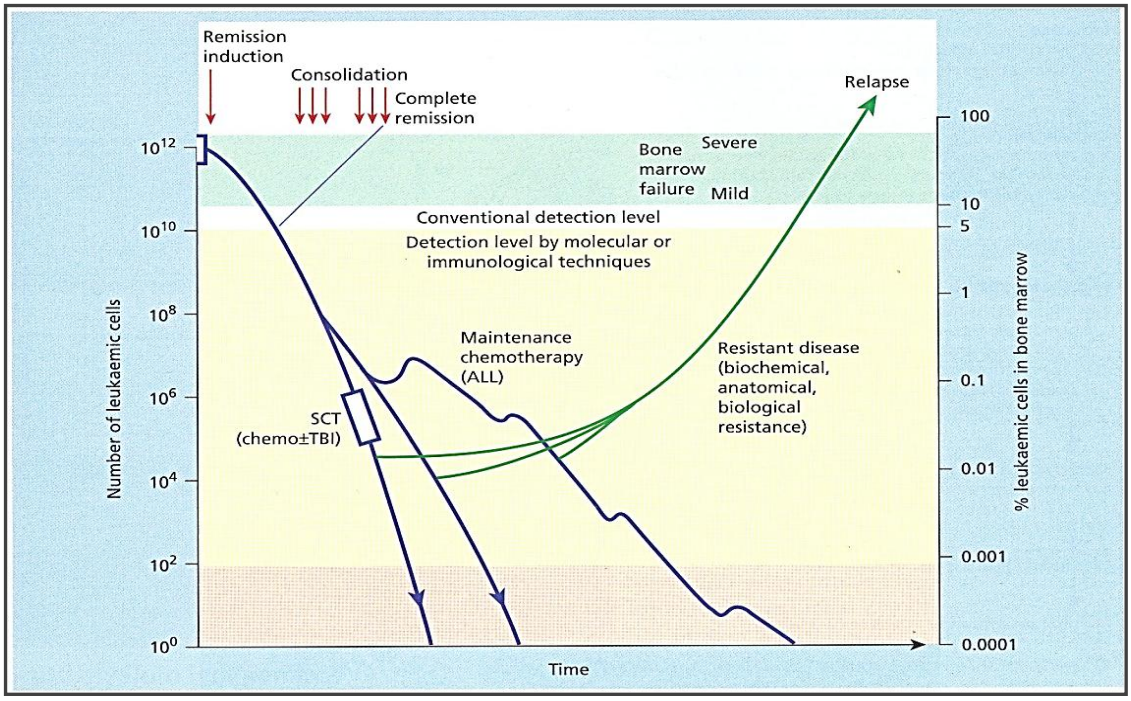

Figure 1.3 Principle of therapy in acute leukaemia. SCT – stem cell transplant; chemo±TBI – chemotherapy ± total-body irradiation. (Hoffbrand, Moss et al. 2006).

The initial aim of remission/induction therapy in children with ALL is to induce remission with elimination of 99% leukaemic cells and restoration of normal haematopoiesis. The standard induction protocol involves a combination of vincristine, glucocorticoid (prednisolone or dexamethasone) and asparaginase which results in complete remission in over 95% of low risk cases (Eden, Harrison et al. 2000). On completion of induction chemotherapy there is usually no evidence of leukaemia found on physical examination or examination of the bone marrow or peripheral blood.

Intensive chemotherapy given during the consolidation period of therapy shortly after induction of remission improves the outcome of patients with an otherwise poor prognosis. Drugs used in this phase include etoposide, cytarabine, cyclophosphamide and anthracyclines and treatment lasts for several months.

Maintenance therapy follows intensified therapy to effectively prevent relapse from development of resistant clones. The protocol used includes a combination of mercaptopurine and methotrexate. Standard CNS prophylaxis by craniospinal irradiation is usually given to patients over the course of maintenance therapy to prevent relapse, particularly patients with CNS disease at diagnosis.

The Medical Research Council (MRC) UK has carried out trials on children with ALL since 1980 to improve treatment for the disease (Table 1.4). Series of clinical trials aimed at finding the best therapy had tested drugs that not only treat the cancer but also treat the symptoms and side-effects. Progress has been made as a result of many gradual improvements in treatment achieved through these trials. This success has led to improvement in survival of children with ALL that four in five children with ALL now recover from the disease compared to three decades ago. For certain subgroup of patients, more intensive studies and trials are required to improve treatment plan for the survival of these children.

Trial	Induction	Intensification	CNS Therapy	Continuing	Randomisation
VIII (1980-1984)	Vincristine Prednisolone Asparaginase +/- Daunorubicin	None	Intrathecal MTX Cranial irradiation	6-MP Oral MTX Vincristine Prednisolone	A: ± Daunorubicin during induction B: 2 or 3 years continuing therapy
X (1985-1990)	Vincristine Prednisolone Asparaginase Daunorubicin	Daunorubicin Cytocine arabinoside Etoposide Vincristine Prednisolone 6-TG	Intrathecal MTX Cranial irradiation	6-MP Oral MTX Vincristine Prednisolone	A: no intensification B: week 5 intensification C: week 20 intensification D: both intensifications
XI (1990-1992)	Vincristine Prednisolone Asparaginase Daunorubicin	Daunorubicin Cytocine arabinoside Etoposide Vincristine Prednisolone 6-TG	WBC <50 x 10^9/L : Intrathecal MTX ± high dose MTX WBC >50 x 10^9/L : High dose MTX or Cranial irradiation	6-MP Oral MTX Vincristine Prednisolone	A: week 20 intensification B: intrathecal MTX, high dose MTX or cranial irradiation
XI (92) (1992-1997)	Vincristine Prednisolone Asparaginase	Daunorubicin Cytocine arabinoside Etoposide Vincristine Prednisolone 6-TG	WBC <50 x 10^9/L : Intrathecal MTX ± high dose MTX WBC >50 x 10^9/L : High dose MTX or Cranial irradiation	6-MP Oral MTX Vincristine Prednisolone	A: intrathecal MTX, high dose MTX or cranial irradiation B: ± week 35 intensification
97 (1997-2003)	Vincristine Prednisolone or Dexamethasone Asparaginase Methotrexate	Daunorubicin Cytocine arabinoside Etoposide Vincristine Prednisolone 6-TG	WBC <50 x 10^9/L : Intrathecal MTX ± high dose MTX WBC >50 x 10^9/L : High dose MTX or Cranial irradiation	6-MP or 6-TG Oral MTX Vincristine Prednisolone	A: Prednisolone or Dexamethasone B: 6-MP or 6-TG C: ± week 35 intensification

Table 1.4 The MRC childhood ALL trials carried out since 1980. MTX = Methotrexate, 6-MP = 6-Mercaptopurine, 6-TG = 6-Thioguanine.

1.3.7.2 Treatment of Relapse

Treatment resistance and relapse in ALL remains a significant clinical problem despite the high cure rate percentage. Complete remission is defined by less than 5% lymphoblast cells in the marrow, the absence of leukaemic blast cells in the blood and cerebrospinal fluid (CSF), normal peripheral blood count and the absence of localized disease. Relapse is defined as the recurrence of more than 25% blast cells in the marrow or presence of localized leukaemic infiltrates at any site after completion of induction therapy (reviewed in Ng, Lin et al. 2000).

The vast majority of relapses occur due to the failure of therapeutic drugs to completely eradicate the original leukaemic clone and its subsequent re-expansion. It has been reported that over 70% of relapses happen within 3 years of initial diagnosis (Chessells, Veys et al. 2003). Intensive exposure to antileukaemic drugs is thought to be the most likely cause for a patient to subsequently develop chemoresistance (Klumper, Pieters et al. 1995) or alternatively, chemoresistance may be caused by treatment-related selection of primary drug-resistant subclones originally present at initial diagnosis (Stankovic and Marston 2008).

The leukaemic stem cell (LSC) is likely to be the most crucial target in the treatment of leukaemias. However, like normal HSC, LSCs are quiescent cells and this resting status protects them from the commonly used cell cycle-specific chemotherapeutic agents used in leukaemia treatment (Essers and Trumpp 2010). This characteristic contributes to treatment failure. Furthermore, these cells may undergo mutation and epigenetic changes which leads to drug resistance and relapse (Ravandi and Estrov 2006).

Options for the treatment of relapse patients include repeated course of systemic and intrathecal chemotherapy with or without radiation therapy. Bone marrow or stem cell transplantation is considered another option if relapse treatment is still a failure. Clinical trials of new drugs or combination chemotherapy regimens are significantly important for improving the therapy management of children with relapse in ALL.

1.3.7.3 Chemotherapeutic Agents

Chemotherapeutic agents are chemical agents with cytotoxic or cytostatic effects used for treating cancerous cells, generally by directly killing or arresting cells with high proliferation rate. In haematological malignancies, specific therapy is aimed at reducing the malignant cell burden by the use of drugs or radiotherapy. A wide variety of therapeutic drugs are used in the management of children with ALL. Several drugs are often combined together in regimens that minimize the potential for resistance to occur against a single agent. The common multiagent chemotherapeutic regimens used include DNA damaging agents, alkylating agents, mitotic inhibitors, antimetabolites, corticosteroids and also cytotoxic antibiotic drugs. Although combinations of chemotherapeutic drugs are very effective in eradicating leukaemic cells in ALL, they are associated with significant side effects. Common side effects of chemotherapy are nausea and emesis (acute), and hair loss (chronic) (JLS Foundation Children with Leukemia; Cancer Health Center WebMD 2010). The mechanism of action and adverse effects of some of the commonly used therapeutic agents in ALL are detailed below. Chemical structures of the drugs used are as shown in Figures 1.4 and 1.5.

Cytarabine (Ara C) is a pyrimidine analogue which acts as a cytotoxic antimetabolite. The drug incorporates into DNA where it inhibits DNA polymerase and subsequently blocks replication in the S phase, arresting cells from mitotic stage (Ogbomo, Michaelis et al. 2008). Long term effects of cytarabine treatment include secondary malignancies and infertility.

6-Thioguanine (6-TG) is an antimetabolite drug that exerts its cytotoxic effect by incorporation into RNA and DNA and triggers cell cycle arrest. It interferes with the purine and pyrimidine synthesis and epigenetic gene regulation by perturbing cytosine methylation. Serious but uncommon side effects include veno-occlusive liver disease and secondary malignancies (King and Perry 2001; Lancaster, Patel et al. 2001).

6-Mercaptopurine (6-MP) is an efficient cytostatic anti-metabolite drug that interrupts the DNA synthesis phase of cell cycle, stopping development and division of cancer cells. It inhibits purine nucleotide synthesis and metabolism by interfering with nucleotide interconversion and glycoprotein synthesis. Possible side effects of 6-MP are diseases

such as acute non-lymphocytic leukaemias and lymphomas (Maekawa, Nagaoka et al. 1990; King and Perry 2001; Lancaster, Patel et al. 2001).

Cyclophosphamide, an alkylating agent from the nitrogen mustards group, alkylates DNA at N-7 on the guanine base. This purines affinity drug initially impairs fundamental metabolic processes such as replication and transcription, resulting in a block at G_2 and death of the cell by apoptosis particularly in rapid-dividing cancer cells (Hoffbrand, Moss et al. 2006). Cyclophosphamide can affect frequently dividing cells such as those in the testes and ovaries leading to infertility. Since an alkylating antineoplastic agent is also carcinogenic, long term side effects of cyclophosphamide treatment include a risk of treatment induced cancer.

Vincristine is one of the earliest antineoplastic drugs used as treatment in patients with leukaemia. A vinca alkaloid from *Catharanthus roseus* plant (Johnson, Armstrong et al. 1963), vincristine binds to specific site on tubulin inhibiting assembly into microtubules, hence arresting mitotic process in cell division. It is administered intravenously, often in combination with other antineoplastic drugs (Qweider, Gilsbach et al. 2007). Long term side effects of vincristine treatment include peripheral neuropathy, hyponatremia, and hair loss.

Daunorubicin is a cytotoxic antibiotic drug that intercalates into DNA and binds strongly to topoisomerase, impairing DNA helical shape and DNA replication of cancer cells. Side effect includes tissue necrosis to the extent of damage to the nervous system.

Methotrexate is in a class of antimetabolites that inhibit metabolism of folic acid and slowing the growth of cancer cells. Side effects of the drugs are hepatotoxicity and cytopenia.

Etoposide inhibits topoisomerase II from re-ligating unwound DNA strands following replication. Long term use of etoposide induces secondary AML.

Prednisolone, a synthetic glucocorticoid, is an anti-inflammatory and immunosuppressive drug that binds irreversibly with cytosolic glucocorticoid receptors found in almost all cells. The drug/receptor complex induced apoptosis in neoplastic lymphoid cells (Rang, Dale et al. 2010). Long term side effects of prednisolone treatment include cataract, osteoporosis, Cushing's syndrome, diabetes mellitus, and insomnia.

Dexamethasone is a glucocorticoid drug that has a potent lymphocytotoxic activity. The drug provides better penetration into the CNS but has a higher incidence of side effects including psychological disturbance and avascular necrosis.

Asparaginase is an important drug in the treatment of childhood ALL. Leukaemic cells require a high amount of asparagine but lack the ability to synthesize the amino acid, thus the malignant cells depend on circulating asparagine. Asparaginase however, catalyses the conversion of L-asparagine into aspartic acid and ammonia, thus depriving the leukaemic cells of the substance and subsequently killing the cells. Common side effects of asparaginase include anaphylaxis, pancreatitis and coagulopathy (Appel, van Kessel-Bakvis et al. 2007).

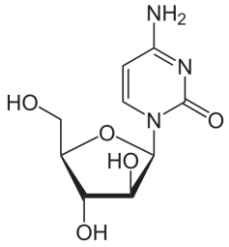

Cytarabine

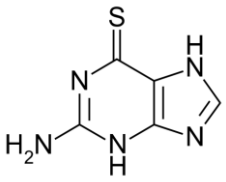

6-Thioguanine

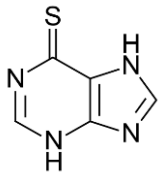

6-Mercaptopurine

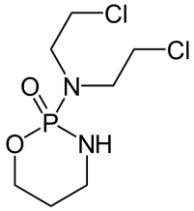

Cyclophosphamid

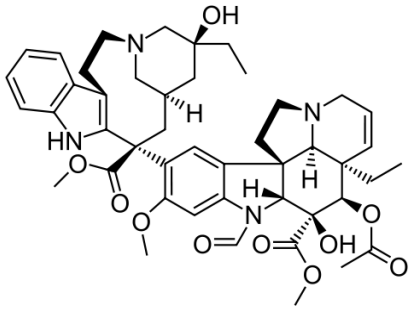

Vincristine

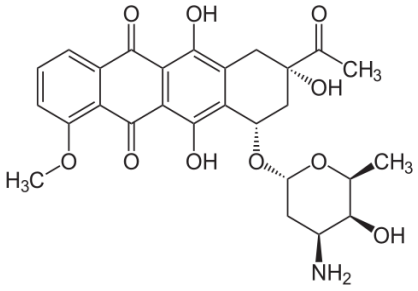

Daunorubicin

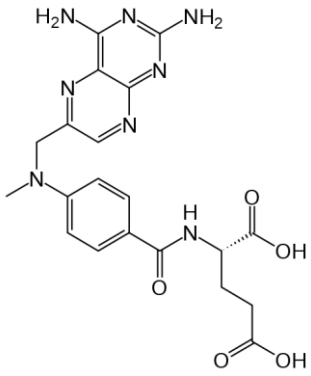

Methotrexate

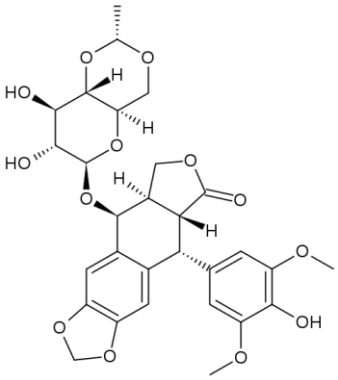

Etoposide

Figure 1.4 Chemical structures of chemotherapeutic agents used in treatment of acute leukaemia.

1.4 Glucocorticoids

Steroid hormones are divided into five groups by the receptor to which they bind: glucocorticoids, mineralocorticoids, androgens, estrogens and progestins. In general, they are pregnenolone derivates which is basically synthesized from cholesterol molecule. The endogenous glucocorticoid is cortisol, a biocompound produced in the adrenal gland. Its main function is to maintain normal homeostasis. Secretion of cortisol is regulated by the hypothalamus-pituitary-adrenal (HPA) axis. In response to stress and low level of circulating glucocorticoid, hypothalamus releases corticotrophin-releasing hormone (CRH) which triggers adrenocorticotropic hormone (ACTH) secretion by pituitary and in turn stimulates adrenal to produce glucocorticoids (Vegiopoulos and Herzig 2007). Cortisol has biologically pleiotropic role including regulation of fat, protein and carbohydrate metabolism, and activates anti-stress and anti-inflammatory pathways. Abnormality in the regulation of HPA axis leads to irregular patterns of cortisol levels as observed in Cushing's syndrome, Addison's disease, clinical depression and psychological stress.

Synthetic analogues of cortisol which are widely used in therapy of haematological malignancies are the prednisolone and dexamethasone (Figure1.5).

1.4.1 Glucocorticoid Receptors

Steroid receptors are located in the cytosol and the nucleus of the target cells. The receptors located in the cytosol are activated and moved to the cell nucleus upon binding of intracellular hormone or synthetic steroids entering the target cells. Steroids may also directly enter the nucleus and activate the steroid receptors in the nucleus by binding to them. The most studied steroid receptors are members of the nuclear receptor subfamily 3 (NR3). There are three groups of NR3: group A and B are mainly subdivided into the estrogen and estrogen-related receptors whereas group C are 3-ketosteroid receptor. Group C of the NR3 consists of four members which are: (1) glucocorticoid receptor (GR; NR3C1), (2) mineralocorticoid receptor (MR; NR3C2), (3) progesterone receptor (PR; NR3C3), and (4) androgen receptor (AR; NR3C4).

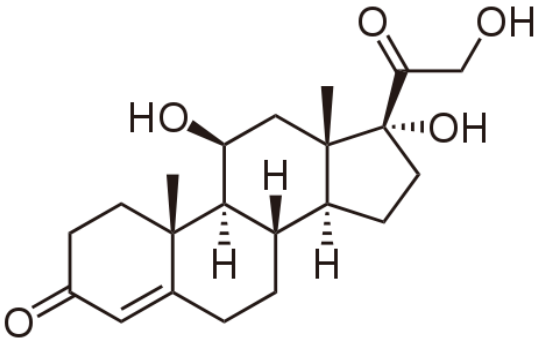

Cortisol

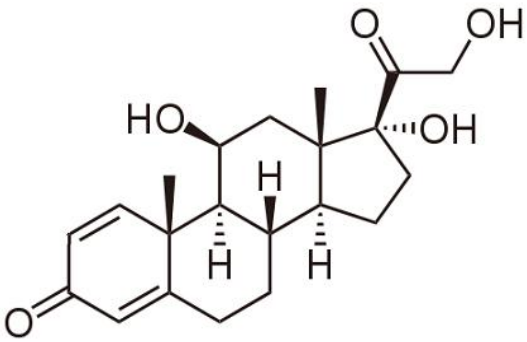

Prednisolone

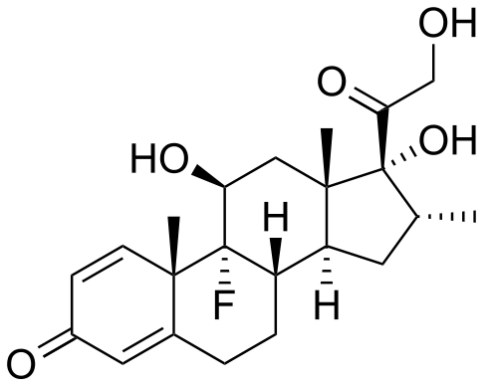

Dexamethasone

Figure 1.5 Chemical structure of the endogenous glucocorticoid, cortisol, and synthetic glucocorticoids, dexamethasone and prednisolone.

Glucocorticoids (GCs) generally are a class of steroid hormones (endogenous or synthetic derivatives) that bind to the glucocorticoid receptor (GR; NR3C1). GCs enter the cell passively and form a dimerization of GC/GR complexes, which subsequently translocate to the nucleus (Lambrou, Vlahopoulos et al. 2009) and activate or repress specific genes. It is known that GR is expressed in virtually all cell types, but both GR mRNA and protein levels vary considerably between tissues (Turner, Schote et al. 2007).

1.4.2 Structure

GC induces apoptosis in lymphoid malignancies and this action is mediated by GR protein, a ligand-induced transcription factor of the nuclear receptor family of transcription factors. GC-bound GR dimerizes, translocates to the nucleus and functions as transcription factor by binding to glucocorticoid response element (GRE) sequences (Geng, Pedersen et al. 2005).

The human GR gene encodes a protein with a molecular weight of 85 – 97 kDa and covers a region of more than 80 kb within chromosome 5, specifically located at 5q31. The GR gene contains eight coding regions (exons 2 – 9) and heterogenous non-coding first exon (Turner and Muller 2005) consist solely of 5'-untranslated sequence (Encio and Detera-Wadleigh 1991). Additionally, the 3'untranslated region of exon 9 is also a non-coding sequence (Charmandari, Kino et al. 2004). The GR gene in the eight coding region consists of three functional domains (Tissing, Meijerink et al. 2003) (Figure 1.4): (1) an N-terminal modulatory domain, (2) DNA-binding domain, and (3) a C-terminal ligand-binding domain. Within these domains are shorter structural motifs involved in nuclear localization, receptor dimerization and protein-protein interaction (Giguere, Hollenberg et al. 1986).

The N-terminal domain is encoded by exon 2 and contains a transactivation domain, AF1. This segment is required for the transcriptional activation of GR target genes (Hollenberg and Evans 1988) and involved in protein-protein interaction with various cofactors (Yudt and Cidlowski 2001; Geng, Pedersen et al. 2005). The N-terminal domain covers half the total length of the GR.

The internal DNA-binding domain (DBD) is a highly conserved 66 amino acid core consisting of two putative zinc fingers motifs separately encoded by exons 3 and 4 (Encio

and Detera-Wadleigh 1991). The first zinc finger encodes domains essential for the binding of the transcription factors, NFκB and AF-1, through which GR exerts its transrepression function. The DBD is essential for DNA binding to the GRE sequence located within the promoter regions of target genes (Yudt and Cidlowski 2001). Receptor dimerization and GRE-mediated transactivation functions through the encoded second zinc finger domain. DBD also contains the first nuclear localization signal (NLS1).

The ligand-binding domain (LBD) located in the carboxyl terminus of the receptor specifically binds glucocorticoids and contains a second activation function (AF-2) and nuclear localization signal (NLS2). This domain also contains sequences important for interaction with heat shock proteins (hsps) and nuclear transcription factors, nuclear translocation and receptor dimerization (Charmandari, Kino et al. 2004). A total of five exons combined to form the LBD.

Two native human GR protein have been described, a 777 amino acids hGRα and a 746 amino acid hGRβ (Wright, Zilliacus et al. 1993). Each hGR is encoded by nine exons with the first 727 amino acid in eight exons aligned identically, whereas the ninth exons are heterologous and the sequence diverge beyond this position (Encio and Detera-Wadleigh 1991). In contradistinction to hGRα, hGRβ resides primarily in the nucleus of cells, and due to its defective LBD, does not bind glucocorticoids (Charmandari, Kino et al. 2004). hGRβ has an intact DBD identical to hGRα, and competes with hGRα in binding to GREs (Geng, Pedersen et al 2005).

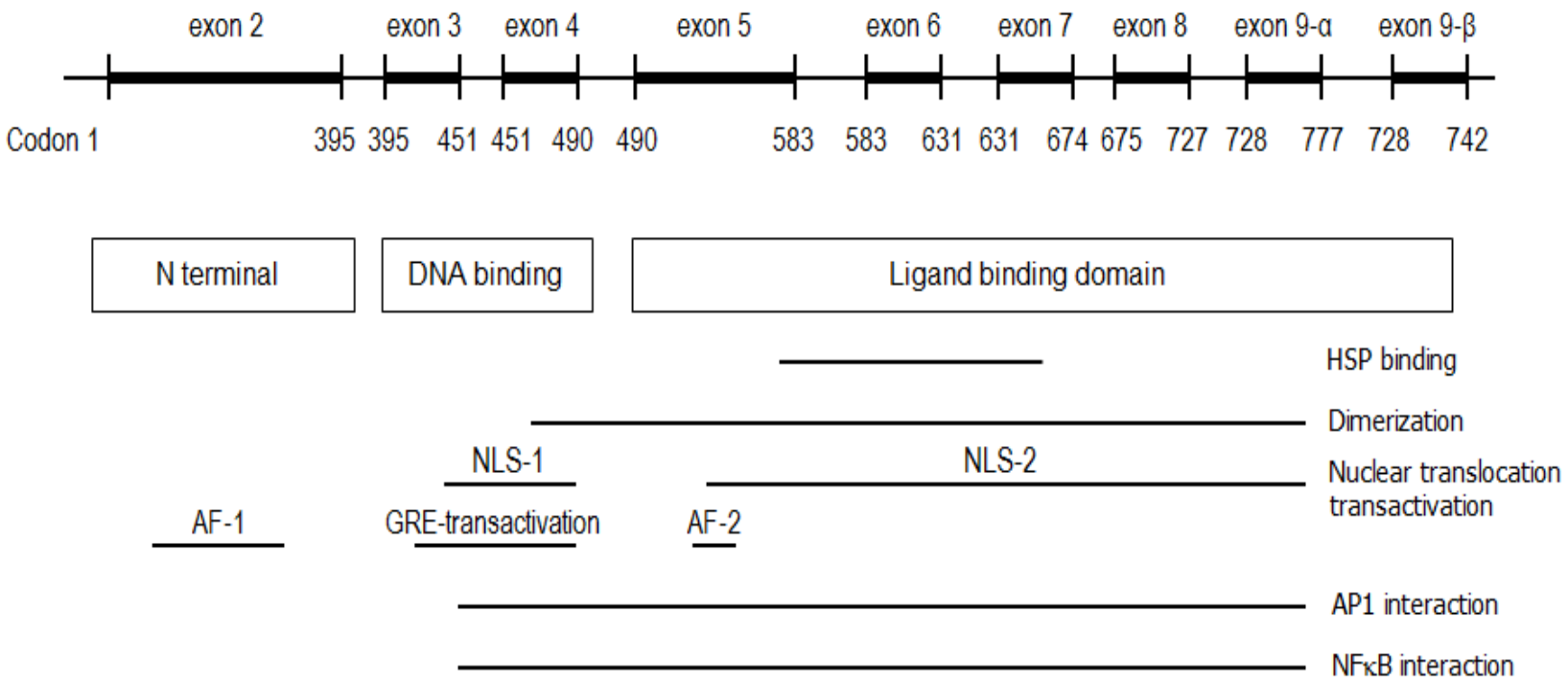

Figure 1.6 Schematic overview of the glucocorticoid receptor (GR) gene. The GR gene localized on chromosome 5 consists of 9 exons which can be divided into 3 functional domains, N terminal domain, DNA-binding domain and Ligand-binding domain. (Tissing, Meijerink et al. 2003).

1.4.3 Mechanism of Glucocorticoid Action

In the absence of ligand, the intracellular GR resides mostly in the cytoplasm as part of a large multiprotein complex which consists of the receptor polypeptide, two molecules of hsp90, hsp70, immunophilins and other proteins (Cheung and Smith 2000). GCs enter the cell through passive diffusion facilitated by their small size and lipophilic nature. Upon binding to the GR, the receptor undergoes an allosteric change which results in dissociation from hsp90 and other protein, unmasking/activation of the NLSs and phosphorylation at five serine sites (Charmandari, Kino et al. 2004). Additionally, the conformational change reveals domains which are necessary for nuclear translocation, dimerization, DNA binding and transactivation. The phosphorylated ligand-bound GC translocates into the nucleus and binds as homodimer to GREs in the promoter region of target genes. The bound GC interaction with basal machinery induces or represses the expression of target genes (Bamberger, Schulte et al. 1996). By physically interacting with other transcription factors such as activator protein AP1 and nuclear factor (NK) κB, the receptor can independently modulate gene expression of GREs (Jonat, Rahmsdorf et al. 1990; Scheinman, Gualberto et al. 1995). Additionally, through the AF1 and AF2 of the receptor in combination with coactivators which recruit the basal transcription machinery, regulates the GR transcriptional activity. The coactivators include p160 such as the steroid receptor coactivator 1 (SRC1) and the glucocorticoid receptor-interacting protein 1 (GRIP1), the p300/CREB binding protein cointegrators, and the vitamin D receptor-interacting protein/thyroid hormone-associated protein complex (Hittleman, Burakov et al. 1999; Auboeuf, Honig et al. 2002).

Endogenous steroid hormones that act with the GR are progesterone and DHEA which have antagonist effects on the GR. Some examples of synthetic steroids are Dexamethasone, as an agonist of the receptor whereas Mifepristone (RU486) and Cyproterone, act as antagonists, of the receptor.

1.4.4 Glucocorticoids in Therapy of ALL

Glucocorticoids were the first drugs to be used successfully in the treatment of ALL. The synthetic analogues of cortisol, prednisolone and dexamethasone (Figure 1.4), are used extensively as routine chemotherapeutic agents in various hematologic malignancies

including multiple myeloma, non-Hodgkin's lymphoma, chronic lymphoblastic leukaemia and ALL. This is due to their cytolytic actions in lymphoid and leukaemic cells, especially in childhood ALL (Galili 1983; Distelhorst 2002). GC drugs induce apoptosis and lysis of lymphoblast cells in those cases, however, the mechanisms are still poorly understood (Greenstein, Ghias et al. 2002). Since the late 1940s, prednisolone and dexamethasone have formed an integral part of treatment of childhood ALL. Although prednisolone has been the most commonly used glucocorticoid in treatment protocol, conventional glucocorticoid activity measurement showed dexamethasone is 6.5 times superior to prednisolone. *In vitro* experiment on defining sensitivity of patient blasts to glucocorticoid suggested that dexamethasone are 16-fold more potent than prednisolone (Kasper, Veerman et al. 1996). Dexamethasone also has a better penetration to the central nervous system (CNS) and more enhanced lymphoblastic cytotoxicity which results in lower bone marrow relapse rate, lower CNS relapse rate and the advantage in event-free survival recorded in children receiving the drug as in Figure 1.4 (Gaynon and Carrel 1999; Bostrom, Sensel et al. 2003). Recent MRC trial protocol ALL97 has reported that the use of dexamethasone significantly improved event-free survival and decreased the risk of relapse in all risk groups and is now standard therapy for childhood ALL.

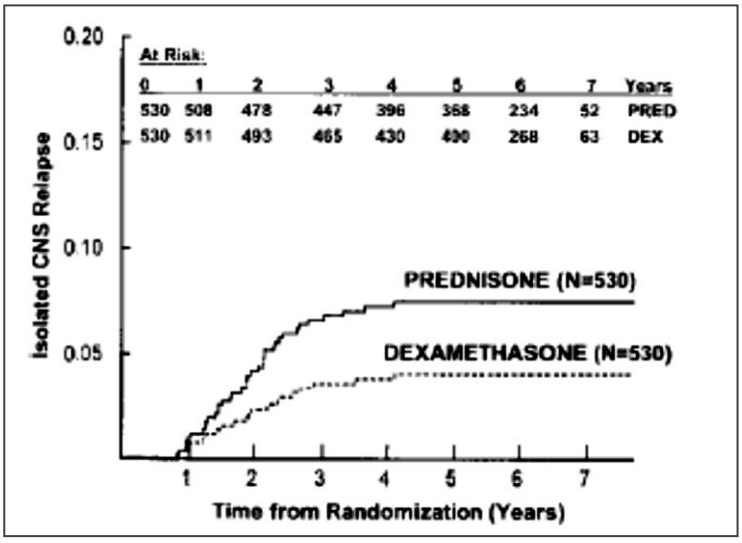

Figure 1.7 Isolated central nervous system (CNS) relapse patients randomised for steroid treatment. The 6-year risk of isolated CNS relapse in patients randomized to receive dexamethasone and prednisolone (Bostrom, Sensel et al. 2003).

1.5 E2A/HLF t(17;19)(q22;p13)

Of the known genetic events leading to leukaemia, translocations involving the fusion of transcription factors or activated signalling kinases are among the most common causes in childhood leukaemia (Wiemels 2008). In approximately one-half of cases of childhood ALL, chromosomal translocations are detected cytogenetically.

The t(17;19)(q22;p13) chromosomal translocation in early B-lineage ALL results in creation of *E2A-HLF* fusion gene that links the paired transactivation domains of E2A (E12/E47) to the basic region/leucine zipper DNA-binding and dimerization domain of hepatic leukaemic factor (HLF). The fusion produces an oncogenic fusion protein with structural and functional properties of a chimeric transcription factor (Inaba, Roberts et al. 1992; Hunger, Devaraj et al. 1994). The transforming activity of E2A-HLF requires at least one of the two transactivation domains of E2A, together with DNA-binding region and the leucine zipper dimerization domain of the HLF (Yoshihara, Inaba et al. 1995; Inukai, Inaba et al. 1998).

A more detailed explanation of the disease is given in Chapter 3 section 3.2.

1.6 Mouse Models for Leukaemia

The use of immunodeficient mice in studying the in vivo repopulation of normal hematopoietic cells as well as cells from patients with leukaemia has been reported for four decades. In the first attempts to establish mouse models for leukaemia, it was reported that nude mice injected subcutaneously with myeloid or lymphoid cell lines or primary cells developed myelosarcomas and solid vascularised tumours instead of leukaemias, although cells in the tumour were similar to those seen in the patients in long-term culture (Lozzio, Machado et al. 1976).

In 1983, severe combined immunodeficient (SCID) mice were described (Bosma, Custer et al. 1983). Homozygous SCID mice have few, if any, lymphocytes; therefore they are hypogammaglobulinaemic (Malynn, Blackwell et al. 1988) and deficient for functional B and T lymphocytes (Bosma and Carroll 1991). In addition these mice also have defects in activating components of the complement system, making them suitable recipients for in vivo experimental study since they cannot reject tumours and transplants.

The first successful engraftment of human stem cells in SCID mice was published in 1988 (McCune, Namikawa et al. 1988). Normal human hematopoietic cells and human tumours can be engrafted into SCID mice and these mice are better recipients than nude mice for the transplantation of human leukaemic cells (Kamel-Reid and Dick 1988). It was shown that human ALL cell line transplanted into SCID mice proliferated in the hematopoietic tissues and that the distribution and invasion of the organs followed a similar pattern to the disease in children (Kamel-Reid, Letarte et al. 1989).

Further experiments had treated SCID mice transplanted intravenously with human leukaemic cells with cytokine and growth factors to improve engraftment. These cells homed and proliferate extensively in the bone marrow, disseminate with a pattern similar to that seen in original patients and presenting cells morphologically identical to the patients leukaemic cells (Dick, Lapidot et al. 1991; Lapidot, Sirard et al. 1994). It has been shown that the prognosis of patients can be correlated with the growth rate of engrafted cells in these mice (Kamel-Reid, Letarte et al. 1991). More recently, a test model was published in which patient ALL and AML blast cells were used in subcutaneous (s.c.) injection into SCID mice. The growth of subcutaneous tumours compared to the clinical data demonstrated that the more aggressive the subcutaneous SCID tumours, the poorer the clinical outcome in patients (Yan, Wieman et al. 2009). Although human peripheral blood mononuclear cells, foetal hematopoietic tissues and hematopoietic stem cells were able to engraft in SCID mice, the number of engrafted cells was low and, in the case of experiments using normal haematopoietic cells failed to generate a functional human immune system (Greiner, Hesselton et al. 1998).

The SCID mouse strain was later crossed with the NOD (non-obese diabetic) mouse strain, which can better support the in vivo repopulation assay of human hematopoietic and leukaemic stem cells. The NOD mice were originally used as a model for type I diabetes where destruction of the pancreas involved B and T lymphocytes. Additionally, these mice have an impaired immune system with depleted natural killer (NK) cells and defective complement system (Shultz, Schweitzer et al. 1995). By crossing these NOD and SCID strains, mice lacking B- and T- cells and reduced functional NK cells were generated. These mice have been shown to be superior to the SCID strain in the modelling of lymphoid malignancy (Hudson, Li et al. 1998).

Studies on lymphoid leukaemia utilizing NOD/SCID mice have demonstrated the engraftment of children ALL blasts obtained at diagnosis or relapse in the mice and highlighted the similarities of the xenograft assays to the clinical disease (Lock, Liem et al. 2002; Liem, Papa et al. 2004). NOD/SCID mice conditioned with total body irradiation were reported to rapidly home and accumulate human scid repopulating cells in the bone marrow and spleen of the mice (Kollet, Spiegel et al. 2001). It was reported that intrahepatic injection of cells from adults with ALL into unirradiated newborn NOD/SCID mice led to successful engraftment after 6-18 week and the levels of bone marrow engraftment were linked to those in peripheral blood (Cheung, Fung et al. 2010).

ALL blasts with CD133 expression together with primitive phenotypes were found to be important in the engraftment in NOD/SCID mice as these cells showed long term in vivo proliferation (Cox, Diamanti et al. 2009).

Despite these successful engraftments of normal or leukaemic cells in mice, the disadvantage of using NOD/SCID mice in lymphoid xenograft was the high incidence of thymic lymphomas in some cases and a short lifespan of the mice with an average 8.5 months (Chiu, Ivakine et al. 2002).

The NOD/SCID mouse strain was further improved by homozygous mutation of the interleukin-2 receptor gamma chain locus (IL-2Rγ-chain; IL-2Rγ-null; Il2rg; NSG) where engraftment of human hematopoietic stem cells and peripheral-blood mononuclear cells in this immunodeficient strain is greater than the previously described humanized mouse strains (Shultz, Ishikawa et al. 2007). Importantly the lifespan of the NSG mice is extended to 15 months, making the strain a more ideal selection as a xenograft model for a long term study of haematological malignancy engraftment (Ishikawa, Yasukawa et al. 2005). In addition, the implementation of orthotopic technique by intrafemoral injection of bone marrow or leukaemic cells into their natural microenvironment can improve engraftment in the implanted mice. This technique is now widely used in the study of haematopoietic cells in xenograft models.

In a very recent published finding utilising NSG mice, Schmitz et al. (2011) reported *de novo* resistant very high risk (VHR) ALL cells reconstitute leukaemia earlier in mice compared to standard risk ALL cells. The VHR-ALL cells were able to maintain high engraftment levels in the bone marrow and spleen of xenografted mice after six serial

transplantations but not the standard risk-ALL cases. This finding demonstrated the ability of NSG mice to conserve repopulating capacity (Schmitz, Breithaupt et al. 2011).

It has been reported that intrafemoral injection of flow sorted ALL cells into non-irradiated NSG mice increased the bone marrow assay sensitivity by tenfold compared to intravenous injection (Mazurier, Doedens et al. 2003). Additionally, Le Viseur et al. (2008) have demonstrated that in limiting dilutions experiments, leukaemic blasts, which were sorted into specific committed lymphoid lineage with different markers, were able to transfer leukaemia in NSG mice in at least four sequential transplantations (Le Viseur, Hotfilder et al. 2008). Notta et al. reported that injection of human HSCs into NSG mice showed higher engraftment in female mice and concluded that self-renewal, proliferation and survival of the engrafted cells were influenced by gender associated factors (Notta, Doulatov et al. 2010).

1.7 Aims of Study

Aim 1:

To evaluate the kinetic, self-renewal and clonal evolution capacity of a t(17;19) E2A-HLF-positive matched paired patient samples in *in vivo* model.

A matched paired L707 presentation and relapse patient materials will be xenografted into NSG mice to evaluate and compare the proliferation and expansion capacity between the blast cells. Combination of both presentation and relaspe cells in different propotions will be carried out as well evaluating which cells have the advantage of repopulating and expanding in the absence and presence of glucococrticoid drugs. This experiment will determine if the engraftment of the matched paired materials is able to recapitulate the human disease condition, which organ is infiltrated and whether the engraftment is continuously reproducible in subsequent transplantation.

Aim 2:

To generate lentiviral vectors harbouring different reporter gene sequences coupled with fluorescent protein sequences.

The purpose of this section is to generate tracking markers that could be used to label target cells to facilitate the monitoring progression of the cells in vivo. HIV-based lentivirus will be utilized in the cloning of different luciferase reporter genes coupled with different fluorescent protein genes. These cloned lentiviruses will be transduced into cell lines to evaluate the transduction efficiency.

Aim 3:

To monitor progression of leukaemic cells xenografted in mice by luminecscence imaging.

This section utilized the transduced cell lines in mouse model xenografts. The purpose of this study is to prove the monitoring capability in tracking the progression of cells using luminescence imaging and the ability to compare expansion of different cells in vivo.

CHAPTER 2

MATERIALS AND METHODS

CHAPTER 2

MATERIALS AND METHODS

2.1 General Materials

2.1.1 Equipment

ABI 7900HT Sequence detection system (Applied Biosystems, USA)

Agarose gel electrophoresis unit BIO-Rad (Hemel-Hempsted, Herts., UK)

Allegra® X-12 benchtop centrifuge (Beckman Coulter, High Wycombe, UK)

Centrifuge 5415C (Eppendorf, Hamburg, DE)

Centrifuge 5417R refrigerated (Eppendorf, Hamburg, DE)

Class II microbiological safety cabinet (BIOMAT-2 Medical Air Technology Ltd., Manchester UK)

FACS Calibur Flow Cytometer (Becton Dickinson, Oxford, UK)

FACS Canto II Flow Cytometer (Becton Dickinson, Oxford, UK)

FACS Sorting (Becton Dickinson, Oxford, UK)

Fluorescent microscope (Nikon Eclipse TE2000-U) with Camera (Digital Sight SD-2MBWc, Amstelveen, Netherland)

Gel Doc BIO-Rad (Hemel-Hempsted, Herts., UK)

Luminescence Bioimager (Caliper Ltd, USA)

Mistral 2000 centrifuge (Fisher Scientific, Loughborough, Leicestershire, UK)

Mistral 3000 refrigerated centrifuge (Fisher Scientific, Loughborough, Leicestershire, UK)

ND-1000 Spectrophotometer (Nanodrop Technologies Ltd., USA)

Olympus CK30 Light microscope (Olympus Corperation, Japan)

Spectramax 250 Multiwell plate reader (Molecular Devices, Crawley,UK)

Thermomixer comfort (Eppendorf Thermoblock, UK)

Tissue culture incubators (Heraeus Equipment Ltd., Essex, UK)

Universal Hood II BIO-Rad (Hemel-Hempsted, Herts., UK)

2.1.2 Disposables and Labware

All disposable and plasticware were purchased from Greiner Bio-one (Frickenhausen, Germany), Eppendorf (Hamburg, Germany) and Becton Dickinson (New York, USA) unless stated otherwise.

Thickwall-style polyalloer conical tubes (Beckman Instruments Inc., High Wycombe, UK).

Derlin PKGED'1 tubes adapters (Beckman Instruments Inc., High Wycombe, UK).

2.1.3 Chemicals and Reagents

All standard chemicals, reagents and buffers used in the experiments were either analytical or molecular grades and purchased from Sigma-Aldrich Chemical Company (Dorset, UK), Fischer Scientific (Leicestershire, UK) or BDH (Dorset, UK) unless otherwise stated.

2.1.4 Buffers

***E.coli* growth and transformation**

Luria-Bertani (LB) Medium (1 Liter)

10 g Bacto-Trypton
10 g Sodium Cloride
5 g Yeast Extract
pH 7.4, Sterilized by autoclaving

Luria-Bertani (LB) Agar (1 Liter)

10 g Bacto-Trypton
10 g Sodium Cloride
5 g Yeast Extract
15 g Agar
pH 7.4, Sterilized by autoclaving

SOC medium

2 g Bacto®-tryptone
0.5 g Bacto®-yeast extract
1 ml of 1M NaCl
0.25 ml of 1M KCl
Add water to 90 ml
Autoclaved and let cooled, then add;
1 ml of 1M $MgCl_2 \bullet 6H_2O$
1 ml of 2M glucose
Bring to 100ml with distilled water
pH 7.0
filter-sterilized with 0.2 µm syringe filter unit

Electrophoresis buffers

50x TAE buffer (stock solution)

242 g Tris-base dissolved in 200 ml distilled water
Add 57.1 ml glacial acetic acid
Add 100 ml of 500 mM EDTA solution (pH8.0)
Bring the final volume up to 1000 ml with distilled water

1x TAE buffer (working solution)

20 ml stock solution 50x TAE buffer
Bring to 1000 ml with distilled water

The Tris-acetate-EDTA (TAE) working solution contains 40 mM Tris, 20 mM acetic acid and 1 mM EDTA.

0.5 M EDTA solution

84.05 g Ethylenediaminetetraacetic acid (EDTA)
Add 100 ml of distilled water
Add 5 M NaOH until pH8.0 reaches and EDTA dissolved
Bring to 500 ml volume with distilled water

Phosphate buffer

1x PBS

Phosphate buffered saline (PBS) was prepared by dissolving PBS tablet into appropriate volume of distilled water and was sterilized by autoclaving.

2.1.5 Molecular Cloning

2.1.5.1 Conventional Restriction Enzymes

All restriction enzymes used as listed below were supplied by Fermentas. The standard activity of all the enzymes was 10u/µl.

BamHI	PstI
BglII	PvuI
Bsp119 (BstBI)	SacI
Cfr42I (SacII)	SalI
EcoRI	ScaI
GsuI	SgsI (AscI)
MunI (MfeI)	XbaI
NcoI	XhoI
NheI	

2.1.5.2 Modifying Enzymes

T4 DNA Polymerase I	5u/µl (Fermentas)
T4 DNA Ligase	5u/µl (Fermentas)
DNA Polymerase I Large (Klenow) Fragment	1u/µl (Promega)

2.1.6 Cell Analysis

Antibodies for Flow cytometry analysis were purchased from Becton Dickinson Pharmingen.

	Clone	**Dilution used**
CD10-FITC	Hl10a	10 µl / 10^6 cells
CD19-PE	SJ25C1	10 µl / 10^6 cells
CD20-PerCP-Cy5.5	L27	10 µl / 10^6 cells
CD33-PE	P67.6	10 µl / 10^6 cells
CD34-APC	8G12	2.5 µl / 10^6 cells
CD45-APC	2D1	2.5 µl / 10^6 cells
CD45-PE-Cy7	30-F11	2.5 µl / 10^6 cells
TER119-APC	TER-119	2.5 µl / 10^6 cells
TER119-PE-Cy7	TER-119	2.5 µl / 10^6 cells

2.1.7 PCR and q-PCR

RevertAid™H Minus First Strand cDNA Synthesis Kit (Fermentas, York, UK).

REDTaq®ReadyMix™ PCR Reaction Mix (Sigma-Aldrich, Missouri, USA)

Taqman MasterMix (Applied Biosystem, Warrington, Cheshire, UK)

2.1.8 Kits

The following kits were purchased from Qiagen (Crawley, West Sussex, UK) and assays from Promega Corporation (Madison, Wisconsin, USA).

QIAamp DNA Blood Mini Kit

QIAquick PCR Purification Kit

QIAqiuck Gel Extraction Kit

Miniprep Plasmid Isolation Kit

Maxiprep Endofree Plasmid Isolation Kit

Luciferase Assay System

2.1.9 Primers and Oligonucleotides

All primers and probes were purchased from Sigma-Aldrich (Dorset, UK).

Self-designed oligonucleotides (polylinker)

SacI-XhoI PL sense	5’ – CGGATCCTTCGAAGCTATCTAGAGAATTCA GCTCCATGGAGATCTGATCCAATTGGTCGACCGT AC – 3’
SacI-XhoI PL antisense	5’ –TCGAGTACGGTCGACCAATTGGATCAGATC TCCATGGAGCTGAATTCTCTAGATAGCTTCGAAG GATCCGAGCT – 3’

Primers for RT-PCR

E2A exon 12	5’-GACATGCACACGCTGCTGCC-3’
E2A exon 13	5’-GCCTCATGCACAACCACGCG-3’
HLF exon 4	5’-CCCGGATGGCGATCTGGTTC-3’

Primers and probe for Q-PCR

NR3C1 forward	5’- AGGACGCCACCCCATTG-3’
NR3C1 reverse	5’- TGTCTGAAGGGTCCCAGTTTG-3’
NR3C1 probe	[6FAM]ACTCAAATGCACACTCACA[TAM]
ATP10A forward	5’- AGCCCCATGGTGAGTGTACAG-3’
ATP10A reverse	5’- GTAGGATTAAATATAGACACCTTCCATGAG-3’
ATP10A probe	[6FAM]CCACGTCTCTTCCCCATTTTCACCATC[TAM]

2.1.10 Cell Lines

SEM: a B-cell precursor leukaemia cell line, established in 1990 from peripheral blood of a 5-year old girl at relapse, carrying t(4;11) MLL-AF4 malignancy (Greil, Gramatzki et al. 1994).

Kasumi-1: a FAB M2 classification AML cell line, established in 1989 from the peripheral blood of a 7-year old Japanese boy at second relapse, carrying t(8;21) AML1-ETO fusion gene (Asou, Tashiro et al. 1991).

SKNO-1: a maturated myeloblast cells isolated from bone marrow of a 22-year old Japanese woman bearing the t(8;21) traslocation with AML1-MTG8 fusion gene (Matozaki, Nakagawa et al. 1995).

RS4;11: a B-cell precursor leukaemia line, established from bone marrow of a 32-year old woman at relapse, classified as ALL L2 subtype of t(4;11) malignancy with MLL-AF4 fusion gene (Stong, Korsmeyer et al. 1985).

PreB 697: a B-cell precursor leukaemia line, established in 1979 from the bone marrow of 12-year old male at relapse of ALL (Findley, Cooper et al. 1982).

REH: a B-cell precursor leukaemic cell line, established in 1975 from the peripheral blood of a 15-year old North African girl with ALL at first relapse (Rosenfeld, Goutner et al. 1977; Matsuo and Drexler 1998).

HAL-01: a B-cell precursor leukaemia of ALL-L2 subtype cell line, established in 1990 from the peripheral blood of a 17-year old woman diagnosed with ALL, carrying Type 1 t(17;19)(q22;p13) with E2A/HLF fusion gene (Ohyashiki, Fujieda et al. 1991). This cell line has a morphological and cytochemical appearance of lymphoid cells, with a myeloid-associated marker in patients' cells but not in the cell line.

293T: a cell line derived from human embryonal kidney cell line 293, expressing large T antigen, of fibroblast morphology and highly transfectable (del Rio, Clark et al. 1985).

2.1.11 Competent Cells Bacteria

JM109

JM109 are *E.coli* competent cells lacking recA which improves DNA yield in plasmid isolation. These competent cells are also deficient in β-gal and carry the genotype of: *end*A1, *rec*A1, *gyr*A96, *thi*-1, *hsd*R17 (r_k–, m_k+), *rel*A1, *sup*E44, Δ (*lac-pro*AB), F' [*tra*D36, *pro*AB+, *lac*I^q, *lacZ* Δ M15]. The JM109 competent cell was purchased from Promega, Madison, USA.

Stbl3

The Stbl3 are *E. coli* strain designed for cloning direct repeats found in lentiviral expression vectors. These cells reduce the frequency of unwanted homologous recombinations of long terminal repeats (LTRs) found in lentiviral and other retroviral vectors. Stbl3 cells are highly stable bacterial cells which help in increasing the efficiency of lentiviral cloning. The cells carry the genotype of: F-*mcr*B*mrr hs*dS20 (r_B^-, m_B^-) *rec*A13 *sup*E44 *ara*-14 *gal*K2 *lac*Y1 *pro*A2 *rps*L20 *(Strr) xyl-5* λ^-*leu mtl-1r*. The Stbl3 competent cell was purchased from Invitrogen, UK.

Self-produced competent cells

E.coli competent cells JM109 and Stbl3 were prepared in high volume from the stocks using a $CaCl_2$ / PEG protocol.

2.1.12 Mouse Strain

All animal experimentation used the same strain of immunodeficient mice.

NSG mice

Also known as NOD/SCID gamma, NOD.Cg-*Prkdc*^{scid} *Il2rg*^{tmIWjl} immune deficient mice, NOD-SCID IL2Rgamma^{null} or NOD-SCID IL2Rg^{null} or NSG, this mouse strain was purchased from Jackson Laboratory, USA.

Mice are deficient in mature B, T and NK cells and carry the true null interleukin-2 receptor gamma mutation. These mutant mice have been shown to readily support

engraftment of human $CD34^+$ HSC and represent a superior, long-lived model suitable for studies employing xenotrasplantation strategies.

2.2 Methods

2.2.1 Methods Chapter 3

2.2.1.1 Cell lines and Maintenance of Cells

All cell lines used in this study were previously tested with the Mycoalert Elisa Assay and confirmed as being Mycoplasma negative. Cell culture work was carried out under aseptic condition in class II microbial safety containment hoods. All surfaces and equipment, disposables and glassware were sterilized with 70% ethanol. Cells were grown in flasks (Corning) or multi-well plates (NUNC, Invitrogen). All cell lines used grew in suspension, unless otherwise mentioned, and were incubated at 37°C in a humidified tissue incubators (IncuSafe, Sanyo) supplied with 5% CO_2.

Cell lines are supplied by DSMZ (German Collection of Microorganisms and Cell Cultures, Braunschweig, Germany) unless otherwise stated. All cell lines used in the experiments were routinely grown in their respective medium. SEM, Kasumi-1, RS4;11 and HAL-01 were grown in RFh10, a RPMI 1640 media with Hepes modification (Gibco) supplemented with 10% fetal calf serum (FCS) and 200 µM L-glutamine. SKNO-1 was cultured in RFh20G, a RPMI 1640 media with Hepes modification supplemented with 20% FCS, 200 µM L-glutamine and 7 ng/ml GM-CSF. PreB 697 and REH were cultured in RF10, a RPMI 1640 supplemented with 10% FCS only. All cells were passaged depending on their doubling times at a cell density of 0.5 x 10^6 cells/ml, as summarized in Table 2.1.

Cell line	Morphology	Medium	Subculture	Doubling time	Source
REH	small, round, single cells in suspension	RF10	every 3-4 days; at 0.5 x 10^6 cells/ml; maintain at high density (>2 x 10^6 cells/ml);	50-70 hours	DSMZ No.: ACC22
697 pre-B	round, single cells and clusters of cells in suspension	RF10	every 2-3 days; at ca. 1.0 x 10^6; maintain at 0.5-1.5 x 10^6 cells/ml	30-40 hours	DSMZ No.: ACC42
HAL-01	single, round cells in suspension, some cells are slightly adherent	RFh10	twice a week; at 1 x 10^6 cells/ml; adherent cells can be detached by tapping the flask;	48 hours	DSMZ No.: ACC610

Table 2.1 Summary of morphology and maintenance of REH, 697 pre-B and HAL-01 cell lines.

2.2.1.2 Mycoplasma Testing

All cell lines used in the studies maintained in cultures were routinely checked for mycoplasma contamination. Cultures contaminated with mycoplasma can affect cell metabolism, antigenicity and growth characteristics of the cells. Contaminated cell lines will invalidate any experimental data achieved from the cells. Mycoplasma infection was analysed using MycoAlert® (Lonza, UK). The MycoAlert® Assay is a selective biochemical test that exploits the activity of mycoplasmal enzymes. The presence of these enzymes is utilized in a rapid screening procedure allowing sensitive detection of mycoplasma contamination in a test sample. The viable mycoplasmas are lysed and the enzymes released react with the MycoAlert® Substrate by catalyzing the conversion of ADP to ATP. The level of ATP in the tested samples is measured before and after addition of MycoAlert® Substrate to obtain a ratio which is indicative of the presence or absence of mycoplasma.

2.2.1.3 Counting of Viable Cells

Cell counts were performed using an Improved Neubauer counting chamber (Fisher Scientific), a hematocytometer which was used to determine the number of cells per unit volume of a suspension. The coverglass of the counting chamber was placed over the counting surface prior to adding the cell suspension. To count viable cells, an aliquot of single cell suspension was mixed 1:1 with 0.4% Trypan blue solution. 10 µl of the mixture was applied to the edge of the coverglass which completely filled the counting area by capillary action. The cells within four large squares with grids (made up of 4x4 squares each) were counted under light microscope (Olympus) and the numbers of cells

scored were averaged. The total number of cells per ml of solution was equal to the average number of cells x 2 (of dilution with Trypan blue solution) x 10^4.

2.2.1.4 Resurrecting Frozen Cell Stocks

All cell line stocks were stored in liquid N_2 at -180°C. In order to defrost them, vials were warmed at 37°C in a water bath. Cells were transferred to 20-ml universal tubes (Sterilin) and 5 ml of pre-warmed growth media was added to dilute the frozen medium containing dimethyl sulphoxide (DMSO). Cell suspensions were spun at 1500 rpm for 5 min in MSE 2000 centrifuge (GMI). Supernatants were aspirated off, the cell pellets were resuspended in fresh growth medium and transferred into 25 cm^2 plastic flasks (Corning). Cells were incubated at 37°C in a humidified incubator supplied with 5% CO_2.

To recover frozen cryopreserved patients cells, the frozen vials of cells were thawed rapidly in a 37ºC waterbath and diluted in 5 ml of RF10 medium. Viable cells were counted by trypan blue exclusion method as mentioned in section 2.2.1.3. Cells were pelleted by centrifugation at 1500 rpm for 5 minutes. The medium was aspirated and cells were resuspended in RF10 medium at an appropriate volume for cell analysis or xenograft mouse model.

2.2.1.5 Freezing Down Cells for Storage

To freeze down cells for storage in liquid N_2, suspension cells were grown in 75 cm^2 or 175 cm^2 flasks at high density. Viable cells were counted according to section 2.2.1.3 and suspensions containing the desired number of cells were spun down to remove the growth medium. The cell pellet was resuspended in a relevant amount of freezing medium to be frozen down at a concentration of 5 to 6 million cells per vial. The freezing medium contained 90% FCS and 10% DMSO. Cell stocks were stored in -80°C overnight or up to two weeks, in order to freeze the cells at a rate of approximately 1ºC per minute. Within 1-14 days vials were transferred into liquid N_2 for long term storage.

2.2.1.6 Harvesting of Cells

Cells were harvested for DNA, RNA and protein studies or other cells experiments when in exponential growth. The cultured cell suspension was aliquoted into a 20-ml sterillin tube and centrifuged at 1500 rpm for 5 minutes at room temperature. The supernatant was aspirated and the cell pellet was washed with PBS, centrifuged and repelleted. Cells were finally resuspended in the appropriate volume of medium or PBS.

2.2.1.7 Cytospins of Cells

Fresh or frozen samples of leukaemic blast cells were prepared for cytospins by diluting the cells to a concentration of 10^6 cells/ml in RF20 (RPMI 1640 medium containing L-glutamine (Invitrogen) supplemented with 20% foetal calf serum). 100 µl of cell suspension was dropped into a cell concentrator chamber attached to a glass slide. The slides were centrifuged at 400 rpm for 3 minutes at room temperature in a Cytospin 2 centrifuge (Shandon Southern Products Ltd., UK). The slides then were allowed to air-dry at room temperature. Slides were directly used for cell staining or were wrapped with cling film and stored in -20ºC freezer. To use the frozen slides for staining, slides were defrosted at room temperature for one hour prior to use.

2.2.1.8 May-Grünwald-Giemsa Staining of Blast Cells

The May-Grünwald-Giemsa stain is an eosin-methylene blue solution which was modified for easier viewing of haematological specimens under microscopy. This stain is also among the widely used solutions in histological staining of blood smears that allows the different types of cells and components within the cells to be distinguished from one and another by their colour and shapes. Lymphocytes are generally round cells with large round nucleus and within a considerable size range. The lymphocyte nuclei stain a deep red or violet colour, while the cytoplasm is either a dark blue ring or not visible due to large nuclei.

Protocol

1.5 ml of May-Grünwald stain (Fisher Scientific) was added onto the cytospinned cells on slides prepared as discussed in section 2.2.1.7 and incubated for 3 minutes at room

temperature. Then 1.5 ml of water was added to dilute the stain on the slides and was incubated for a further 5 minutes at room temperature. Approximately 10 drops of Giemsa (Sigma) were diluted in 10 ml of water. The diluted May-Grünwald stain was poured off the slides (into a sink with running water). The slides were flooded with the freshly prepared diluted Giemsa stain and were incubated for 15 minutes at room temperature. Following this step, the slides were rinsed in water and air-dried. Slides were mounted in DPX stain and were covered with coverslips.

2.2.1.9 Cell Growth and Growth Curves

Assessment of cell growth is required for cell lines intended for use in drug induction assays. Cells in culture follow a characteristic growth cycle of a lag phase, a period of exponential growth or log phase and finally reaching a plateau in which the growth of the cells was arrested with zero or reduced growth period. Different cell lines have different characteristic of these growth phases which allows determination of the doubling time of the cell line. The population doubling time is the time taken for the culture to increase two-fold in the middle of the log phase. This assessment facilitates routine subculture of cells lines and is used in determining drug exposure for cytotoxicity assays.

Protocol

Cell lines in well maintained routinely passaged cultures were used for cell growth assessment. Cells in exponential phase of the growth cycle were passaged in a 25 cm^2 flask at a concentration of 0.5 x 10^6 cells/ml in 10 ml of fresh medium. Cell growth was determined by counting the cells daily for seven consecutive days using trypan blue exclusion method as described in Section 2.2.1.3. To maintain the cells growing in culture without too much change in medium for the growth assessment, cell suspension was aliquoted 20 µl daily for cell counting. Growth curves were analysed using simple Excel worksheet.

2.2.1.10 Cell Growth and Cytotoxicity Assays

Cytotoxicity assays measure drug-induced alterations on cell growth. The colorimetric assay based on WST-1 is suitable for the non-radioactive quantification of cell proliferation, cell viability and cytotoxicity. For this purpose, Cell Proliferation Reagent

WST-1 (Roche Applied Science, Germany) was used. Proliferation assays utilizing this kit are useful for analyzing the number of viable cells by the cleavage of tetrazolium salts added to the culture medium. This technique does not require washing or harvesting of cells. The tetrazolium salts are cleaved to formazan by cellular mitochondrial enzymes. Overall activity of mitochondrial dehydrogenases in the sample correlates with the number of viable cells. Increased enzyme activity leads to an increase in the amount of formazan dye formed, which directly correlates to the number of metabolically active cells in the culture. Quantification of the formazan dye produced is measured by multiwell plate reader spectrophotometer.

Protocol

Cell lines PreB 697 and REH were maintained in culture in RF10 (RPMI supplemented with 10% FCS) medium and HAL-01 was cultured in RFh10 (RPMI with hepes modification supplemented with 10%FCS and 200 µM L-glutamine) medium. Cells at the exponential phase of the growth cycle were collected in universal tubes and centrifuged at 1500 rpm for 4 minutes. Supernatants were removed and cell pellets were resuspended in respective media. Cells were then seeded in 96-well plates at a density of 1 x 10^5 cells in 150 µl medium per well. For the t(17;19) patient presentation and relapse cells, one vial of each frozen sample of cells harvested from spleens of xenografted mice were used in this experiment. Cells were recovered from cryopreservation as in Section 2.2.1.4. Cell suspensions were seeded in 96-well plates at a density of 1 x 10^6 cells/well in150 µl RF10 medium. Each cell was aliquoted in triplicate for each treatment dilution. Fifty microliters of dexamethasone (Sigma, USA) at various concentrations of 1 nM, 10 nM, 100 nM, 1 µM and 10 µM were added to each triplicate of cells, in addition to 20 µl WST-1 reagent. Cells were incubated in a humidified incubator at 37ºC supplied with 5% CO_2 for 96 hours prior to measuring the colorimetric of the dye produced using the multiwell plate reader Spectramax 250 (Molecular Devices, UK). Dye absorbances in the samples were measured at 450 nm and an additional absorbance value at 650 nm were measured for correction to medium colour. Data were analysed using PrismPad v4.0 software.

2.2.1.11 Extraction of Genomic DNA

Genomic DNA was extracted from cell pellets using the QIAamp DNA Mini and Blood Mini Kit (Qiagen, Crawley, UK). The kit simplifies rapid isolation and purification of DNA from 200 µl of whole human blood, 5 x 10^6 lymphocytes, or cells with a normal karyotype. The DNA was eluted with a fast spin column without phenol-chloroform extraction. The DNA binds specifically to the QIAamp silica gel membrane while contaminants pass through. PCR inhibitors such as divalent cations and proteins are completely removed in two efficient wash steps. The pure nucleic acid is eluted in water or buffer provided in the kit. The technique yields DNA sizes from 200 bp to 50 kb depending on the age and storage of the samples. DNA extraction was performed according to manufacturer's protocol. The proprietary reagents included in this kit were QIAGEN® Protease or proteinase K, Buffer AL, Buffer AW1, Buffer AW2 and Buffer AE.

Protocol

Approximately 5 x 10^6 cells were pelleted as previously described. Cell sample was pelleted in a 1.5 ml microcentrifuge Eppendorf tube for the following processes. The washing solution was aspirated out and the cell pellet was resuspended in PBS to a final volume of 200 µl. A total of 20 µl of proteinase K solution (20 mg/ml) was added to the cell suspension followed by 200 µl of Buffer AL for cell lysing. The sample was mixed thoroughly in the suspension using pulse-vortexing for 15 seconds. The mixture was incubated at 56ºC for 10 minutes in a heat block to lyse the cells. Following this step, 200 µl of 100% ethanol was added to the sample and mixed twice by pulse-vortexing for 15 seconds. The sample was then centrifuged briefly to remove any drops from the inside of the lid and the mixture was transferred to a QIAamp spin column with attaching 2-ml collection tube. The column was centrifuged at 13,000 rpm for one minute at room temperature. The DNA remained in the column filter and the collection tube containing the filtrate was discarded and replaced with a clean collection tube. The QIAamp spin column was washed by adding 500 µl Buffer AW1 and centrifuged at 13,000 rpm for one minute at room temperature. The collection tube containing the filtrate was discarded and replaced with a clean collection tube provided. The column was washed again by adding 500 µl of Buffer AW2 followed by centrifugation at 13,000 rpm for 3 minutes. The final step was to elute the DNA from the column. The column was placed in a clean 1.5 ml

Eppendorf tube and 50-200 µl pre-warmed Buffer AE or nuclease-free water was added to the column, depending on the size of the initial pellet or cell count. The column with elution buffer was incubated for 1 minute at room temperature before centrifugation at 13000 rpm for 1 minute. To increase the DNA yield, column was incubated for 5 minutes at room temperature before centrifugation. The DNA was stored at 4ºC ready for use. The concentration and purity of DNA was estimated using the NanoDrop® ND-100 spectrophotometer.

2.2.1.12 Extraction of Total RNA

Total RNA was extracted from cell pellets using the Qiagen RNeasy Mini kit (Qiagen, Crawley, UK). The method relies on the selective binding properties of a silica-based membrane. The kit utilizes buffer containing a highly denaturing guanidine-thiocyanate to immediately inactivate RNases that ensures purification of intact RNA from the lysed and homogenized biological samples. Addition of ethanol provided appropriate conditions of the silica-gel membrane in the spin column to bind RNA to the membrane when the contaminants were efficiently washed away. Water provided in the kit was used to elute the high quality RNA. The proprietary reagents included in this kit were RLT buffer containing guanidium thiocyanate, RW1 buffer, RPE buffer containing 80% ethanol and RNase-free water.

Protocol

Appropriate numbers of cells (usually $\geq 10^6$ cells) were aliquoted into centrifuge tubes and spun down for 5 minutes at 300 x g. Supernatants were discarded completely removing all media. Cell pellets were washed once with PBS and spun down to remove the washing buffer. Cell pellets were loosened by flicking the tubes. 350 µl of Buffer RLT (1% of 2 Mercaptoethanol added) was added to the pellet and the mixture was vortexed to mix. The homogenized lysates were pipetted directly onto QIAshredder columns with 2-ml collection tubes (supplied in the kit), and centrifuged for 2 minutes at maximum speed to homogenize. One volume or 350 µl of 70% ethanol was added to the flow-through and mixed well by pipetting. Lysates were transferred to RNeasy spin columns with 2-ml collection tubes, and centrifuged for 15 seconds at 8000 x g (10,000 rpm). 700 µl of Buffer RW1 was pipetted onto the RNeasy columns and centrifuged for 15 seconds at 8000 x g to wash the columns. Columns were transferred into new 2-ml

collection tubes (supplied). 500 µl Buffer RPE was pipetted onto the column and centrifuged at 8000 x g to wash. This step was repeated twice. Flow-through was discarded and columns were centrifuged again for 2 minutes at maximum speed to dry the RNeasy membrane. RNeasy columns were transferred into 1.5-ml collection tubes (supplied). 50 µl of RNase-free water was pipetted directly onto the RNeasy membranes. The columns were centrifuged for 1 minute at 8000 x g to elute. RNAs were either kept in -80ºC for long-term storage or used directly to synthesize cDNA.

2.2.1.13 Assessing DNA and RNA Concentration and Quality

The concentration of DNA and RNA samples yielded were assessed using a ND-1000 Spectrophotometer (Nanodrop Technologies, Labtech International, UK). The Nanodrop measures the concentration of DNA or RNA using only 1µl of sample. Spectrophotometric absorbance at 260 nm (A260) and 280 nm (A280) were measured against water blank. The ratio of A260:A260 was taken as a guideline of sample purity, with values between 1.8 and 2.0 indicating pure DNA or RNA. Lower ratio values indicated protein contamination.

2.2.1.14 Synthesis of cDNA

The total RNA isolated from the samples was first converted into cDNA by a reverse transcriptase step before it can be analyzed. RevertAid^{TM}H Minus First Strand cDNA Synthesis Kit was used for this purpose. The cDNA synthesis kit was supplied with Random Hexamer Primers, 5x Reaction Buffer, Ribolock RNase Inhibitor, RevertAid H Minus Reverse Transcriptase and DEPC-treated water. The incubation steps for cDNA synthesis were performed using the Applied Biosystem GeneAmp PCR System 9700 thermal cycler machine.

Protocol

To prepare the cDNA from RNA samples, 200 µl PCR tubes were used and the cDNA synthesis was performed according to manufacturer's procedures. A volume of 20 µl reaction mix was prepared using reagents from the kit. Two microliters of RNA samples with concentrations between 250 ng to 1 µg was used in the initial step. One microliter of Random Hexamer primers and 9 µl of DEPC-treated water were mixed with the RNA in

the PCR tube. The first step reaction mixture was incubated at 70℃ for 5 minutes followed by a cooling-off step with a reduction of temperature to 4℃ for 10 minutes. During this time, a mixture of 4 µl 5x reaction buffer, 2 µl of 10 nM dNTPs, 1 µl RNase inhibitor and 1 µl of reverse transcriptase were added. The second step reaction mixture was run for a full cycle of incubation at 25°C for 10 minutes, 42°C for 60 minutes and 70°C for 10 minutes followed by cooling at 4°C. The synthesized cDNA was kept at 4°C for short term storage and at -20°C for long term storage.

2.2.1.15 RT-PCR

Reverse transcription polymerase chain reaction (RT-PCR) is a technique used to amplify minute amount of specific DNA sequence. This technique utilizes DNA polymerase enzyme (often Taq polymerase) together with specific primers and single nucleotides to produce complementary copies of the template DNA. The reactions take place in different temperature conditions – heating to denature DNA strands, decreasing temperature to allow primers to anneal to DNA, optimum temperature to allow enzyme to extend the primers – with repeated cycles to amplify the amount of DNA. REDTaq® ReadyMix™ PCR Reaction Mix supplied by Sigma-Aldrich was used in this technique. The REDTaq ReadyMix is a ready-to-use mixture of Taq DNA polymerase, 99% pure deoxynucleotides, reaction buffer, and an inert red dye in a 2x concentrate. With the red dye already added in the ReadyMix, the PCR products can be loaded directly onto an agarose gel without having to add loading/tracking dye prior to electrophoresis.

Protocol

The cDNA prepared in Section 2.2.1.14 at a concentration of 50 ng/µl was used in this procedure. A volume of 50 µl reaction mixture was prepared in a 200 µl PCR tube. Primers used for RT-PCR are as shown in Section 2.1.9. E2A exon 12 and E2A exon 13 are forward primers while the reverse primer is HLF exon 4. 25 µl REDTaq ReadyMix was mixed with 1 µl of 50 µM forward primer, 1 µl of 50 µM reverse primer, 1 µl template cDNA and 22 µl water. The mixture was mixed well, centrifuged to collect the components in the bottom of the tube and run for PCR in an optimized thermal condition. The reactions mix was run for initial denaturation at 94°C for 5 minutes followed by 35 cycles at denaturing temperature at 94°C for 30 seconds, annealing temperature at 56°C

for 30 seconds, and elongation step at 72°C for 1 minute. The final step was elongation at 72°C for 15 minutes.

2.2.1.16 Agarose Gel Electrophoresis

To determine the bands of amplified genes, the PCR products were run on agarose gel by electrophoresis. 2% agarose gel was prepared in a conical flask by adding 2 g of Agarose (Sigma) into 100 ml 1x TAE buffer prepared as in Section 2.1.4. Gel was prepared in a mould with the desired number of wells. PCR products were pipetted into the wells and gel was run by electrophoresis in 1x TAE buffer for 60 minutes at 80V. Gel was later viewed for bands produced under UV light in a dark chamber using the GelDoc system.

2.2.1.17 Real-time PCR

Real-time quantitative PCR (qPCR) was developed to monitor DNA amplification as it occurred with data collected throughout the reaction. The specific DNA product from the target sequence is detected as it accumulates (Figure 2.1). The first PCR product is detected in the early exponential phase and the product doubles during every cycle in the Log-linear phase. The cycle threshold (Ct) is determined during this phase where the Ct is the number of cycles required to meet a predefined threshold. In this study the TaqMan™ (Applied Biosystems) was used. This technique uses a probe with fluorogenic label which binds to the target sequence. The probe is tagged with a high energy reporter dye fluorescein (FAM) at the 5' end, and a low energy quencher dye (TAMRA) at the 3' end. When FAM is excited by the light source, instead of emitting fluorescence it transfer the energy to TAMRA through fluorescence resonance energy transfer (FRET).

In this technique, the TaqMan Universal Master Mix was used in preparation together with NR3C1 forward and reverse primers and NR3C1 probes for the target gene which were designed using Primer Design program earlier by Marian Case from Julie Irving's group. The control gene uses ATP10A forward and reverse primers and a probe, which were available from Applied Biosystems. Genomic DNA was isolated from blasts collected from highly engrafted spleen of mice in xenograft experiment.

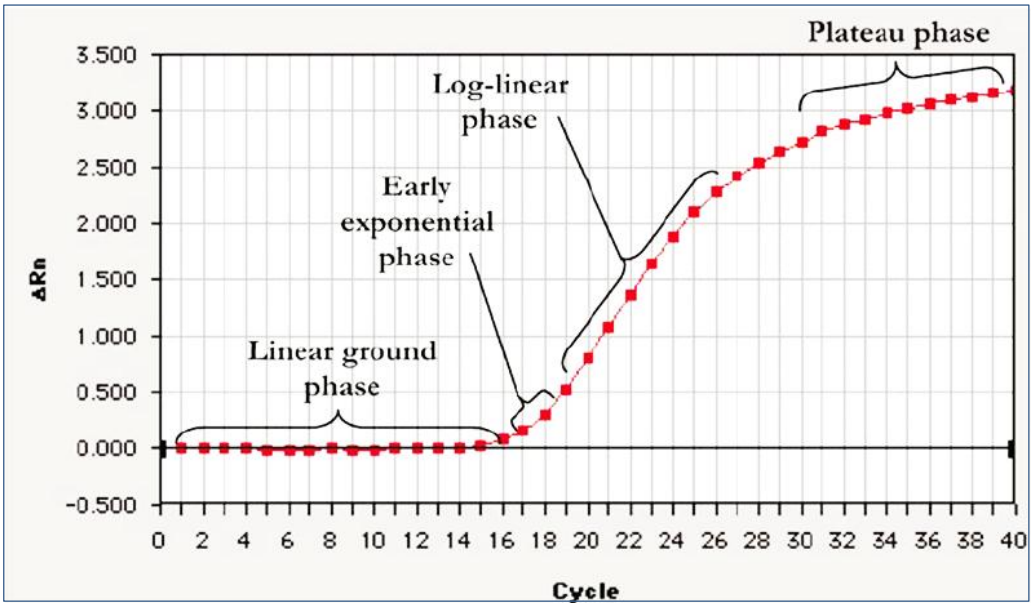

Figure 2.1 Phases of the PCR amplification curve. The PCR amplification curve depends on the accumulation of fluorescent emission at each reaction cycle. Rn is the intensity of fluorescent emission of the reporter dye divided by the intensity of fluorescent emission of the passive dye. ΔRn represents the magnitude of signal generated during PCR. (Adapted from www.dorak.info/genetics/realtime)

Protocol

Reactions were carried out in 384-well plates. The total reaction volume for each well was 10 µl. Each reaction was performed in triplicate on each plate. The reagent mixture for each sample is as summarized below. Volumes of reagents have been optimised by Marian Case previously and the same concentrations were used as this in house protocol.

	Volumes required per well (µl)	
Reagent	**NR3C1**	**ATP10A**
Taqman MMix	5	5
DNA 25 ng	1	1
Forward primer	1.8	0.375
Reverse primer	0.6	1.125
Probe	0.45	0.4
Water	1.15	2.1
Total volume	10 µl	10 µl

Plates were spun at 1,500 rpm for 1 minute in a 4K15 centrifuge (Sigma) to remove air bubbles trapped in the well. The plates were run on a 7900 HT-RT-PCR system (Applied Biosystems) with the SDS software. The qPCR was run by commercial thermal cycling for activation of Taqman Mastermix at 50ºC for 2 minutes, initial denaturation at 95ºC for 10 minutes, 40 cycles of 95% for 15 seconds and annealing and extension at 60ºC for 1 minute.

The results were analysed using the SDS 2.2 software (Applied Biosystems). Amplification plots were generated for each well with the plots for magnitude of signal (ΔRn) versus number of cycles. The unknown (target gene NR3C1) results were normalized against the control ATP10A results. The unknown values were calculated relative to the standard curve.

2.2.1.18 Fluorescence *In Situ* Hybridization (FISH)

Preparing cells for analysis

Fluorescence in situ hybridization (FISH) was performed on cells from the highly engrafted spleens from xenografts of L707 presentation, relapse and mixed populations of the cells in the treated and non-treated groups. Thawed viable cells were made into cell suspension following methods used previously in sections 2.2.1.3 and 2.2.1.4. 10 ml of 0.75 M KCl was mixed in the suspension and incubated for 15 minutes in a 37ºC incubator. The suspension was then centrifuged at 1,500 rpm for 7 minutes and supernatant was removed, pellet was resuspended by vortexing in 1 ml of fresh Methanol:Acetic acid (3:1) fixative added drop by drop to avoid cells clumping. A volume of 10 ml fixative was added and this was then centrifuged at 1,500 rpm for 7 minutes. Supernatant was discarded and cell pellet was suspended in 1 ml of fixative. Approximately 3 µl of cells were pipetted and dropped onto slides with 2 – 3 drops per slide. Cells were left to air-dry prior to FISH probing. Cells in fixative were stored in –20ºC for future use.

Preparation of probes

Probes for labelling the target gene and a control gene in an unaffected region, both on chromosome 5, were selected from lists of available probes from the *Ensembl* website (Figure 2.2). The BAC (Bacterial Artificial Chromosome) clones of the RP11-92B6,

RP11-790H4, RP11-614D16, RP11-320G11 (Chr5-32k-2P22) and RP11-1259L22 probes were purchased from Roswell Park Cancer Institute (Buffalo, New York, USA). To prepare the probes for FISH analysis, initially Luria-Bertani (LB) agar plates and broth were prepared supplemented with 12.5 µg/ml Chloramphenicol. The supplied probes were cultured separately on the LB agar plates and were incubated overnight in a 37ºC incubator. Following this, single colonies from each of the probe cultures were picked and precultured in 3-5 ml LB broth for 8 hours, prior to a large 200 ml overnight culture in LB broth, incubated at 37ºC in an orbital shaker with 300 rpm shaking. The following day, the cultures were spun down at 5,000 x g for 10 minutes at 4ºC to pellet the plasmid, and the supernatant was discarded.

For purification of plasmid DNA, the Plasmid DNA Purification NucleoBond®Xtra Midi Kit (Macherey-Nagel GmbH & Co., Dūren, Germany) was used. By following the manufacturer's instruction, the plasmid pellet was resuspended in 16 ml Buffer RES (RNase added). Then equal volume of Buffer LYS was added and mixed thoroughly followed by incubation at room temperature for 5 minutes. To neutralize the lysis, 16 ml of Buffer NEU was added to the suspension and mixed by swirling to form precipitates. The suspension was centrifuged at 5,000 rpm for 15 minutes at 4ºC and the supernatant was transferred into a filter-column pre-equilibrated earlier with Buffer EQU. Column filter was washed with 5 ml equilibration Buffer EQU followed by 8 ml of Buffer WASH. The bound DNA was eluted by adding 5 ml elution Buffer ELU and the eluate was collected in 50-ml falcon tube. 3.5 ml isopropanol was added to the eluate to precipitate plasmid DNA. The mixture was mixed by pulse vortexing, incubated for 2 minutes at room temperature and centrifuged at 12,000 rpm for 30 minutes at 4ºC. Supernatant was discarded and the DNA pellet was purified with 2 ml 70% ethanol and centrifuged at 12,000 rpm for 5 minutes at room temperature. Ethanol was removed and the DNA pellet was dried at room temperature for 10 minutes before dissolving in 200 µl sterile distilled water. DNA was measured using Nanodrop for use in the next step. Probe DNA was kept at –20ºC for long-term storage.

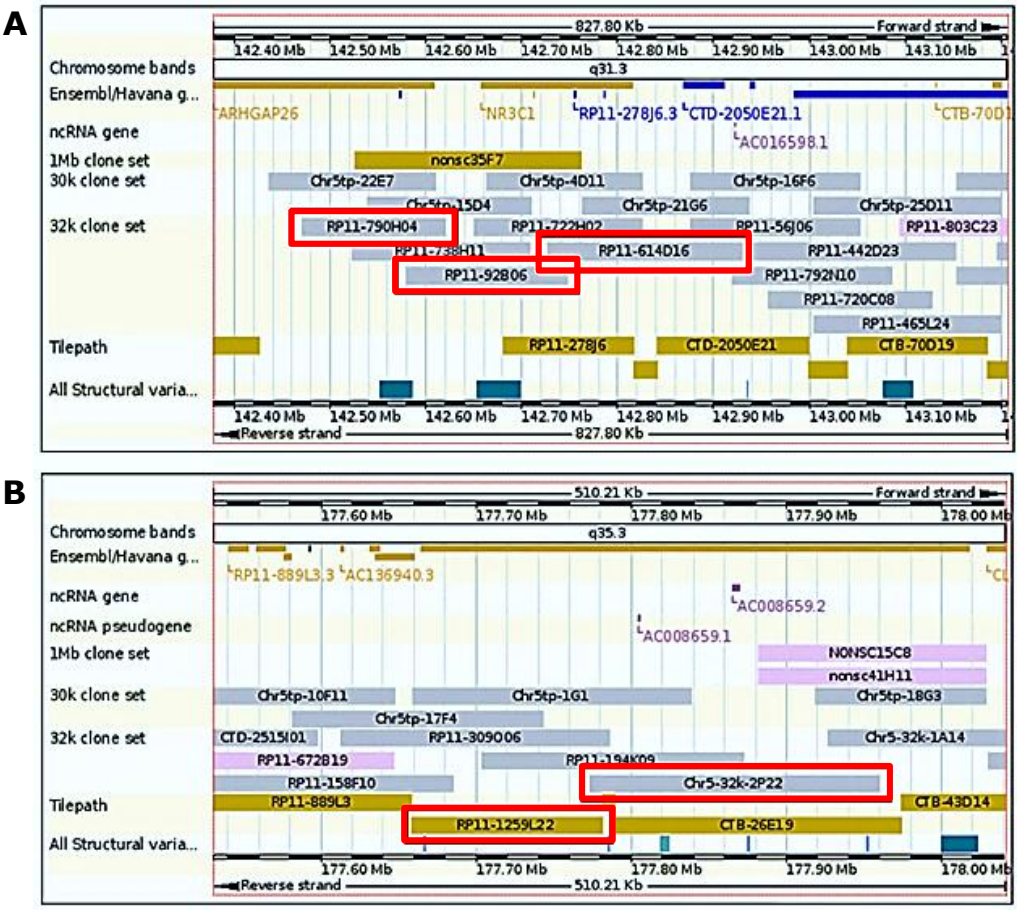

Figure 2.2 Selection of probes for genes labelling in FISH. *Ensemble* web page was used to select suitable probes covering the deleted targeted gene, *NR3C1* (A), a region in the q31.3, and control unaffected gene, (B), a region in the q35.1. Red boxes indicated selected probes.

Nick Translation protocol

In this protocol, probes for labelling target gene were labelled with spectrum green and probes for labelling control gene were tagged with spectrum red. These probes were prepared using Nick Translation Kit (Abbot Molecular Inc., Germany) which involves mixing of 10 µl dNTPs and 5 µl dTTP, 5 µl NT buffer, 2.5 µl dUTP spectrum red or green, 17.5 µl DNA of target gene probes and control gene probes and 10 µl NT enzyme. Following overnight incubation at 15ºC, labelled probes were mixed with 3 µl 0.5M EDTA, filtered through resin column, added 10 µl human cot-1 DNA, 6 µl of 3M sodium acetate and 160 µl ice cold ethanol and incubated. After incubation in –80ºC for 3 hours

and spun down, supernatant removed and pellet air dried, probes were resuspended in 14 µl hybridization buffer and 6 µl nuclease-free water then stored in –20ºC until used.

Performing FISH with labelled probes

Fixed cells were dropped onto slides and heated on a hot plate at 60ºC for 5 minutes. Three probes labelling the target gene, RP11-92B6, RP11-790H4 and RP11-614D16, labelled with spectrum green, and control gene probes, RP11-320G11 (Chr5-32k-2P22) and RP11-1259L22, labelled with spectrum red, were mixed equal volume each. Of this, 2 µl was used to hybridize each drop of cells and covered with round coverslip. Rubber glue was put around the coverslips and slides were incubated at 37ºC overnight. Following this, the rubber glue and coverslips were removed, slides were placed into a coplin jar with 0.4x SSC/0.3% NP-40 at 73ºC for 2 minutes then removed and placed into 2x SSC/0.1% NP-40 at room temperature for 2 minutes. Slides were then air dried in darkness, then 3 µl DAPI was applied to each drop and covered with a coverslip. The hybridized cells were visualized under a fluorescent microscope and red (R) and green (G) signals were counted in each cell. For each drop of cells, 100 cells were scored for the presence of the signal patterns: either 2R2G, 2R1G or 2R0G.

2.2.1.19 SNP6K Microarray Analysis

For microarray analysis of L707 presentation and relapse blasts, one vial of cryopreserved blasts from engrafted spleen were processed as the previous protocol (section 2.2.1.4) for labelling with CD19 human antibodies in combination with CD45 and TER119 mouse antibodies for exclusion of murine cells. CD19 cells were sorted by FACS cell sorting and DNA was isolated as previously mentioned. DNAs were sent out for microarray analysis by Vikki Rand. Raw data received were analyzed using Genome Console software.

2.2.1.20 Xenotransplantation of Leukaemic Cells

Animal work was approved and covered by project licence PPL 60/3846. Non-obese diabetic/severe combined immunodeficient IL2Rgamma^{null} (NSG) mice were used in all animal studies unless otherwise mentioned. Animals were housed in the Comparative Biology Centre (CBC) of Newcastle University, where all experimentation with live animals was carried out.

Animal preparation and intrafemoral leukaemic cell transplantation

To prepare the animals for implantation of leukaemic cells, mice were anaesthetized with an isoflurane/oxygen gas mix (25% isoflurane and 0.5 l O2 per minute) and 50 ng carprofen (Rimadyl, Pfizer) per 10 g body weight was injected subcutaneously as an analgesic. All leukaemic cell samples were injected into the right femur of NOD/scid mice. The femur was punctured with a 27G needle and sample volumes up to 30 µl were subsequently injected with a 0.5 ml (30G needle) insulin syringe.

Primary cells – L707 presentation and relapse cells

One vial each of frozen stocks of L707 presentation and relapse cells were thawed in a waterbath at a temperature of 37ºC. Cells were transferred to universals with 2 µl of medium and viable cells were counted using trypan blue exclusion method as described in Section 2.2.1.3. Medium was added to a 5 ml volume. Cell suspensions were centrifuged at 1500 rpm for 5 minutes and supernatant was removed. Cells were resuspended in an appropriate volume of medium for a 20 µl injection into each mouse with required cell numbers for xenotransplantation into NSG mice.

Mix population

For a competitive clonal repopulation study, mixtures of L707 presentation and relapse cells at different ratios were prepared. Frozen stocks of cells collected from the spleen of primary transplanted mice were used for this experiment. Each vial of presentation and relapse spleen cells were thawed at room temperature. Cells were transferred into universal tubes and 10 ml fresh medium RFh10 was added gently to the cell suspensions. Suspensions were centrifuged for 1500 rpm for 5 minutes. Supernatant was removed and pellet was resuspended in 5 ml medium. Cells were counted and calculated for different percentage mixture as shown in Table 2.2 below. Cell mix was prepared for experiments with 5 mice each and finally resuspended with medium for 20 µl transplants of 10^5 cells. Mixed cells in 1.5 ml centrifuge tubes were centrifuged for 1 minute at 3000 rpm. Supernatant was removed and cells were resuspended in fresh medium.

Percentage of cells		Cells ratio
Presentation	Relapse	
100	0	10P:0R
90	10	9P:1R
70	30	7P:3R
50	50	5P:5R
30	70	3P:7R
10	90	1P:9R
0	100	0P:10R

Table 2.2 Percentages for mixture of cells in different ratios for transplantations.

2.2.1.21 Fluorescence-Activated Flow Cytometric Analysis of Retrieved Cells

FACS analysis was performed using antibodies purchased from BD Pharmingen Research Products (San Diego, Calif.). Specific antibodies used for common human B-ALL cells were as follows: anti-CD10 (fluorescein isothiocyanate-conjugated), anti-CD19 (phycoerythrin-conjugated), anti-CD20 (peridinin-chlorophyll protein-Cy5.5-conjugated) and anti-CD34 (allophycocyanin-conjugated). Mouse antibodies used to label mouse cells and mouse erythrocytes were anti-CD45 (phycoerythrin-Cy7-conjugated) and anti-TER119 (phycoerythrin-Cy7-conjugated) respectively.

One million cells from thawed stocks of tissue suspensions (refer to section 2.2.1.4) were aliquoted into FACS tubes. Cells were washed with PBS twice. Supernatants were removed and cells were resuspended in 100 µl PBS. Mixture of antibodies was added to each sample: 10 µl CD10, 10 µl CD19, 10 µl CD20, 2.5 µl CD34, 2.5 µl CD45 and 2.5 µl TER119. Mixtures were incubated for 20 minutes in the dark with occasional vortex for mixing. After 20 minutes, antibodies labeled-cells were washed twice with PBS and resuspended in 500 µl for analysis using FACS Canto II machine with the FACS-Diva v6.1.2 software.

2.2.1.22 Survival Analysis

Survival curves of the mice engrafted with leukaemic blasts were analysed using Kaplan-Meier method. Data used were number of days the xenografted animals survived before succumbing (endpoint) to the disease. Data were plotted as a percentage of mice surviving against number of days elapsed.

2.2.2 Methods Chapter 4

2.2.2.1 Restriction Digest of DNA Sequence

Digestion of DNA sequence was performed to isolate specific target genes from vectors or plasmids in molecular cloning. Restriction enzymes used either produce a single cut or multiple cuts depending on restriction sites of the enzyme present in the vector. To linearize the vector or insert sequence, the same restriction enzymes were used to produce the same flanking overhang for the vector and insert. Digestion was performed by adding the appropriate buffer, restriction enzymes and DNA as recommended by Fermentas webpage. Digestion was performed at 37ºC for 1 hour and enzymes were inactivated by increasing the temperature to 80ºC for 20 minutes.

2.2.2.2 Gel Electrophoresis

Agarose gel electrophoresis was performed following the technique in Section 2.2.1.16. Agarose gel was prepared as 0.8% or 1% agarose in 1x TAE buffer depending on the size of vector. Whole volumes of the digested vector and insert were transfered into agarose gel wells and electrophoresis was run at 80V until clear cut separated bands were produced when viewed under UV light. The correct sizes of band for ligation were excised and put into 1.5 ml tubes separately.

2.2.2.3 DNA Purification by Gel Extraction

QIAquick Gel Extraction Kit (Qiagen) was used in this protocol. The kit was supplied with Buffer QG, buffer PE, Buffer EB, and QIAquick spin columns. To purify DNA of

fragments excised from agarose gel, the gel fragments were weighed in colourless 1.5 ml tube. 3 volumes of Buffer QG was added and gel slices were incubated at 50ºC for 10 minutes with 600 unit shaking or until the gel had completely dissolved. For DNA fragments < 500 bp or > 4 kb, isopropanol was added at 1 gel volume to increase the yield of DNA. The mixtures were transferred into QIAquick spin columns and centrifuged for 1 minute at 13,000 rpm to bind DNA to the membranes. Flow-through was discarded and 750 µl of Buffer PE was added to the column to wash the bound DNA. Columns were centrifuged at 13,000 rpm for 1 minute and the flow-through was discarded. Columns were spun for an additional 1 minute to dry the ethanol from the washing buffer off the membrane. 50 µl of nuclease-free water was used to elute the DNA from the membrane.

2.2.2.4 Ligation of DNA Sequence

To clone a fragment into a plasmid vector, several ratios of vector:insert DNA were used. Normally the ratios used were 1:1, 1:3 and/or 3:1 depending on the type of vector. The formula used for calculation of DNA required was as follows.

$$\frac{\text{ng of vector} \times \text{kb size of insert}}{\text{kb size of vector}} \times \text{molar ratio of insert/vector} = \text{ng of insert}$$

Protocol

T4 DNA Ligase (Promega) was used in this ligation technique. Typically, ligation reactions use 100-200 ng of vector DNA. To insert a 500 bp insert into a 3 kb vector in a 1:1 ratio, for a preparation of 10 µl ligation volume, reaction mixture assembled 1 µl of 10x Ligase buffer, 1 µl of 100 ng vector DNA, 1 µl of 50 ng insert DNA, 1 µl of 1unit/µl T4 DNA Ligase and 6 µl of nuclease-free water. The ligation mix was incubated at 12ºC overnight. Some modifications were made in preparing the ligation mixture and incubation temperature and duration depending on the success of the following steps in cloning.

2.2.2.5 Transformation of Competent Cells

For transformation into competent cells using heat shock technique, 10 µg of the lentivector clone DNA or 6-8 µl of ligation reaction mix was added to bacterial strain JM109 or Stbl2 with no preference. After 10 minutes incubation on ice, the cells was incubated in 42°C water bath for 50-60 seconds and immediately immersed into ice for 2 minutes. 900 µl SOC medium prepared as in Section 2.1.9 was added to the cells and incubated at 37°C with vigorous shaking for 1 hour. The transformed competent cells were spread onto agar plates supplemented with 100 µg/ml Ampicillin. Agar was incubated overnight (16-20 hours) in 37°C incubator.

2.2.2.6 Expansion of Cloned Plasmids

Single colonies of transformed clone were inoculated overnight (16-20 hours) in 5 ml of Luria-Bertani broth (refer to Section 2.1.9). The following day, 2 ml of the cultures were processed for isolation of DNA using Qiagen Miniprep Kit. The DNAs were digested with compatible restriction enzymes for confirmation of lentivector clones with inserted sequence. The remainder of the overnight culture from the confirmed lentivector clone was cultured in 200-250 ml Luria-Bertani broth for maxiprep preparation with endotoxin-free Qiagen kit.

2.2.2.7 Extraction of Plasmid DNA

For large volumes of endotoxin-free plasmid DNA extraction from cultured broths, EndoFree Plasmid Maxi Kit (Qiagen) was used. Cultured broths were transferred into several 50-ml polypropylene tubes for easy handling. Bacterial cells were harvested by centrifugation at 6000 x g for 5 minutes at 4ºC. Bacterial pellets were resuspended in 10 ml Buffer P1. 10 ml Buffer P2 was added and mixed gently by inverting tubes 4-6 times before incubating the blue viscous lysate at room temperature for 5 minutes. 10 ml of chilled Buffer P3 was added to the lysate and was mixed immediately by inverting the tube gently for 4-6 times to produce fluffy white precipitates containing genomic DNA, proteins and cell debris. Lysate was then poured into the barrel of a QIAfilter Cartridge with a screw cap nozzle and incubated for 10 minutes at room temperature. The plunger was inserted after the cartridge nozzle was uncapped and the lysate was filtered through

the cartridge into a 50-ml tube. Then 2.5ml Buffer ER was added to the filtered lysate and was mixed by inversion 10 times before incubating on ice for 30 minutes. During this time, a QIAGEN-tip 500 column was equilibrated by adding 10 ml Buffer QBT and allowing the column to empty by gravity flow. After incubation, the filtered lysate was applied to the QIAGEN-tip and allowed to flow through the resin by gravity. The QIAGEN-tip was washed twice with 30 ml of Buffer QC. 15 ml Buffer QN was added to elute DNA into a 30-ml endotoxin-free tube. 10.5 ml isopropanol was added to the eluate to precipitate DNA and centrifuged at 15,000 x g for 30 minutes at 4ºC. The supernatant was carefully decanted. The DNA pellet was washed with 5 ml endotoxin-free 70% ethanol and centrifuged at 15,000 x g for 10 minutes. The supernatant was carefully decanted and the pellet was dried for 5-10 minutes. The DNA was redissolved in a suitable volume of endotoxin-freeBuffer TE. This DNA is suitable to be used in cloning, direct transformation into competent cells, transfection and transduction if the DNA has a cloned lentivirus.

2.2.2.8 Hybridization and Ligation of Oligonucleotides

To generate a lentivirus vector harboring *Renilla luciferase* reporter gene and red fluorescence protein, a 10.2 kb lentivector pHR-SINcPPT-SIEW, a pRL-SV40 vector carrying a 947 bp *Renilla luciferase* gene, and a pcDNA3.1-mcherry(Zeo) vector with a 724 bp red fluorescence protein (mcherry) sequence in the backbone were used. To simplify the transfer of genes of interest, a 76 bp oligonucleotide containing a series of restriction enzymes was designed as shown in Table 2.3 below.

Sense and antisense of the oligonucleotides were hybridized at 95°C for 30 seconds in a heat block and then left to cool off gradually to room temperature in the block. The reaction mixture was prepared in a total volume of 100 µl, with final concentrations of 0.8x Buffer O (Fermentas), and 10 µM of each sense and antisense oligonucleotides prepared at the concentrations of 100 µM each. The annealed oligonucleotides were further diluted for ligation with the pBlueScript KS+ vector.

SacI – BamHI – Csp45I –N– XbaI – EcoRI –N– NcoI – BglII –N– MunI –N– SalI – XhoI

Restriction enzymes (RE)	**RE Sequence 5'– 3'**
SacI	G A G C T C
BamHI	G G A T C C
Csp45I	T T C G A A
XbaI	T C T A G A
EcoRI	G A A T T C
NcoI	C C A T G G
BglII	A G A T C T
MunI	C A A T T G
SalI	G T C G A C
XhoI	C T C G A G

Table 2.3 Designed oligonucleotides with series of enzymes. N represents random sequence of 4 nucleotides serves as insertion sites.

For ligating the hybridized oligos into pBlueScript KS+ vector, the vector was prepared by digestion with SacI and XhoI restriction enzymes for 1 hour at 37°C in a final volume of 20 µl. Reaction mixture was prepared as recommended by Fermentas for double digestion. The digested mixture was then run for gel electrophoresis with 1% agarose gel in 1x TAE buffer (tris-acetate-EDTA) and the expected band was cut out and purified using Qiaquick Gel Extraction Kit (Qiagen) following the protocol provided.

Ligation of annealed oligos and purified digested pBlueScript KS+ was prepared by mixing the reagents and DNAs as shown in Table 2.4 below. All reagents used were from Fermentas. Mixture was incubated for 3 hours at room temperature and 5 µl of ligation mix was used for transformation of JM109 competent cells. The protocol for transformation and subsequent steps were standardized and used as detailed in Section 2.2.2.5.

Reaction mix	Final concentration
10x Ligase Buffer	1x
10nM pBlueScript KS+ digested	2.5 nM
200nM oligonucleotide hybrid	10 nM
5U/µl T4 DNA Ligase	5U in 20 µl
dH_2O	-
Final volume	20 µl

Table 2.4 Mixture of reaction reagents for ligation of oligonucleotides and pBlueScript vector.

2.2.2.9 Blunt-ending

Blunting of DNA ends involves fill-in 5'-overhangs or/and removal of 3'-overhangs. T4 DNA Polymerase is a 104 kDa monomer enzyme and a template-dependent DNA polymerase in which it catalyzes 5'→3' synthesis from primed single-stranded DNA. The enzyme has 3'→5' exonuclease activity but lacks 5'→3' exonuclease activity. The T4 DNA Polymerase consists of DNA polymerase enzyme supplied in 20 mM potassium phosphate (pH7.5), 200 mM KCl, 2 mM DTT and 50% (v/v) glycerol, and 5x Reaction Buffer with a composition of 335 mM Tris-HCl (pH 8.8 at 25ºC), 33 mM $MgCl_2$, 5mM DTT and 84 mM (NH_4) SO_4.

Protocol

Five micrograms of DNA was linearized with appropriate restriction enzymes and compatible buffers in a 20 µl volume. The DNA was digested at 37ºC for 1 hour followed by heating up to 80ºC for 20 minutes to stop the reaction enzymes. The linearized DNA with overhang ends was blunt-ended by mixing 1 µg of the DNA with 4 µl of 5x reaction buffer, 1 µl of dNTP mix with 2 mM of each dNTP and 0.2 µl T4 DNA Polymerase. The reaction mixture was prepared in 20 µl volume with addition of nuclease-free water and incubated at 11ºC for 20 minutes. The reaction enzyme was inactivated by heating at 75ºC for 10 minutes. The blunt-ended DNA was ready for use for ligation in the cloning procedure.

2.2.2.10 Klenow Fill-in

Klenow fill-in technique utilizes the DNA Polymerase I Large (Klenow) Fragment (Promega) which consists of a single polypeptide chain (68 kDa) that lacks the 5'→ 3' exonuclease activity of intact *E.coli* DNA polymerase I. However, the fragment retains its 5'→ 3' polymerase, 3'→ 5' exonuclease and strand displacement activities. The 5'→ 3' polymerase activity of Klenow Fragment can be used in many applications, which include: (a) to fill-in 5'-protruding ends with unlabelled or labelled dNTPs; (b) to sequence single- or double-stranded DNA templates; (c) for *in vitro* mutagenesis experiments using synthetic oligonucleotides; (d) for cDNA second strand synthesis; (e) to generate single-stranded DNA probes. The 3'→ 5' exonuclease activity is used in experiments that require to generate blunt ends from a 3'-overhang. Klenow Fragment is active in many restriction enzyme buffers which is useful in which the fill-in reaction can be performed directly in the restriction buffer. In the cloning of pSLIEW lentivector, Chapter 4 utilizes the applications of Klenow Fragment for filling 5'-protruding ends in the presence of dNTPs in the reaction.

The Klenow Fragment kit consists of Klenow Fragment supplied in 50 mM Tris-HCl (pH 7.5), 1 mM DTT, 0.1 mM EDTA and 50% (v/v) glycerol, and Klenow 10x Buffer with a composition of 500 mM Tris-HCl (pH 7.2) 100 mM $MgSO_4$ and 1 mM DTT.

Protocol

Approximately 1 – 4 µg of DNA was digested with appropriate enzymes and buffers to generate 5'-overhang. The digestion was prepared in 20 µl volume and incubated at 37ºC for 1 hour. Restriction enzymes were inactivated at 65ºC or 80ºC depending on the enzyme following manufacturer's recommendation for 20 minutes. Klenow fill-in technique was performed directly in the digestion buffer. One unit of Klenow Fragment was used per microgram of DNA in optimal reaction conditions of 50 mM Tris-HCl (pH 7.2), 10 mM $MgSO_4$, 0.1 mM DTT, 40 µM of each dNTP and 20 µg/ml acetylated BSA. The reaction was incubated at room temperature for 10 minutes followed by heating the reaction at 75ºC for 10 minutes to stop the enzyme reaction.

2.2.2.11 Cell Culture Preparation

293T cells are embryonic kidney cells of fibroblast morphology and are highly transfectable with lentivirus system. These cells are also known as a lentivector producer cell line. For transfection purposes, early passages (not more than passage 20) of 293T cells are preferable for higher yield of provirus concentration. 293T are adherent cells cultured in DMEM media supplemented with 10% FCS.

To passage the cells cultured in 75 mm^2 flask, the culture medium was removed and PBS was added to the adherent cells to wash the remaining medium off the culture. The washing buffer was aspirated, 2 ml of 1x Trypsin was added and the culture flask was tapped vigorously to detach the cells from the surface. Approximately 5 ml culture medium was added to neutralize the trypsin reaction. The detached 293T cells were mixed in the flask by pipetting up and down to give a single cell suspension. Viable cells were counted by trypan blue exclusion method as detailed in Section 2.2.1.3 to prepare a culture with appropriate cell counts for transfection purposes.

2.2.2.12 Transfection of 293T Cells

293T cells were precultured in a 90 mm culture dish at 2 x 10^6 cells in 10 ml medium one day prior to transfection with lentivirus. Transfection procedures using lentiviral work was performed in the Level 2 Biosafety culture hood. Lentivirus was prepared by mixing 20 μg of lentivectors (pSLIEW or pSRLICW) with 5 μg of envelope plasmid (pMD2.G) and 15 μg of packaging plasmid (pCMVdelta8.91) into Hepes buffered water made up to 250 μl. The mixture was added to an equal volume of 0.5 M $CaCl_2$. The solution was then added by dropping slowly into 500 μl of 2x HeBS (0.28 M NaCl, 0.05 M Hepes, 1.5 mM $NaHPO_4$) with continuous bubble blowing with pipette in the other hand. The mixed solution was allowed to stand for 30 minutes at room temperature in the culture hood for $CaPO_4$ precipitates to form. After exactly 30 minutes, the final mixture was added dropwise to precultured 293T cells and was incubated overnight in 37°C with 5%CO_2 humidified incubator. The following day the culture medium was removed and cells were washed once with PBS gently before adding fresh medium and returning to incubator for another 3 days.

2.2.2.13 Concentration of Lentivirus

On the third day of 293T cell transfection in Section 2.2.2.12, medium with free lentivirus was collected from the culture into a 20-ml Sterilin tube and was centrifuged at 3000 rpm for 15 minutes at 4°C to pellet the debris. Supernatant was filtered through 0.45 µm Acrodisc Syringe Filter to removed remaining debris. The filtrate containing lentivirus was concentrated in polyallomer Konical tubes in an ultracentrifuge with swinging bucket, at 26,000 rpm for 2 hours. Supernatant was removed and the pellet was resuspended in 3 ml medium containing cells to be infected.

2.2.2.14 Transduction of ALL and AML Cell Lines

Cells to be transduced (SEM, RS4;11, Kasumi-1 or SKNO-1) were precultured a day prior to use. Cells were seeded at 2.0 x 10^6 cells per well in 6-well plates in 2 ml culture medium. 1 ml of concentrated lentivirus was added into each precultured cells and polybrene was added for a final concentration of 8 µg/ml. The plates were covered with parafilm and the cells were spinoculated at 1500 x g for 2 hours in 32°C condition. After spinoculation, the culture plates were incubated in CO_2-incubator and for an additional 24 hours. The following day, cells were collected, centrifuged and washed with medium once to remove unbound lentivirus and polybrene. Cells were resuspended with fresh media and cultured in new 6-well pates for 3-4 days before analyzing for expression signals with flow cytometry.

2.2.2.15 Evaluation of Transduced Cells by Flow Cytometry

500 µl of cultured-transduced cells were aliquoted into FACS tubes. Cells were washed once with PBS and resuspended in 1 ml PBS. Cells were tested using green channel for measuring the transduced and non-transduced cells in FACScan Caliber BD.

2.2.2.16 Sorting of gfp Cells

Aliquots of 10^7 transduced cells were spun at 1500 rpm for 5 minutes. Medium was removed and cell pellet was washed with PBS and spun again. Cell pellets were resuspended in 3 ml of PBS for sorting of gfp+ cells using green channel in

FACSVantage cell sorter. Gfp+ cells were sorted into 1 ml medium supplemented with 2% penicillin/streptomycin. Sorted cells were spun at 1200 rpm for 3 minutes and resuspended into 200 µl media with 1% penicillin/streptomycin. Cell suspensions were transferred into one well each of 24-well plate and left to recover from sorting. Proliferated cells were later transferred into appropriate well or plates.

2.2.2.17 Luciferase Assay

Luciferase assay was performed using the Luciferase Assay System (Promega). Approximately 10^5 of transduced cells were aliquoted into 1.5 ml tubes. Cells were spun at 13,000 rpm for 1 minute and supernatant was discarded. The cell pellets were washed with 500 µl PBS spun again. Supernatant was removed and cells were mixed with 50 µl 1x Reporter Lysis Buffer. Cells were then incubated at 37ºC for 10 minutes followed by freezing down at –80ºC for 20 minutes. The frozen cells were then thawed and resuspended well before aliquoting 10 µl into opaque lumi-plate (Wallac). 50 µl of substrate reagent was added prior to running plate in Scintillation/Luminometer Counter for luminescence count.

2.2.3 Methods Chapter 5

2.2.3.1 Growth Curve Study

Cells were grown in flasks (Corning) or multi-well plates (NUNC, Invitrogen). All cell lines used grew in suspension and were incubated at 37°C in a humidified incubators (IncuSafe, Sanyo) supplied with 5% CO2. All cell lines used in the experiments were routinely grown in their respective medium. SEM and Kasumi-1 were grown in RFh10, a RPMI 1640 media with Hepes modification (Gibco) supplemented with 10% fetal calf serum (FCS) and 200 µM L-glutamine. SKNO-1 was cultured in RFh20G, a RPMI 1640 media with Hepes modification supplemented with 20% FCS, 200 µM L-glutamine and 7 ng/ml GM-CSF. Cells were maintained and subcultured as described in Section 2.2.1.1.

Cell line	Morphology	Medium	Subculture	Doubling time	Source
SEM	round to polygonal single rather small cells in suspension, some cells slightly adherent	RFh10	every 2-3 days at 0.5 x 10^6 cells/ml;	30 hours	DSMZ No.: ACC546
Kasumi-1	round cells growing singly or in small clumps in suspension	RFh10	every 3-4 days; at 0.5 x 10^6 cells/ml	48-72 hours	DSMZ No.: ACC220
SKNO-1	round cells growing singly and in clumps in suspension	RFh20G	every 3-4 days; at 0.5 x 10^6 cells/ml; maintain at about 0.5-1.0 x 10^6 cells/ml	48-72 hours	

Table 2.5 Summary of morphology and maintenance of SEM, Kasumi-1 and SKNO-1 cell lines.

2.2.3.2 Animal Handling

Animals were handled according to the approved animal project licence. The immune deficient mice were kept in sterile conditions in a specialised room in CBC. Handling of animals was carried out in a laminar flow hood using aseptic techniques to avoid infections in these mice. Sterile food and water were provided ad libitum. Mice were regularly checked for any sign of distress or pain throughout the experiments. Painful procedures were handled under anaesthetic condition accompanied by analgesic (Carprofen) injection. Suffering animals were humanely killed.

2.2.3.3 Intraperitoneal Injection (i.p)

To administer i.p injection, the mouse was held by scruffing the loose skin at the nape of the neck and restraining the tail and the leg. A 26G needle was used to inject 150 µl of 30 mg/ml Rediject D-luciferin (XenoLight, Caliper, USA) into the lower quadrant (left or right) of the abdomen. It was acertain that the needle was within the peritoneal cavity before slowly injecting the luciferin, ensuring not to penetrate any internal organ. If there was a shot of blood coming through the needle, this indicated that the needle had entered an organ.

2.2.3.4 Intrafemoral Injection (i.f)

For i.f injection, the mouse fur surrounding the knee was shave and sterilized with ethanol. The knee was bent and held firmly. The femur was punctured on the upper part of the kneecap towards the femoral cavity with a 27G needle and the needle was removed without shifting the position of the puncture. Cells were transplanted by inserting a 0.5 ml

(30G needle) insulin syringe into the same puncture and volumes of up to 20 µl of desired cell concentrations were subsequently injected in to the femoral cavity.

2.2.3.5 Transplantation of Transduced Leukaemic Cells

Lentiviral infected cell lines, the SEM, Kasumi-1 and SKNO-1 cells, were stably maintained in culture for the procedure. Cells were prepared for transplantation into three mice each with 10^6 cells in every 20 µl injection.

Animals were anaesthetized and injected intraperitoneally with 150 µl/30 g body weight of 30 mg/ml D-luciferin (Caliper Life Sciences, USA) before putting the animals in the dark chamber for imaging. After imaging, animals were returned to the cage and monitored for regaining consciousness before returning the cage to the racks. Animals implanted with lentivirus labeled-cells were imaged weekly for the detection of luminescence emitted by transduced cells.

2.2.3.6 Bioluminescence Imaging

All imaging was done using IVIS® Spectrum Imaging System 100 Series (Caliper Life Sciences, USA). Images acquired were processed by Living Image® Software (Caliper Life Sciences, USA). For bioluminescence imaging, the imaging system requires a photographic image and bioluminescence image. In principle, the photographic image is taken in a grayscale mode whereas the luminescence image is in pseudocolor mode. In the overlay display mode, the pseudocolor luminescent image is displayed on the associated grayscale photographic image. The Living image software automatically coregisters the images to generate an overlay image. The luminescence image displayed in pseudocolor represents intensity of luminescence emission. A longer exposure time of the subject taken in darkness is required to capture low levels bioluminescence emission. When cells occur in tissue, photon emission from the tissue surface is called surface radiance (photons/sec/cm^2/sr). The in vivo IVIS Imaging System consists of cooled CCD (charge-coupled device) camera mounted on a light-tight specimen chamber (dark box), a camera controller, a camera cooling system and a Windows computer system for data acquisition analysis.

Prior to imaging for luciferase activity, transplanted mice are injected intraperitoneally with 150 mg/kg of 30 mg/ml Xenolight Rediject D-Luciferin (Caliper LifeSciences Inc., Massachusetts, US). Luciferin distributes quickly and easily throughout the animal and does not affect the animals deleteriously (no evidence of toxicological or immunological effects).

2.2.3.7 Processing Tissue and Specimen

Tissue specimens collected from terminated animals in the experiment include spleen, liver, kidney and tumour. The specimens are cut into 4-5 mm^3 pieces then passed through a 70 mesh tissue filter and washed with media into a 50-ml tube. Cell suspension was transferred into sterilin tube and centrifuged at 1,500 rpm for 5 minutes. Supernatant was removed and cells were suspended in freezing medium containing 90% FCS and 10% DMSO and aliquoted at 1 ml per cryovial. Cells were cryopreserved in liquid nitrogen for future use. Prior to centrifugation, cell suspensions were aliquoted at 100 µl into FACS tube for flow cytometry analysis.

2.2.3.8 Flow Cytometry Analysis of Retrieved Cells

FACS analysis was performed by labelling cells with specific antibodies for different cell lines. SEM cells were labelled with CD133-APC, Kasumi-1 cells with CD34-APC and SKNO-1 with CD38-APC in combination with mouse antibodies CD45 and TER119 conjugated with PE-Cy7 to exclude murine cells. Cells aliquoted from organs as described in Section 2.2.3.7 were washed with PBS twice. Cells were spun at 1,500 rpm for 5 minutes and the supernatant was removed. Cells were resuspended in 100 µl PBS. Mixture of appropriate antibodies was added to specific cells and was incubated for 20 minutes in the dark with occasional vortex for mixing. After 20 minutes, antibody labeled-cells were washed twice with PBS and resuspended in 500 µl for analysis using FACS Canto II machine with the software FACS-Diva v6.1.2.

CHAPTER 3

COMPETITIVE CLONAL REPOPULATION OF t(17;19) CELLS

CHAPTER 3

COMPETITIVE CLONAL REPOPULATION OF t(17;19) CELLS

3.1 Introduction

Non-random, somatically acquired chromosomal translocations are detected cytogenetically in approximately one-half of cases of childhood ALL. One of the major classes of these chromosomal translocations is those that create fusion genes and chimeric proteins that have structural and functional properties (Raimondi 1993; Hunger, Devaraj et al. 1994) such as those that encode transcription factors (Look 1997). Various types of chromosome translocation in ALL have been widely studied. One of such cases is the childhood ALL translocation t(17;19).

3.1.1 Translocation t(17;19)(q22;p13)

The translocation t(17;19) is a recurring chromosomal translocation that is rarely found (0.5-1%) in a subset of childhood B-lineage ALL (Ramanujachar 2009). This translocation results in an in-frame fusion of the 5'-region, amino-terminal transcriptional activation domains 1 and 2 of *E2A* gene on chromosome 19, and the 3'-region, the carboxyl-terminal DNA-binding and protein dimerization domains of leucine zipper and basic protein of *HLF* gene on chromosome 17. The fusion product, E2A-HLF chimeric protein, is associated with a poor prognosis (Hunger, Devaraj, et al 1994), and is responsible for the pathogenesis of t(17;19)-ALL in that it inhibits lymphoid precursor cells from going into apoptosis (Hunger, Devaraj, et al 1994; Takahashi, Goto, et al. 2001). In addition, the chimeric oncoprotein in its homodimeric form can bind directly to promoter/enhancer elements of downstream target genes and abnormally alter the expression for the growth, differentiation or survival of early B-cell progenitors and contribute to leukemogenesis (Inukai, Inaba et al. 1997).

To elucidate the mechanism by which E2A-HLF escapes the normal development pathway, Inaba et al. has shown that dominant-negative inhibition of E2A-HLF in transformed lymphocyte progenitors induces apoptosis (Inaba, Inukai et al. 1996). This suggested the E2A-HLF fusion protein increases the number of immature B-lymphocytes by preventing their death (Look 1997). Moreover, E2A-HLF blocks apoptosis in mouse

pro-B cells deprived of growth factor and inhibits p53-mediated apoptosis triggered by ionizing radiation (Inukai, Inaba et al. 1998). Additionally, the block of apoptosis imposed by E2A-HLF in pro-B lymphocytes depends critically on the transactivating regions of E2A (Dang, Inukai et al 2001) supported by functional transcription factor within HLF that promotes survival of the mutated cells (Ikushima, Inukai et al. 1997; Altura, Inukai et al. 1998).

3.1.1.1 E2A

E2A is an immunoglobulin enhancer binding protein which is also known as transcription factor 3 (TCF3). This gene is located on the short arm of chromosome 19 at band p13. The *E2A* gene is comprised of transcriptional activation domains 1 and 2 (AD1 and AD2) and basic helix loop helix (bHLH) coding region (Figure 3.1). Basically, the *E2A* gene is a member of the bHLH family. This gene encodes two alternatively spliced bHLH transcription factors, the E12 and E47 which is expressed in most cell types. These transcription factors act together in promoting the maturation of B-lymphocytes (Bain, Robanus-Maandag et al. 1994; Bain, Robanus-Maandag et al. 1997; Dang, Inukai et al. 2001). The transactivation domains AD1 and AD2 activate programmed cell death in normal cells.

In human leukaemias, *E2A* gene is found in two translocations. The t(1;19) which generates the E2A-PBX1 chimera, and the t(17;19) that generates the E2A-HLF chimera. Both translocations consist of the AD1 and AD2 transactivation domains of E2A fused to their respective translocated sites. Therefore, these fusion genes are considered as variants of each other (Inukai, Inaba et al. 1998; Dang, Inukai et al. 2001).

Figure 3.1 Schematic presentation of E2A gene which encodes the basic helix loop helix (bHLH) transcription factors E12 and E47 and contains transactivation domains (AD1 and AD2).

3.1.1.2 HLF

Hepatic leukaemia factor, also known as HLF, is a human gene normally expressed in liver and kidney but not lymphoid cells. This gene is located on the long arm of chromosome 17 at locus q22. The *HLF* gene encodes a member of the proline and acidic amino acid-rich (PAR) protein family, a subset of the bZIP transcription factors and contains a transcriptional activation domain (TAD) (Figure 3.2). The encoded protein forms homodimers or heterodimers with other PAR family members and binds sequence-specific promoter elements to activate transcription. The bZIP proteins are a major family of transcription factors characterized by a highly charged basic region which is responsible for DNA binding. An adjacent leucine zipper, the amphipatic α-helical domain, mediates protein dimerization (Inukai, Inaba et al. 1998). Chromosomal translocations fusing portions of this gene with the E2A gene cause a subset of childhood B-lineage acute lymphoid leukaemias. Alternatively spliced transcript variants have been described, but their biological validity has not been determined.

Figure 3.2 Schematic presentation of HLF gene consists of basic leucine zipper (bZIP) transcription factor which normally expressed in hepatocytes and, at lower level, in lung and renal cells but not in hematopoietic cells, prolin / acidic amino acid rich domain (PAR) and a transactivation domains (TAD).

3.1.1.3 Fusion Gene of *E2A-HLF*

As previously mentioned, E2A-HLF is rare occurring in less than 1% of all childhood B-ALL. It is associated with a poor prognosis and patients with t(17;19) abnormality are stratified as very high risk of early refractory relapse (Vora 2006). With the cytology of pro-B lymphocytes ALL and a precursor-B cell immunophenotype, the *E2A-HLF* fusion gene anomaly is characterized by expression of the surface markers CD10, CD19, TdT and HLA-DR. The morphology presents usually as a balanced translocation t(17;19)(q22;p13), however, in some unbalanced cases, the der(19)t(17;19) is observed. The *E2A-HLF* gene encodes 574 amino acids (Inaba, Roberts et al. 1992).

The hybrid gene involved a fusion between the amino terminal activation domains 1and 2 of E2A to the carboxyl-terminal leucine zipper and basic domain of HLF (Figure 3.3). The fusion gene encodes a chimeric transcription factor E2A-HLF with altered binding affinity. In leukaemic cell transformation, the chimera functions as an antiapoptotic transcription factor. The E2A-HLF oncoprotein disrupts signalling pathways that are normally responsible for cell death, allowing the cells to accumulate as transformed lymphoblasts (Inukai, Inaba 1998).

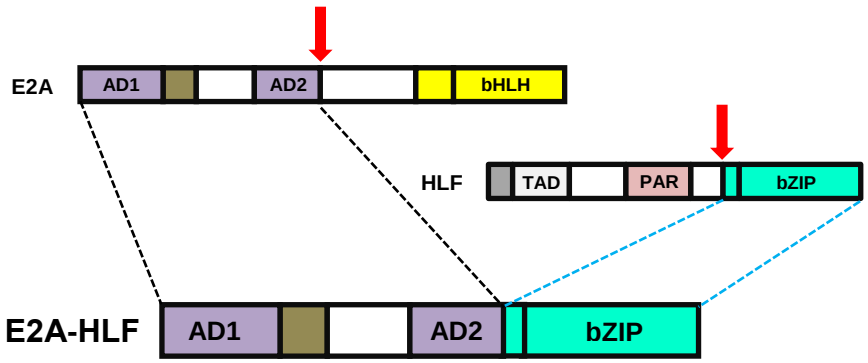

Figure 3.3 Schematic presentation of hybrid gene E2A-HLF created by fusion of transactivation domains (AD1 and AD2) of E2A from chromosome 19 (black dotted line) to the leucine zipper and basic domain (bZIP) of HLF from chromosome 17 (blue dotted line). Red arrow indicated breakpoint on chromosome 19 (E2A) and chromosome 17 (HLF) which generated the E2A-HLF chimera.

Breakpoints in fusion genes generally occur in non-coding introns of each gene. Alternative mRNA splicing joins the exons of the two genes together in the same reading frame, in which this fusion are translated into functional chimera (Hunger, Devaraj et al. 1994).

Two types of E2A-HLF has been described: whereas type 1 fusion is produced by a link between exon 13 of E2A and exon 4 of HLF with insertion of a cryptic exon known as joining region which maintain the open reading frame, type 2 fusion is generated by a link between exon 12 of E2A and exon 4 of HLF in the same reading frame (Figure 3.4) (Takahashi, Goto et al. 2001; Inukai, Hirose et al. 2007). The type 1 and type 2 E2A-HLF fusion proteins showed similar DNA binding activities but with a slight difference in the transcriptional activation properties analysed in *in vitro* assay (Hunger, Brown et al. 1994). This was thought may explain the distinct clinical differences between patients with these two types of t(17;19)-ALL (Takahashi, Goto et al. 2001). Additionally the type

1 E2A-HLF rearrangement is associated with disseminated intravascular coagulation (DIC) and type 2 rearrangements are associated with hypercalcemia (Yeung, Kempski 2006).

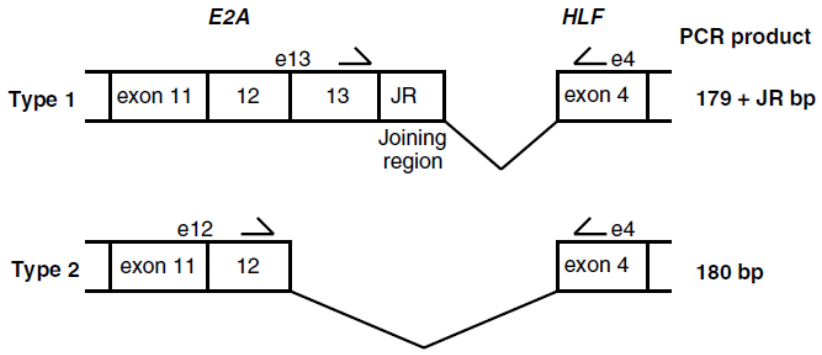

Figure 3.4 Schematic presentations of Type 1 and Type 2 of E2A-HLF fusion gene. Type 1 is generated by fusion between exon 13 of E2A and exon 4 HLF with insertion of joining region. Type 2 is generated by fusion between exon 12 of E2A and exon 4 of HLF. (Adopted from Inukai, Hirose et al. 2007).

3.1.2 *NR3C1* Gene

The *NR3C1* (nuclear receptor subfamily 3, group C, member 1) gene, or commonly known as glucocorticoid gene, encodes protein for glucocorticoid receptor (GR). This GR protein has two functions: (1) as a transcription factor that binds to glucocorticoid response elements (GRE) in the promoters of glucocorticoid responsive genes to modulate their transcription, and (2) as a regulator of other transcription factors (Rhen and Cidlowski 2005; Lu, Wardell et al. 2006).

As previously mentioned, the GR is typically found in the cytoplasm until it binds with ligand glucocorticoids (GCs), which induce transport of the GR into the nucleus. This protein can also be found in heteromeric cytoplasmic complexes along with heat shock proteins and immunophilins. It is involved in inflammatory responses, cellular proliferation, and differentiation in target tissues. Mutations in this gene are a cause of generalized glucocorticoid resistance.

3.1.3 Dexamethasone Treatment in Mouse Model of Childhood Leukaemia

A few studies have developed childhood ALL in vivo by xenograft in mice models and retrieved the engrafted cell for dexamethasone sensitivity assays in vitro (Bachmann, Gorman et al. 2005; Igarashi, Medina et al. 2005; Bachmann, Gorman et al. 2007). Although these studies could guide the in vitro growth inhibition assay, in this chapter, the in vivo blasts sensitivity to drug treatment requires other similar experimental evidence.

A number of studies have reported on established xenograft of childhood ALL in mouse models and assessment of their in vivo sensitivity to dexamethasone (Liem, Papa et al. 2004; Kang, Kang et al. 2007; Bhadri, Cowley et al. 2010; Bonapace, Bornhauser et al. 2010).

In Liem et al. study, tertiary inoculation of four cases of ALL blasts in NOD/SCID mice was treated with 15 mg/kg dexamethasone for 5 days a week for 4 weeks, when the engraftment reached 1% in peripheral blood. As a result, dexamethasone prolonged survival of mice in all four tested ALL blasts, although with different responsive capacity (Liem, Papa et al. 2004). Another study by Kang et al. used a combination of drugs, vincristine (0.15 mg/kg), dexamethasone (5 mg/kg) and L-asparaginase (1000 IU/kg) in secondary inoculation of patient ALL blasts at diagnosis and relapse in NOD/SCID mice. Treatment was given for four consecutive weeks on a 5 days per week basis. Combined with a small molecule (ABT-737) that inhibits antiapoptotic Bcl-2 family protein overexpressed in leukaemia, VXL treatment greatly delayed the progression of both diagnosis and relapse blasts in mice (Kang, Kang et al. 2007).

Bhadri et al. xenografted NOD/SCID mice with ALL blasts from a child with B-cell precursor ALL and injected dexamethasone at 15 mg/kg when engraftment reached more than 50% to investigate GC-induced gene expression. Thereafter they harvested blasts from spleen in serial durations within 0 to 48 hours and reported that at the 8 hour timepoint, gene set enrichment analysis showed significant upregulation of genes in the catabolic pathways and down regulation of genes in the pathways associated with cell proliferation (Bhadri, Cowley et al. 2010). In the same year, Bonapace et al. in their studies transplanted NSG mice with primary ALL blasts recovered from first xenotransplantation. Similar to the study by Kang et al., a significant delay in leukemia

progression was achieved when Bonapace et al. injected 5mg/kg dexamethasone into the secondary xenografted mice for 5 days per week for 3 consecutive weeks, in combination with a small molecule obatoclax that inhibits antiapoptosis Bcl-2 family protein (Bonapace, Bornhauser et al. 2010).

In this chapter, we selected NSG mice as a model for leukemia cell engraftment, which has been in practice in our group and for the reasons explained in chapter 5 (Section 5.1.1). NSG mice lack B, T and NK cells which give the advantage of xenotranplantion of human leukaemic cells without rejection or decreased engraftment compared to NOD/SCID mice. In addition, in one study the investigators engrafted HSC in NOD/SCID and NSG mice to compare the reconstitution capacity of the stem cells in both models. They reported that both NOD/SCID and NSG models adequately supported human HSC reconstitution and in vivo-selection in the primary recipient mice, but the NSG mice were far superior to the NOD/SCID model for secondary reconstitution (Cai, Wang et al. 2010). For glucocorticoid treatment, dexamethasone administration in mice was given following the work of Liem et al. who reported on survival of ALL-cell engrafted-mice. As part of the study within this chapter evaluates the survival of engrafted mice, the mice will be given 15 mg/kg dexamethasone for 4 consecutive weeks on a 5 day a week basis.

3.1.4 Case Study

In this chapter, the experiments performed were based on a single case with a matched pair of diagnosis (presentation) and relapse cells from the same patient. The 16 year old female patient was diagnosed with B-cell progenitor (BCP) ALL. Cytogenetic analysis confirmed that the patient presented with a t(17;19) with white blood count of $39.1x10^9$ cells/L. Cytogenetic analysis also confirmed that the patient had der(19)t(17;19), an unbalanced form of the translocation. The presentation karyotype of the patient was 46,XX,der(19)t(17;19)(q2?;p13)[12]/46,idem,fra(10)(q25)[17]/46,XX[1].ishder(19)t(17;19)(19ptel-,wcp17+,wcp19+,19qtel+) and the relapse karyotype was 46,XX,der(19)t(17;19)(q2?;p13)[5]. The patient was treated on regimen B of ALL2003 and achieved MRD (minimal residual disease) after 28 days. However, she suffered from relapse within 5 months from first diagnosis and despite treatment given (R3 and then FLAG) it was not possible to reinduce remission. The

patient developed encephalopathy and deceased post-intracranial bleed after 2 months of relapse.

This chapter details the xenograft of paired presentation and relapse blasts from this patient in NSG mice and evaluates the clonal expansion and progression of the disease by single as well as combinations of the blasts in various proportions. Dexamethasone was used to measure the effects on clonal expansion.

3.2 Results

3.2.1 Dexamethasone response in cell

3.2.1.1 Growth curves for cell lines

Growth curves of the cell lines were generated to determine the growth characteristic of the cells in vitro and to determine the optimal growth duration for the subsequent drug toxicity assays.

HAL-01, REH and PreB 697cell lines were cultured in their respective medium as described in Material and Methods Section 2.2.1.10, with initial seeding density of 0.5 x 10^6 cells/ml. Cell growth was counted daily for 7 consecutive days using trypan blue exclusion method as described in the Section 2.2.1.3, without changing of medium throughout the experiment. The characteristic growth curves obtained for the cell lines is shown in Figure 3.5, with each cell lines showing a lag, exponential and plateau phases.

All three cell lines showed a normal growth curves with a short lag phases followed by a long exponential phases and cells started to reach plateau phases after 96 hours (4 days) in culture. This was chosen as the optimal time for drug exposure in the following dexamethasone cytotoxicity assays.

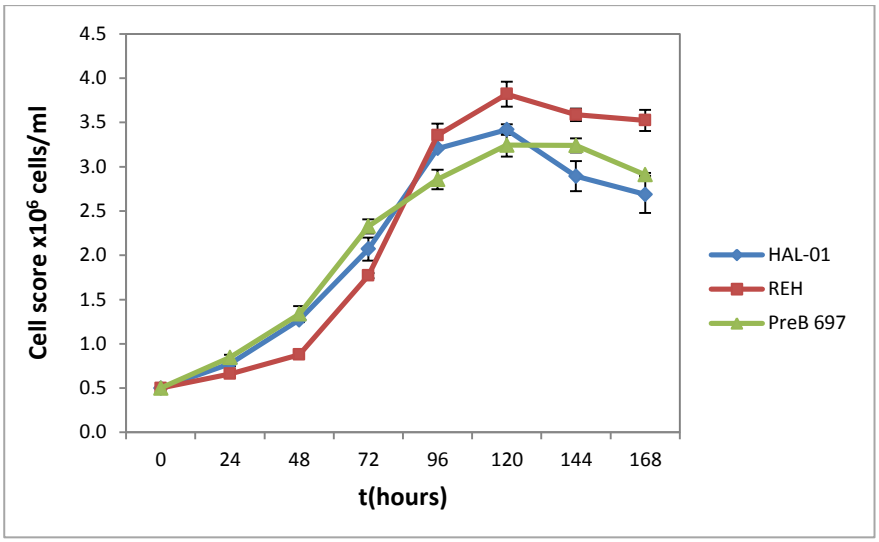

Figure 3.5 Growth curves of HAL-01, REH and PreB 697 cell lines. HAL-01 cell was grown in RPMI 1640 with Hepes modification medium supplemented with 10% FBS (v/v) and 2 mM L-glutamine (v/v). REH and PreB 697 cells were grown in RPMI 1640 medium supplemented with 10% FBS (v/v). Cells were seeded at 0.5 x 10^6 cells/ml at the start of experiment and cell growth was counted daily for 7 consecutive days using Neubauer hematocytometer counting chamber with trypan blue exclusion method as describe in *Materials and Methods*. The data presented are mean ± s.e.m of three independent experiments.

3.2.1.2 Growth inhibition by dexamethasone

To determine the glucocorticoid-sensitivity in the cell lines and the L707 presentation and relapse cells of t(17;19) studied in this chapter, dexamethasone cytotoxicity was carried out as described in Materials and Methods Section 2.2.1.10. Briefly, cells in exponential phase of the growth cycle were harvested and the viability of the cells prior to the assay was determined using trypan blue exclusion method as mentioned earlier (Section 2.2.1.3). In this experiment, cells were seeded in flat-bottomed 96-well plates in triplicates. For all cell lines, cells were seeded at a density of 1 x 10^5 cells/well while the seeding density for patient presentation and relapse cells from xenotransplantation were 1 x 10^6 cells/well. These seeding densities of cell lines and 'primary' patient cells were determined by Julie Irving's group earlier (Lindsay Nicholson 2008). All cell lines and the L707 cells were exposed to an increasing concentration of dexamethasone or a vehicle control (0.05% ethanol) for 96 hours as described in Section 2.2.1.9. The cells viability was measured using Cell Proliferation Assay WST-1 and data was calculated as a percentage of vehicle control-treated cells.

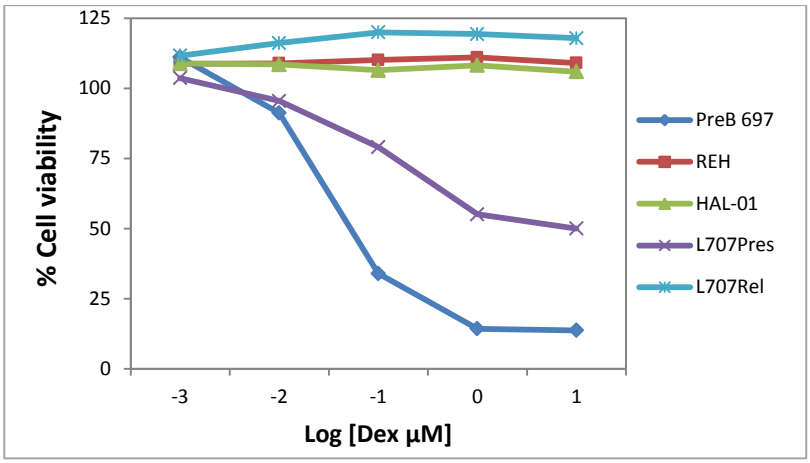

Figure 3.6 Growth inhibition by dexamethasone. The effect of dexamethasone on cell viability was assessed using Cell Proliferation Assay WST-1. The viable number of cells at each concentration of dexamethasone was calculated relative to vehicle control-treated cells. Data were presented as mean of at least two independent experiments.

The PreB 697 cell line is known to express high glucocorticoid receptor (Geng and Vedeckis 2011) while REH and HAL-01 cell lines have impaired express of the receptor (Bachmann, Gorman et al. 2007). Therefore, as expected, the PreB 697 cell line was highly sensitive to dexamethasone treatment in which REH and HAL-01 cell lines were resistant and had no response to (Figure 3.6). For the L707, presentation cells expressing glucocorticoid receptor were sensitive to dexamethasone treatment however, with less effective than the PreB 697 cell line whereas relapse with deletion on glucocorticoid receptor gene (explained in this chapter section 3.3.4) had no effect on the treatment.

3.2.2 Engraftment of t(17;19) in mice

3.2.2.1 Primary and secondary xenotransplantation of L707 into NSG mice

In order to understand the clonal expansions and kinetics of patients with t(17;19) malignancy *in vivo*, studies using xenograft mice model is the best way to elucidate this phenomenon. Mouse work experimentation was covered partially by grant no. LREC06/Q0906/79 and was under approved of R&D Project No.07/H0906/109, funded by Leukaemia and Lymphoma Research Fund and sponsored by The Newcastle upon Tyne Hospitals NHS Foundation Trust. Animals were housed and worked on in the

Comparative Biology Centre (CBC) of Faculty of Medical Sciences, Newcastle University.

Frozen cryopreserved stocks of match paired primary materials from the patient were obtained from Newcastle Haematology Biobank. The bone marrow samples were assigned as L707 presentation and relapse blasts. Viable cells were assessed by trypan blue exclusion method to determined number of cells to be transplanted in mice. The L707 presentation and relapse cell were pelleted and resuspended in appropriate volume of RF10 medium. Cells were implanted directly into the femur of 8–10 weeks old female NSG mice by intrafemoral injection (Figure 3.7). This orthotopic injection has been implemented in our group (Josef Vormoor's and Olaf Heidenreich's) because of the much improved engraftment since the cells are transplanted into their natural environment in the bone marrow. All transplantation work in this study was performed by Mike Batey and Klaus Rehe. Preparation of cells and animals for transplantation were as detailed in Materials and Methods Sections 2.2.1.20

Figure 3.7 Route of leukemic cell transplantation.
Intrafemoral injection (i.f) into a mouse femur.

Primary transplantation

From the cryopreserved bone marrow stocks supplied, viable patient primary material available were 6 x 10^5 presentation blasts and 4.5 x 10^6 relapse blasts. For primary transplantation, with available viable L707 blast cells, 20 µl of 2 x 10^5 presentation cells and 20 µl of 1.5 x 10^6 relapse cells were transplanted into 3 mice each to expand the cells excessively for modulation in future. The mice were monitored daily for progression of the disease. Unexpectedly, mice engrafted with presentation cells succumbed to the

disease earlier than those with relapse cells, despite the low number of cells initially transplanted. Mice xenotransplanted with presentation cells showed severe manifestation of the disease after 6 to 7 weeks, where all three mice in this group were lethargic and had total loss mobility of their hind limbs. They were humanely killed at day 43, 44 and 51. At week 8, mice implanted with relapse cells were severely engrafted when animals looked pale and were lethargic. All relapse mice had significant enlargement in the right legs, at site of implantation. However, other than difficulty moving the right leg due to this enlargement, mice engrafted with relapse cells did not show lost mobility of their leg compared to that displayed by mice engrafted with presentation cells. All 3 mice were killed at day 59 post xenograft. All animals were killed after consultations and as adviced by CBC Animal Care personel. Bone marrows from the femurs of all mice were flushed out and organs grossly showing infiltration were collected.

In both groups, the spleens of all the engrafted mice were noticeably enlarged, approximately 4-5 times from the normal size with weight ranging between 400 mg to 600 mg. The normal spleen was collected from non-transplanted mouse, weighing approximately 100-120 mg. In the relapse cell engrafted group, surprisingly mice showed infiltration of the ovaries, which was not seen in presentation cell engrafted mice. These organs appear whitish and rubber-like hard and with the size 5-6 times larger than the normal size. The ovaries and other possibly infiltrated organs including kidneys with white spots and gastric lining which appeared whitish in both groups (but not all mice), and the leg tumours in relapse mice were also collected for analysis. Organs were processed for immunophenotyping and cell suspensions aliquots were cryopreserved for future use.

Secondary transplantation

The subsequent secondary transplantation of the presentation and relapse L707 cells were also done by randomly selecting frozen stocks of bone marrow sample from primary engraftment. For both presentation and relapse L707 cells, three mice of each group were xenotransplanted with the same number of cells, 5×10^5 blast cells each. After 6 weeks post xenograft, mice with presentation cells were severely engrafted, showing similar conditions with the ones in primary xenotransplantation, with lethargy and loss mobility of hind limb. Mice in relapse group were engrafted and killed after 8 weeks and also

displayed similar conditions with the mice in primary implant except without leg tumour. This showed that the leg tumour seen in the primary relapse was due to excess cells implanted into the femur which was thought to overspill into the femoral cavity to the surrounding vicinity and overgrown as tumour. Bone marrow and spleens of these mice were collected for analysis and cryopreserved. Mice engrafted with relapse cells also had enlarged ovaries (not seen in presentation mice), which were collected as well. Other organs were not collected due to random infiltration of the blasts cells.

Another subsequent secondary transplantation was carried out using randomly selected cryopreserved spleen suspensions from primary engraftment. In this secondary transplantation, various combination ratios of presentation and relapse L707 cells were carried out to study the competitive repopulation of the clones, which is explained later in Section 3.3.5.

3.2.2.2 Morphology of engrafted cells

Blasts cells retrieved from bone marrow and spleen of primary engraftment were stained for morphological analysis as detailed in Materials and Methods Section 2.2.1.8, for comparisons with the patient primary biopsies (Figure 3.8). Initial patient presentation and relapse biopsies were stained and scored by Lynne Minto from Julie Irving's group. The biopsies showed high population of blast cells identified as large nucleus and ring of cytoplasm in which patient presentation biopsy was accounted for 99% blasts cells (Figure 3.8A) and relapse biopsy indicated 97% of blast cells (Figure 3.8B). For blast cells retrieved from xenograft bone marrow, however cytospin failed to produce good quality of cells for staining after several repetitions. This was abandoned due to preserving limited primary xenograft materials for subsequent xenograft purposes. Figure 3.8 C and D showed high population of match blast cells retrieved from engrafted spleens with similar morphologies to that of corresponding patient's biopsies.

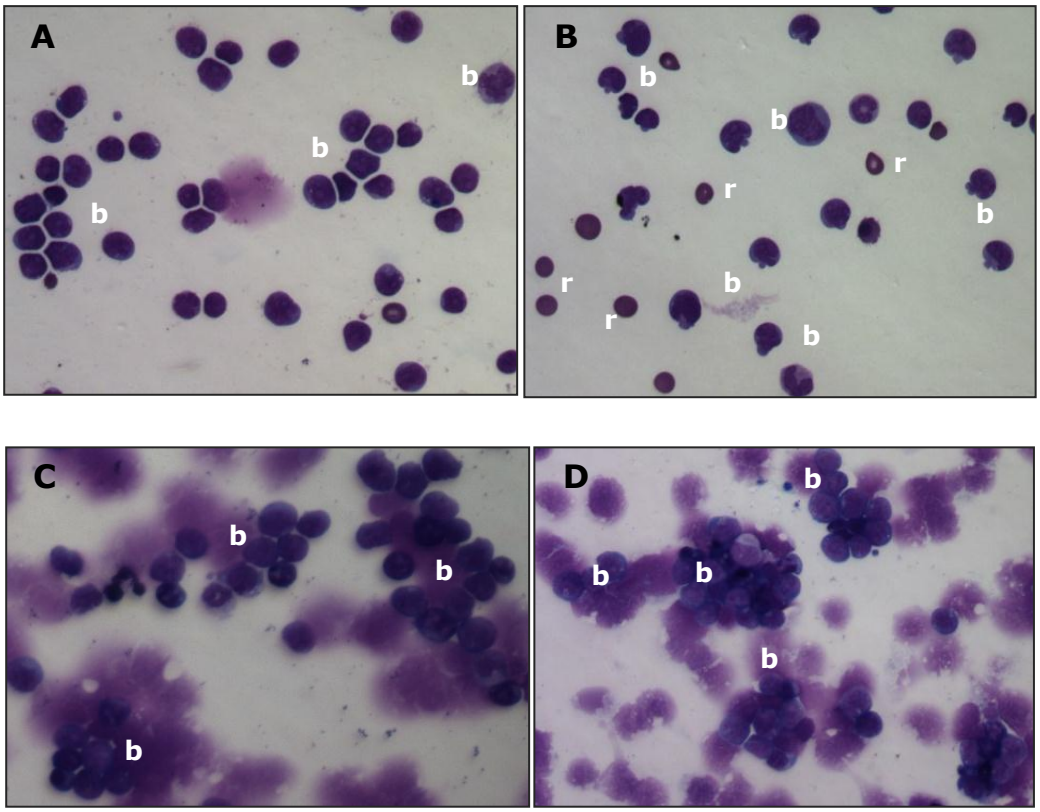

Figure 3.8 May-Grünwald-Giemsa stain of L707 blast cells. Patient bone marrow at presentation, A, with high blast cells accounted for 99%, and patient bone marrow at relapse, B, with blasts count of 97%. Presentation blasts in spleen of an engrafted mouse, C. Relapse blasts from spleen of an engrafted mouse, D. b = blast cell or group of blast cells; r = red blood cell in vicinity. 400x magnification.

3.2.2.3 Infiltrated organs

As mentioned in Section 3.3.2.1, the engrafted spleen and ovaries were enlarged compared to normal condition of the tissues. Figure 3.9 showed gross anatomy of the tissues mentioned. Whereas the normal spleen was small with healthy dark red colour, the enlarged spleen was 4 to 5 times larger measuring 25 mm x 8 mm and appeared paler and whitish indicating high infiltration of blast cells (figure 3.9 A and B respectively). The normal ovaries taken from control non-transplanted mice (Figure 3.9C) measuring approximately 2 mm x 2 mm were relatively smaller than the highly infiltrated ovaries which appeared white and measuring 7 mm x 9 mm (Figure 3.9D). Ovaries from the presentation mice were similar to those of control normal mice. Figure 3.9E showed uneven size of ovaries collected from mixed population studies. However, this phenomenon was only seen in three mice (8.6%) which was thought to be a random occurrence.

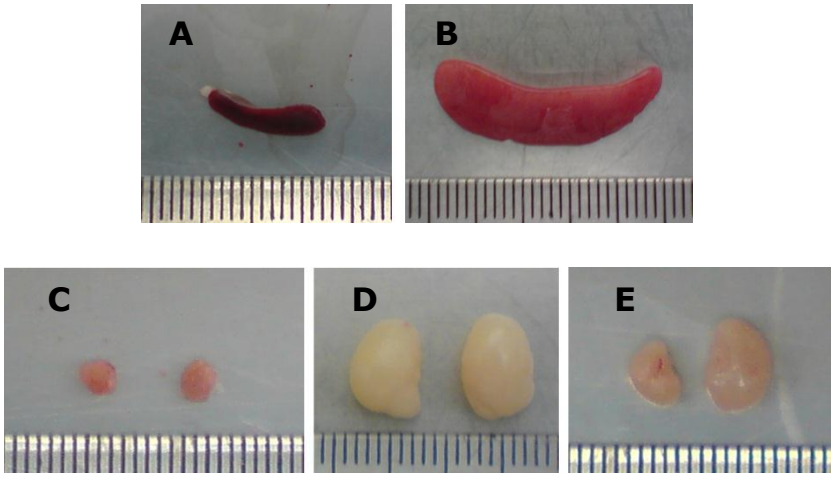

Figure 3.9 Infiltrated spleen and ovaries. Enlarged spleen and ovaries grossly noted in the blasts engrafted organs. (**A**) A normal spleen from a non-transplated mouse, and (**B**) an enlarged spleen which appears paler, which is similarly seen in both presentation and relapse engrafted mice. (**C**) Normal ovaries from a non-transplanted mouse, (**D**) evenly enlarged relapse ovaries and (**E**) uneven enlargement of ovaries collected from mouse engrafted with mixed population.

3.2.2.4 Immunophenotyping of engrafted cells by flow cytometry

Blasts cells retrieved from bone marrow, spleen and other infiltrated organs were labelled with conjugated human antibodies CD19-PE, CD10-FITC, CD20-PerCP-Cy5.5 and CD34-APC to determined immunophenotype of the blast cells. To distinguish and exclude mouse cells from human blasts, murine antibodies, CD45- and TER119-PE-Cy7, were added in combination with the human antibodies.

Flow cytometry analysis of presentation blasts retrieved from bone marrow and spleen were as shown in Figure 3.10. Human blast cells were gated out from mouse cells in the histogram graph and to ensure only human cells were counted for, this cell population was further purified in the dot plot graph by setting the threshold and gate on blast population (Figure 3.10 A and C). Dot plot graphs in Figure 3.10 B and D showed high populations of blast cells populating the bone marrow and especially highly depositing in the spleen. These dot plots graphs indicated the presentation blasts as high CD10 and CD19 expression, low or non-CD20 and non-CD34 expressing blasts.

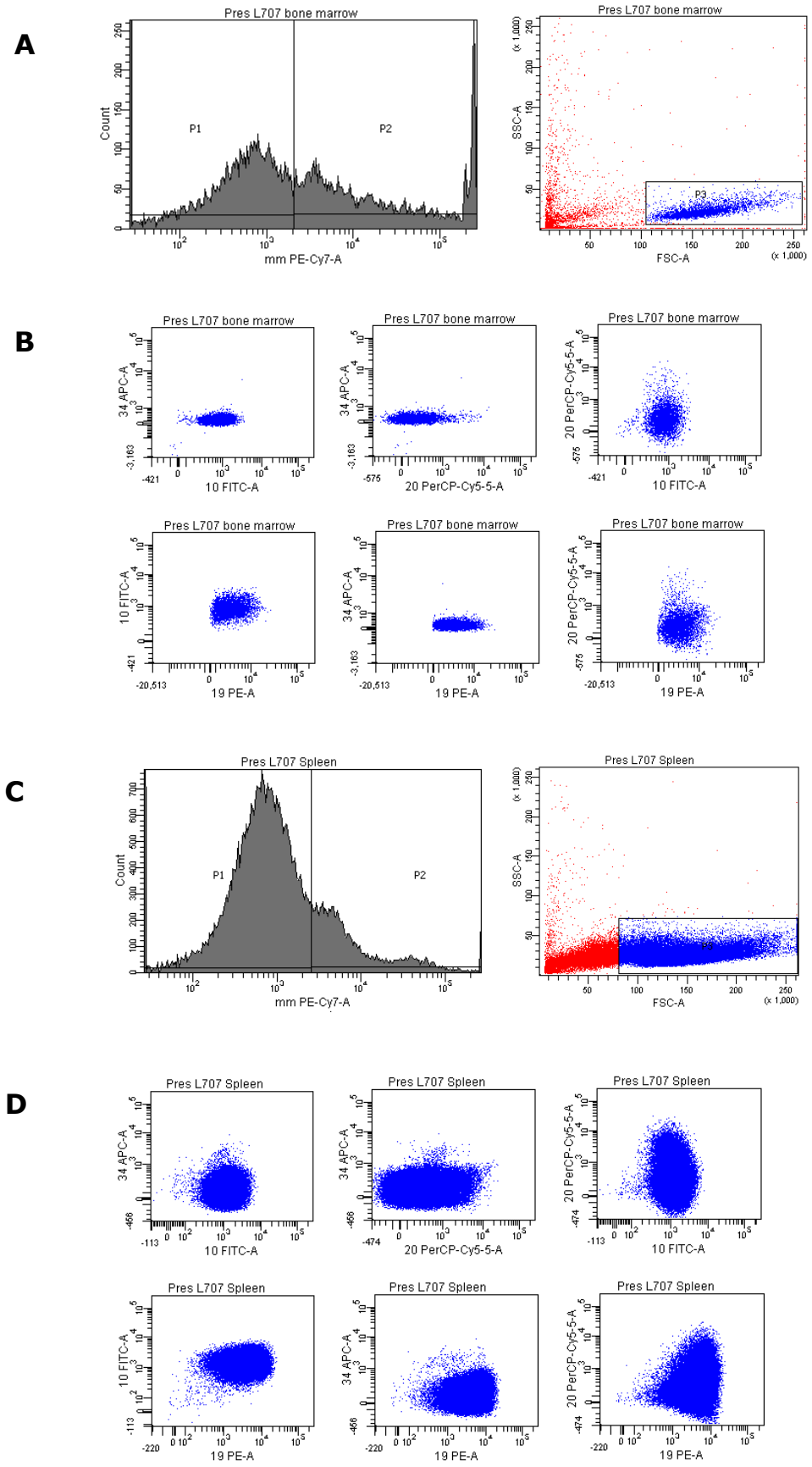

Figure 3.10 Flow cytometry analysis of engrafted L707 presentation blast cells. Histogram and dot plot graphs showed gating of the blast cells in bone marrow (A) and spleen (C). Dot plot graphs (B and D) showed blast cells were expressing CD10 and CD19, low or non-expressing CD20 and non expressing CD34.

Figure 3.11 showed flow cytometry analysis of relapse blasts isolated from the bone marrow and spleen of an engrafted mouse. Similar gating was applied as those with the presentation cells. Relapse blasts showed similar pattern of phenotypic markers as those with presentation blasts. This indicated the relapse cells had no changes immunophenotypically from presentation cells. Figure 3.11 B and D showed high populations of blast cells populating the bone marrow and infiltrating spleen of a xenografted mouse. Detailed percentages of blasts analyzed by flow cytometry are as presented in Appendix 1.

These flow cytometry analysis results were similarly seen in primary xenograft, subsequent secondary xenograft and secondary xenograft with mixed populations of the presentation and relapse cells. These flow analysis results distinguished the L707 blast cells with a typical $CD19^{+}CD10^{+}CD20^{-}CD34^{-}$ immunophenotype. In normal hematopoietic conditions, Rimsza et al. (2000) has stated that B-blast cells are CD34+, CD10+, CD19+ and CD20- (Rimsza et. al. 2000).

As mentioned in Section 3.3.2.1 and shown in figure 3.9 (D and E), ovaries of the relapse blast xenografts were persistently infiltrated with blast cells resulting in enlarged tumoric tissue. Mice xenografted with the primary relapse cells were presented with leg tumour, thickened and whitish gastric lining and pale kidneys. Flow cytometry analysis of cells isolated from these tissues was as shown in Figure 3.12. Histogram A and B showed high population of blast cells in the leg tumour and the ovaries with more than 95% of the populations were relapse blast cells. This clarifies our thought that the xenografted cells overfilled the bone marrow cavity and filled the surrounding cavity that produce tumour. The ovaries and the tumour were frozen and stored as high percentage of blast cells. Histogram C and D showed analysis of cells from kidneys with low infiltration and stomach lining with 80% blast cells infiltration. However, gastric lining infiltration was a random occurrence since subsequent xenotransplanted mice showed no similar findings.

All presentation cell xenotransplanted mice, as mentioned previously, had lost mobility of their hind limbs towards the end point. As this condition was thought to involve the CNS, the spinal cord distal to the brain stem of a mouse was removed. As expected, the spinal cord was affected by populating blast cells as shown in flow cytometry analysis in Figure 3.13. The populations in red in the dot plot graphs showed the blasts cells from the brain stem.

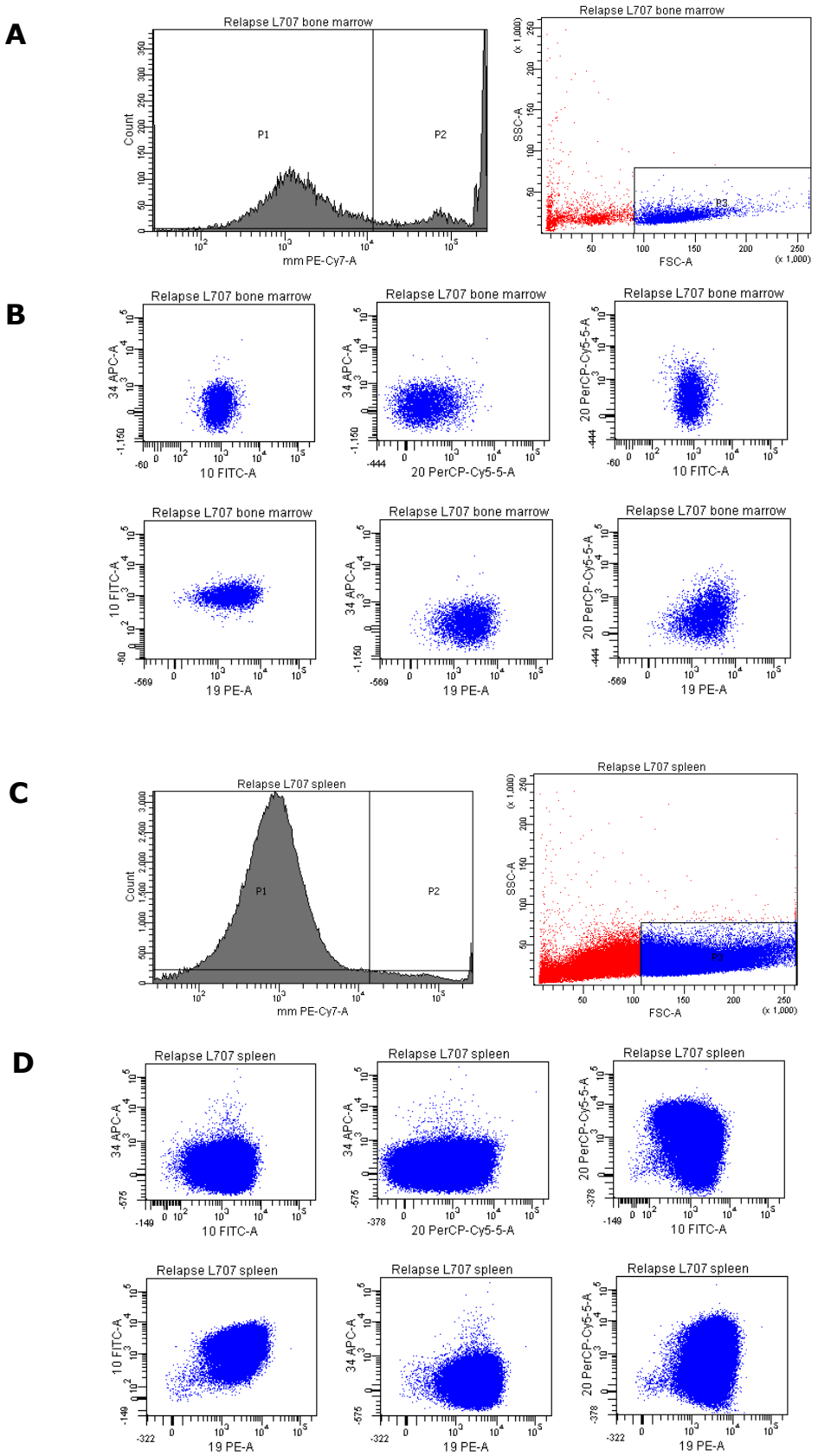

Figure 3.11 Flow cytometry analysis of engrafted L707 relapse blast cells. Histogram and dot plot graphs showed gating of the blast cells in bone marrow (A) and spleen (C). Dot plot graphs (B and D) showed blast cells were expressing CD10 and CD19, low or non-expressing CD20 and non expressing CD34.

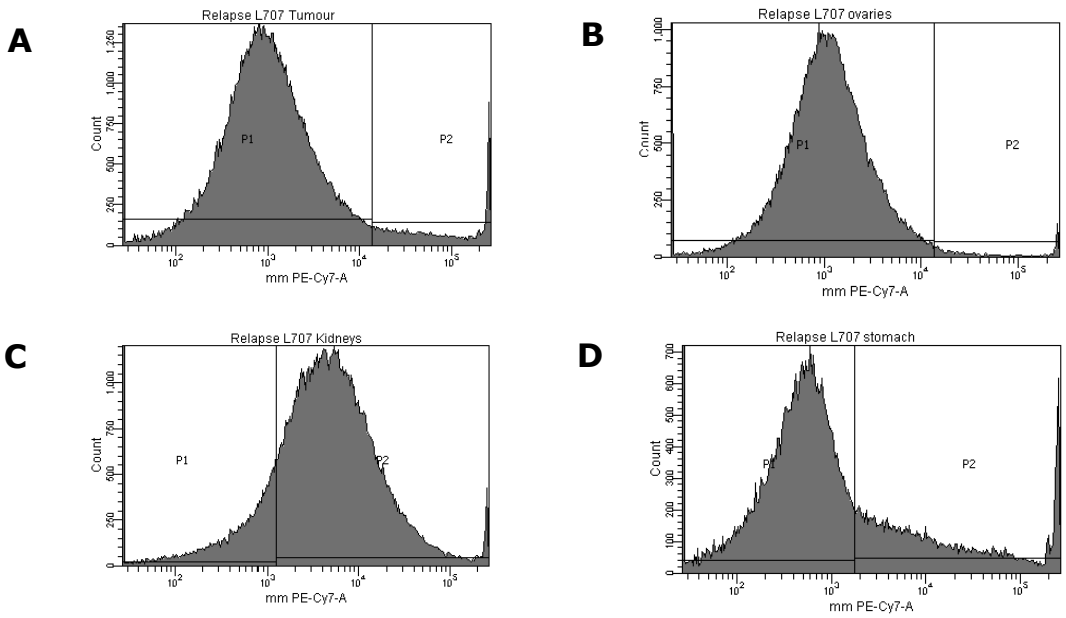

Figure 3.12 Flow cytometry analysis of infiltrated tissues in L707 relapse blasts engraftment. Analysis of relapse xenografted mice showed: High population of blast cells in leg tumour (A) and ovaries (B). Kidneys has low infiltration (C) and stomach lining has infiltration (D).

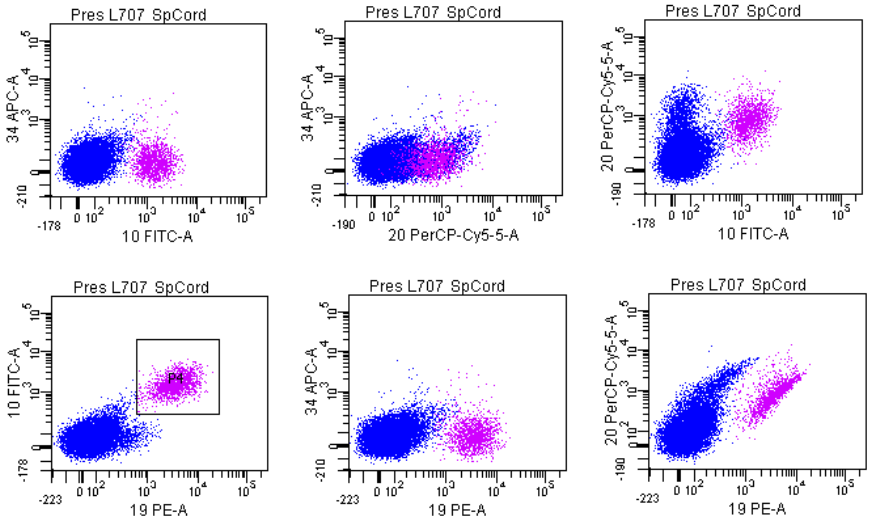

Figure 3.13 Flow analysis of L707 presentation infiltration in spinal cord. The presence of presentation blast cells (in purple) in spinal cord could explain condition of lost mobility in these mice.

3.2.3 Identifying type of t(17;19) fusion by RT-PCR

As Inukai et al. (2007) has reported, there are two types of E2A-HLF fusion in t(17;19) malignancy which involved either exon 13 of *E2A* fused to exon 4 of *HLF* (Type 1) or exon 12 of E2A fused to exon 4 of *HLF* (Type 2), as explained in the Introduction in this chapter. To identify the type of fusion the L707 bear, the techniques and protocol used by Inukai et al. were implemented.

RT-PCR was performed on complementary DNA (cDNA) of RNA isolated from patient L707 primary presentation (P pt) and relapse (R pt) cells and cells retrieved from xenografted mice (P and R) using the primers that were homologous to sequences in E2A exon 12 and exon 13, and HLF exon 4 as detailed in Materials and Methods Sections 2.2.1.12 to 2.2.1.16.

Figure 3.14 showed agarose gel analysis on the amplified gene with fusion between exon 13 and exon 4 (gel A) and fusion between exon 12 and exon 4 (gel B). Bands produced in gel A confirming that the L707 cells is a Type 1 t(17;19) malignancy. No band was produced in gel B with primers which was confirmed functional prior. HAL-01 cells (H) was used as a positive control since this cells was confirmed bearing the Type 1 fusion.

Although the L707 was confirmed having the Type 1 E2A-HLF fusion, there were three bands produced by the L707 cells differed from that of HAL-01 with only a single band was amplified. This was thought to be due to the joining region present within the fusion (refer to Figure 3.4). To confirm the fusion, excised bands were sent for sequencing (Gene Service, Cambridge). However, due to time constraint and limited time, Vikki Rand is continuing this work onwards.

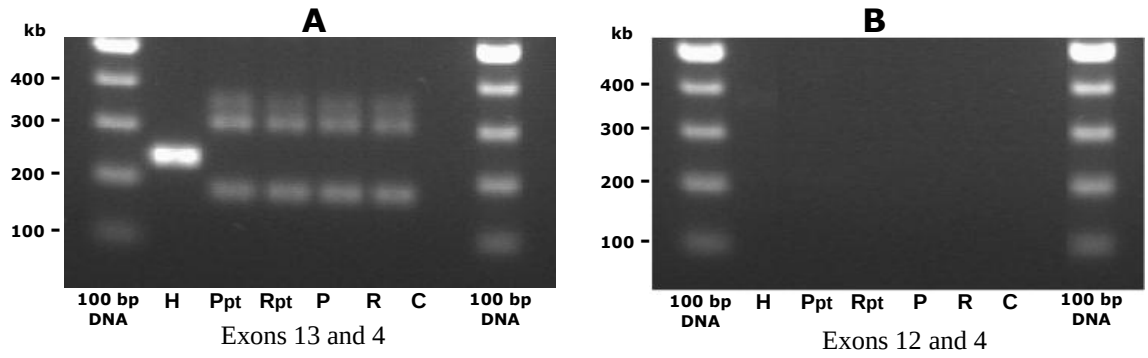

Figure 3.14 Representative analysis of RT-PCR amplification of *E2A/HLF*. Total RNA were isolated, cDNA were generated, PCR performed using primers of exons 4, 12 and 13. Primary presentation and relapse blasts from patient and corresponding mice engrafted cells were processed identifying L707/t(17;19) as Type 1. Primers from exon 13 or exon 12 of *E2A* and exon 4 of *HLF* were used. H, HAL-01 cell line; Ppt, presentation cells from patient; Rpt, relapse cells from patient; P, xenografted presentation cells; R, xenografted relapse cells; C, control without DNA

3.2.4 Genetic changes identification using Affymetrix SNP microarrays

Affymetrix microarrays platform is used in determining the copy number alteration in human whole genome. The paired L707 blast cells used in this chapter were subjected to the analysis.

DNA from paired primary presentation and relapse cells as well as the matching DNA from xenografts were isolated according to Materials and Methods Section 2.2.1.11. Presentation and relapse cells were labelled with human CD19 antibody sorted for CD19+ using FACS cell sorter (FACVantage). Figure 3.15 showed dot plot graphs of presentation cells (A) and relapse cells (B) sorted by the cell sorter FACS. Both cell populations were gated to exclude murine cells in the pre-sort graphs. Sorted cell were short run through FACS in post-sort graphs to confirm purity of sorted cells. DNA of the presentation and relapse cells were extracted and were sent for genotype analysis. This work was undertaken by Vikki Hall.

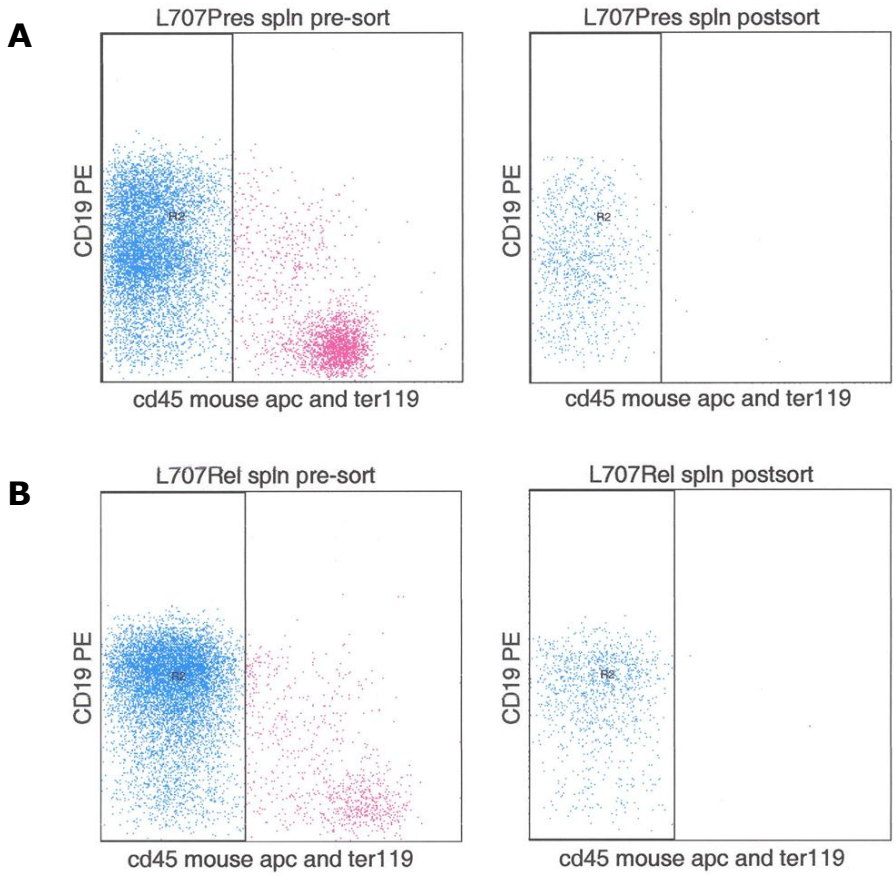

Figure 3.15 FACS sorting of CD19+ cells for microarray analysis. L707 presentation and relapse cells isolated from spleen from engrafted mice were processed and labelled with human anti-CD19 antibody in combination with murine anti-CD45 and anti-Ter119 as detailed in *Materials and Methods*. Dot plot graphs from FACS cell sorter shows pre-sort (left panel) and post sort (right panel) of presentation blast cells (A) and relapse blast cells (B). CD19-labelled blast cells were gated in the pre-sort to exclude mouse for sorting human blast cells population. Sorted cells were short run through FACS for confirmation of blast cells isolation.

Whereas the primary samples from patients earlier (in 2005) were hybridized on Affymetrix Human Mapping 500K Array Set according to the manufacturer's protocols (performed by Geneservices, Cambridge, UK), the matching xenograft DNA samples were hybridized on microarrays from Affymetrix Genome-Wide Human SNP Array 6.0 performed by Atlas Biolabs GmbH.

To analyse the data, Andy Hall and Vikki Rand carried out the analysis and provided the region of interest for this study. Raw intensity data from primary materials were analyzed using Affymetrix Genotyping Console v4.0 for quality control and Partek Genomic Suite v6.5 (Partek Incorporated) to determine paired DNA copy number alterations, the xenograft raw data were analyzed using Partek Genomic Suite v6.5 for copy number and

segmentation analysis. Regions of the aberration were mapped according to the human reference sequence GRCh37.

Figure 3.16 showed data processed using Affymetrix Genotyping Console v4.0 on chromosome 5. Results obtained showed a deletion occurred in this chromosome at 5q31.3–q32 in relapse cells (green histogram) which was not present in presentation cells (blue histogram).

Figure 3.17 showed comparison between dot plot data from array analysis on chromosome 5 between paired patient primary presentation and relapse blasts (A) and the matching xenografts data (B). The deleted region on relapse cells occurred from location 141.9 Mb to 143.6 Mb on the chromosome (C) as determined from the analysis software. The deleted location were run through *Ensembl* Human Genome Archive (Ensembl 54: May 2009) website. Figure 3.17D showed the deleted region in chromosome 5 affected the NR3C1 (nuclear receptor subfamily 3 group C member 1) gene located in the middle of the region (blue box). NR3C1 is an intracellular glucocorticoid receptor gene, which plays a major role for binding steroids to the nucleus. Deletion of this particular steroid receptor gene is responsible for the immunochemo-resistance in relapse cells.

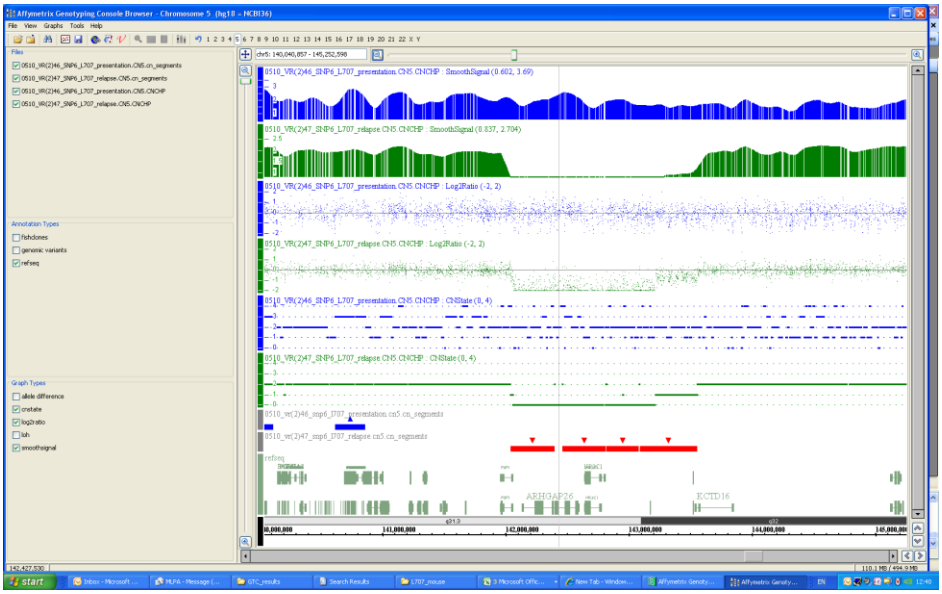

Figure 3.16 Raw data processing software Affymetritrix Genotyping Console. Analysis on chromosome 5 displayed histogram of presentation cells (top, blue) and relapse cells (below, green) showing deletion on relapse cells. Red bar with arrows (below) mapped the downregulation of the region.

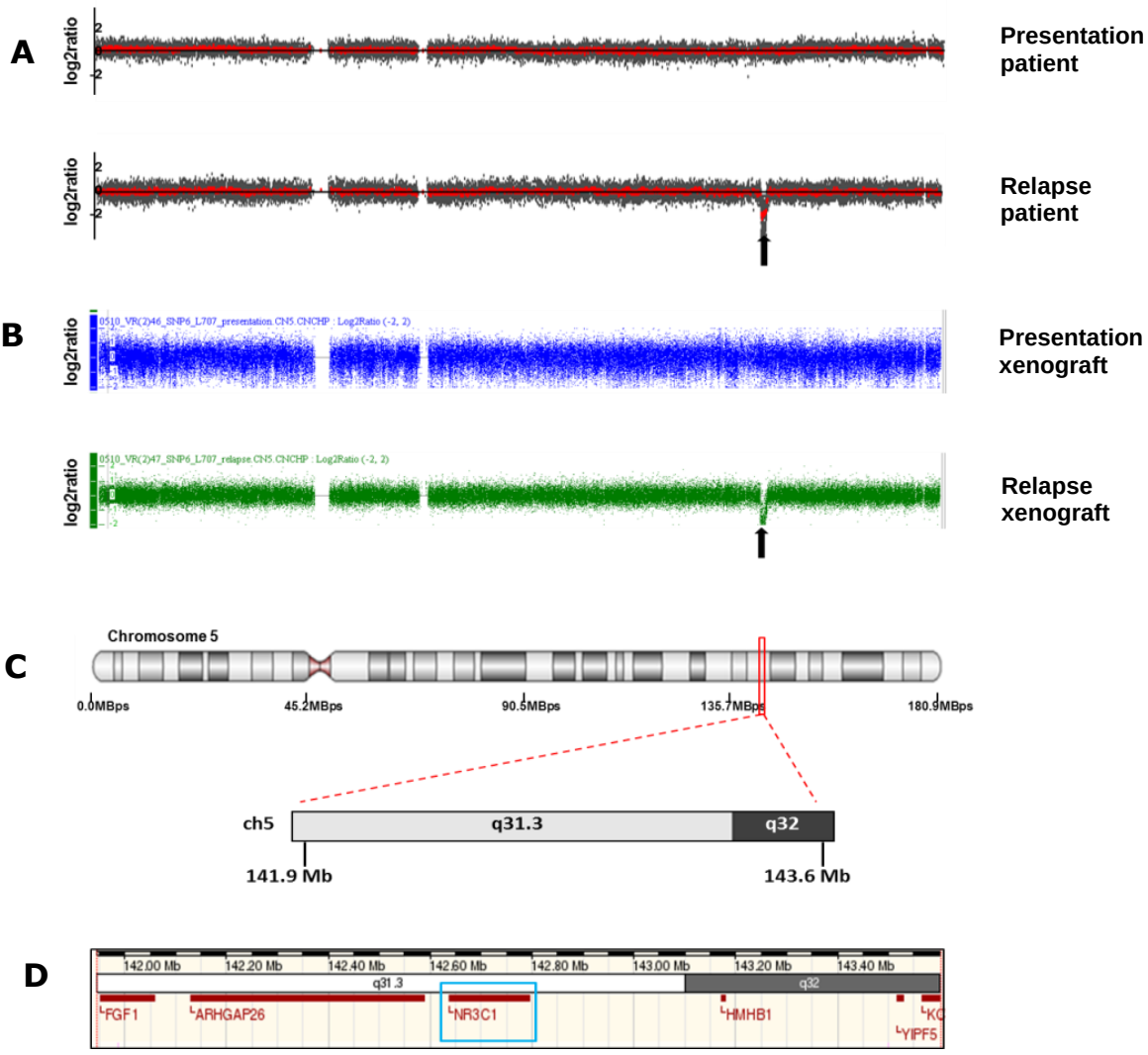

Figure 3.17 Relapse specific deletion on chromosome 5. (A) Array analysis on patient presentation and relapse cells. (B) Array analysis on presentation and relapse cells xenografted mice. Deleted region identified in relapse cells in A and B was mapped to chromosome 5 to identify the length of the region, C, and deleted region was searched in *Ensembl* website for chromosome 5 which displayed the deleted region encompassing *NR3C1* gene (blue box), D.

3.2.5 Evaluation of competitive repopulation of t(17;19) mix cells *in vivo*

In this section, NSG mice were xenotransplanted with combination or mix L707 presentation and relapse blast cells at different ratios to determine which clone has greater advantage in expanding and repopulating *in vivo*. All intrafemoral transplantation of blast cells was performed by Mike Batey and Klaus Rehe. Effect of dexamethasone treatment

on the repopulation of cells was also studied on the similar mixed populations of cells at similar ratios. The ratios of the mix cell populations were as shown in Table 3.1. For the dexamethasone treated study, ratios of 90% and 10% presentation cells were omitted. Five mice were used in each combination ratio. A 100% presentation (10P:0R) and 100% relapse (0P:10R) cells were also included in the mix population study as comparison. Each mouse was transplanted via intrafemoral injection with 1 x 10^5 blast cells which were retrieved from primary xenograft of patient's primary presentation and relapse leukaemic cells in NSG mice prior. After the cells were engrafted, animals with severe manifestation of the disease were humanely killed and bone marrow and spleen were collected to retrieve the engrafted leukaemic cells.

Cells implant in mice (100,000 cells each)	Ratio of cells
100% P	10P:0R
90% P + 10% R	9P:1R*
70% P + 30% R	7P:3R
50% P + 50% R	5P:5R
30% P + 70% R	3P:7R
10% P + 90% R	1P:9R*
100% R	0P:10R

Table 3.1 Ratios of combination cells transplanted into mice in mix population studies.
P=presentation cells; R=relapse cells. * indicates ratio omitted in dex-treated groups.

For the dexamethasone (Dex) treated groups, peripheral blood of randomly selected mice were collected on day12 post xenograft and were analysed for engraftment of blast cells. Figure 3.18 showed the flow cytometry analysis of peripheral blood of three mice. Figure 3.18A showed a low engraftment of blast cells was detected in a mouse with 10P:0R (100% presentation cells). Therefore, it was decided for Dex treatment to commence on day 14. Treatment was administered via intraperitoneal injection on a five days a week basis for four weeks. At the end point of the mice where the xenografted mice in this

group were killed, none of the mice was presented with loss of hind leg mobility as seen in the xenografted mice in the non-treated group. However, all mice showed extreme lethargy, pale, immobolized and weight loss of almost 20% at the time of sacrificed. Mice were killed as advised by the CBC Animal Care personnel. The femur of almost all xenografted mice in Dex-treated group was noticeably fragile, making bone marrow collection difficult. This condition was not seen in the untreated group.

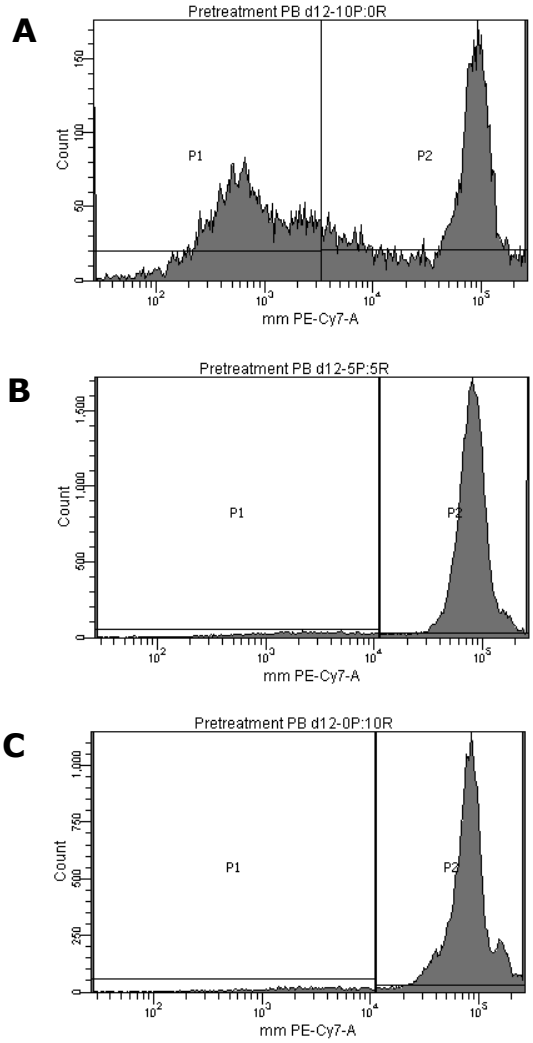

Figure 3.18 Flow cytometry analysis of peripheral blood on day 12 post xenograft. Peripheral blood was isolated from random mice on day 12 to analyse for engraftment before starting dexamethasone treatment on day 14. Low engraftment of was detected in presentation cells (10P:0R) xenografted mice A. No engraftment was seen in mix population (5P:5R) B, and relapse cells (0P:10R) xenografted mice C.

3.2.5.1 Survival analysis

The survival of the mice following engraftment was estimated using Kaplan-Meier analysis. The starting point was the start of leukaemic cell inoculation in mice, which is the day 0 of intra femoral xenotransplantation of L707 cells, and the end point was the day the mice was killed depending on the severity of illness due to the disease, following guidelines from CBC. At the end point of each mouse in the mix cell populations study, percentages of survival after mix cells engraftment were analyzed. Figure 3.19 showed Kaplan-Meier curves of survival rates of mice engrafted with mix populations of L707 without treatment. Mice engrafted with L707 relapse cells (0P:10R) survived significantly longer than those with presentation cells (10P:0R) ($p=0.0034$, log rank test) (A), while survival rate for mice with different ratios of the mix cells fall in between the two curves. Mice engrafted with ratios of 9P:1R and 1P:9R both survived significantly shorter than those with relapse cells (B) ($p<0.05$, $p<0.05$, log rank test). The survival rates of mice engrafted with blast cell ratio 7P:3R, 3P:7R and 5P:5R were moderately in between survival of mice with presentation cells and relapse cells only (C and D).

In the Dex-treated experiment on mice xenografted with the mix cells at different ratios, Dex was administered at concentration of 15 mg/kg body weight and treatment was given for 4 weeks. Figure 3.20 showed Kaplan-Meier curves of survival rates of mice engrafted with mix populations of L707 with Dex treatment. As the relapse blast cells have deletion on the steroid receptor gene, as expected Dex-treatment has no significant effect on the survival rate of mice xenografted with 0P:10R (A) compared to those without treatment. Dex treatment successfully prolonged survival rates of mice engrafted with 10P:0R, towards those of 0P:10R (A). With Dex treatment given mice xenografted with all ratios of mix cell populations survived as long as the relapse 0P:10R (B and C).

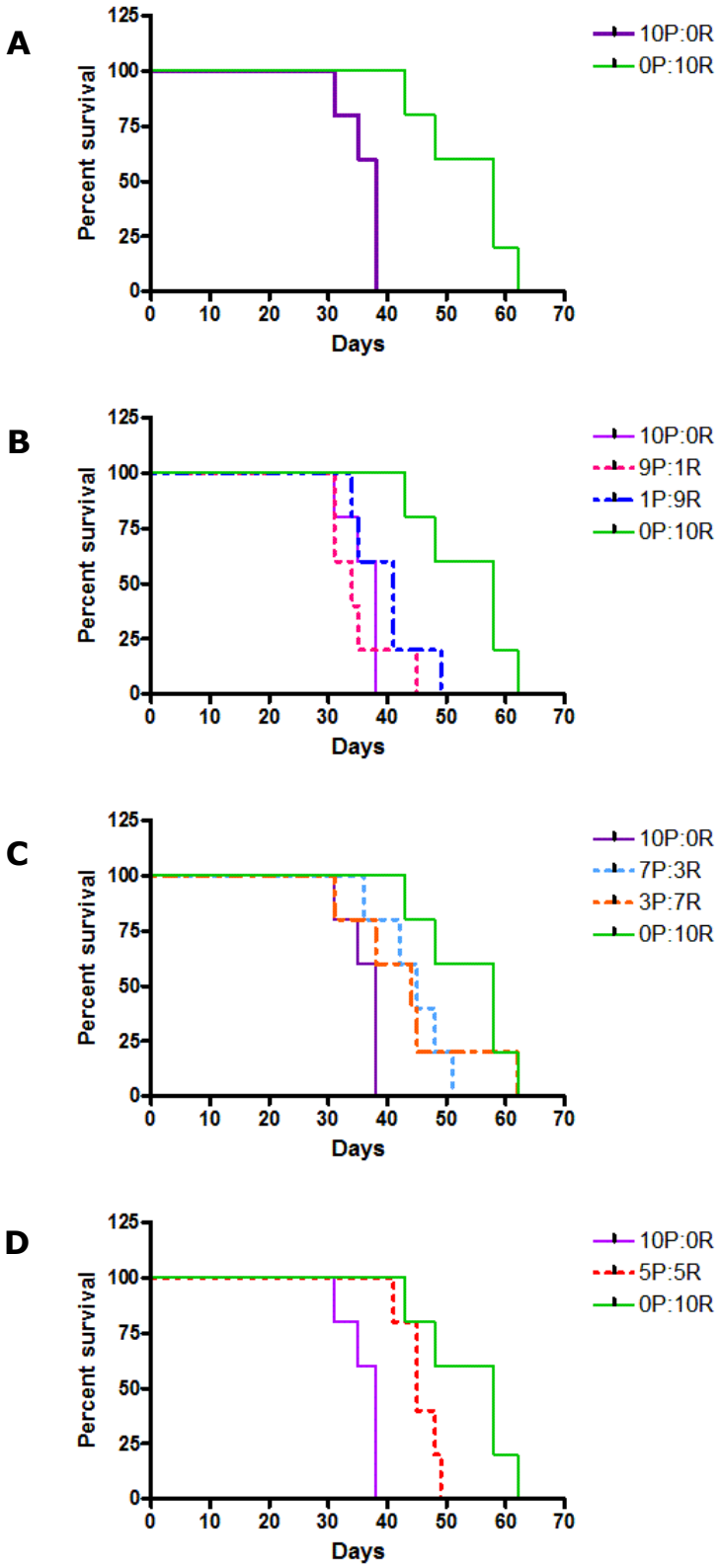

Figure 3.19 Kaplan Meier analysis of survival in non-treated mice. A, Presentation cells xenografted mice and relapse cells xenografted mice. B, 90%P and 10%P cells mix populations with presentation and relapse cells xenografted mice. C, 70%P cells and 30%P cells mix populations with presentation and relapse xenografted mice. D, 50%P mix population with presentation and relapsed cells xenografted mice.

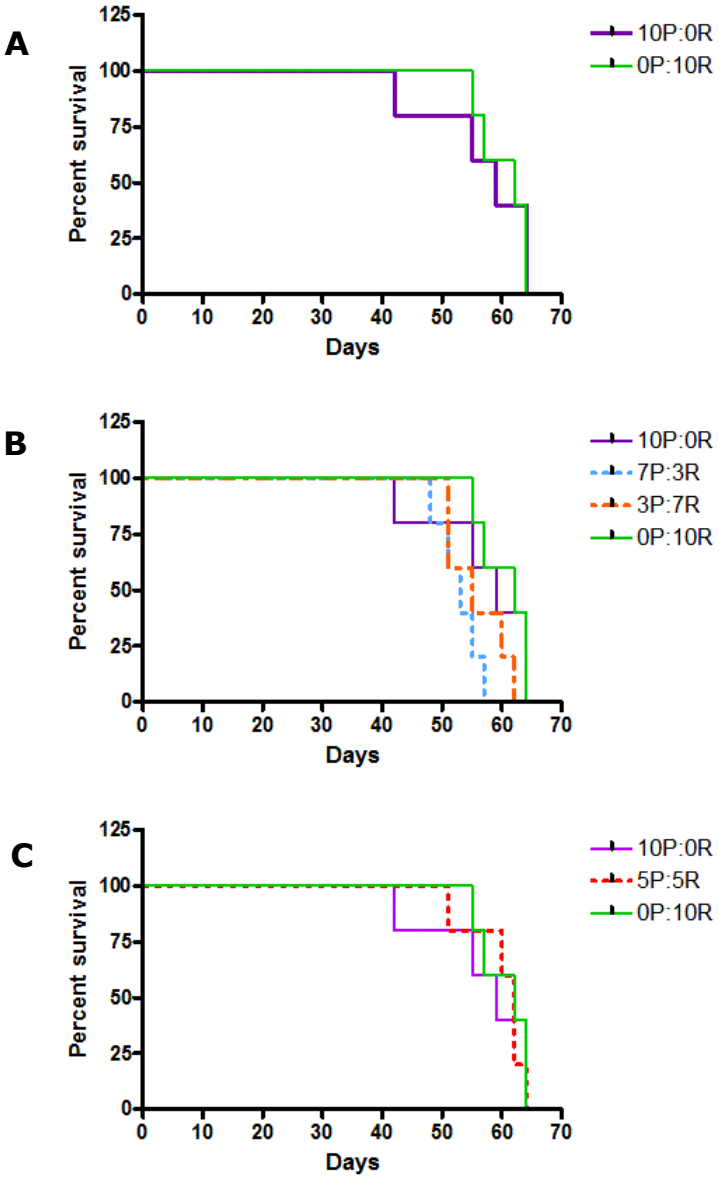

Figure 3.20 Kaplan Meier analysis showing survival of mice treated with dexamethasone. A, Presentation cells xenografted mice and relapse cells xenografted mice. B, 70%P cells and 30%P cells mix populations with presentation and relapse xenografted mice. C, 50%P mix population with presentation and relapsed cells xenografted mice.

3.2.5.2 Cytogenetic analysis of engrafted cells

From the SNP microarray analysis result in Section 3.2.4 which identified deletion in the *NR3C1* gene, the percentages of cells with this deletion present in the mixed cell engrafted mice could be determined using fluorescence *in situ* hybridization (FISH) technique. Probes covering the *NR3C1* gene and a control non-affected gene on the far end of chromosome 5 at q35.3 were selected from the same *Ensembl* webpage as shown in Section 2.2.1.18.

Cryopreserved cells were thawed and fixed with methanol/acetic acid (3:1). To perform FISH technique, cells dropped on slides were hybridized with target gene probes, RP11-92B6, RP11-790H4 and RP11-614D16 labelled with spectrum green (G), and control unaffected gene probes, RP11-320G11 (Chr5-32k-2P22) and RP11-1259L22 probes labelled with spectrum red (R), as described in Materials and Methods Section 2.2.1.18.

In this analysis, cells were scored based on the presence of the biallelic target gene. Cells with unaffected *NR3C1* gene were identified by homozygous 2G2R, cells with heterozygous *NR3C1* deletion by 1G2R or homozygous deletion of *NR3C1* by 0G2R. For every sample analysed, 100 cells were scored. The cut-off values for the chance finding of a deletion were established to be 5% by Claire Schwab. The preparation of samples and scoring of cells were partially assisted by Claire Schwab and Heather Morrison from Leukaemia Research Cytogenetics Group, (NICR, Newcastle University).

In Figure 3.21, fluorescent photographs A and B showed initial patient primary presentation and relapse cells respectively. Presentation cells with intact *NR3C1* gene showed the presence of both green and red signals (2G2R). Patient relapse cells showed a population of bilateral loss (0G2R). There was also a presence of a single cell with 2G2R in the population seen in photograph B. Given the size of the cell, this was thought to be the origin LSC clone, residing dormant in the bone marrow niche, which was resistant to antiproliferative chemotherapy.

Figure 3.21 C, D and E showed cells retrieved from presentation cells xenografted mouse, relapse cells xenografted mouse and a mix population xenografted mouse respectively. The presentation xenograft sample showed cells expressing 2G2R whereas relapse xenograft cells expressed only red signal as expected. Mix cells engrafted sample showed presence of both 2G2R and 0G2R.

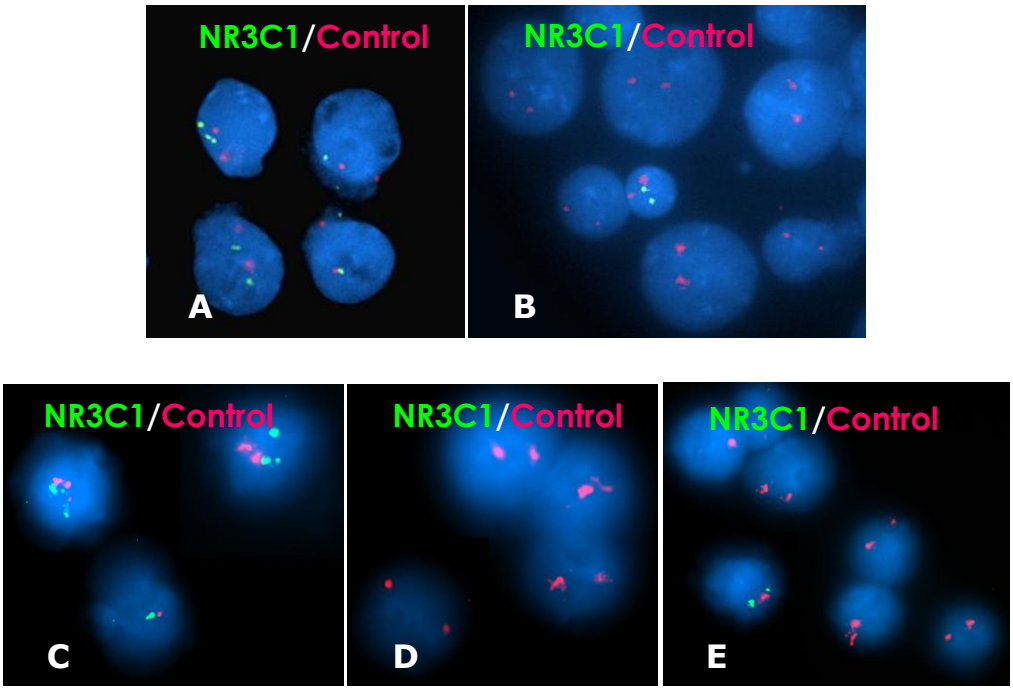

Figure 3.21 Fluorescence microscopic representative of *NR3C1* gene detection in blast cells. Target gene *NR3C1*were labelled with spectrum green and control gene were labelled with spectrum red. A, Primary presentation cells from patients. B, Primary relapse cells from patients. C, Presentation cells in xenograft mouse. D, Relapse cells in xenografted mouse. E, Mix population in xenografted mouse.

To evaluate the effect of drug treatment on clonal evolution and expansion of patient presentation and relapse blasts in xenografted mice, cytogenetic analysis was performed on the blast cells retrieved from treated and untreated mice engrafted with mixed population of the blasts.

Figure 3.22 shows percentages of presentation cells present in the xenograft mice with and without Dex treatment. In the non-treated group (A), the graphs showed the percentage of presentation cells in the engrafted mice with mix populations of cells were higher than the initial ratios of the cells transplanted. In xenografts of 10P:0R and 0P:10R, percentages of P cell 100% and 0% respectively. For the mix populations, percentage of P cells in 9P:1R, 7P:3R, 5P:5R, 3P:7R and 1P:9R were (99 ± 0.7)%, (74 ± 8.2)%, (66.3 ± 17.5)%, (69.3 ± 19.4)% and (53.7 ± 8.6)% respectively. Detailed breakdown of cell scored is given in Appendix 2. This indicated that the presentation cells were expanding and repopulating faster than the relapse cells *in vivo*. In Dex-treated group (B), the percentage of presentation cells in xenografted mice were lower than the initial ratios of the presentation cells transplanted indicating that dexamethasone successfully suppressed the growth of presentation cells in the mix population. The

percentages of presentation cells in 10P:0R, 7P:3R, 5P:5R, 3P:7R and 0P:10R were (95.8 ± 4.3)%, (49.0 ± 23.2)%, (45.6 ± 17.9)%, (7.8 ± 1.7)% and 0% respectively. By comparison with the non-treated group, dexamethasone significantly reduced the percentage of presentation cells in mice xenografted with 3P:7R ratio of mix cells ($p<0.01$; t-test). Surprisingly, in the 10P:0R (100% presentation cells) group, one mouse was presented with 16% of cells expressing single green signal (2R1G). This could possibly indicate that these cells have loss of heterogeneity (LOH) condition, selected by dexamethasone.

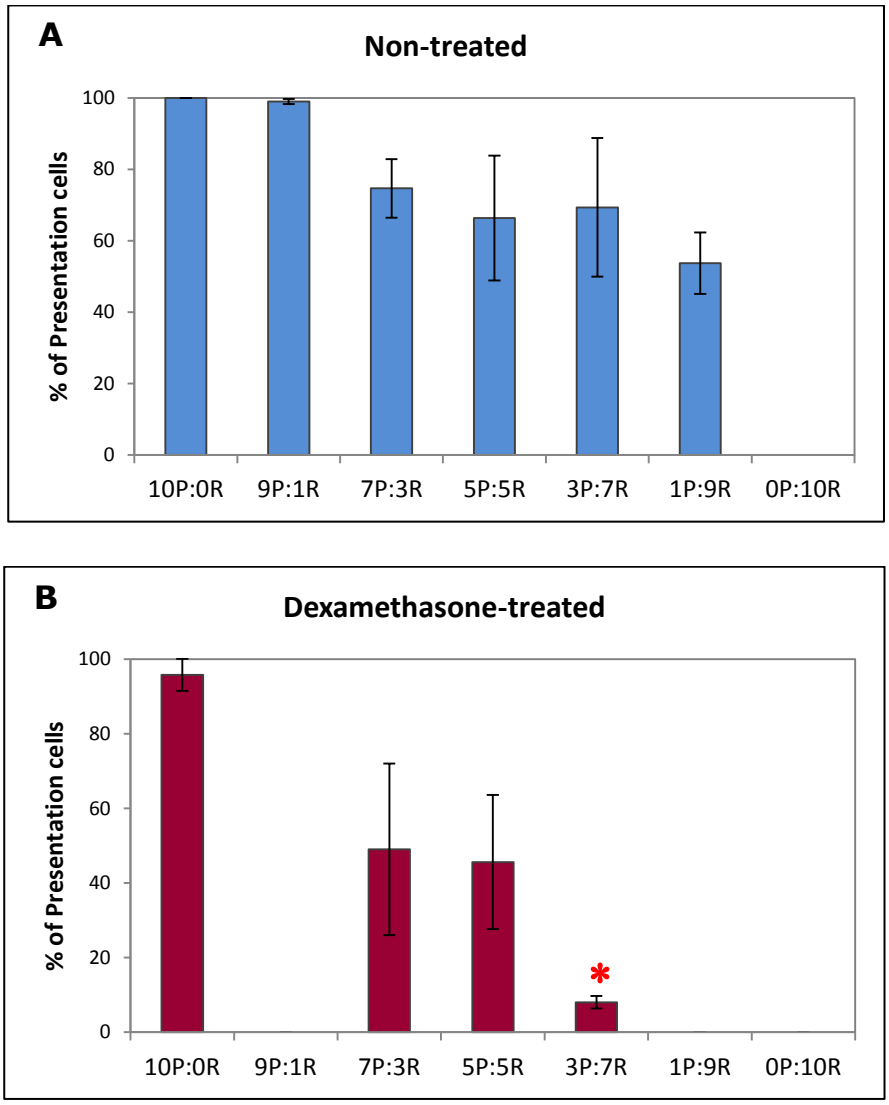

Figure 3.22 FISH analysis representing percentage of presentation cells engraftment in non-treated and dexamethasone-treated mice. A, Percentages of presentation cells in non-treated xenografted mice. B, Percentages of presentation cells in dexamethasone treated xenografted mice. * indicates significant value ($p<0.01$, t-test) compared to the corresponding non-treated mice in A.

3.2.5.3 Determination of NR3C1 levels in engrafted cells

Complementary to the FISH analysis, real-time PCR was carried out to quantify *NR3C1* level in genomic DNA of cells retrieved from mice xenografted with mix cell populations. A Taqman real-time PCR method with primers and fluorogenic oligonucleotide probe was used in this analysis. Standard curve was built up from mixture of DNA of 10P:0R and 0P:10R from the non-treated group, prepared at the same ratios as the transplanted mix cell populations. C_T values of target gene *NR3C1* were normalized against C_T values of a control ATP10A gene. To quantify the *NR3C1* level, the $\Delta\Delta C_T$ values of the untreated 10P:0R was used as an internal control and data were presented in $2^{-\Delta\Delta CT}$ as detailed in Materials and Methods Section 2.2.1.17.

Figure 3.23 shows the levels of NR3C1 in the xenografted mice with Dex treatment and those without treatment. Standard curves in both graphs were indicated as blue lines. In the non-treated group (A), the *NR3C1* gene copy levels in the engrafted cells were higher than the corresponding standard mixes. As an internal control, the NR3C1 level in 10P:0R was 1.0 and NR3C1 level in 0P:10R was undetectable. For the mix cell populations groups, the levels of NR3C1 in 9P:1R, 7P:3R, 5P:5R, 3P:7R and 1P:9R were 1.4 ± 0.07, 1.15 ± 0.26, 1.28 ± 0.32, 0.81 ± 0.40 and 0.59 ± 0.17 respectively. This indicated the presence of high numbers of presentation cells across all the mix cell engraftments. In contrast, in Dex-treated group (B), NR3C1 levels were lower than the standard curves indicating lower numbers of presentation cells. The level of NR3C1 measured were 0.72 ± 0.07 in 10P:0R, 0.35 ± 0.09 in 7P:3R, 0.29 ± 0.14 in 5P:5R, 0.02 ± 0.01 in 1P:9R and non-detectable in 0P:10R. By comparing these Dex-treated and non-treated groups, the NR3C1 gene copy numbers were significantly different with $p<0.05$ (t-test) in ratios of 10P:0R, 7P:3R, 5P:5R and 3P:7R.

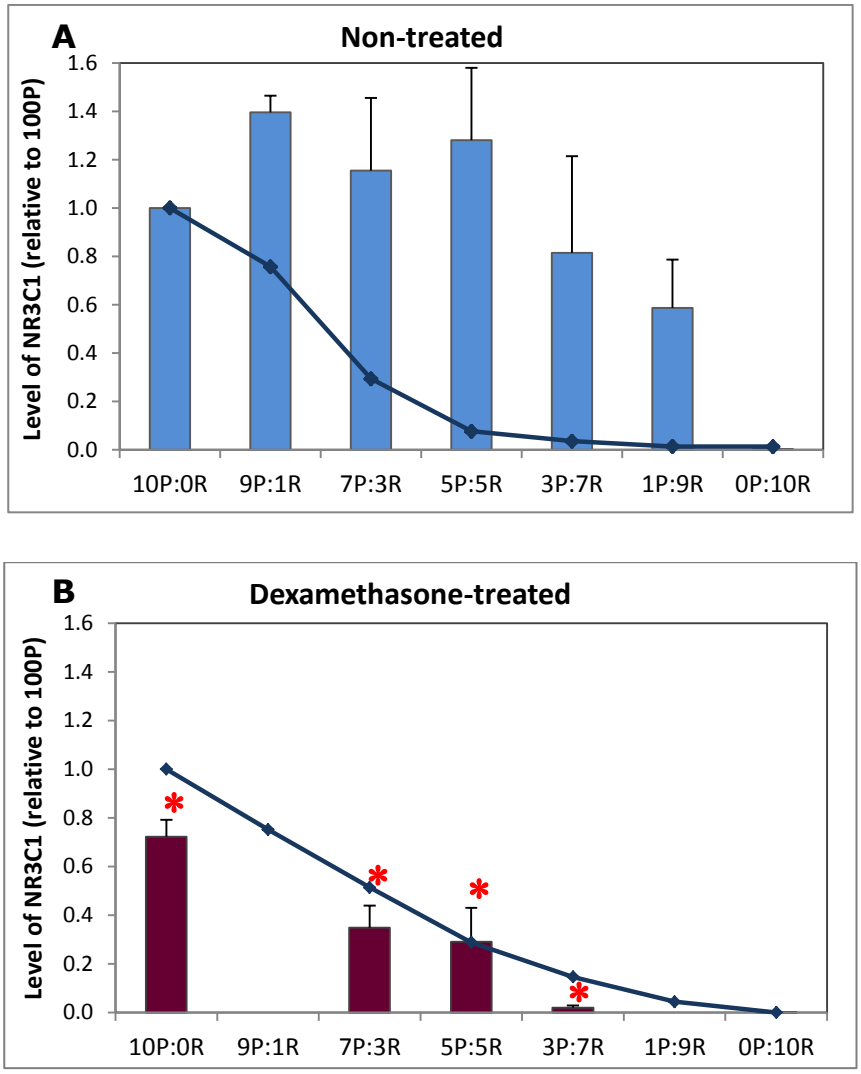

Figure 3.23 Real-time PCR analysis on NR3C1 level in non-treated and dexamethasone-treated xenograft. A, Analysis on the level of *NR3C1*gene in non-treated xenografted mice. B, Analysis on the level of *NR3C1*gene in dexamethasone treated mice. Blue lines indicate standard curves were generated by mixing DNA from 10P:0R and 0P:10R of non-treated group at the same ratios of initial engraftment of mix cell ratios. * indicates significant value (in all, $p<0.05$, t-test) compared to the corresponding non-treated mice in A.

3.2.6 Engraftment of t(17;19) – second case

To compare the clonal expansion and kinetics between two t(17;19) cases, a second match paired presentation and relapse of t(17;19) samples were obtained from Dublin Hospital. This sample pair was assigned as L878. The frozen samples were processed and viable cells were counted by trypan blue exclusion method as described in Materials and Methods. The viable presentation cells counted were 1.2×10^5 cells and unfortunately, for relapse sample there was hardly any cells seen in the provided vial. The vials were spun down and cells pellet were washed with RF10 medium and suspended with medium for xenograft in NSG mice. The relapse vial contained a very tiny cell pellet, despite this, the cell pellet was xenotransplanted as well. L878 presentation cells were transplanted into two mice and relapse cells was transplanted into one mouse to bulk-up the cells *in vivo*. However, after 7 months transplantation, the mice did not show any manifestation of the disease. Bone marrow puncture was performed to collect samples for analysis. Due to old age, the mice was killed 2 months later after transplanting bone marrow aspirates of presentation cells into three NSG mice for subsequent (secondary) engraftment. Figure 3.24 shows histograms from flow cytometry analysis of the bone marrow sample collected at 7 month and cells retrieved from spleens of the killed mice.

Analysis on the bone marrow puncture showed there was low engraftments by the presentation cells in both xenografted mice (left panel, top and middle) whereas the relapse cells xenografted mouse did not show any engraftment in the bone marrow (left panel, bottom graph). However, histogram of the flow analysis on the spleen showed low, but detectable presentation and relapse cells deposited in the organ (right panel). The subsequent secondary xenograft work is still on going to this date. Because of the limited time left in the lab, this experiment was passed unto other colleague to continue and care for.

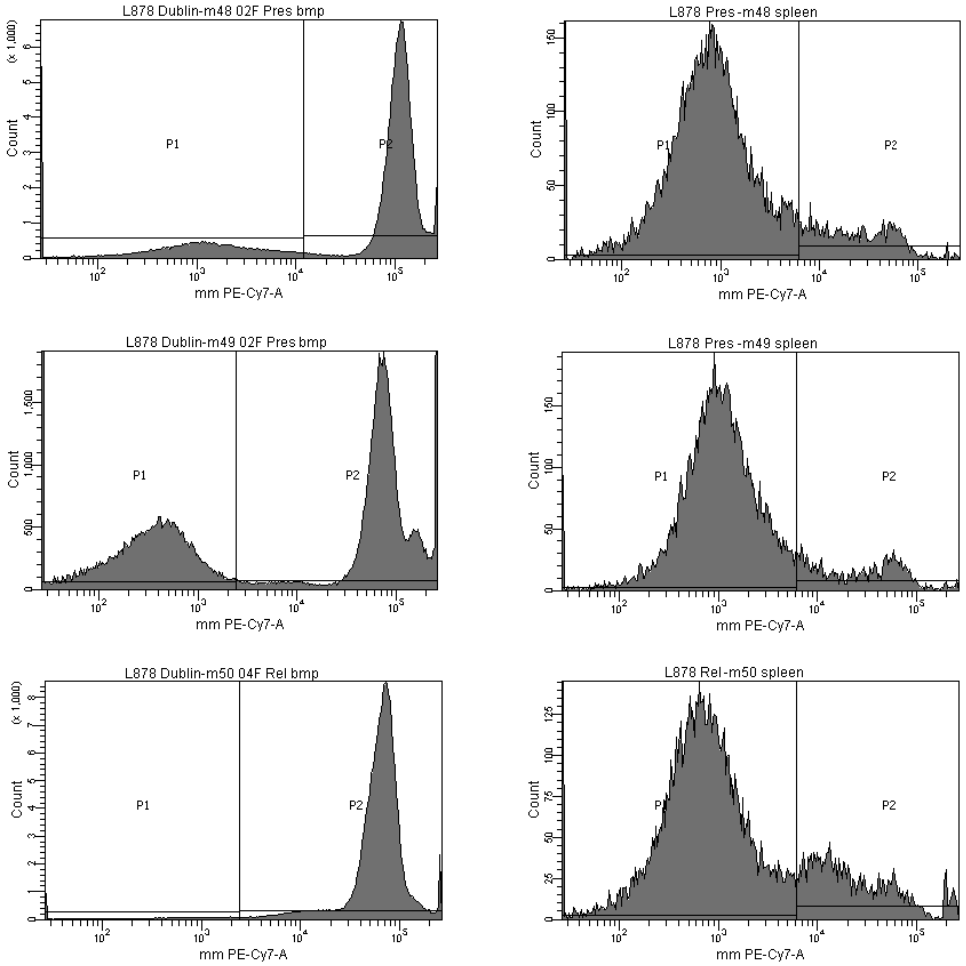

Figure 3.24 Flow cytometry analysis of engrafted L878 blasts cells. Histograms showed analysis of bone marrow puncture on the left panel and isolated spleen on the right. The top and middle histograms represented corresponding bone marrow and spleens results of L878 presentation cells xenografted mice. Bottom histogram represented bone marrow and spleen results from the L878 relapse cells xenografted mouse.

3.3 Discussion

The main aim of this chapter is to evaluate competitive clonal repopulation of the mix combinations of presentation and relapse cells in various proportions in xenograft mouse models to determine which clone has greater advantage of repopulating and expanding in vivo. A dexamethasone treatment was applied in another similar xenograft set up as a comparison for the advantage of repopulating and expanding cells.

Only a single case of matched paired presentation and relapse cells of t(17;19)-positive pro-B ALL was studied in this chapter. Since the translocation t(17;19) occurs rarely in childhood ALL, similar cases of t(17;19) was rarely available and those that were available did not have matching pairs of samples.

The principle of xenografting of leukaemic cells, either fresh or cryopreserved, into immunodeficient mice was to establish a continuous supply of samples from these patients without having to establish an in vitro culture. The presentation and relapse blast cells of L707 were by preference xenotransplanted into female mice since the paired samples were taken from female patient. Moreover, John Dick's group has reported that female mice more efficiently engrafted human haematopoietic stem cells with 1.6- and 1.7-fold higher engraftment in bone marrow and spleen, respectively, in comparison to males (Notta, Doulatov et al. 2010).

High engraftment of the L707 blasts in the xenografted mice was demonstrated in the infiltration of the spleen, ovaries and occasionally other organs randomly. This study has shown that for L707 case, relapse cells persistently infiltrated the ovaries and presentation cells penetrated the CNS as seen in primary and subsequent secondary transplantation. This is supported by the similar morphology of blasts isolated from spleen and brain stem of the respective mice, and flow analysis of the engrafted cells.

Immunophenotyping of primary and secondary engrafted L707 blast cells showed similar features of presentation and relapse blasts phenotype of CD10+CD19+CD20–CD34–. As Rimsza et al. (2000) reported, normal B-blast cells have a phenotype of CD10+19+20–34+ (Rimsza, Larson et al. 2000). However, the t(17;19) HAL-01 cell lines were reported to have antigens of CD10+CD19+CD20+CD22+ (Ohyashiki, Fujieda et al. 1991) and another cell line, YCUB-2 with t(17;19) was reported to express CD10, CD19, CD20 but

not CD34 (Takahashi, Goto et al. 2001). This indicates that the L707 phenotypes of CD10+CD19+CD20-CD34- are typical for this particular ALL subtype.

The L707 presentation and relapse blast cells were similarly identified as Type 1 t(17;19), however the band produced differed from those of HAL-01 which was used as a positive Type 1 t(17;19) control. Takahashi et al. reported the same three bands produced from RT-PCR of the YCUB-2 cells (Takahashi, Goto et al. 2001). The reason was possibly that the E2A gene was truncated in the middle of exon 13 and fused to HLF exon 4 with insertion in between which produced the upper two bands. The lower band was a direct fusion of the exon 12 E2A and exon 4 HLF (Takahashi, Goto et al. 2001) which gives the Type 2 t(17;19) as reported by Inukai et al. (Inukai, Hirose et al. 2007). Clearer evidence may be produced by sequencing the produced band, which is still in progress.

The Affymetrix SNP microarray analysis of the whole genome identified that the relapse L707 blast cells had deletion on chromosome 5, which totally removed the *NR3C1* gene from the affected region. This deletion was not seen in the L707 presentation blasts. The deletion results in resistance to glucocorticoid treatment, which was seen in the glucocorticoid inhibition study. The L707 relapse blasts were not affected by dexamethasone treatment while the L707 presentation cells were sensitive to the treatment. This phenomenon may explain why at relapse the patient was non-responsive to chemotherapy which may include glucocorticoid drugs.

In competitive repopulation of the mixed L707 blast cells, survival curves showed mice xenografted with presentation cells had a shorter life span than those of relapse, indicating the ‘aggressiveness’ and faster evolution and kinetics of the presentation cells. This phenomenon has no possible evidence reported so far on such study. One possible reason might be that the clonal proliferation and expansion of the relapse cells were slightly impaired because the relapse cells unlike presentation cells, has gone through chemotherapies with drugs targeted directly to kill the cells. Cell proliferation capacity could have been affected making the relapse cells propagate much slower. Thus, tumour burden potential of relapse cells is much lower than presentation cells, which in turn prolonged the survival of mice engrafted with relapse cells. Xenografted mice with mixed cells in various ratios of the L707 presentation and relapse cells had an intermediate life span which was expected to be.

Treatment with dexamethasone prolonged and shifted the survival curve of the presentation cell xenografted mice and the mix cell population xenografted mice towards those of relapse xenografted mice, for which survival was similar to those without treatment. This indicated that dexamethasone successfully killed if not all, most of the presentation cells engrafted, without any effect on the GR-deleted relapse cells. However, dexamethasone treatment may have had a side effect on mice, given that the treated xenografted mice seemed to be moving slower and the femurs were visibly thinner and fragile, easily broken. Those conditions were not seen in the non-treated xenografted mice.

Glucocorticoids are widely used not only as combination therapy to treat leukaemia but also in the clinic to treat a variety of diseases including inflammation, other cancer, and autoimmune disorders (Rhen and Cidlowski 2005). Responsiveness to glucocorticoid therapy, however, differs considerably among patients, and even within the same individual, different tissues have different glucocorticoid responsivenesses (Bronnegard 1996). In addition, patients, particularly in the elderly treated chronically with glucocorticoids such as in the cases of rheumatoid arthritis, osteoarthritis, Crohn's disease, ulcerative colitis, and asthma (Kino, De Martino et al. 2003) suffer side effects including metabolic syndrome, muscle wasting, and osteoporosis, which are frequently accompanied by fracture and fatality. Glucocorticoid-induced osteoporosis has been attributed to multiple mechanisms such as impaired intestinal calcium absorption, increased osteoclast activity, suppressed osteoblastic formation, and stimulated osteoblast apoptosis (O'Brien, Jia et al. 2004), since the glucocorticoids exert their cell-killing effects directly on bone cells (Weinstein 2001). These could possibly explain the condition seen in dexamethasone treated mice.

Cytogenetic analysis on the xenografted mice revealed that without treatment, the presentation cells outgrown relapse cells which was seen in the mix population groups. Regardless of initial ratios of presentation cells in mix populations, the percentage of the cells engrafted were higher. Dexamethasone selectively reduced or suppressed the presence of presentation cells in the engrafted mice. In the treated group as well, although uncommon, one mouse from the presentation cells only group (100%P) was presented with 16% single green signal of the target gene (*NR3C1*). The other four mice showed 100% of two red signals and two green signals. The presence of single signal could possibly be because the deletion of one allele of the chromosome 5 which indicate loss of

heterozygosity (LOH). In primary ALL cases, loss of heterozygosity (LOH) or mutations within the *GR* gene are rarely found (Irving, Bloodworth, et al. 2005; Tissing, Meijerink et al. 2003; Bachmann, Gorman et al. 2007) although a number of studies have described the association between endocrinological glucocorticoid resistance syndromes with genetic mutations within the *GR* or *NR3C1* gene (Ruiz, Lind et al. 2001; Charmandari, Tsigos, et al. 2005). Therefore, from this finding, it appears that dexamethasone treatment has induced a heterozygous deletion in this patient and it could be suggested that the finding of homozygous deletion of relapse is exceptionally rare.

The FISH cytogenetic analysis was complemented by the real-time q-PCR analysis of *NR3C1* gene expression level. Without treatment, NR3C1 levels in mixed populations of engrafted mice were higher than the levels for standard mixes across all ratios, in contrast dexamethasone markedly reduced these levels. This indicated the presentation cells outgrown relapse cells which was suppressed by dexamethasone.

In summary, NR3C1 deletion seen by copy number microarray was confirmed by cytogenetic and real-time PCR analysis at relapse. In competitive transplantation in vivo, cytogenetic and real time copy number analysis of different ratios showed that xenografted mice treated with dexamethasone demonstrated lower presentation cells than relapse cells in these experiments. These mice also exhibited shorter survival.

In normal conditions, without dexamethasone treatment, the presentation cells had an advantage of outgrowing the relapse cells. In presence of drug treatment, this advantage was diminished.

These competitive repopulation and clonal evolution in mixed populations studies would be much clearer if the presentation and relapse cells could be tracked using real-time bioimaging. To be able to this, these cells have to be labelled differently. Lentivirus vector system could be developed to facilitate this need.

CHAPTER 4

LENTIVIRAL: CLONING, PRODUCTION AND TRANSDUCTION

CHAPTER 4

LENTIVIRAL: CLONING, PRODUCTION AND TRANSDUCTION

4.1 Introduction

Viruses were first discovered and presented in 1892 by Dimitry Ivanovsky in which he stated that the infected tobacco leaf filtrate from the Chamberland filter used to filter bacteria could still infect new tobacco plants (Lustig and Levine 1992). In a similar study, this filterable infectious non-bacterial agent was later named virus by Martinus Beijerinck in 1898, in recognition of Ivanovsky's work. Since these discoveries, to date over 5000 viruses have been described in detailed.

Viruses are non-living particles that do not require nutrients or energy and cannot replicate themselves. However, like living forms, they do carry genetic information in form of RNA or DNA. They need living hosts to replicate. Viruses can infect all genera of living organisms including animals, plants, bacteria and archaea. Viruses are the most abundant type of biological entity and they are found in almost every ecosystem.

Virus particles, known as virions, consist of two or three parts: the RNA or DNA as mentioned above which contains genetic material, a protein coat that protects these genomes and, in some cases a lipid encapsulating the core of structural and catalytic protein once outside the host (Pedersen and Duch 2001). In addition, a virus also has signalling and enzymatic functions which are needed during multiplication in host cells. As the size of viruses ranges from 20 nm to 300 nm, they can only be seen under an electron microscope.

There are seven groups of viruses classified by the structure of their genomes and their shared properties. The viral genome, RNA or DNA, can either be single-stranded (ss) or double-stranded (ds), and may or may not use reverse transcriptase (RT) to convert ssRNA into dsDNA. Additionally ssRNA maybe either sense (+) or antisense (–). The seven classes of viruses as categorized by David Baltimore are simplified in the table and diagram below.

Class of virus	Type of virion genome	Example of viruses
I	dsDNA viruses with double stranded DNA	Adenoviruses Herpesviruses Poxviruses
II	ssDNA viruses with single stranded (+) sense DNA	Parvoviruses
III	dsRNA viruses with double stranded RNA	Reoviruses
IV	(+)ssRNA viruses with single stranded (+) sense RNA	Picornaviruses Togaviruses
V	(–)ssRNA viruses with single stranded (–) sense RNA	Orthomyxoviruses Rhabdoviruses
VI	(+)ssRNA-RT viruses with single stranded (+) sense RNA, with DNA intermediate in the life cycle using reverse transcriptase (RT)	Retroviruses
VII	dsDNA-RT viruses with double stranded DNA using RT	Hepadnaviruses

Table 4.1 Classes of virus according to type of genome in the virion (adapted from Baltimore Cassification of Viruses website).

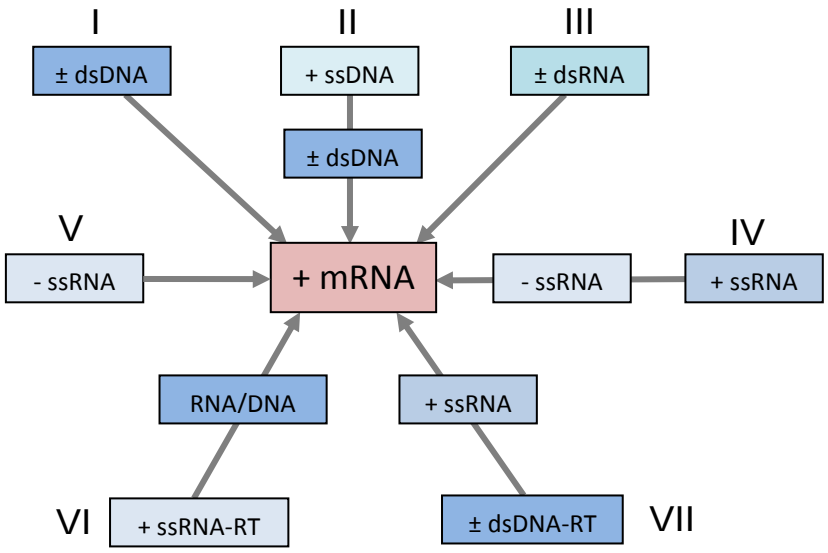

Figure 4.1 The Baltimore Classification of Viruses – Classes I-VII. The diagram shows relationship between the viral genome and its mRNA. (+) indicates sense RNA/DNA and (-) indicates antisense or complementary RNA/DNA. ds=double stranded, ss=single stranded, RT=reverse transcriptase.

4.1.1 Lentiviruses

Lentiviruses are a type of retrovirus from the Class VI, the most commonly used amongst the seven classes of viruses in the Baltimore classification system.

The HIV is the most clinically relevant lentivirus as it is responsible for AIDS. As lentivirus means a slow virus, the progression of HIV-related disease has a slow onset, which may take years for the symptoms to develop.

There are various types of retroviruses which show different interactions with their specific hosts. Although these retroviruses have different biological properties, they share the same basic genomic organization and mode of replication. In the infected cells, the genome of the virions, the RNA, is reverse transcribed into a DNA forming a provirus.

4.1.2 Genomic Structure of Retroviruses

In the simplest form, the retrovirus genome contains two positive single stranded RNA. The retroviral RNA genome carries an m7G5'ppp5'Gm cap group at the 5' end and a poly(A) tail at the 3' end (Figure 4.2). The coding regions of the retroviral genome are located in between two untranslated flanking ends. The coding regions are the key elements for viral replication. The retroviral genome is large, consisting of 7000 – 10000 nucleotides, including a short repeated (R) sequence at both 5' and 3' ends. The R region is involved in strand transfer during reverse transcription in which the PBS (primer binding site) and the PPT (polypurine tract) play the main part. The packaging signal (ψ) main function is to assemble the viral RNA into new virions.

All retroviruses, with simple or complex genomic structure, contain *gag, pol* and *env* ORFs (open reading frames). *gag* (group specific antigen) encodes polyproteins such as the capsid protein (CA), the matrix protein (MA) and the nucleoprotein (NC), which are found in all retroviruses. Cleavage of these polyproteins exposes the core protein of the viral particle. *pol* encodes enzymes for viral replication, the RT (reverse transcriptase) and IN (integrase). In some retroviruses, the retroviral protease enzyme (PR) is either encoded by the 3' of the *gag* ORF, the 5' of the *pol* ORF or in between the *gag-pol* ORF. Proteins of the viral envelop, the surface glycoprotein (SU) and the transmembrane

glycoprotein (TM) are encoded by *env* (Coffin, Hughes et al. 1997; Pedersen and Duch 2001).

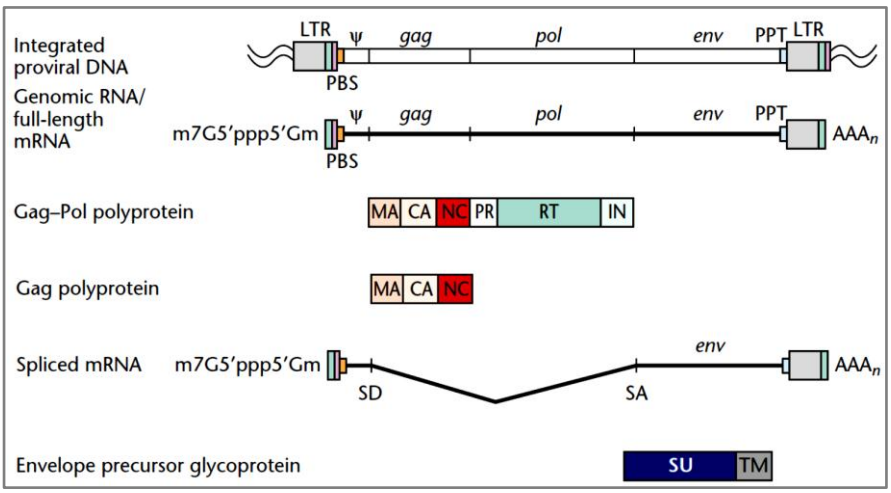

Figure 4.2 Genomic structure of a simple retrovirus. The organization of genome and gene expression pattern of a simple retrovirus shown the structure of an integrated provirus linked to flanking host cellular DNA. This is located at the terminal of the virus at the LTR sequence (U3-R-U5). The full length RNA serves as genomic RNA and mRNA for translation of the gag and pol ORFs into polyproteins. The splicing of the mRNA generated the env mRNA which encodes the Env precursor glycoprotein. CA, capsid (contains RNA genome); IN, integrase; LTR, long terminal repeat (U3-R-U5 for proviral DNA, derived from RU5 downstream of 5' cap and U3-R upstream of 3' poly(A) in RNA genome); MA, matrix of retrovirus; NC, nucleoprotein; PBS; primer binding site; ψ, packaging signal; PPT, polypurine tract; PR, protease; RT, reverse transcriptase; SD, splice donor site; SA, splice acceptor site; SU, surface binding glycoprotein; TM, transmembrane protein. (adopted from Pedersen and Duch 2001).

An HIV-1 genome is much more complex than the simple retrovirus genome (Figure 4.3A). The HIV-1 provirus DNA is 9.7 kb long which includes nine ORF that translate into nineteen proteins. The major part of the provirus DNA is protein encoding regions which are flanked by 5' and 3' long terminal repeats (LTRs). Both 5' and 3' LTRs termini contain the 3'unique element (U3), the repeat element (R), and the 5' unique element (U5). The trans elements of the provirus consist of the retroviral basic ORFs, the gag-pol, gag, and env, which encode the structural proteins and enzymes involved in replication. Other additional ORFs includes tat and ref genes coding for essential regulatory proteins, vif, vpu, vpr and nef genes coding for accessory proteins. These are the nine ORFs mentioned above. The cis elements located on the 5' and 3' LTRs are the att repeats, which contain signals for provirus integration into the host genome, enhancer/promoter sequence, transactivation response elements (TAR) and polyadenylation signal (polyA). Other cis acting sequence includes those downstream of 5' LTRs which are primer binding site (PBS) and viral RNA packaging and dimerization signal (ψ and DIS). Central

cis elements are the central polypurine tract (cPPT) and central termination sequence (CTS). Additional cis elements are on the upstream of 3'.

LTR including rev response element (RRE) are involved in exporting viral mRNA into the cytosol and purine-rich region (PPT) is important for plus strand DNA synthesis (Pluta and Kacprzak 2009).

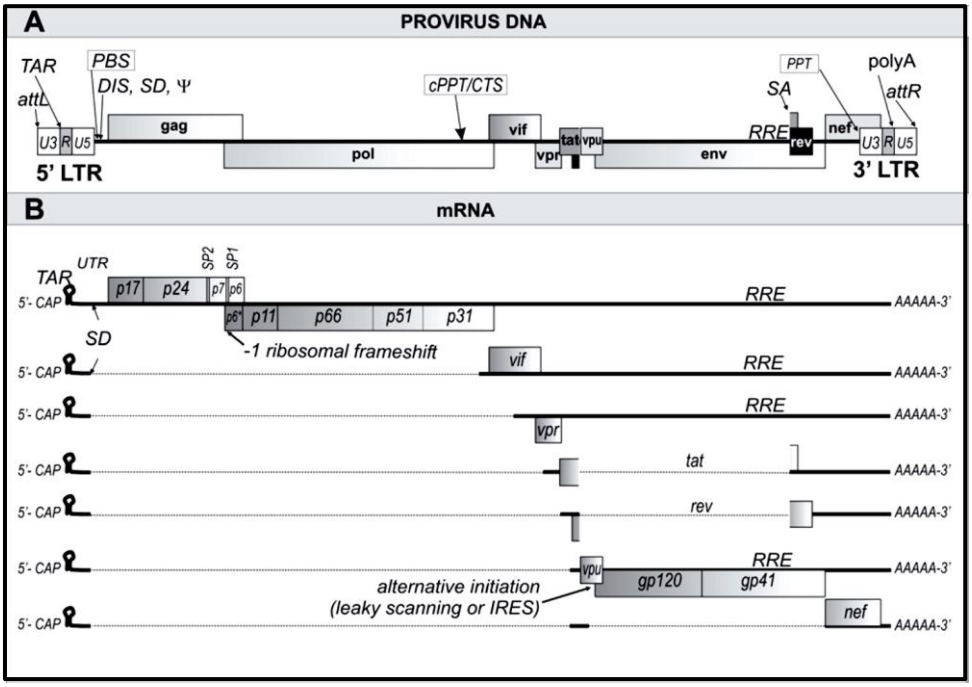

Figure 4.3 Genomic structure of HIV-1. A. Provirus DNA consist of 5' and 3' LTRs with U3, R and U5 regions at both ends. The ORFs gag, gag-pol and env encode for protein and enzymes for the virus. The PBS, cPPT, CTS and PPT are important elements for viral replication. The attL and attR involve in the integration into host genome. The DIS and ψ are elements for dimerization and packaging of virus RNA. TAR and polyA involved in transcription of mRNA, the SA and SD involved in slicing of RNA. The RRE is responsible for transporting viral mRNA from nucleus to cytosol. **B**. Viral DNA splicing exposed the three open reading frames for producing viral proteins. tat, transactivator protein; rev, regulator of viral protein expression; nef, negative factor; vif, viral infectivity; vpr, viral protein R; vpu, viral protein U; att, attachment sites; cap, terminal 7-methylguanosine. (Adopted from Pluta and Kacprzak 2009).

The three longest ORF are the gag, gag-pol and env, while the smaller central and 3' ORFs are the vif, vpu, vpr, tat, rev and nef. Alternative splicing of proviral mRNA is a way for complex retroviruses to reduce the size of their genome, allowing for expression of their genetic information (Figure 4.3B). Cleavage of gag polyprotein produces 6 structural proteins: MA (p17) responsible for transport of Gag-RNA complex to cytosol; CA (p24) and NC (p7) responsible for membrane binding, capsid formation, packaging and dimerization during viral assembly; SP1 and SP2 regulate cleavage rates, membrane

binding, virus budding and virion formation; p6 is involved in interaction with host proteins. The gag-pol polyprotein cleavage produces enzymes RT (p66, p51), PR (p11) and IN (p31). Cleavage of env produces two glycoproteins, SU (gp120) and TM (gp41), responsible for membrane fusion and virus uptake. The original regulatory proteins are the transactivator protein (tat; p16/p14) which initiates transcription of viral LTR and regulate expression of viral proteins (rev; p19). Finally, the accessory proteins are comprised of negative factor (nef; p27) which is crucial for down-regulating CD4 and other receptors, viral infectivity factor (vif; p23) which inactivates host immune response, viral protein R (vpr; p14) which is involved in nuclear import of viral PIC and viral protein U (vpu; p16) which is responsible for degrading the CD4 receptor, release of viral particles and apoptosis (Pluta and Kacprzak 2009).

4.1.3 Replication of Lentivirus

Viruses must generate mRNAs from their genomes to produce proteins and replicate themselves, and, depending on the host, different mechanisms are used to achieve this in each virus family.

Viral replication depends on host cell factors and species-specific characteristics. However, anti-viral mechanisms in the host including the restriction factor can directly inhibit retrovirus replication. To overcome this inhibition, some viruses such as the HIV-1 produce additional gene products that counteract host inhibitors (Valente and Goff 2009).

The HIV replication cycle starts with the binding of envelope glycoprotein gp120 to host the CD4 surface receptor (Landau, Warton et al. 1988) and host the secondary receptor CCR5 forming gp120-coreceptor/CD4 complexes (Dobrowsky, Zhou et al. 2008). This formation triggers the gp41 subunit to release free energy sufficient to induce fusion of the virus to the cell membrane (Melikyan, Markosyan et al. 2000). The viral core content is then released into the host cell cytoplasm. It was proposed that HIV-1 Nef protein is responsible for actin rearrangements that facilitate core content to penetrate the plasma membrane after fusion (Campbell, Nunez et al. 2004). Viral genome is then reverse transcribed by reverse transcriptase within the capsid (Arhel, Souquere-Besse et al. 2007) and the reverse transcription complex (RTC) is transported towards the nucleus. The completed provirus DNA forms preintegration complex (PIC) with other viral proteins

such as RT, IN, NC, Vpr, MA and cellular proteins (Bukrinsky, Sharova et al. 1993). The PIC is then transported through the nuclear pore into the nucleus, where the provirus DNA is integrated into the host genome at a specific site selected by IN (Lewinski, Yamashita et al. 2006). Cellular RNA polymerase II (RNAP II) together with viral tat protein forms a stem-loop RNA (Feng and Holland 1988) and transcribes the inserted sequence into proviral DNA. Viral rev protein stabilizes the unspliced and partially spliced mRNA transcripts, promoting the transport to cytosol and synthesis of viral protein (Schmid and Jensen 2008). The RNA molecules, gag, gag-pol and env proteins assemble the new virus particles and direct the gp120 and gp 41 glycoproteins to the cell membrane. Virus particles are released from the cells through budding and protease enzyme promotes capsid formation that maturates the virus (Pluta and Kacprzak 2001).

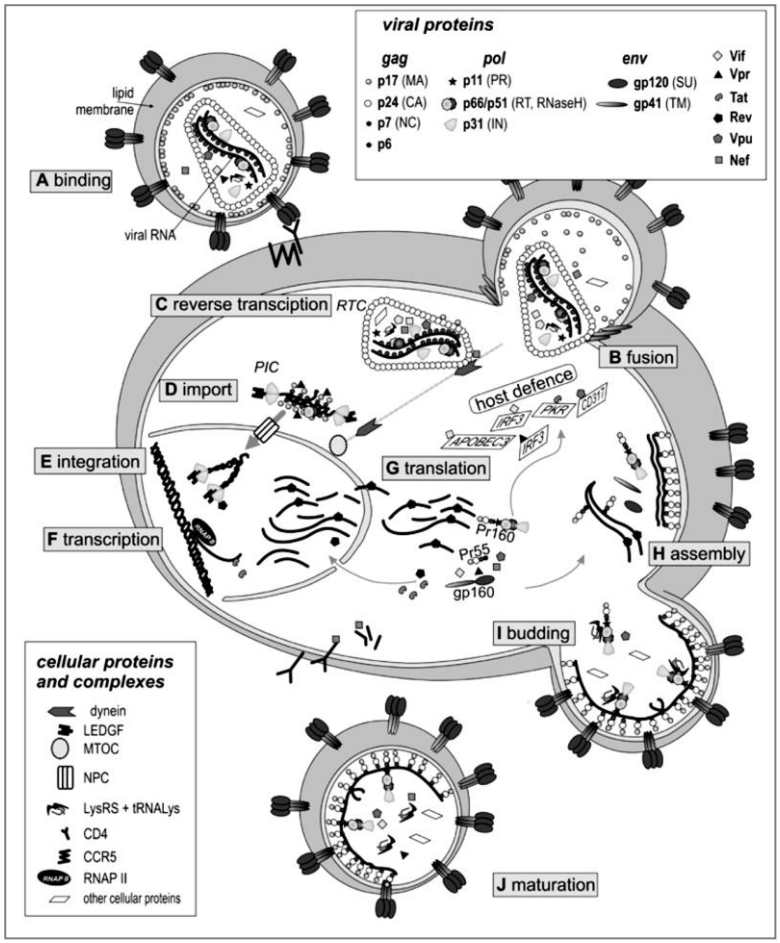

Figure 4.4 Scheme of HIV-1 lifecycle. A, HIV virus binds to CD4 cell surface receptor. B, Fusion of viral envelop membrane with cell membrane releases the viral content into cytosol. C, Virus genome is transcribed and preintegration complex (PIC) is formed. D, PIC is imported into the nucleus. E, Viral DNA is integrated into the cell genome. F, Genomic viral DNA is transcribed into viral RNA and exported into the cytocol. G, Coding viral RNA is translated into viral proteins. H, Viral proteins and the viral RNA assemble at cell membrane. I, Viral contents are encapsulated into membrane by budding. J, Release of fully encapsulated virus. (adopted from Pluta and Kacprzak 2001).

4.1.4 HIV-derived (based) Lentiviral Vectors

Viral vectors including HIV-based vectors are widely used these days in basic research and gene therapy applications because of their high rates of gene transfer ability. Retroviral vectors have an ability to integrate into the host DNA. Therefore, the retrovirus-based systems offer long-term, stable transgene expression.

The advantage of using lentiviral-based vectors is their ability to infect dividing and non-dividing cells. Lentiviral vectors can transduce a wide range of quiescence cells including progenitors and stem cells (Ricks, Kutner et al. 2008; Santoni and Naldini 2009).

The first recombinant retroviral vector systems, with a replication-defective virus, were developed in the 1980s. Following that, a system for recombinant HIV-based vector production was described in which a HIV-1 vector with replication defective and deleted sequence encoding the viral envelope (Env) glycoprotein was cotransfected with an expression vector encoding heterologous envelope protein to from HIV-1 pseudotypes (Page, Landau et al. 1990; Landau, Page et al. 1991). Along with the unique lentiviral vector properties that includes selection of 'safe' integration site in the host genome, efficient long term gene delivery to dividing and non-dividing cells, relatively large loading capacity and target specificity achieved by pseudotyping, these are key factors for the popular use of HIV-based lentiviral vector as a vehicle for gene transfer application (Pluta and Kacprzak 2009).

To date, experiments utilizing a lentivirus as a gene delivery tool have adopted a well-established production system. This system uses three vectors; a packaging vector, a transfer vector and an envelope vector, with the concept to separate trans elements encoding for structural, accessory and enzymatic proteins from cis elements required for reverse transcription, integration, RNA synthesis and packaging.

The packaging vector encodes genes responsible for structural proteins for the formation of infectious particles as well as viral enzymes. In the vector, the 5'-LTR is replaced by a CMV promoter and the packaging signal (ψ) sequence has been deleted. The original polyA signal has been replaced by those from simian virus 40 (Naldini, Blomer et al. 1996). This prevents the packaging of full-length mRNA encoding trans elements into viral particles. The RRE sequence was maintained unchanged in the vector. Further modification generated the second generation of the packaging vector. This includes the

removal of accessory proteins not required in virus replication. Deletion of vif, vpr, vpu and nef reduces the cytotoxicity and virulence, leaving only the tat and rev proteins, expressed together with gag, gag-pol and env glycoprotein (Gibbs, Regier et al. 1994). Other modifications describe additional deletions leaving only the gag-pol, tat and rev ORFs (Zufferey, Nagy et al. 1997; Mochizuki, Schwartz et al. 1998).

The transfer vector usually carries the sequence for the gene to be expressed with its own promoter. The vector contains elements such as the PBS, gag, RRE, cPPT and modified LTR (Naldini, Blomer et al. 1996). The elements are needed for reverse transcription, nuclear import, integration and packaging. The RRE is dependent on gag to enhance gene transfer efficiency (Clever, Sassetti et al 1995). As a safety measure, the U3 region in the 3' LTR of the vector is deleted, producing the self-inactivating (SIN) vector (Dull, Zufferey et al. 1998). Replacement of 5' LTR U3 by CMV promoter has been shown to enable tat dependent vector cassette expression (Kim, Mitrophanous et al. 1998). The SIN vector showed reduction in the expression of transcript and a marked reduction in producing viral particles in host cells (Bukovsky, Song et al. 1999). The SIN vectors are less harmful viruses. It was proven that the genotoxicity mainly depends on active LTRs (Montini, Cesana et al, 2009).

The envelope vector provides envelope glycoprotein in the lentiviral vector system and enhances specificity towards target cells. This vector also improves viral particle stability during viral concentration and long term storage (Page, Landau et al.1990).

4.1.5 IRES and WPRE

As mentioned previously, during viral infection, host defence mechanisms can inhibit virus replication by blocking protein synthesis. To combat this intrinsic immunity, most viruses often use the internal ribosome entry site (IRES) to ensure that translation is activated. The IRES facilitates initiation of protein synthesis independent of the 5' end. Over 56 viral and 80 cellular IRES sequences have been characterized and this sequence has been widely used in lentiviral vectors (Baird, Turcotte et al. 2006; Mokrejs, Vopalensky et al. 2006). It was shown that when two ORF are linked by IRES, the expression of the second ORF is driven by IRES by enabling and enhancing downstream

ORF translation. If the upstream ORF is not functional, the second ORF is still productive enhanced by IRES (Balvay, Soto Rifo et al. 2009).

The woodchuck hepatitis virus (WHE) post-transcriptional regulatory element (PRE) is one of the cis activating elements (Zufferey, Donello et al. 1999). With the insertion of WPRE sequence in the 3' untranslated region of a transcript, the overall transgene expression increased more than 6 fold (Oh, Bajwa et al. 2007).

4.2 Results

4.2.1 Cloning of lentivector harbouring luciferase reporter gene and fluorescent protein expressing gene

To generate lentiviral vector expressing luciferase reporter gene coupled with fluorescent protein gene, the pHR'-SINcPPT-SIEW (pSIEW) lentivector was used for this purpose (Figure 4.5). pSIEW contains 5'LTR (long terminal repeats) and 3'LTR, an SFFV promoter, a linker element IRES, an enhanced green fluorescent protein (EGFP) reporter gene, an Ampicillin resistance gene (Amp) and several viral elements such as GaG, RRE, cPPT and WPRE. In the transduction of targeted cells with the lentivectors, the cassette between 5'LTR and 3'LTR was integrated into the genome of the cells. Therefore, the genes intended for expression in the transduced cells have to be inserted between the two LTR regions in order for the lentivector to be able to express the inserted gene.

The generation of two lentiviral vectors is described in this chapter. The first lentivector is the pSLIEW, an addition of firefly luciferase (*luc*+) on the pSIEW lentivector backbone, and the second lentivector is the pSRLICW, additions of *Renilla* luciferase (RLuc) and mCherry fluorescent protein (mCherry) on a modified pSIEW. For the second lentivirus, utilization of other vectors was needed because of non- compatible sites for insertion of the reporter genes required.

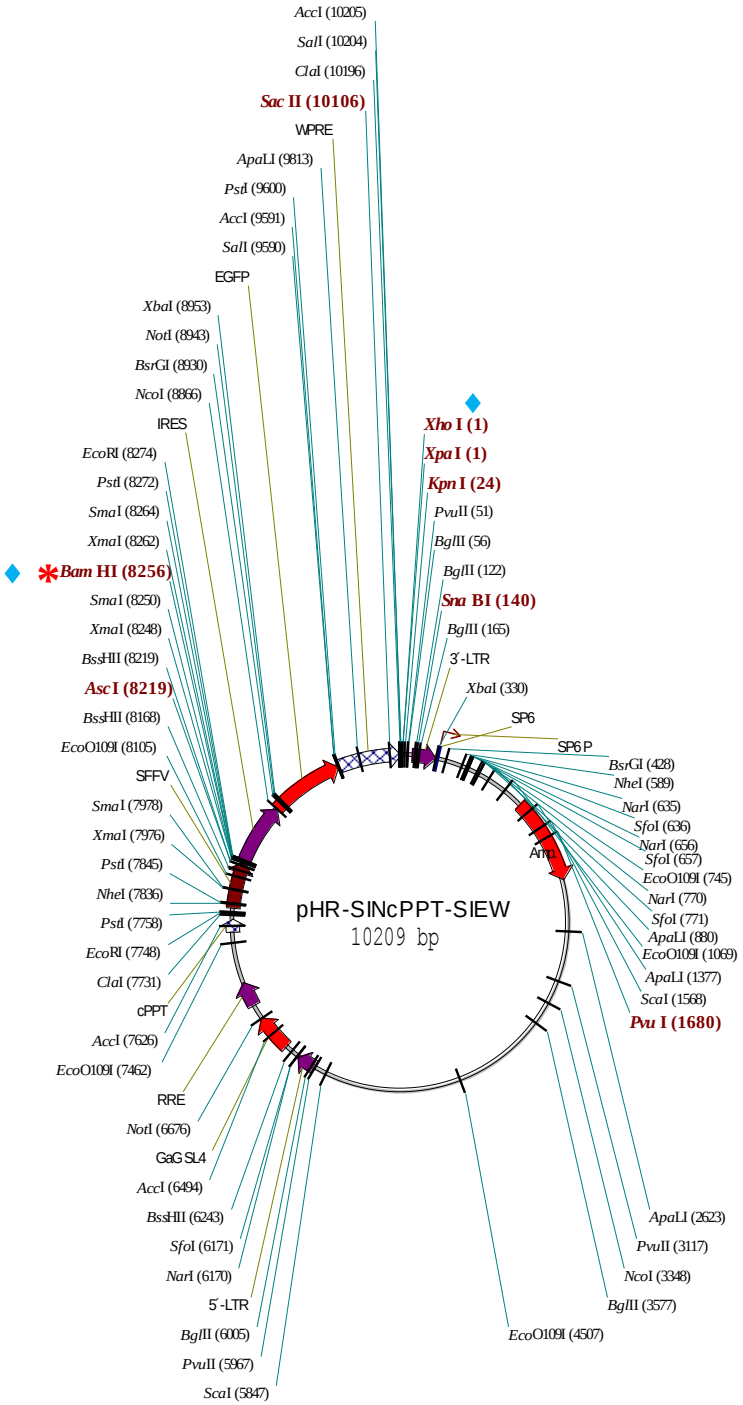

Figure 4.5 Map of pHR-SINcPPT-SIEW Lentivector (pSIEW). This lentivector was utilized in cloning of luciferase-fluorescent protein genes harbouring lentivirus. The vector backbone consists of 5' and 3' LTR (long terminal repeat), GaG, RRE (Rev-responsive element), cPPT (central polypurine tract), a promoter SFFV (spleen focus forming virus), IRES (internal ribosome entry site), EGFP (enhanced green fluorescent protein) and WPRE (woodchuck posttranscriptional regulatory element). * indicates the site of insertion of firefly luciferase reporter gene (luc+) and ♦ indicates the region modified and replaced by oligonucleotides.

4.2.1.1 Luc+ and EGFP expressing lentivector (pSLIEW)

The pSLIEW lentivector harbouring the firefly luciferase (*luc+*) and green fluorescence protein (EGFP) was successfully constructed before this work was undertaken by Dr Olaf Heidenreich. However, the clones generated had not been tested. In brief, the pGL3-Basic plasmid (Figure 4.6) carrying *luc+* reporter gene cassette was used in the cloning of pSLIEW vector. To generate a functional luc+/EGFP expressing vector, the luc+ cassette from the plasmid could be inserted only before the IRES and EGFP cassette in the pSIEW lentivector (refer to Figure 4.4). Downstream of IRES is a unique single cutting site at the 8256 nt, the BamHI, which is also available downstream of the *luc+* cassette from the pGL3-Basic plasmid at 2004 nt site. However, the luc+ reporter SV40 upstream of BamHI was not needed and had to be removed.

All the mentioned techniques and protocols used in this section were as described in the Materials and Methods Section 2.2.2.

The plasmid was double digested with XbaI and BamHI at 1742 nt and 2004 nt sites respectively in a 1x buffer Tango as suggested by Fermentas Double Digestion (Fermentas, UK). In order to be able to use the BamHI site for insertion into pSIEW, following digestion the Klenow fill-in technique was applied using the Klenow Fragment of the DNA Polymerase I enzyme (Promega, USA) to restore the BamHI sequence and blunt-ended the overhanging open frame. The digested and blunt-ended plasmid was religated, followed by DNA purification. With the BamHI cutting site directly upstream of *luc+* cassette, the plasmid was again double digested with BglII (at the 36 nt site) and BamHI to remove the *luc+* cassette. At the same time, the pSIEW lentivector was digested with BamHI for insertion of the *luc+* cassette. The restriction enzyme BglII has the same overhang as the BamHI (as shown below), therefore the fragment cut out by these two enzymes can be inserted into a site which has been cut by either one of the enzymes. However, the disadvantage is that the intended insert could ligate to pSIEW in the wrong direction.

BamHI sequence:	5'…G^GATC C…3' 3'…C CTAG^G…5'	^ indicates the cutting site of the enzymes
BglII sequence:	5'…A^GATC T…3' 3'…T CTAG^A…5'	

The digested plasmid and lentivector were run through agarose gel electrophoresis and the linearized open frame single band of pSIEW lentivector (10.2 kb) and the *luc*+ cassette (1.7 kb) fragment were cut out of the gel and purified for ligation, followed by transformation into competent cell Stbl3, agar plating, inoculation of colonies and extraction of plasmids (termed clones) DNA from each colony inoculated using miniprep kit (Qiagen).

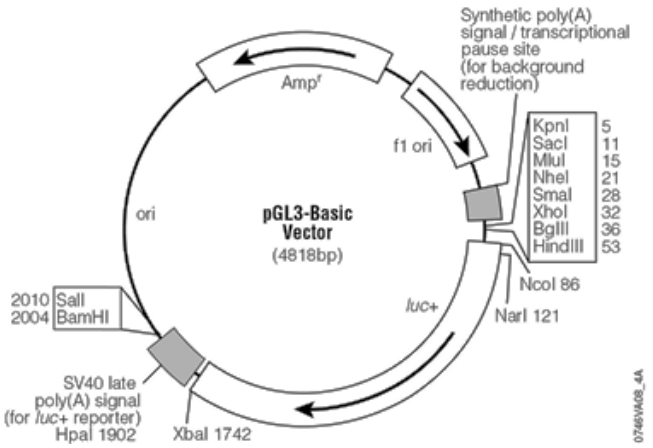

Figure 4.6 Map of pGL3-Basic vector. The 4818 bp plasmid contains firefly luciferase (*luc*+) region required for the generation of pSLIEW. Plasmid was double digested with BamHI (site: 2004 nt) and XbaI (site: 1742 nt) to remove the SV40 region from the vector. Klenow fill-in method was performed to religate the plasmid to retain the BamHI sequence. Modified vector without the SV40 promoter region were double digested with BglII (at 36 nt) and BamHI (now at 1742 nt) to get the *lu*+ reporter cassette (1.7 kb) to be inserted into pSIEW to generate the pSLIEW lentivector. Techniques used were as detailed in the *Materials and Methods*. (vector map was taken from Promega).

To verify successful insertion of *luc*+ into the pSIEW vector and to prove that the insert was in the right direction, clones (plasmids) DNA were triple digested with XhoI (at 1 nt), AscI (at 8219 nt) and BamHI (at 8956 nt) in 2x Buffer Tango which was compatible for the three enzymes. To inactivate the enzymes, the digestion was incubated at 80°C for 20 minutes, and the digested plasmids were run through electrophoresis in 1% agarose gel. Ligated pSIEW–*luc*+ plasmid is expected to yield three bands of 8.2 kb, 1.9 kb and 1.7 kb whereas non-ligated pSIEW plasmid will produce two fragments of 8.2 kb and 2.0 kb.

Figure 4.7 shows that, out of 10 clones tested, two clones were successfully ligated with insertion of *luc*+ cassette in pSIEW vector at the right direction. Clones 2 and 5 produced the 3 bands described above; therefore these clones were successfully generated pSLIEW plasmids.

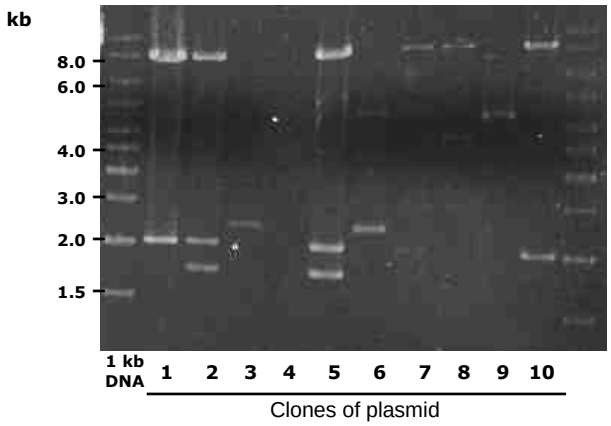

Figure 4.7 Digestion of the cloned plasmids DNA for verification of *luc*+ insert in pSIEW. Aliquots of 1 µg of plasmids DNA were triple digested with XhoI, AscI and BamHI restriction enzymes in 2x buffer Tango and incubated in 37°C for 1 hour before enzymes were heat inactivated at 80°C for 20 minutes. Aliquots of 6 µl of digested plasmids were separated by on 1% agarose gel electrophoresis run for 90 minutes. Gel was stained in 2 ng/ml ethidium bromide solution before viewing under UV-light. Clones were run against 1 kb DNA ladder for bands size determination. Gel showed 10 clones were tested. Clones 2 and 5 with successful *luc*+ insertion yielded bands at 8.2 kb, 1.9 kb and 1.7 kb.

The single colony inoculations of these pSLIEW plasmids were aliquoted into a larger volume of LB broth for overnight culture at 37°C in orbital shaker to amplify the plasmid in order to get a higher concentration of the plasmid DNA for the lentiviral production work described later in this chapter. DNA of the plasmid from overnight incubation was isolated and purified using an endotoxin-free maxiprep kit (Qiagen). The concentration of the plasmid DNA was measured using a nanodrop spectrophotometer, and then, along with pSIEW DNA, the pSLIEW DNA was digested with restriction enzymes XhoI, AscI and BamHI for reconfirmation of the presence of the right plasmid. Figure 4.8 showed the digested plasmids where pSIEW without the insert yielded two bands and the pSLIEW with the *luc*+ insertion yielded three bands.

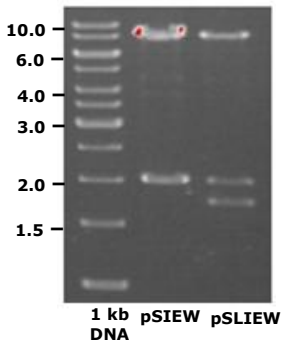

Figure 4.8 Digestion of the pSLIEW plasmid by XhoI, AscI and BamHI. Plasmid DNA isolated and purified using endotoxin-free maxiprep kit according to manufacturer's procedures as detailed in *Materials and Methods*. Aliquots of 1 µg DNA of pSIEW and pSLIEW vector were incubated with restriction enzymes XhoI, AscI and BamHI in 2x Buffer Tango (Fermentas) at 37°C for 1 hour as detailed in *Materials and Methods*. Enzymes were inactivated by increasing the temperature to 80°C for 20 minutes. Agarose gel electrophoresis at 0.8% in 1x TAE was run for 1 60 minutes. Gel was stained in 2 µg/ml ethidium bromide for 20 minutes prior to viewing under UV light. Digested DNA was run against 1 kb DNA ladder for bands identification. Gel showed digested pSIEW produced 2 bands at 8.2 kb and 2.0 kb lengths (v) whereas digested pSLIEW yielded 3 bands at 8.2 kb, 1.9 kb and 1.7 kb lengths which confirmed the insertion of *Luc+* at BamHI recognition site.

The insertion of *luc+* reporter gene cassette of 1.7 kb length into the backbone of pSIEW plasmid (10.2 kb) generated a pSLIEW plasmid of 11.9 kb length, as illustrated in Figure 4.9.

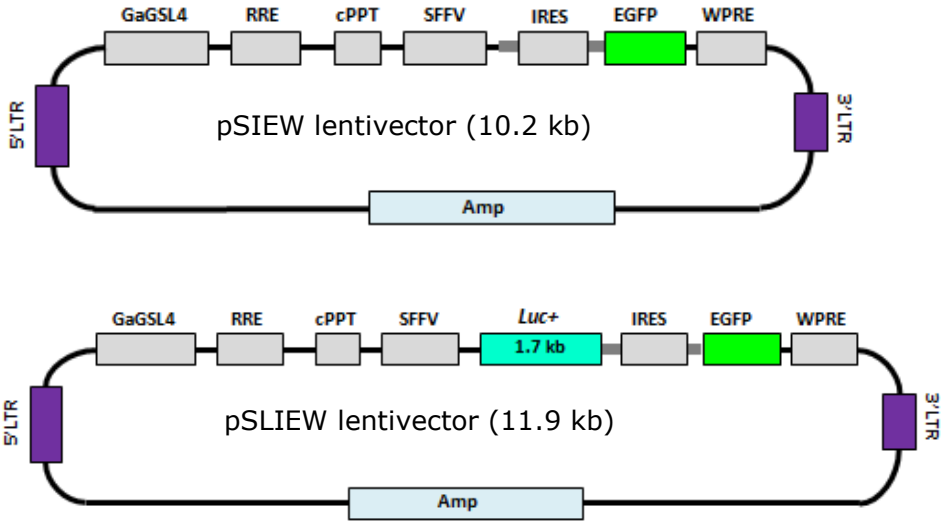

Figure 4.9 Schematic representation of generated pSLIEW. The insertion of *luc+* reporter gene (1.7 kb) upstream of IRES and EGFP in the pSIEW lentivector (10.2 kb) backbone generating a 11.9 kb pSLIEW plasmid. The backbone of pSIEW contains 5'LTR, 3'LTR and all the important viral elements and Ampicllin resistant cassette in for selection in bacterial competent cells.

4.2.1.2 *RLuc* and mCherry expressing lentivector (pSRLICW)

The pSRLICW lentivector harbouring the *Renilla* luciferase (RLuc) reporter gene and mCherry fluorescence protein (mCherry) was generated by using pSIEW from Figure 4.5 as a main backbone vector. To construct a functional pSRLICW lentivector, the RLuc reporter gene has to be inserted upstream of IRES and mCherry protein gene downstream, replacing EGFP in the main pSIEW backbone. The pRL-SV40 (Figure 4.10) and pcDNA3.1-mCherry (Zeo) (Figure 4.11) vectors were selected for this purpose for the RLuc and mCherry reporter genes respectively. However, as there were no compatible restriction enzyme sites for these reporter genes to be inserted directly into the pSIEW plasmid, a more complex strategy had to be planned.

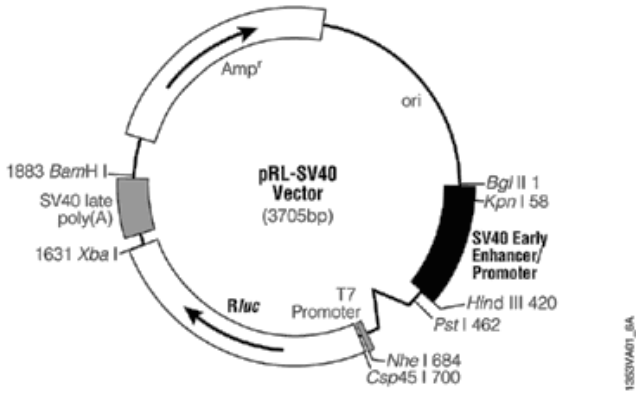

Figure 4.10 Map of pRL-SV40 vector. *Renilla* luciferase (RLuc) reporter gene is located in between NheI and XbaI recognition sites. This vector contains Ampicillin (Amp) resistant gene to enable selection of bacteria that contain the plasmid for amplification. (from Promega).

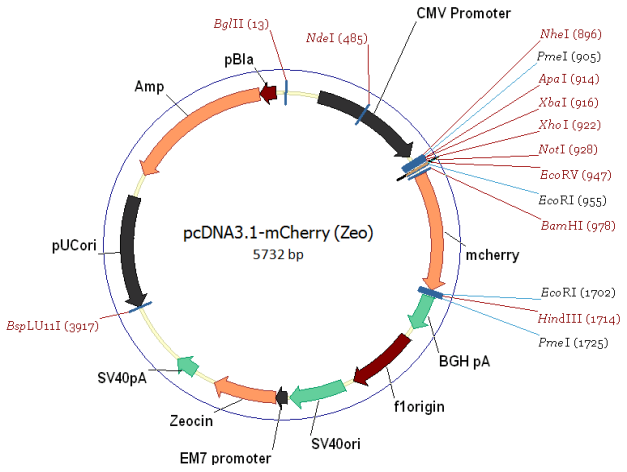

Figure 4.11 Map of pcDNA3.1-mCherry (Zeo). The intended mCherry is located between BamHI and EcoRI recognition sites. The vector contains Ampicillin (AMP) resistance gene for selection of bacteria that contain the plasmid and for amplification purposes. (provided by Christian Berens, Microbilogy Unit, University Erlangen-Nuernberg).

The reporter genes cassettes, RLuc and mCherry, could be inserted together into another vector with compatible insertion sites available. For this purpose, the pBluescript II KS+ vector (Figure 4.12) was selected because of the availability of the multiple cloning sites (MCS) to be manipulated, and a range of unique (single) restriction enzyme recognition sites. The sequence from SacI to XhoI was selected for manipulation as circled in red in the MSC of the vector.

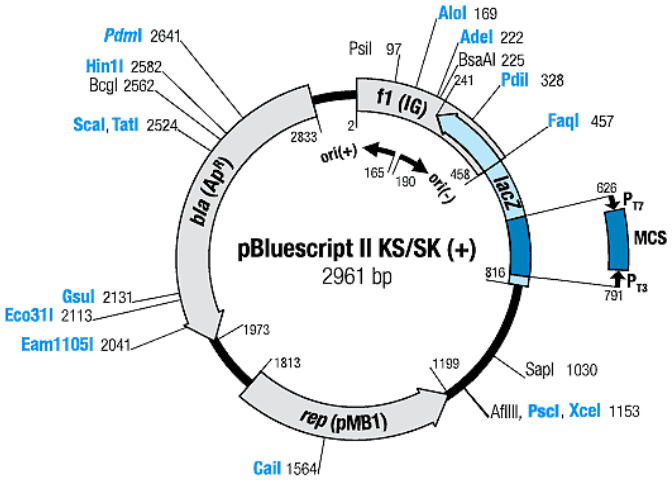

Multiple cloning site (MCS)

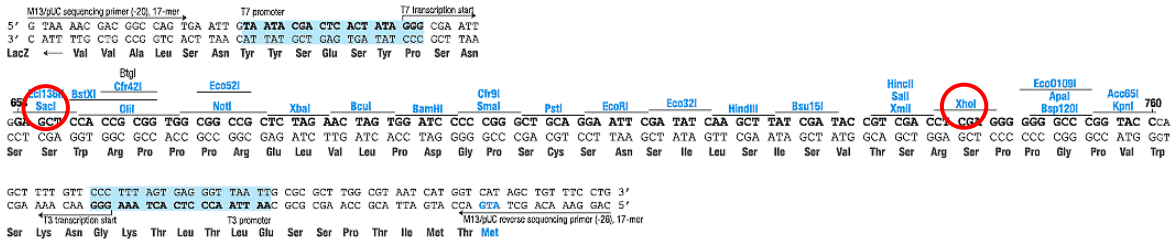

Figure 4.12 Map of pBluescript II KS+ with MCS sequence. pBluescript II KS(+) vector contains a multiple cloning site (MCS) with series of unique (single) restriction enzymes recognition sites which facilitates insertion of genes of interest. A range of 93 bp nucleotides from SacI and XhoI (circled in red) was replaced by a designed 79-bp polylinker oligonucleotides with series of unique restriction enzymes sequence. (source: Thermo Scientific).

A polylinker of oligonucleotides containing a series of restriction enzymes was designed as illustrated in Figure 4.13. The restriction enzymes in the polylinker were assembled so that the inserted genes would be in the right position and order. Figure 4.13A illustrates the series of restriction enzymes with gaps between Csp45I and XbaI, EcoRI and NcoI, BglII and MunI, and SalI and XhoI, within which these gaps were filled in with at least four nucleotides (allocated as n). Figure 4.13B illustrates the gaps were intended in order for RLuc, IRES, mCherry and WPRE. The actual sequence of the polylinker (5'→3') is as shown in Figure 4.13C, with the gaps replaced with random nucleotide arrangements so as not to interfere with the functions of the downstream or upstream genes of the polylinker. Sequence in red showed the complementary sequence (3'→5') of the polylinker.

The idea of this polylinker is to replace SacI – XhoI sequence in the pBluescript II KS+ vector (approximately 93 bp nucleotides) with the polylinker of SacI – XhoI (approximately 76 bp nucleotides) and to insert the gene cassettes into the selected position in the polylinker sequence one after another. As the final event, when the polylinker was completely filled with the inserts, the BamHI—XhoI segment from the pSIEW vector will be replaced with the BamHI—XhoI sequence of the polylinker.

A

Sac I – BamHI – Csp45I – nnnn – Xba I – EcoRI – nnnn – Nco I – Bgl II – nnnn – Mun I – Sal I – nnnn – Xho I

B

Sac I – BamHI – Csp45I – *RLuc* – Xba I – EcoRI – IRES– Nco I – Bgl II – mCherry– Mun I – Sal I – WPRE – Xho I

C

5' – GAGCTCGGATCCTTCGAAGCTATCTAGAGAATTCAGCTCCATGGAGATCTGATCCAATTGGTCGACCGTACTCGAG – 3'

3' – CTCGAGCCTAGGAAGCTTCGATAGATCTCTTAAGTCGAGGTACCTCTAGACTAGGTTAACCAGCTGGCATGAGCTC– 5'

Figure 4.13 Polylinker oligonucleotides. ***A,*** Series of restriction enzymes constructed from SacI to XhoI with gaps within enzymes filled in by four nucleotides (n in blue). ***B,*** The nucleotides gaps were illustrated to be replaced by the intended inserts RLuc, IRES, mCherry and WPRE. ***C,*** The actual sequence of the polylinker (5'→3'; sense) with random nucleotides filling in the gap; underlined sequences are to indicated sequence of one restriction enzyme from the adjacent restriction enzyme sequence; nucleotides in blue are Red sequence indicates the complementary (3'→5'; antisense) of the polylinker.

The oligonucleotides were designed so that upon annealing, there is a 5'-SacI restriction enzyme recognition site overhang at the 3' end and 3'-XhoI restriction enzyme recognition site overhang at the 5' end.

The sense and antisense of the polylinker oligonucleotides were hybridized as detailed in Materials and Methods Section 2.2.2.9. To ligate the annealed oligonucleotides with the pBluescript II KS+ vector, the vector was digested with SacI and XhoI enzymes to linearise and remove the 93 bp of SacI to XhoI segment. Figure 4.14 shows a fragment of 2961 bp of the linearized pBluescript II KS+ vector. The band was excised under UV-

light and purified using Qiaquick gel extraction kit. The purified vector was ligated with 76 bp polylinker oligonucleotides and transformed into JM109 competent cells for production of clones as described in Materials and Methods. Plasmid DNA was prepared from these clones.

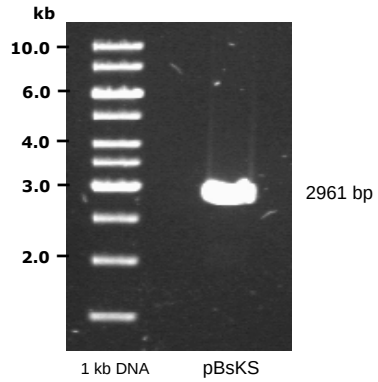

Figure 4.14 Digestion and gel purification of pBluescipt II KS+ with SacI and XhoI. Aliquot of 1.2 µg of pBluescript II KS+ vector was incubated with restriction enzymes SacI and XhoI in 1x Buffer SacI at 37ºC for 1 hour. Enzymes were inactivated at 80ºC for 20 minutes following 1% agarose gel electrophoresis for 60 minutes. Gel was stained in 2 µg/ml ethidium bromide solution prior to viewing under UV-light. Digested DNA was run against 1kb ladder for identification of the band size. Gel showed linearized vector at 2.9 kb. Band was excised and purified as described in *Materials and Methods* for ligation with hybridized polylinker oligonucleotides.

The clone DNA was digested with restriction enzyme Csp45I, which is a unique single cutting recognition site in the oligonucleotide. With the polylinker insert ligated in the vector, the expected band was 2944 bp. Figure 4.15 shows clones 2 and 3 to be positive for the oligonucleotide insert. Clones 1 and 4 were not ligated. Clones 2 and 3 were amplified by overnight LB broth culture to prepare a purified higher concentration of DNA as detailed in Materials and Methods.

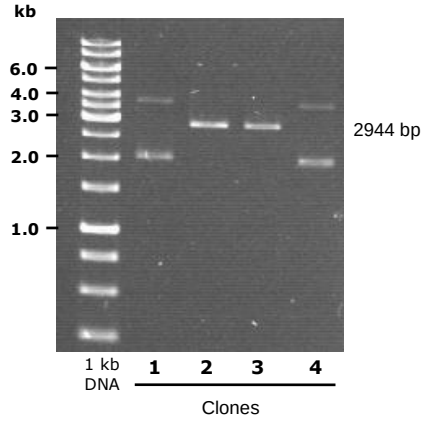

Figure 4.15 Restriction digest of oligonucleotides–pBluescript II KS+ by Csp45I. Aliquots of 1µg DNA from plasmids were incubated with Csp45I in 1x Buffer Tango at 37ºC for 1 hour. Enzyme was heat inactivated at 80ºC for 20 minutes following by 1% agarose gel electrophoresis for 90 minutes. Gel was stained in 2 µg/ml ethidium bromide solution for 20 minutes before viewing under UV-light. Gel showed clones 2 and 3 yielded a single band at 2.9 kb. These clones indicated successful ligation of polylinker oligonucleotides and pBluescript II KS+ vector.

For insertion of IRES into the modified pBluescript II KS+ vector-oligo ligated (pBsKS-PL vector), the IRES fragment was isolated from pSIEW by digesting the vector with EcoRI and NcoI restriction enzymes. In parallel, the pBsKS-PL vector was also digested with the same enzymes. Figure 4.16 showed single band of the linearized two preparation of pBsKS-PL vector in lane 2 and 3. The digested pSIEW vector produced three bands of 526 bp, 592 bp and 6000 bp. The IRES fragment isolated was further confirmed as shown in gel on the right to be a 592 bp fragment. The linearized pBsKS–PL and the IRES bands were excised under UV-light and purified using gel extraction kit.

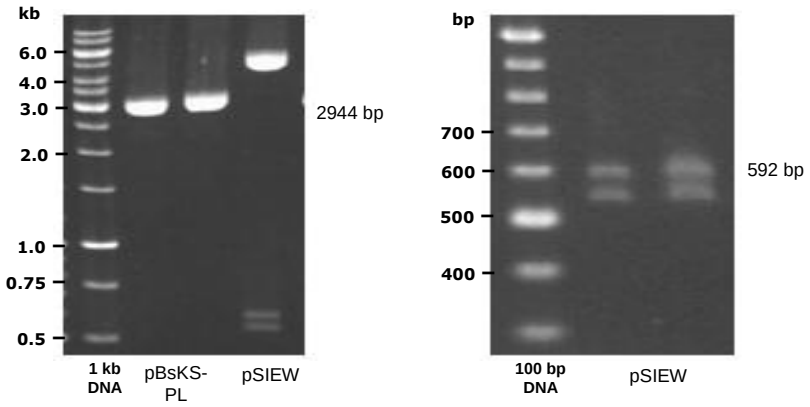

Figure 4.16 Restriction digest of pBsKS-PL and pSIEW vectors with EcoRI and NcoI. Aliquots of 1 µl vectors DNA were incubated with restriction enzymes EcoRI and NcoI in 2x Buffer Tango at 37ºC for 1 hour. Enzymes were inactivated at 80ºC for 20 minutes followed by 1% agarose gel electrophoresis for 60 minutes. Gel was stained in 2 µg/ml ethidium bromide solution for 20 minutes prior to viewing under UV-light. Digested DNA was run against 1kb DNA ladder (gel on the left) and 100 bp DNA ladder (gel on the right) for identification of the band size. Gel on the left showed linearized pBsKS-PL giving bands sizes of 2.9 kb in the two digestions prepared. pSIEW digestion gave 3 separated fragments sizes; expected band size for IRES was at 592 bp which was confirmed on the gel on the right to be the upper band. Linearized pBsKS-PL and IRES bands were excised and purified for ligation as described in the *Materials and Methods*.

The purified vector and IRES DNA was ligated and transformed into competent cells JM109 for colony formation on LB agar plates. Plasmid DNA was prepared from these colonies. To verify that the vector contained the inserted IRES fragment, plasmid DNA was digested with Csp45I restriction enzyme. Figure 4.17 shows different plasmid DNA samples following digestion with Csp45I enzymes. With the IRES fragment inserted, the predicted band size was 3536 bp, without IRES fragment insertion the band size would be 2944 bp. Out of nine colonies tested, eight colonies were positive for the IRES insert, one clone did not have the insert in. The cloned vectors from positive 3536 bp bands were amplified in LB broth and vector DNA was isolated and purified as described in Materials and Methods Section 2.2.2.7 and 2.2.2.8.

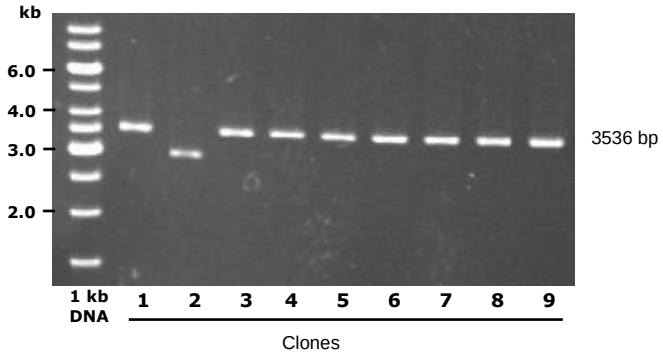

Figure 4.17 Restriction digest of pBsKS-PL – IRES ligation by Csp45I. Aliquots of 1µg DNA from plasmids were incubated with Csp45I in 1x Buffer Tango at 37ºC for 1 hour. Enzyme was heat inactivated at 80ºC for 20 minutes followed by 1% agarose gel electrophoresis for 60 minutes. Gel was stained in 2 µg/ml ethidium bromide solution for 20 minutes prior to viewing under UV-light. Digested DNA was run against 1kb DNA ladder for identification of the band size. The numbers indicated the DNA of clones in the lanes. Gel showed 9 plasmid clones was digested for verification of the insert. All clones except clone 2 linearized yielded a band size of 3.5 kb contained insertion of IRES fragment.

To insert the WPRE fragment into the cloned pBsKS-PL-IRES vector, the WPRE segment was isolated from pSIEW. In the original plan, when designing the polylinker oligonucleotides, WPRE was supposed to be inserted between the SalI and XhoI restriction enzymes recognition sites. However, in the pSIEW vector (refer to Figure 4.5), there were two SalI recognition sites at both ends (upstream and downstream) of WPRE, in which the SalI recognition sites were upstream of XhoI recognition site. Therefore, the pSIEW lentivector was digested with restriction enzyme SalI to isolate the WPRE fragment. In the same manner, the cloned pBsKS-PL-IRES vector was also digested with the same restriction enzyme to prepare for ligation with WPRE. Gel electrophoresis as shown in Figure 4.18 shows digestion of the pBsKS-PL-IRES vector in which the restriction enzyme SalI linearized the vector into a 3536 bp band, and digestion of two preparations of pSIEW vector with SalI produced two bands at 614 bp and 9595 bp. The linearized pBsKS-PL-IRES vector and the 614 bp WPRE fragment bands were excised and purified for ligation. The ligated vector and WPRE were transformed into competent cells JM109 and plated on LB agar for colonies formation as detailed in Materials and Methods Section 2.2.2.5. Plasmid DNA prepared from these colonies was digested with EcoRI for verification of insertion.

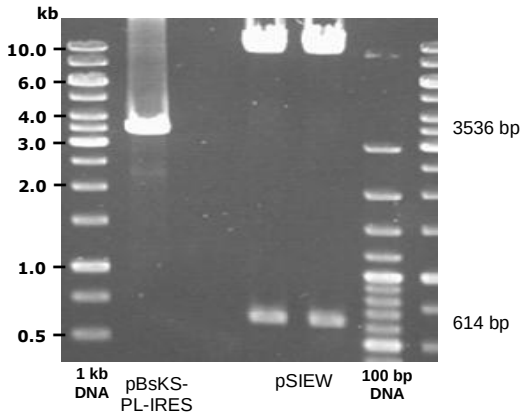

Figure 4.18 Digestion of pBsKS-PL-IRES and pSIEW by SalI. Aliquots of 1 µl vectors DNA were incubated with restriction enzyme SalI in 1x Buffer Tango at 37ºC for 1 hour. Enzymes were inactivated at 80ºC for 20 minutes followed by 0.8% agarose gel electrophoresis for 60 minutes. Gel was stained in 2 µg/ml ethidium bromide solution for 20 minutes prior to viewing under UV-light. Digested DNA was run against 1kb DNA ladder and 100 bp DNA ladder for identification of the band size. Gel showed linearized pBsKS-PL-IRES giving bands sizes of 3.5 kb and pSIEW digestion yielded bands at 9.5 kb and 614 bp lengths. Linearized pBsKS-PL-IRES and 614 bp WPRE bands were excised and purified for ligation as described in the *Materials and Methods*.

Figure 4.19 shows the agarose gel electrophoresis of 13 plasmid DNA digested with restriction enzyme EcoRI. Plasmids with WPRE insertion in pBsKS-PL-IRES were expected to give a single band at 4159 bp. Without insertion of WPRE colonies would retain a 3545 bp band. The gel showed plasmid 1, 3, 5, 9, 11, 12 and 13 showed the expected band indicating positive insertion of WPRE in the vector. The other plasmids were negative for insertion.

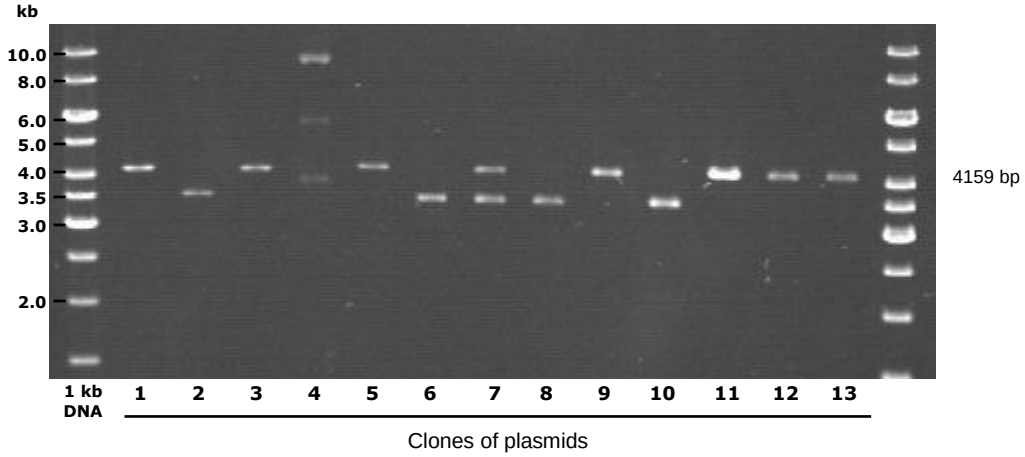

Figure 4.19 Restriction analysis of pBsKS-PL-IRES–WPRE ligation. Aliquots of 1µg DNA from plasmids were incubated with EcoRI in 1x Buffer Tango at 37ºC for 1 hour. Enzyme was heat inactivated at 80ºC for 20 minutes followed by 1% agarose gel electrophoresis for 90 minutes. Gel was stained in 2 µg/ml ethidium bromide solution for 20 minutes prior to viewing under UV-light as described in *Materials and Methods*. Digested DNA was run against 1kb DNA ladder for identification of the band size. Gel showed 13 clones were digested for verification of insert. Positive WPRE inserted in pBsKS-PL-IRES plasmid yielded band at size of 4159 bp. Clones 1, 3, 5, 9, 11, 12 and 13 were positive generation of pBsKS-PL-IRES-WPRE plasmids.

To confirm the insertion was in the right direction, plasmids DNA positive for insertion of WPRE were randomly selected and digested with restriction enzymes PstI and XhoI followed by gel electrophoresis of the digested DNA. In the correct direction of the inserted WPRE, the expected bands will be at 608 bp and 3551 bp lengths. Of seven DNA samples tested, four plasmids were inserted with the right direction of WPRE as shown in Figure 4.20. The positive correct direction of WPRE plasmid, pBsKS-PL-IRES-WPRE, was further amplified in large volumes of LB broth to prepare a higher endotoxin-free DNA as detailed in Materials and Methods Section 2.2.2.7 and 2.2.2.8.

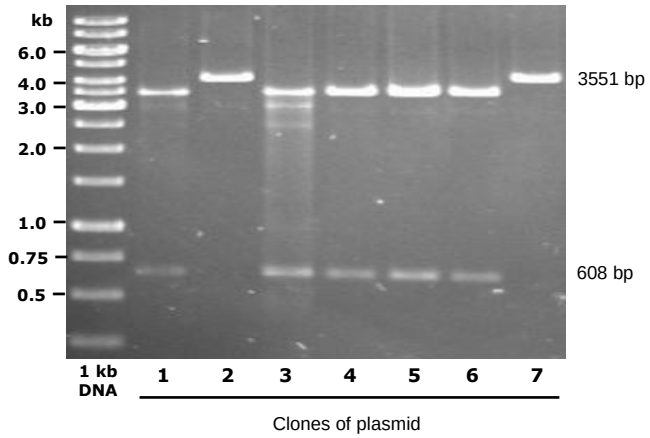

Figure 4.20 Digestion of pBsKS-PL-IRES-WPRE with NcoI. To confirm insertion of WPRE was in the correct direction, aliquot of 1µg DNA from plasmids were incubated with restriction enzymes PstI and XhoI in 1x Buffer R at 37ºC for 1 hour as detailed in *Materials and Methods*. Enzyme was heat inactivated at 80ºC for 20 minutes. Agarose gel electrophoresis was run in 0.8% agarose gel for 60 minutes. Gel was stained in 2 µg/ml ethidium bromide solution for 20 minutes before viewing under UV light. Digested DNA was run against 1kb DNA ladder for identification of the band size. The numbers indicate the DNA of clone in the lanes. Gel showed 7 plasmid clones was tested. Clones 1,3,4,5 and 6 contained insertion of WPRE fragment in correct direction.

The next step was insertion of the RLuc reporter gene into the pBKS-PL-IRES-WPRE vector. To insert the RLuc reporter gene, the RLuc segment was digested out from pRL-SV40 vector (refer to Figure 4.10). In designing the polylinker, the RLuc gene was supposed to be inserted between the Csp45I and XbaI restriction sites. In the pRL-SV40 vector, the Csp45I recognition site was located upstream of the RLuc gene and the XbaI recognition site was downstream of the gene. However, on looking at the sequence of the gene, the Csp45I site was located at the beginning of the ATG reporter RLuc gene. If the vector was cut with the mentioned restriction enzyme, this would render the RLuc gene non-funtional. Therefore, the NheI restriction enzyme in the upstream of the RLuc gene was used instead. However, some modification was made in the preparation of the genes for ligation.

The pBsKS-IRES-WPRE vector was digested with restriction enzyme Csp45I whereas the pRL-SV40 vector was digested with restriction enzyme NheI. After incubation with the restriction enzymes, the T4 DNA Polymerase was added to blunt-ended sticky ends of the linearized vectors, as detailed in Materials and Methods Section 2.2.2.10. The digested and blunt-ended DNAs of both vectors were purified with Qiaquick PCR Purification Kit. Next, the purified blunt-ended DNAs of the pBsKS-IRES-WPRE and

pRL-SV40 vectors were digested with restriction enzyme XbaI and agarose gel electrophoresis was performed. Figure 4.21 shows that the XbaI digested pPR-SV40 produced two bands of 2768 bp and 947 bp lengths. The RLuc reporter gene was the latter. The pBsKS-IRES-WPRE vector yielded a single 4.1 kb. The vector and the RLuc bands were excised and gel purified before ligation followed by transformation into Stbl3 competent cells for colony formation. Plasmid DNA was prepared from these colonies.

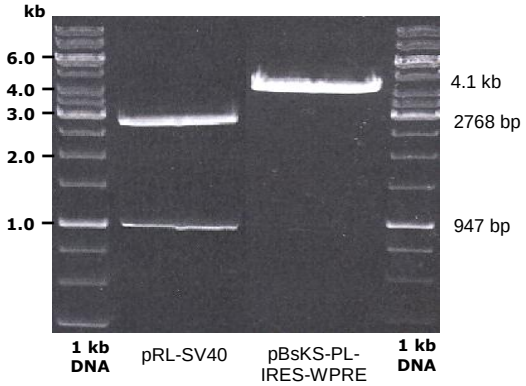

Figure 4.21 Digestion of pRL-SV40 and pBsKS-PL-IRES-WPRE vectors for ligation. To prepare the vectors for ligation, aliquot of 1µg DNA from pRL-SV40 and pBsKS-PL-IRES-WPRE was incubated with restriction enzymes NheI and Csp45I respectively in 1x Buffer Tango at 37ºC for 1 hour. Enzyme was heat inactivated at 80ºC for 20 minutes. For blunt-ending the overhang ends of digested vectors, T4 DNA Polymerase was added with 1x T4 DNA Polymerase Buffer and 100 µM dNTPs in final volume of 30 µl, and incubated at 11ºC for 20 minutes. Enzyme was inactivated at 75ºC for 10 minutes. The blunt-ended vectors were purified using Qiaquick PCR Purification kit. Aliquots of 25 µl of purified vectors were incubated at 37ºC for 1 hour with restriction enzyme XbaI separately. Enzyme was inactivated at 80ºC for 20 minutes. Protocols used were as detailed in *Materials and Methods*. Agarose gel electrophoresis was run on 0.8% agarose gel in 1x TAE buffer for 70 minutes. Gel was stained in 2 µg/ml ethidium bromide for 20 minutes before viewing under UV light. Digested DNA was run against 1kb ladder for identification of the band size.

Plasmid DNA was digested with XbaI for confirmation of the insert. Gel electrophoresis of the digested plasmids was shown in Figure 4.22. Successful ligation was expected to yield a band of 5106 bp length. The gel showed that out of 15 plasmids isolated, only one clone (clone 8) was positive for the RLuc insertion into the pBsKS-IRES-WPRE plasmid. The other clones had no insert. The clone inoculation of the positive pBsKS-IRES-WPRE-RLuc plasmid was cultured in higher volume of LB broth to achieve higher concentration of purified endotoxin-free DNA as detailed in Materials and Methods. The following step was insertion of mCherry into the pBsKS-PL-IRES-WPRE-RLuc plasmid.

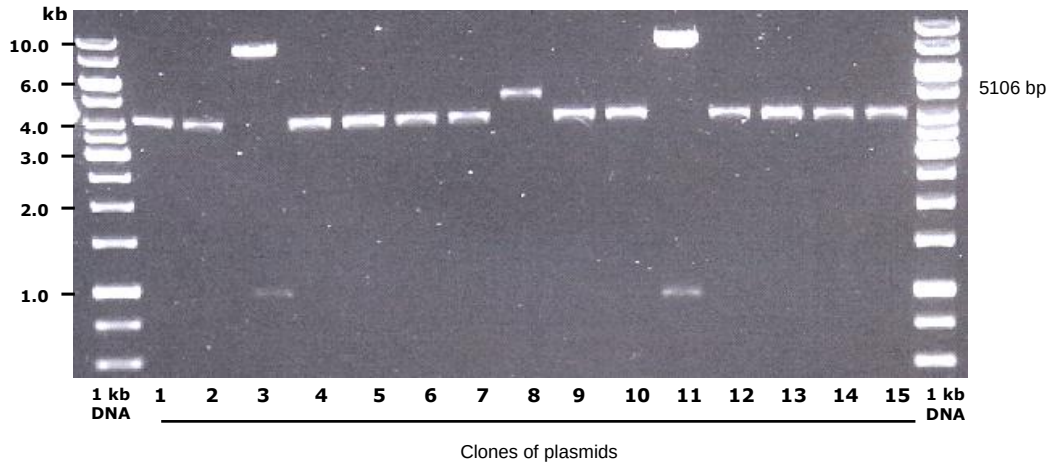

Figure 4.22 Digestion of pBsKS-PL-IRES-WPRE-RLuc with XbaI. To confirm insertion of RLuc in the pBsKS-PL-IRES-WPRE vector, aliquot of 1µg DNA from plasmids were incubated with restriction enzyme XbaI in 1x Buffer Tango at 37ºC for 1 hour as detailed in *Materials and Methods*. Enzyme was heat inactivated at 80ºC for 20 minutes. Agarose gel electrophoresis was run in 0.8% agarose gel for 60 minutes. Gel was stained in 2 µg/ml ethidium bromide for 20 minutes before viewing under UV light. Digested DNA was run against 1kb ladder for identification of the band size. The numbers indicated the DNA of clone in the lanes. Gel showed 15 clones were tested. Clone 8 was positive for producing a 5.1 kb pKS-PL-IRES-WPRE-RLuc vector.

For insertion of mCherry protein gene into the plasmid, the mCherry gene as taken out of the 5732 bp pcDNA3.1-mCherry (Zeo) vector (refer to Figure 4.11). In the polylinker oligonucleotide sequence (refer to Figure 4.9), the mCherry was designed to be inserted in between BglII and MunI recognition sites. To isolate the mCherry fragment from the vector, however, the BamHI and EcoRI recognition sites were used instead. It was possible to use these restriction enzymes because of the presence of the same overhang sequences exposed following digestion. The restriction enzyme BamHI has the same overhang sequence as the BglII enzyme while the EcoRI restriction enzyme has the same sequence as the MunI enzyme as stated below.

BamHI sequence: 5'…G^GATC C…3'
3'…C CTAG^G…5'

^ indicates the cutting site of the enzymes

BglII sequence: 5'…A^GATC T…3'
3'…T CTAG^A…5'

EcoRI sequence: 5'…G^AATT C…3'
3'…C TTAA^G…5'

MunI sequence: 5'…C^AATT G…3'
3'…G TTAA^C …5'

Therefore, for the ligation to take place, the pcDNA3.1-mCherry (Zeo) vector was digested with restriction enzymes BamHI and EcoRI to isolate the mCherry whereas the pBsKS-IRES-WPRE-RLuc plasmid was digested with restriction enzymes BglII and MunI. Figure 4.23 showed gel results of two preparations of digestion for each vector and plasmid. The digestion produced a single band of linearized pBsKS-IRES-WPRE-RLuc plasmid at 5.1 kb and digestion of pmCherry vector yielded two bands at 5.0 kb and 724 bp. The mCherry fragment was the smaller band size. The linearized plasmids and the mCherry fragments were excised under UV-light and were purified for ligation followed by transformation into Stbl3 competent cells and colony formation on agar plates. Purified DNA was prepared from these colonies as detailed in Materials and Methods.

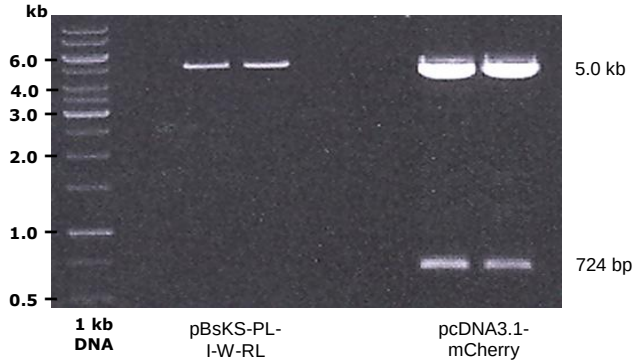

Figure 4.23 Restiction digest of pBsKS-PL-IRES-WPRE-RLuc and pcDNA3.1-mCherry vectors for ligation. To prepare the vectors for ligation, aliquot of 1.5 µg DNA from pcDNA3.1-mCherry was incubated with restriction enzymes BamHI and EcoRI in 2x Buffer Tango for 1 hour whereas aliquot of 1 µg pBsKS-PL-IRES-WPRE-RLuc was incubated with restriction enzymes BglII and MunI in 1x Buffer Tango at 37ºC for 1 hour. Enzyme was heat inactivated at 80ºC for 20 minutes. Protocols were as detailed in *Materials and Methods*. Agarose gel electrophoresis was run on 0.8% agarose gel in 1x TAE buffer for 60 minutes. Gel was stained in 2 µg/ml ethidium bromide for 20 minutes before viewing under UV light. Digested DNA was run against 1kb DNA ladder for identification of the band size. Gel showed two restriction digests prepared for each vectors. Linearized pBsKS-PL-IRES-WPRE-RLuc vector bands were at 5.1 kb. Digestion of pcDNA3.1-mCherry yielded 2 bands at size of 5.0 kb and 724 bp. Bands of linearized plasmid and 724 mCherry fragment were excised and purified for ligation as detailed in *Materials and Methods*.

The cloned plasmid DNA was digested with restriction enzyme Csp45I for confirmation of the insert. Figure 4.24 showed bands produced on gel following electrophoresis. Insertion of mCherry in pBsKS-IRES-WPRE-RLuc plasmid was expected to yield a 5.8

kb clones. Five clones tested were positive for the insertion with bands at almost 6 kb. These clones generated the pBsKS-IRES-WPRE-RLuc-mCherry plasmids.

Figure 4.24 Digestion of pBsKS-PL-IRES-WPRE-RLuc-mCherry by Csp45I. To confirm insertion of mCherry in the pBsKS-PL-IRES-WPRE-RLuc vector, aliquots of 1µg DNA from plasmids were incubated with restriction enzyme Csp45I in 1x Buffer Tango at 37ºC for 1 hour as detailed in *Materials and Methods*. Enzyme was heat inactivated at 80ºC for 20 minutes. Agarose gel electrophoresis was run in 0.8% agarose gel for 60 minutes. Gel was prepared with ethidium bromide at a concentration of 1 µg/ml gel. The gel was viewed directly under UV light following electrophoresis. Digested DNA was run against 1kb ladder for identification of the band size. The numbers indicated the DNA of clone in the lanes. Gel showed all 5 clones tested were positive for insertion of mCherry with expected band at 5.8 kb which indicated clones of pKS-PL-IRES-WPRE-RLuc-mCherry vector was generated.

The completely filled polylinker on the pBsKS-IRES-WPRE-RLuc-mCherry plasmids were ready to be removed and inserted into the pSIEW vector. As usual, the cloned plasmid was produced into higher copies for higher purified DNA concentrations.

To insert the polylinker nucleotide into pSIEW vector, the 1.9 kb fragment from BamHI to XhoI recognition sites containing IRES, EGFP and WPRE in the vector had to be removed. This removal was to be replaced by insertion of a 2.9 kb fragment from the filled oligonucleotides. For this purpose, the pSIEW vector was digested with restriction enzymes BamHI and XhoI. The cloned pBsKS-IRES-WPRE-RLuc-mCherry plasmid was digested with restriction enzymes GsuI followed by BamHI and XhoI. This additional cutting was required to avoid producing two bands at similar size if digested by BamHI and XhoI only. The digested vector and plasmid was run in gel electrophoresis and the bands produced were shown in Figure 4.25. Two preparations of digestion for both vector and cloned plasmid were shown. Digestion of the pSIEW vector produced two bands, the removed 1.9 kb band, and the 8.3 kb band size. The cloned plasmid was digested into three segments producing bands at 2.9 kb, 1.5 kb and 1.4 kb lengths. The vector 8.3 kb band and the cloned plasmid 2.9 kb band were excised and gel purified as described in

Materials and Methods Sections 2.2.2.3 to 2.2.2.5. The purified DNA of both fragments were ligated and transformed into competent cells Stbl3 for colony formation and plasmids DNA isolation.

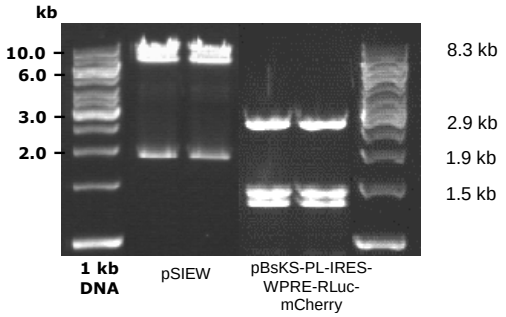

Figure 4.25 Digestion of pSIEW and pBsKS-PL-IRES-WPRE-RLuc-mCherry. Aliquots of 0.3µg DNA from pSIEW vector were incubated with restriction enzymes BamHI and XhoI in 1x Buffer Tango at 37ºC for 1 hour as detailed in *Materials and Methods.* Aliquots of 0.3µg DNA from pBsKS-PL-IRES-WPRE-RLuc-mCherry plasmid were incubated with restriction enzymes GsuI in 1x Buffer Tango at 30ºC for 1 hour followed by addition of restriction enzymes BamHI and XhoI in 2x Buffer Tango at 37ºC for 1 hour as detailed in *Materials and Methods*. Enzymes were heat inactivated at 80ºC for 20 minutes. Gel was prepared with ethidium bromide at a concentration of 1 µg/ml gel. The gel was viewed directly under UV light following electrophoresis. Digested DNA was run against 1kb ladder for identification of the band size. Gel showed two preparations of digestions for each vector and plasmid. pSIEW digestion yielded band at 8255 bp and 1954 bp, pBsKS digestion yielded bands at 2913 bp, 1507 bp and 1465 bp.

DNA exracted form the clone was digested with restriction enzymes BamHI and PvuI for confirmation of the ligation and inserts. Successful ligations were expected to produce a 11169 bp vector. The expected bands size from the digested clone DNA were 6576 bp and 4593 bp. Figure 4.26 showed gel electrophoresis results from the digestion. DNA from 10 clones was digested; all clones except clone 8 produced bands at the expected size, proving that in these 9 clones polylinker was successfully inserted into the pSIEW vector. pSRLICW lentivector was successfully cloned.

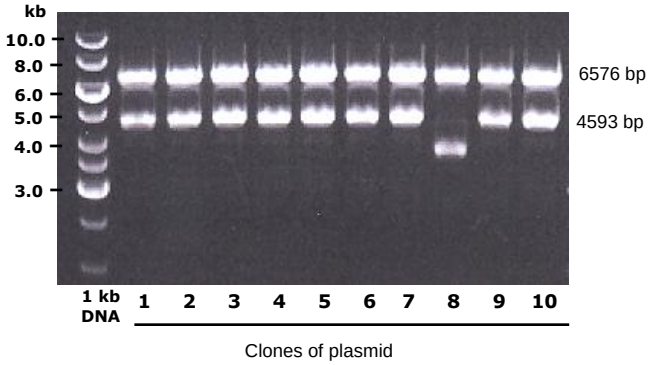

Figure 4.26 Restriction digestion of pSRLICW by BamHI and PvuI for insert confirmation. To confirm insertion of polylinker in the pSIEW vector, aliquot of 1µg DNA from plasmids were incubated with restriction enzymes BamHI and PVuI in 2x Buffer Tango at 37ºC for 1 hour as detailed in *Materials and Methods*. Enzyme was heat inactivated at 80ºC for 20 minutes. Agarose gel electrophoresis was run in 0.8% agarose gel for 80 minutes. Gel was prepared with ethidium bromide at a concentration of 1 µg/ml gel. The gel was viewed directly under UV light following electrophoresis. Digested DNA was run against 1kb ladder for identification of the band size. The numbers indicated the clone in the lanes. Gel showed 10 clones were tested. Except clone 8, all clones were positive for insertion producing expected bands at 6576 bp and 4593 bp length. The pSRLICW vector was generated with a length of 11169 bp.

Schematic representation of the constructed pSRLICW lentivector is as shown below. The RLuc reporter gene is located upstream of mCherry fluorescent protein gene connected by IRES. The expressions of RLuc and mCherry are driven by the SFFV promoter upstream of RLuc.

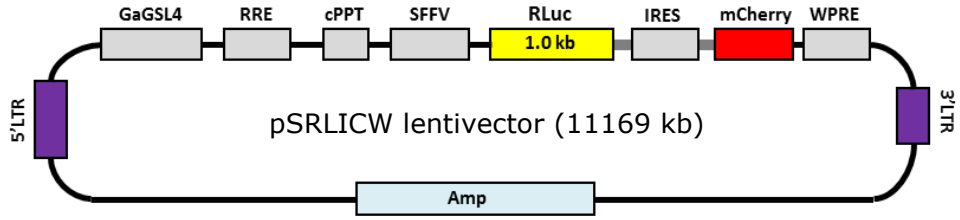

Figure 4.27 Schematic representation of generated pSRLICW vector. The new constructed lentivector contained RLuc reporter gene upstream of IRES and mCherry fluorescent protein gene. The SFFV promoter in the vector backbone promotes the expression of RLuc and mCherry. Lentivector also contains Ampicillin (Amp) resistance gene for a selection of plasmid in bacterial culture.

4.2.2 Production of lentivirus

To be able to use the newly constructed pSLIEW and pSRLICW lentivectors for the intended *in vivo* experiment, the functionalities of the lentivectors were first determined in *in vitro* experiments. To do this, lentivirus was produced by transfecting 293T cells with the lentivirus particles as described in Materials and Methods Sections 2.2.2.11 to 2.2.2.13. Briefly, to produce lentivirus particles, the lentivectors were prepared with packaging and envelope vectors, the pCMV-dR8.91 and the pMD2.G respectively (Figure 4.28). The peudovirus particles were in form of calcium phosphate precipitates.

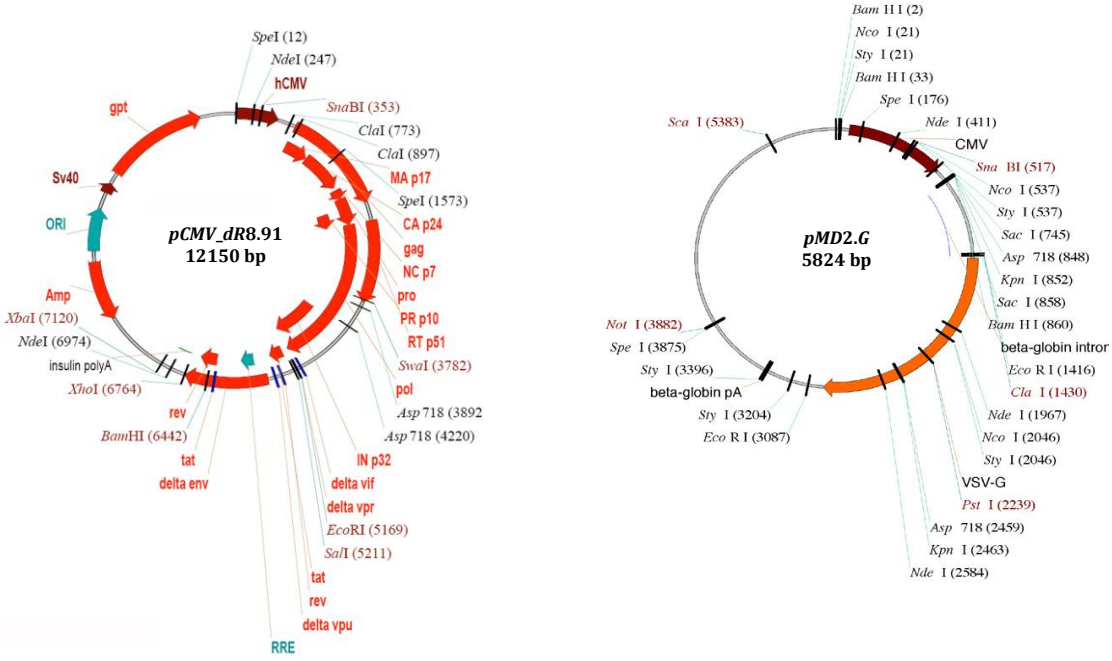

Figure 4.28 Maps of pCMVdR8.91 and pMD2.G vectors. Packaging and envelop vectors used in production of pseudovirus particles with the newly constructed lentivectors. (Vector maps source from LentiWeb.com)

These precipitates were added into 293T cells cultured at the confluency of 30% to 40% plated the day before. Figure 4.29 shows transfection of lentivirus in 293T cells as viewed under a fluorescent microscope. With the presence of EGFP gene in the back bone of pSLIEW and the mCherry gene in the backbone of the pSRLICW the transfected 293T cells expressed the fluorescent protein as expected. Transfection with pSLIEW produced green 293T cells and pSRLICW transfection produced red cells. Viruses were left to replicate and reproduce themselves in the 293T cells for 3 days after removal of

unengulfted particles. The lentivirus produced in the medium was concentrated after 4 days in culture.

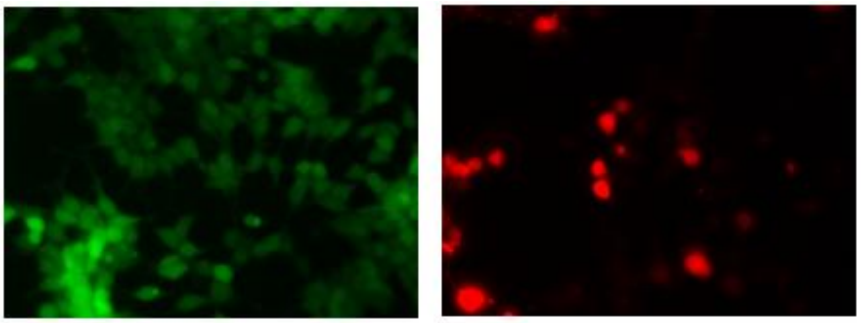

pSLIEW transfected 293T cells pSRLICW transfected 293T cells

Figure 4.29 Transfection of 293T cells with pSLIEW and pSRLICW. 293T cell were seeded at a concentration of 2 x 10^5 cells/ml in plates a day prior to transfection with the lentivirus. Aliquots of 20 µg DNA of pSLIEW or pSRLICW lentivectors were prepared with 15 µg DNA of pCMVd8.91 and 5 µg DNA of pMD2.G vectors for production of calcium phosphate ($CaPO_4$) as detailed in the *Materials and Methods*. Precipitates were left to develop for 30 minutes. The viral particles precipitates were dropped into the 30% - 40% confluent 293T cells. Figures showed pSLIEW transfected 293T cells expressing green fluorescence and pSRLICW transfected 293T cells expressing red fluorescence when view under fluorescence microscope a day after transfection. Imaged were taken at two separate experiments. 400x magnification.

The pSRLICW was newly generated just shortly before the end of this project. Therefore, the utilization of the lentiviral in the following steps were only based on the use of pSLIEW.

4.2.3 Transduction of cell lines with pSLIEW

pSLIEW lentivirus produced and concentrated as described above were used to transduce the leukaemic cell lines. Four cell lines were used for transduction with the lentivirus; two ALL cell lines, SEM and RS4;11, and two AML cell lines, Kasumi-1 and SKNO-1. Cells were transduced by spin inoculation as detailed in the Materials and Methods Section 2.2.2.15. Cells were left for 4 days for stable transduction and proliferation before viewing under a fluorescence microscope. Flow cytometric analysis was performed on the cell lines using a FACScan machine as detailed in Materials and Methods Section 2.2.2.15. Fluorescence photographs of the green fluorescence cells together with the flow cytometric histogram are shown in Figure 4.30. The histogram from FACS analysis showed that, from the same preparations of virus, SKNO-1 cells were easily transduced with a high intensity of green fluorescence cells measured. The RS4;11 cells were the

least infected with high populations of non-infected cells. As measured by FACS, the transduction efficiency for SEM cells was 45%, whereas in RS4;11cells the efficiency was only 5%. In Kasumi-1 cells, 72% cells were efficiently transduced and transduction in SKNO-1 cells was highly efficient with 98% of cells transduced. The flow results were run against non-infected controls. Fluorescent cells in photographs showed large populations of cells with a high intensity of green SKNO-1 cells compared to Kasumi-1 and SEM cells while in RS4;11 there were only a few cells and these had low fluorescence intensity. The photographs of fluorescent cells were consistent with the histogram of transduced cells.

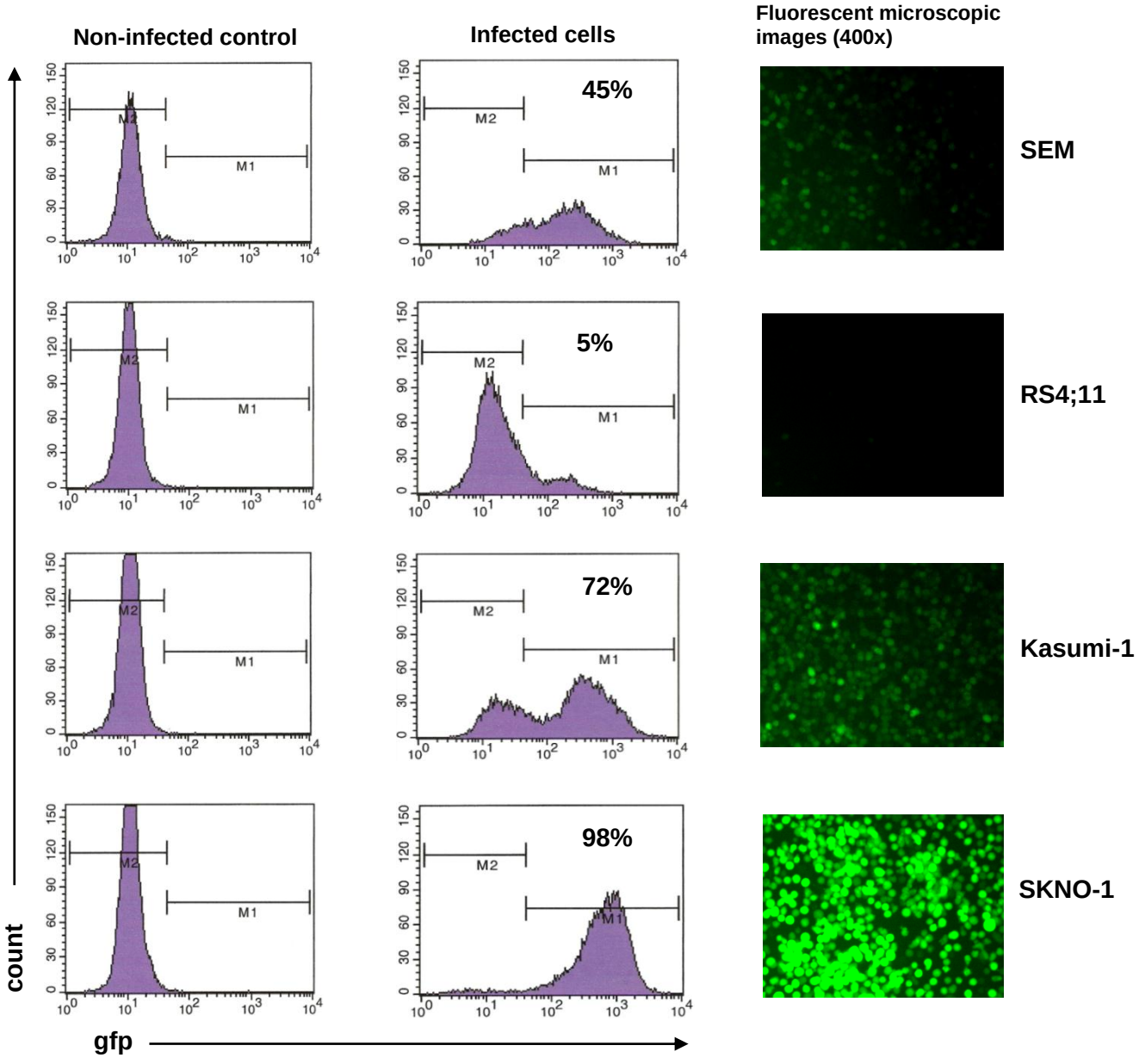

Figure 4.30 Analysis of transduced cell lines by flow cytometry and fluorescent microscopy.

With the exception of RS4;11, all the other transduced cells were kept according to the standard culture regime. RS4;11 was only kept in culture for a short period for analysis, the cells were discarded after when several passages no green fluorescent cells were detected under fluorescent microscopy and by luciferase assay.

4.2.3.1 Luciferase Assay

The luciferase assay was also performed on the transduced cell lines to determine the functionality of the luciferase reporter gene in the lentivirus. The luminescence count was measured using a Scintillation and Luminescence counter. 1 x 10^5 cells were processed for the analysis as detailed in Materials and Methods Section 2.2.2.17. Figure 4.31 showed the results of the analysis. The luminescence count detected in the transduced SEM cells was 15.3 x 10^4 and for the transduced RS4;11 cells was 0.44 x 10^4. Transduced Kasumi-1 was measured as 32.9 x 10^4 for luminescence count and transduced SKNO-1 cells was 134.8 x 10^4. These results complement the flow analysis on the transduced cells suggested that the efficiency of infection in ALL cell lines is much lower than AML lines. The efficiency of Kasumi-1 and SKNO-1 cells infection were 2.2-fold and 8.8-fold higher respectively than the SEM cells.

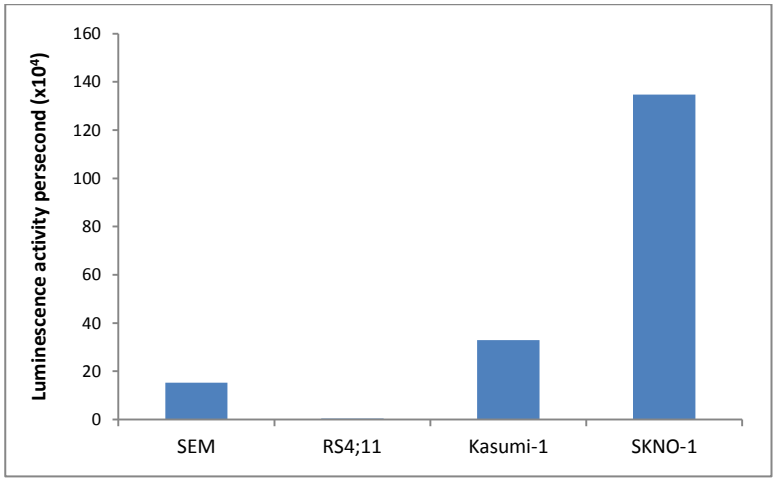

Figure 4.31 Luciferase assay of transduced cell lines. 1 x 10^5 of transduced cells line were washed in PBS and lysed with 1x lysis buffer using Luciferase Assay System (Promega) as described in *Materials and Methods*. 10 µl lysates were aliquoted into luminescence plate-reader. 50 µl Luciferase Assay Reagent was added prior to luminescence count by Scintillation and Luminescence Counter (Perkin Elmer).

4.2.3.2 Sorting of transduced cell populations

From the results of flow cytometric analysis of the transduced cells, it was shown that SEM and Kasumi-1 cells in culture consisted of a mixture of non-transduced and transduced cells. To establish a high percentage of transduced cells in culture, the Kasumi-1 and SEM cells were sorted for green (gfp) positivity using fluorescence-assisted cell sorting (FACS) as described in Materials and Methods Section 2.2.2.16. SKNO-1 cells were not sorted for gfp positivity as the transduction efficiency was very high.

Figure 4.32 shows a dot plot graph and the gating of gfp positive cells. Non-transduced cells were run as controls. Two distinguishable populations were detected as shown in pre-sort dot plots. Cells gated in green were populations of gfp positive cells (in the pre-sort column). For Kasumi-1, 28% of green fluorescence cells were gated as pre-sort and these cells were sorted for gfp positive population whereas for SEM, 39% gfp positive cells were gated in pre-sort and sorted out for gfp positive population. The purity of positive green fluorescence cells sorted (in the post-sort column) were 92% for Kasumi-1 and 95% for SEM. Approximately 1.5-2.0 x 10^6 gfp positive cells were sorted for both cells. Sorted cells were maintained in culture for the xenotransplant experiments described in Chapter 5.

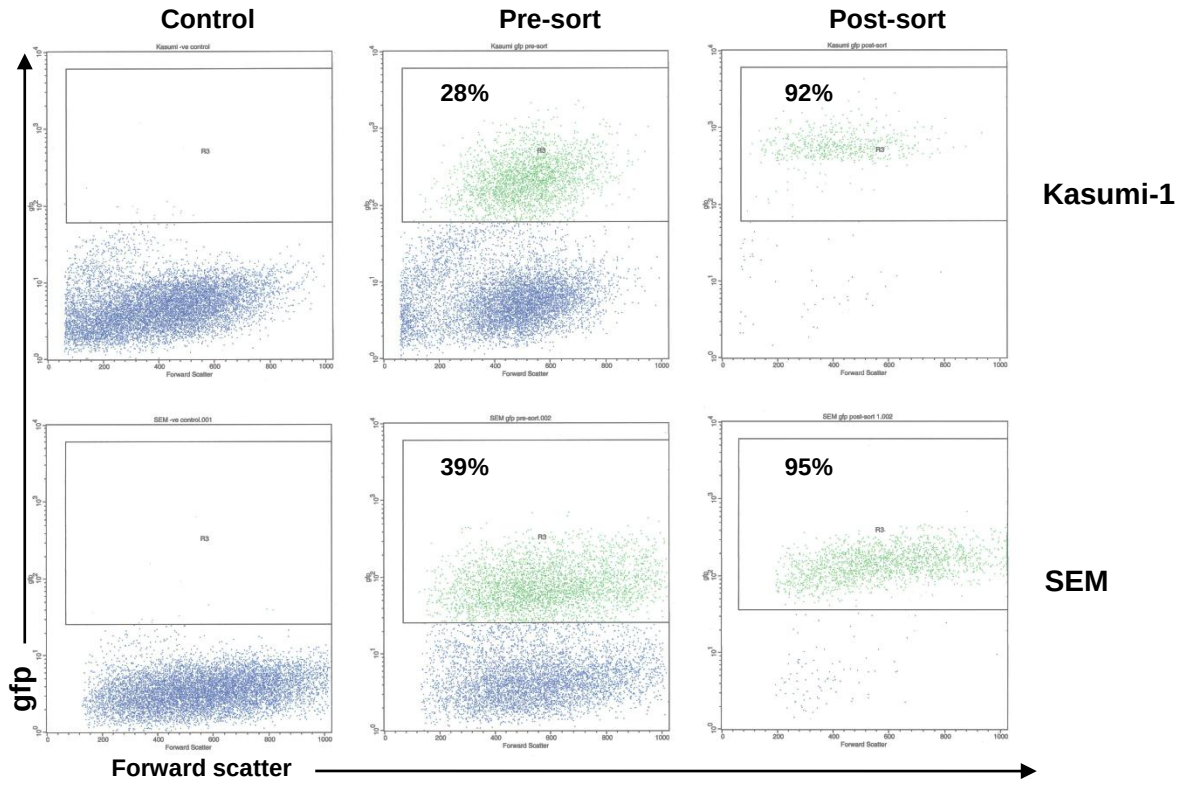

Figure 4.32 FACS sorted green positive (gfp+) cells. Aliquots of 10^7 Kasumi-1 and SEM cells were washed and resuspended with PBS. Cells were sorted into culture medium with addition of 2% Penicillin-Streptomycin as detailed in *Materials and Methods*. Dot plot graphs showed transduced Kasumi-1 and SEM cells were gated on the gfp+ cells in the pre-sort column by comparing to control negative cells. Sorted cells were analysed by FACS to determine the purity of cells as shown in the post-sort column.

4.2.3.3 Gfp/luc+ cells culture

Sorted SEM and Kasumi-1 gfp positive cells were maintained for stable and normal proliferation rates in culture. Cells were then checked by FACS analysis to determine populations of green positive cells. Figure 4.33 shows the FACS analysis and fluorescence images of sorted gfp+ SEM and Kasumi-1 cells. Histograms of the gfp+ sorted cells showed both SEM and Kasumi-1 cells have 89% green cells populations in culture. Approximately 10% of non-transduced cells were contaminating the sorted gfp+ cultures. Images of fluorescence cells confirmed the high populations of green cells in culture.

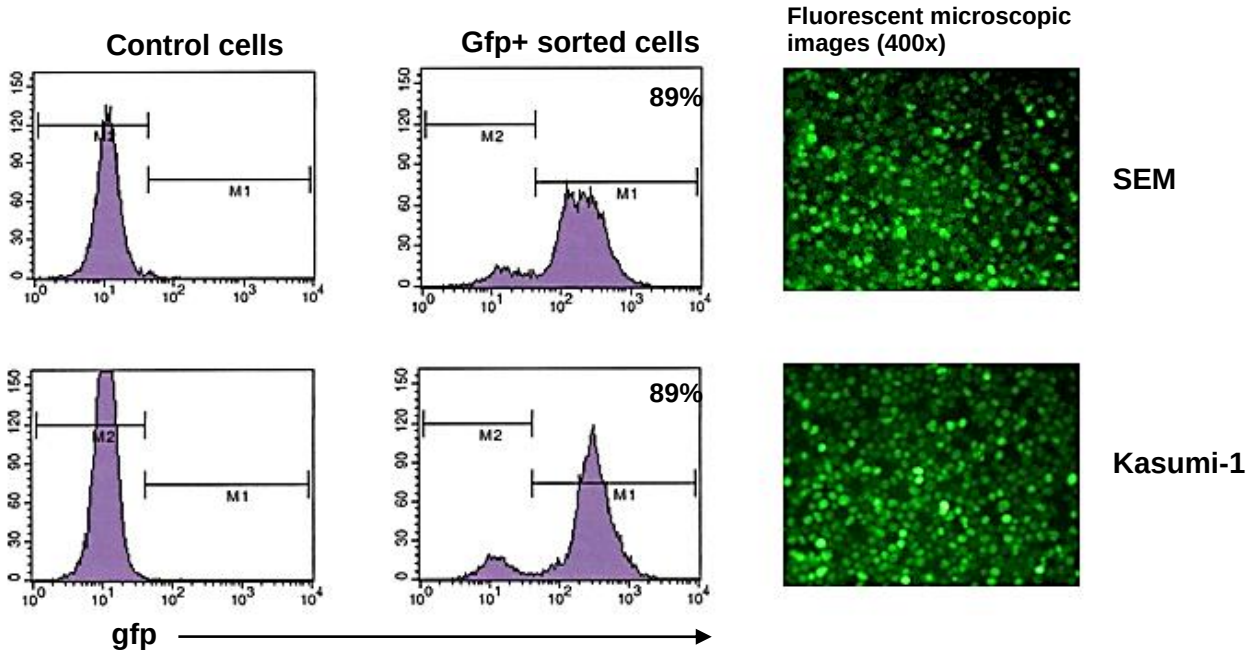

Figure 4.33 Flow cytometry analysis and image of stable sorted cells in culture. Aliquots of 10^6 cells were washed and suspended in 2 ml PBS. Cells were analysed using FACScan. Control cells are non-tranduced cells growing in culture, gated at M2 in histogram. Gfp+ sorted cells are sorted cells in stable condition in culture. Images of sorted cells growing in culture are shown on the right panel.

4.3 Discussion

The experiments described in this chapter aimed to generate lentiviral vectors expressing different luciferase reporter genes and fluorescent protein genes, which could serve as labelling markers for tracking cells *in vivo*. In order to be able to track a random mixture of two different cell populations *in vivo* mentioned in chapter 3, these cells will have to be labelled with different markers. Lentivirus was used to carry the inserted gene of interest into the DNA of infected cells. These genes are incorporated into the genome of the cells and are expressed upon induction.

The cloning of pSLIEW and pSRLICW used a pSIEW lenitival SIN vector backbone. Cloning of pSLIEW was successfully done just before the start of this project. The pSLIEW clone was amplified in broth and was aliquoted and kept in glycerol stocks after confirmation by restriction digest. pSLIEW was used in transfection and transduction of cells as discussed later.

The cloning of pSRLICW was very challenging. Firstly, there were no compatible resctriction sites for the insertion of RLuc and mCherry into the pSIEW vector backbone. An oligonucleotide polylinker was designed to overcome this. Then, there were many failed attempts to get inserts in the polylinker sites. Extensive efforts with various modifications were tried before the inserts were finally integrated into the polylinker. Each cassette inserted into the polylinker used a different approach. IRES was the easiest to be cloned into the linker. Various strategies were used to insert the polylinker into pSIEW. Due to the time taken to successfully clone the pSRLICW, the production of lentivirus was only done once. This second lentivector was still being tested to prove the functionality sequence for the vector to be utilized in future experiments when the fellowship finished. The limitation of the work carried out in this part was the slow progression of successful cloning of relevant inserts into the specific sites in the oligonucleotides.

In producing the lentivirus, this work employed the three vector system, the packaging vector, the transfer vector and the envelop vector. This is to avoid the production of functional provirus. Although the lentivector backbone used was already a self-inactivating vector which cannot produce viral particles, nonetheless, using this system serve as a safety measure.

Lentivirus was produced in the 293T cells. The conventional method for lentiviral vector production relies on efficient cotransfection of the producer cells 293T, with packaging plasmid, helper envelope and vector. The 293T cells are normally used for producing lentivirus because they are highly transfectable and they express the SV40 T-large antigen which enables replication of plasmids containing SV40 ori of replication (Soneoka, Cannon et al. 1995).

As seen in the images of the highly transfected 293T cells in this chapter, transfection of the two constructed lentivirus produced green (pSLIEW) and red (pSRLICW) cells. This showed the fluorescent proteins EGFP and the mCherry inserted into pSIEW were working and could be used in cell transduction. However, fluorescence images of the 293T cells transfected with pSRLICW lentivirus showed the 293T cells were not transfected as high as the previously prepared pSLIEW lentivirus production. The most likely reason is that a high passage of 293T cells was used. Two studies have stated that it is critical the 293T cells are not passaged more than 18-20 times before transfection to produce the viral vectors (Reiser 2000; Mitta, Rimann et al. 2005). Therefore, 293T cells lower than 18 passages have a higher efficiency of cotransfection. The transfected 293T cells were left for 4 days for high virus production. Medium with lentivirus was ultracentrifuged to concentrate the virus. However, it was reported that vectors carrying large inserts above 7kb in their backbones were particularly fragile; they need a careful preparation specifically during ultracentrifugation in concentrating the virus (al Yacoub, Romanowska et al. 2007). Since both of the generated lentivirus, the pSLIEW and the pSRLICW were large, 11.1 kb and 11.9 kb, this information was taken into consideration when preparing the concentrated lentivirus produced by the 293T cells.

By using the same suspension of concentrated pSLIEW virus, transduction of ALL and AML cell lines was done using spinnoculation method. FACS analysis showed that AML cells have higher rates of transduction with the lentivirus. By taking SEM cells as the reference, Kasumi-1 cells was 1.6-fold and SKNO-1 was 2.2-fold higher rates of transduction than SEM and rates of transduction for RS4;11 was 9-fold lower than SEM. Higher transduction rates mean that the virus genome can easily integrate into the DNA of the cells. RS4;11 cells were the most resistant to infection. Low transduction rates may occur because the cells have a defence mechanism against infection. Alternatively the cells may have low expression of surface receptor for binding the virus.

The transduced cells were also tested for functionality of luciferase gene inserted into the backbone of the lentivirus. From transduced cells, we know that the EGFP was functional. However, this does not mean that luciferase is also functional. As previously mentioned, IRES is located upstream of EGFP and luciferase is upstream to IRES. Even if the first gene is not functional IRES can drive the expression of the second gene. A luciferase assay was performed on transduced cells to test the functionality of the reporter gene luciferase. From the bar chart (in figure 4.30) SKNO-1 has very high intensity of luminescence counts while RS4;11 luminescence activity detected was negligible. A similar pattern was seen with the FACS analysis for fluorescence, suggesting that the luminescence results complement the EGFP data. This means that both the reporter genes were functional.

The transduced cells were kept in culture for stable and normal growth rate and to have a high population of cells to work with. Since Kasumi-1 and SEM cultures have a high percentage of nontranduced cells mixed with the transduced cells, transduced green cells (gfp/luc+) were sorted to get high populations of green cells. RS4;11 was not sorted as the green cells were untraceable. Although the FACScan analysis showed transduced Kasumi-1 cells were higher than SEM cells, however, in FACS sorting percentage of green cells gated were lower for Kasumi-1 cells. Cells were sorted into a 2% penicillin and streptomycin treated culture medium since the first attempt of sorting, the cells were sorted in a non-treated medium and as a consequence the sorted cells were highly infected with bacterial contamination. Approximately 10^6 gfp+ cells were sorted. To verify the purity of the gfp+ cells sorted cells were re-analysed on the FACS machine. Post-sorted cells contained a high population of gfp+ cells with more than 90% purity. Sorted cells were kept in dense culture in a 24-well plate to keep the cells in close contact. The sorted cells were dormant for three weeks in culture with an increasing population of apoptotic and necrotic cells. This is thought to be because the cells were exposed to multiple assaults. First, for sorting purpose the cells were suspended in phosphate buffered solution. Sorting of cells took hours to complete using the FACSVantage cell sorter, meaning the cells had been in buffered solution for a long period of time. The sorting itself was also a pressure for the cells. Additionally, cells were kept in penicillin/streptomycin treated medium. Medium was partially removed to replace with a fresh media to initiate cell proliferation. Finally, when the sorted cells started to proliferate at the bottom of well, cells were transferred into a 48-well plate to expand the

cells and to remove if not all, but most of the debris and necrotic cells from culture. The sorted cells were finally stable in culture eight weeks after sorting. Cells were then aliquoted to analyse the percentage of gfp+ cells in culture. FACScan analysis showed high percentage with 83% of gfp+ cells. This is supported by fluorescent image proving the high populations of gfp+ cells in both Kasumi-1 and SEM. However, this percentage of gfp+ cells were approximately 10% lower than the purity checked post sorting. It is likely that most of the necrotic cells were the gfp+ cells. Alternatively the non-transduced cells could have grown more rapidly. Unfortunately, this was not determined for.

In conclusion, the generated lentiviral vector expressing luciferase reporter gene and green fluorescent protein gene are functional for both genes. This lentiviral vector can be used as a marker to track any cells intended for *in vivo* experimentations. The transduced gfp+ sorted cells may be utilized as a primary or secondary marker for studies utilizing other markers as therapeutic or drug testing studies. The generated second lentiviral vector harbouring *Renilla* luciferase reporter gene and mCherry protein gene may serve the same purpose. These two lentiviral vectors may be used as dual markers in *in vitro* or *in vivo* experiments.

CHAPTER 5

MOUSE MODEL FOR LEUKAEMIA – BIOLUMINESCENCE IMAGING

CHAPTER 5

MOUSE MODEL FOR LEUKAEMIA – BIOLUMINESCENCE IMAGING

5.1 Introduction

5.1.1 Humanized Mouse Models

Generating mouse models that can accommodate human haematopoietic cells was started over 30 years ago when severe combined immunodeficiency (SCID) mice were discovered. Engraftments of fetal hematopoietic tissues and HSCs into this model were very low and failed to generate a human immune system, the presence of mouse T, B and NK cells were the reasons for the engraftment failure (McCune, Namikawa et al 1988; Lapidot, Pflumio et al. 1992). Following this, non-obese diabetic (NOD)/SCID mice were generated to have no B and T cells and depleted NK cells. This model allowed higher levels of human PBMCs and HSCs to engraft (Hesselton, Greiner et al. 1995; Lowry, Shultz et al. 1996), but the residual activity of NK cells impeded engraftment of the human lymphoid compartment. The humanized mice were modified to become homozygous for targeted mutations at the interleukin-2 receptor γ-chain locus (*Il2rg*). The absence of IL-2R γ-chain caused severe impairment by preventing development of B, T and NK compartments. These NOD/SCID/*Il2rg*, also known as NSG mice, support greatly increased engraftment of human HSCs and PBMCs compared to all previously developed immunodeficient mouse models (Shultz, Ishikawa et al. 2007). The route of xenotranplanting human hematopoietic cells into mice varied from subcutaneous, intravenous and intrafemoral injections. The most preferable route of xenotransplantation is intrafemoral injection directly into bone marrow, the niche for haematological tissue. Xenotransplating leukaemic cells in these develop humanized mice are detailed in Chapter 1 (Section 1.6) and Chapter 3 (Section 3.1.3).

5.1.2 Bioluminescence *In Vivo* Imaging

Bioluminescence refers to the biochemical generation of light in living organisms. This enzymatic generation of visible light emission is a naturally occurring phenomenon in some non-mammalian species (Contag and Ross 2002). A variety of different bioluminescent systems have been identified in nature, with each requiring a specific enzyme and substrate. The bioluminescent reporters include luciferases from firefly (*Photinus pyralis*), sea pansy (*Renilla*), jellyfish (*Aequorea*), corals (*Tenilla*), beetles (*Pyrophorus plagiophthalamus* and *Lampyris*), and several bacterial species (*Vibrio fischeri* and *Vibrio harveyi*) (Hastings 1996; Sala-Newby, Thomson et al. 1996). Luciferases in general generate light by catalysing the corresponding substrates in the presence of ATP, Mg^{2+} and oxygen.

In vivo bioluminescence imaging is a technique that is based on detection of light emission from cells or tissue utilizing the bioluminescent reporter genes, a tool for non-invasive *in vivo* monitoring of human biology, diseases and molecular processes in small, intact living subjects. Importantly, repetitively imaging using this modality does not have any deleterious effects on the experimental animals as there is no evidence of toxicological or immune effects of the substance used has been reported.

A number of studies have reported the successful application of bioluminescence imaging modalities in monitoring diseases in mice or rats. These include the study on growth of tumours and lung cancer metastases (Sadikot and Blackwell 2005; Zinn, Chaudhuri et al. 2008), effect of treatment on intracerebral tumour (Rehemtulla, Stegman et al. 2000), activation of transcription on a specific gene and bacterial infections (Benaron, Contag et al. 1997), progression of melanoma (Klerk, Overmeer et al. 2007) and various other experiments in validating the bioluminescence measurements of tumour loads and reporter gene expressions (Bhaumik and Gambhir 2002; Contag and Ross 2002) (reviewed in (Klerk, Overmeer et al. 2007)). These studies demonstrate that bioluminescence imaging is rapid, easy to perform and sensitive. This method can detect tumour shortly after inoculation, even in cases when limited and relatively few cancer cells are available.

This chapter utilizes the bioluminescence imaging technique to monitor progression of green fluorescent/luciferase-expressing leukaemic cells in xenografts of NSG mice.

5.2 Results

5.2.1 Growth curve study

In order to understand the expansion of different cell lines engrafted in mice, growth curves of the cell lines used in this chapter were generated to determine the growth characteristics of the cells *in vitro*. SEM, Kasumi-1 and SKNO-1 cell lines were cultured as described in Section 2.1.1.1, without change of medium throughout the experiment. Cell growth was counted daily for 7 consecutive days using the trypan blue exclusion method as described in Section 2.2.1.2. Figure 5.1 shows the characteristic growth curves obtained for the cell lines, each showing a lag, exponential and plateau phases. The lengths of the lag phase of the growth curves in each cell line were similar but the exponential phase differed in all cells. SEM lines showed a longer exponential phase and reach plateau phase after 120 hours (5 days) in culture whereas SKNO-1 showed a shorter exponential phase and reach plateau after 4 days (96 hours) in culture. Kasumi-1 cells has a low and prolonged exponential phase and plateau after 6 days in culture.

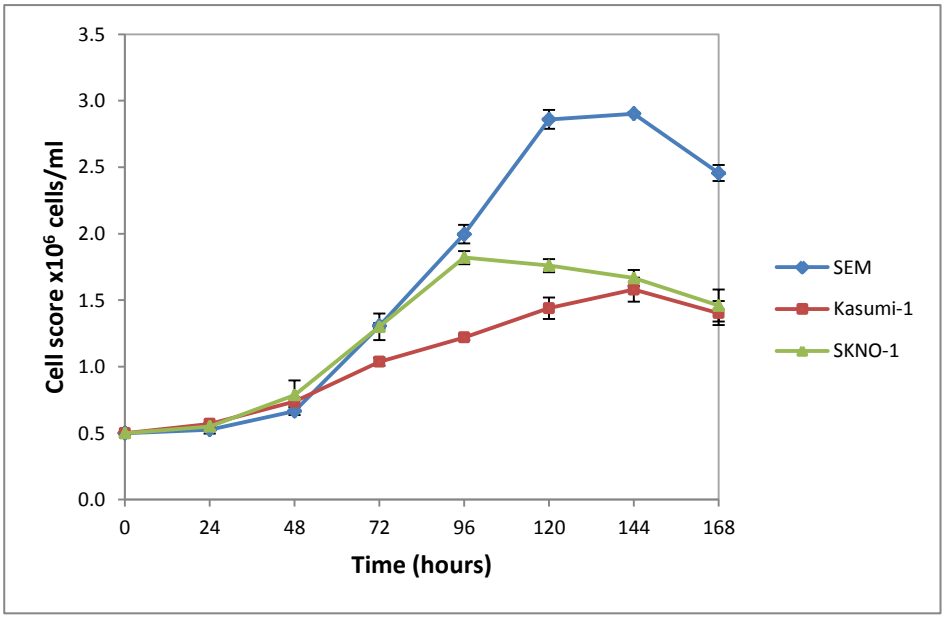

Figure 5.1 Growth curves of SEM, Kasumi-1 and SKNO-1 cell lines. SEM and Kasumi-1 cells were grown in RPMI with Hepes modification medium supplemented with 10% FBS (v/v) and 2 mM L-glutamine (v/v). SKNO-1 cells was grown in RPMI with Hepes modification medium supplemented with 20% FBS (v/v), 2 mM L-glutamine (v/v) and 7 ng/ml GM-CSF (v/v). Cells were seeded at 0.5 x 10^6 cells/ml at the start of experiment and cell growth was counted daily for 7 consecutive days using a Neubauer hematocytometer counting chamber with the trypan blue exclusion method as describe in *Materials and Methods*. The data presented are the mean ± s.e.m of three independent experiments.

5.2.2 Bioluminescence Imaging of Engrafted Mice

To evaluate the expansion and progression of leukaemic cells *in vivo* and to be able to track the cells, lentiviral transduced and green fluorescent positive (gfp+)-sorted SEM and Kasumi-1 cells and unsorted SKNO-1 cells (from Chapter 4 Section 4.3.3) were transplanted intra femorally (i.f) into female NSG mice. Animals were prepared for transplantation and the protocol used in this procedure is described in Materials and Methods Section 2.2.1.15. Briefly, three animals were used in each group and for each animal, 20 µl of 10^6 cells were transplanted separately with each cell line. Immediately after implantation, while still anaesthetised, animals were injected intraperitoneally (i.p) with XenoLight Rediject D-Luciferin (Caliper) and were immediately subjected to bioluminescence imaging in a dark chamber using an IVIS Spectrum Imager (Caliper). D-Luciferin is the substrate for luciferase. Therefore, Luciferase (luc+) from the transduced leukaemic lines (gfp+luc+ cells) in the animals reacted with the administered luciferin and produced luminescence light, which was detected by the imager. Images were captured after 10 sec exposure to luminescence channel and images from the emission filter at 620-640 nm were selected for display (see Section 2.2.3.2 for detailed explanation). Luminescence imaging was carried out weekly to track the expansion of the cell population in the mice. In images from each different cell lines, each mouse was allocated as mouse 1 (m1), mouse 2 (m2) and mouse 3 (m3). If mice showed severe manifestation of leukaemia or signs of distress they were humanely killed by cervical dislocation.

5.2.2.1 $SEM_{(gfp+luc+)}$ engraftment

Images showing the progression of the infected cells *in vivo* are shown in Figure 5.2. On day 0, luminescence light was detected at the site of injection (right leg) in all mice. On day 7, images of mouse taken individually showed the intensity of luminescence light on the right leg had increased showing expansion of the implanted $SEM_{(gfp+luc+)}$ cells *in vivo*. On day 15 mice were imaged simultaneously rather than individually the week before. The images showed a high intensity of luminescence light was detected in m2 indicating presence of a high number of the transduced cells whereas no luminescence light was detected in m1 and m3. Luminescence detection was automatically set at a high intensity range resulting low luminescence emitting cells were not displayed. On day 21, luminescence light emitted in all mice, showed accumulation of the transduced cells in

right leg of m1, wide expansion of the cells in m2, particularly in the midriff section, and dissemination of the cells to left midriff of m3. Mouse 2 had difficulty moving at this point while mouse 1 and mouse 3 were showing effects of the disease. Four days later, at day 25, m2 was physically very weak and had loss mobility of the hind limb, and was dragging the limb when moving about. Images on day 25 showed luminescence light was detected in throughout m2, with high intensity on the midriff and part of the head. When the animal was imaged from the side, it was shown that the spleen and probably the liver and bone marrow of both legs were infiltrated. Mouse 2 was culled at this point and the peripheral blood, bone marrow and organs were collected for flow cytometry analysis. On day 28 post-transplantation, m1 images showed accumulation of the transduced SEM cells on right leg and m3 images showed systemic spread of the cells. Mouse 3 was also culled due to lost mobility of hind limb. Mouse 1 was culled after imaging on day 35 with the similar condition. Bone marrow and spleen of the culled mice were collected for flow cytometry analysis.

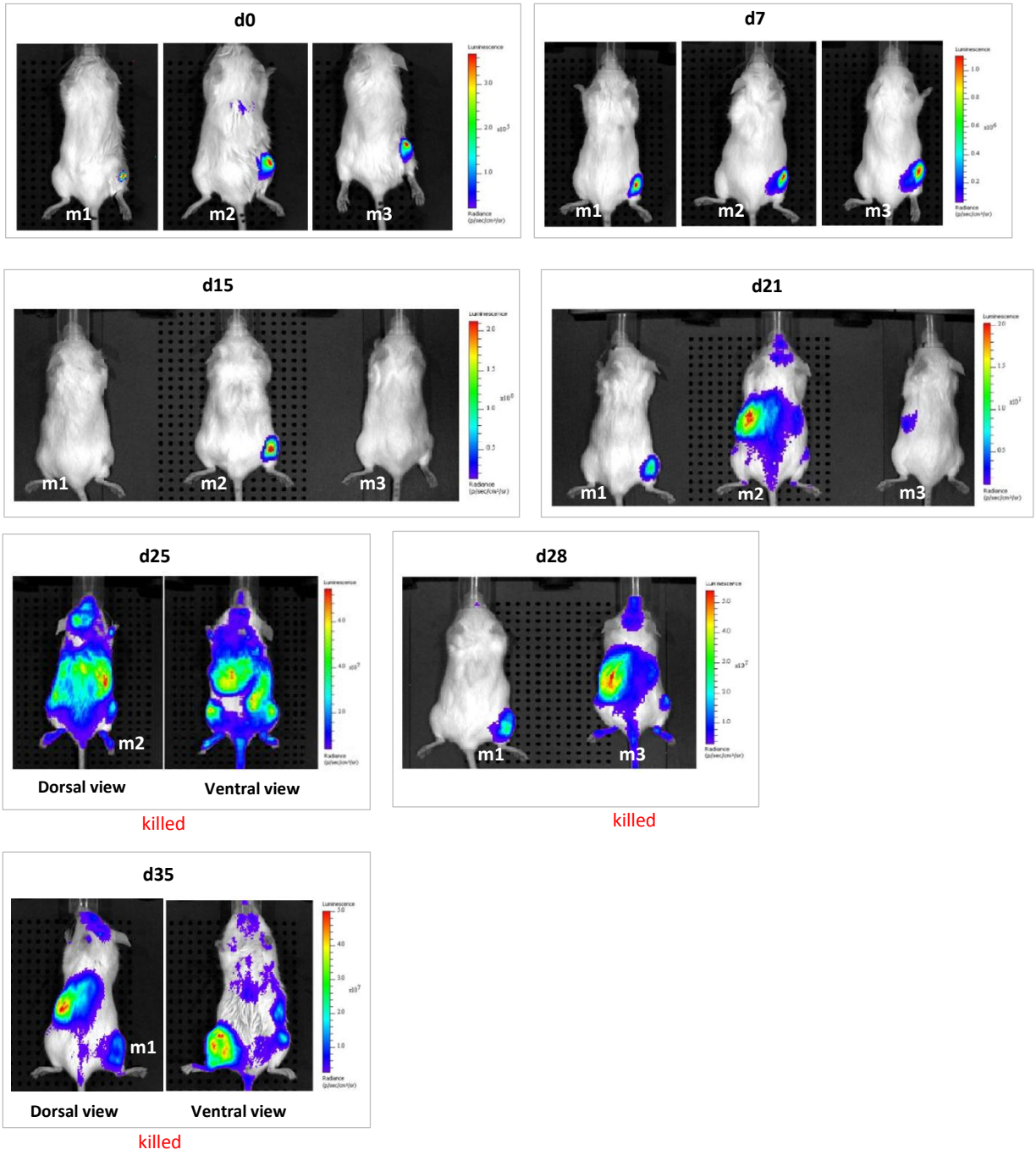

Figure 5.2 Bioluminescence images of SEM$_{(gfp+luc+)}$ engrafted mice. Rediject D-Luciferin (30 mg/ml) was injected intraperitoneally (i.p) at 150 µl/mouse prior to imaging on sedated mice. Images were photographed in dark chamber condition under bioluminescence channel to capture luminescence light emitted from cells *in vivo*. Pseudocolour panels on the right of each image indicate intensity of luminescence measured. Series of weekly images are depicted. Animals were humanely culled due to severe condition following engraftment. d=day; m=mouse.

5.2.2.1.1 Flow cytometry analysis

Flow cytometry analysis was performed by labelling SEM cells with anti-mouse CD45 and TER119 antibodies conjugated with PE-Cy7 and a specific SEM marker anti-human CD133 conjugated with APC, as detailed in the Materials and Methods Section 2.2.1.16.

Figure 5.3A depicts an example of gating of human lymphocytes population from debris in dot plot graph, following gating of human cells from mouse cells contamination on a histogram plot. Figure 5.3B and 5.3C showed histogram and dot plot graphs of non-transduced SEM as negative control and transduced SEM ($SEM_{(gfp+luc+)}$) cells used in xenograft model as a positive control respectively. The dot plot populations in control cells were at the lower quadrant of the PE-Cy7 channel showing the populations were human cells. For this control and peripheral blood part, results are presented below, cells were mistakenly labelled with CD38, which is not specific for SEM cells. Therefore experimental dot plot data was presented comparable with the controls. In the $SEM_{(gfp+luc+)}$ positive control dot plot graph there were two populations measured. As explained in Chapter 4, sorted gfp+ SEM were contaminated with a low percentage of gfp-negative cells and these cells expanded over time in culture.

Peripheral blood of mouse 2 at the end point was collected and processed using lymphoprep reagent according to manufacturer's protocol as detailed in Materials and Methods Section 2.2.3.7 to isolate lymphocytes from whole blood. Flow cytometry analysis on the isolated lymphocytes of mouse 2 showed 15.4% of the lymphocytes were human SEM cells with 51.2% of these cells were positive for gfp (Figure 5.3D), which explained the overall luminescence light detected in the animal terminated on day 25. For mouse 1 and mouse 3, peripheral blood was not collected for analysis.

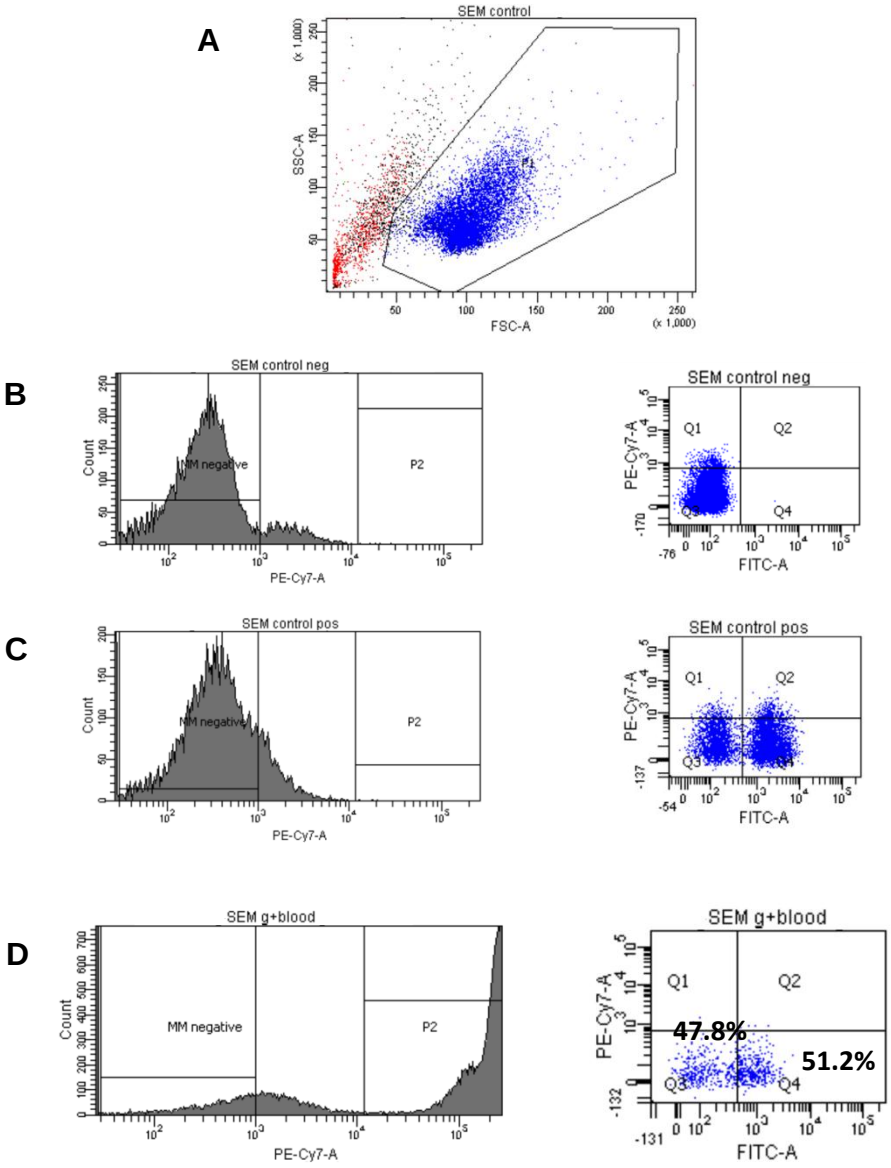

Figure 5.3 Flow cytometry analysis of peripheral blood isolated at terminal point of mouse (m2) engrafted with SEM$_{(g+luc+)}$ cells. Lymphocytes or leukaemic cells were isolated from peripheral blood using lymphoprep technique as detailed in *Materials and Methods*. Isolated cells were labelled with mouse antibody anti-CD45 and anti-TER119 conjugated with PE-Cy7. (A) Dot plot showing population of human leukaemic cells gated out in the analysis. Dot plot data was the result of population gated out from histogram graph. (B) Histogram and dot plot graphs of non-transduced SEM cells as negative control and (C) Histogram and dot plot graphs of SEM$_{(g+luc+)}$ cells from sorted culture. (D) Histogram and dot plot graphs of lymphocytes isolated from peripheral blood showing presence of SEM$_{(g+luc+)}$ cells in the blood circulation of the mouse.

The bone marrow and spleen of all 3 mice were also collected and analysed by flow cytometry. Figure 5.4 shows examples of gating the SEM cell populations in control cells, which was done in a similar manner to the sample analysis. Human cells were gated towards the right from mouse cells in the mmPE-Cy7/Count histogram (Figure 5.4A), followed by purification of the SEM cells by isolating the cell population in a gate in a dot plot graph (Figure 5.4B). Figure 5.4C(i) and 5.4C(ii) depicted unstained SEM cells as a negative control and stained $SEM_{gfp+luc+}$ cells as a positive control respectively.

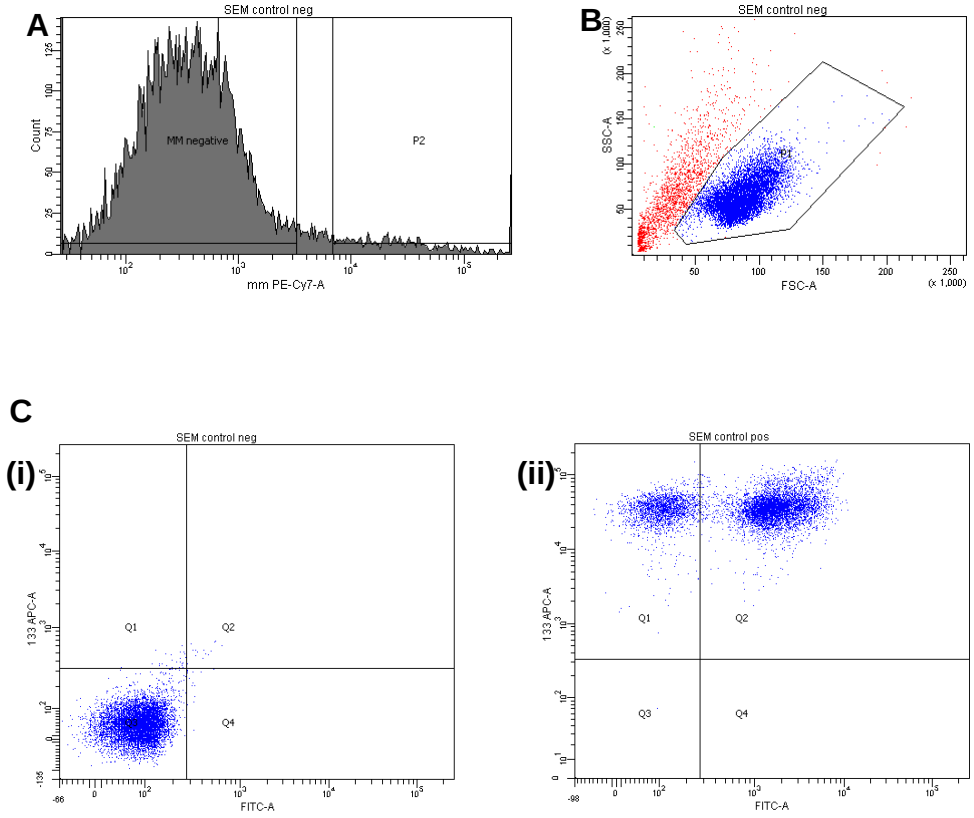

Figure 5.4 Gating of SEM cells in flow cytometric analysis. Non-transduced SEM cells and gfp-positive SEM cells from stable ongoing culture were suspended in PBS as detailed in *Materials and Methods*. Cells were labelled with anti-human CD133-APC antibody in combination with anti-mouse CD45- and TER119-PE-Cy7 antibodies. (A) Histogram showed the gating of human cells towards the right of the graph (marked as MM negative) on the mouse (mm) PE-Cy7 channel. (B) Dot plot graph indicates further gating from MM negative to purify human cells from debris. (C) Dot plot of unstained control negative SEM (i) and positive gfp SEM (ii) showed the cells are CD133 positive. The positive control cells are a mixture of negative and positive green fluorescence cells in FITC channel.

Analysis of bone marrow and spleen from engrafted mice are as shown in Figure 5.5. In mouse 1, 94% of retrieved cells from bone marrow were human leukaemic cells and 71% of these cells were gfp-positive. 53% of the mouse spleen was populated with human cells where 67% of the cells were positive for gfp (Figure 5.5A). These results corresponded with the high luminescence intensity at the site of right leg and the left abdominal part on day 35 when the animal was killed. Analysis of the bone marrow and spleen of mouse 2 showed the sites contained SEM cells with 62.1% gfp-positive of 65.6% human cells and 60.1% gfp-positive from 45.4% gated human cells respectively (Figure 5.5B). In mouse 3 samples analysis, the bone marrow cells population contained 46.6% human leukaemic cells with 64.5% gfp-positive SEM cells and the spleen was infiltrated with 11.6% human leukaemic cells with 69.2% gfp-positive SEM cells (Figure 5.5C). For mouse 1, 50,000 cells was counted for both bone marrow and spleen samples whereas 30,000 cells was counted from spleen samples of mouse 2 and mouse 3, and 12,000 cells and 10,000 cells from bone marrows of mouse 2 and 3 respectively. Liver samples were excluded in the analysis due to the difficulty of gating human cells from mouse cells.

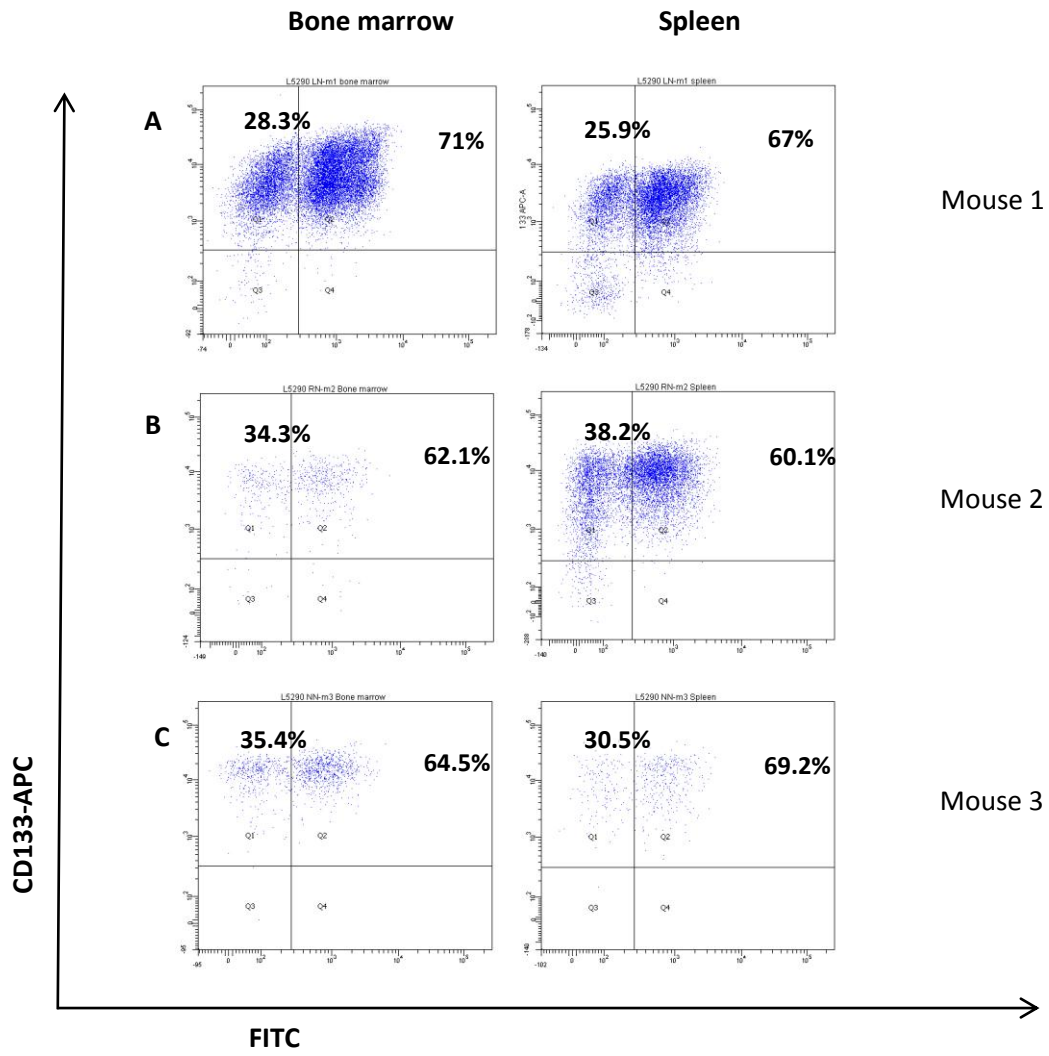

Figure 5.5 Flow cytometric analysis of cells retrieved from bone marrow and spleen at the end-point of mice engrafted with $SEM_{(g+luc+)}$ cells. (A), (B) and (C) represent dot plot data from mouse 1 (m1), mouse 2 (m2) and mouse 3 (m3) respectively, engrafted with the implanted cells. Retrieved cells were processed as describe in *Materials and Methods* and labelled with CD133-APC antibody to identify SEM cells and combining with mouse anti-CD45- and anti-TER119-PE-Cy7 antibodies. Fluorescent gfp cells were measured by FITC channel. Dot plot data on left panel show analysis of cells retrieved from bone marrow and dot plot data on right panel show analysis from spleen of mice. Percentage of $SEM_{(gfp+luc+)}$ cells in dot plot populations were as depicted in the graphs.

5.2.2.2 Kasumi-$1_{(gfp+luc+)}$ engraftment

Images showing progression of post implanted Kasumi-$1_{(gfp+luc+)}$ cells in mice are shown in Figure 5.6. On the day of implantation (d0), luminescence light was detected at the site of implantation on right leg in all three mice, m1, m2 and m3, which continued to increase the following week (d7). However, imaging on day 15, 21, 28, 35 and 41 displayed only that m2 showed increasing intensity on the region of the right leg. No visible luminescent emission was seen on imaging of m1 and m3 on the same days. On day 49, m2 had visibly developed a large lump on the right leg, which was luminescent on imaging. The mouse was having difficulty in movement and the flexibility of the leg was limited. m2 was culled following imaging on day 49 and bone marrow and spleen, as well as the tumour on the right leg were collected. On the same day, m1 did not show any light detected at the same luminescent intensity used, whereas m3 started to show luminescent light emerging on the left abdominal compartment suggesting the expansion of the engrafted cells in vivo. The following imaging on day 55 showed the luminescence light noted in m2 a week before had grown bigger with higher luminescent intensity, m1 remained negative. However, 8 days later (on day 63), luminescence imaging showed a sudden widespread expansion of engrafted cells in m1 on the right lower abdominal region while the luminescent intensity on m3 increased slightly indicating growth expansion of the engrafted Kasumi-$1_{gfp+luc+}$ cells. Luminescent images on day 70, 78 and 84 demonstrated further growing of the human cells in the animals. On day 78, a ventral view of m2 was also imaged showing extension of the engrafted cells proliferated with possible high infiltration of the spleen. Images on day 84 and 91 post transplantation showed the dorsal view and ventral view of both m1 and m3 mice with luminescent light emission covering wider regions, most notably in m3. This mouse was culled on day 91 due to an enlarged abdomen. Bone marrow, spleen and emerging abdominal tumours were collected for analysis. The final image of m1 14 days later (day 135) showed luminescent light from the enlarged abdominal region as seen in the ventral view. The dorsal view of the mouse also showed emergence of human cells in the left abdominal region, which was thought to be the continuation of the region detected on the ventral view. The mouse was killed after the final imaging and bone marrow, spleen and abdominal tumours were collected for analysis. On daily observation until the day the animals were culled, all 3 mice did not show any physical sign of illness from the disease at the time of termination.

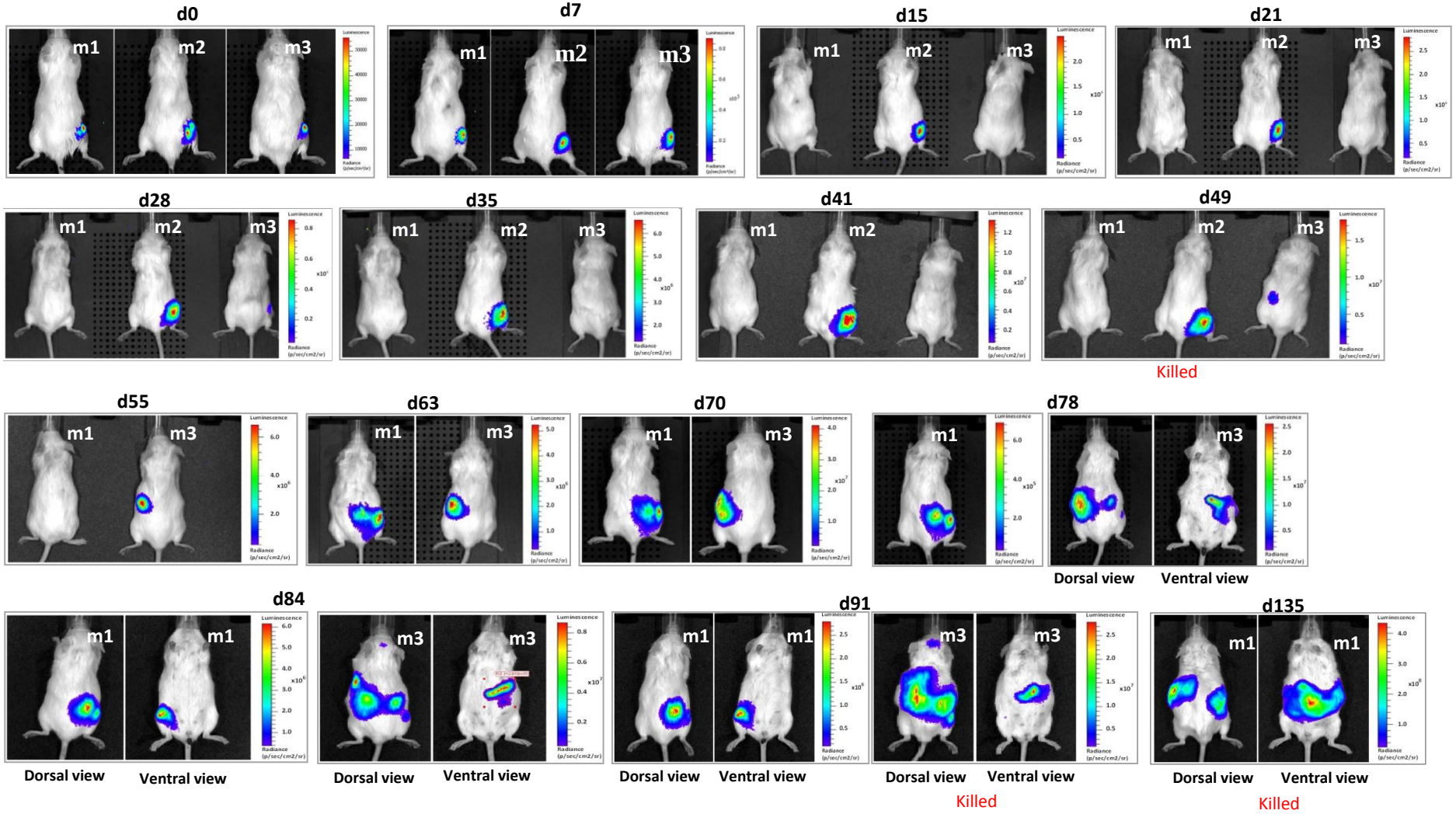

Figure 5.6 Bioluminescence images of Kasumi-1gfp+luc+ engrafted mice. Luciferin was injected intraperitoneally (i.p) into mice prior to imaging. Bioluminescence imaging was taken on weekly basis to track progression of the leukaemic cells in vivo. Animals were humanely culled due to physical conditions following engraftment.

5.2.2.2.1 Flow cytometry analysis

Flow cytometry analysis was performed by labelling cells with Kasumi-1 cell specific marker CD34 conjugated with APC, and with anti-mouse CD45 and TER119 antibodies conjugated with PE-Cy7 to exclude contamination with mouse cells, as detailed in Materials and Methods Section 2.2.1.16.

Figure 5.7 shows examples of gating of human cells in histogram (A) followed by gating of the cells in dot plot (B) to purify the Kasumi-1 cells population from debris. Figure 5.7C showed dot plot populations of stained non-transduced Kasumi-1 cells and transduced Kasumi-$1_{(gfp+luc+)}$ cells as negative and positive controls respectively. The control cells are totally CD34-positive human Kasumi-1 lines. As explained in Chapter 4, sorted Kasumi-$1_{(gfp+luc+)}$ culture were not totally pure green cells but still a mixture of small percentage of non-transduced gfp-negative cells in culture. This resulted in two populations of gfp-positive and gfp-negative cells measured on FITC channel in the dot plot.

Figure 5.8 shows flow analysis of samples collected after culling of mouse 2 on day 49. Bone marrow, spleen and tumour from the right leg of the mouse were isolated and processed as described in Materials and Methods Section 2.2.3.4. Histogram of the flow analysis on bone marrow (top) and spleen (middle) showed negligible human cells in the samples. No or negligible human cells were seen in the corresponding dot plot graphs on the right panel. However analysis from the leg tumour (bottom) showed high percentage of human cells gated (72.6%) in the histogram. The corresponding dot plot graph showed 80% of the cells were of Kasumi-1 gfp-positive cells which give the light intensity in the images.

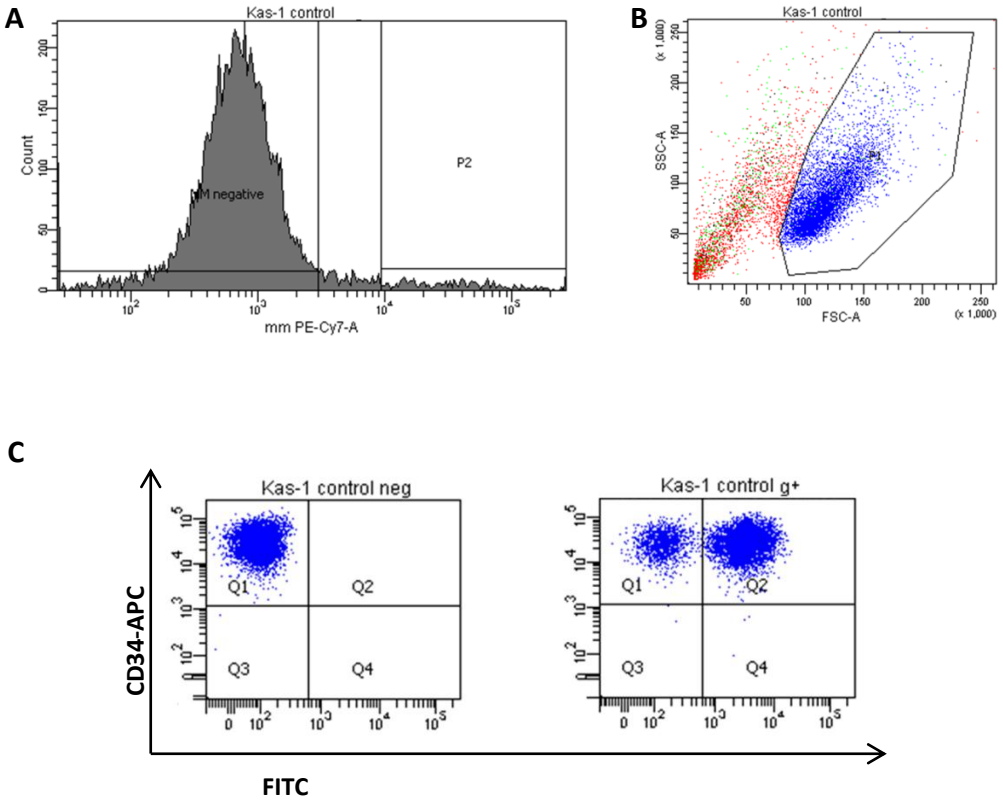

Figure 5.7 Gating of Kasumi-1 cells in flow cytometric analysis. Cultured non-transduced Kasumi-1 cells and gfp-positive sorted culture of transduced Kasumi-1 cells in PBS were labelled with anti-human CD34-APC antibody in combination with anti-mouse CD45- and TER119-PE-Cy7 antibodies. (A) Histogram showed the gating of human cells towards the right of the graph (marked as MM negative) on the mouse (mm) PE-Cy7 channel. (B) Dot plot graph indicates further gating from MM negative to purify human cells from debris. (C) Dot plot stained control negative (left) and positive gfp (right) from ongoing culture showed the Kasumi-1 cells are CD34 positive. Negative control cells are negative for green fluorescence in FITC channel and positive control cells are a mixture of negative and positive green fluorescence cells.

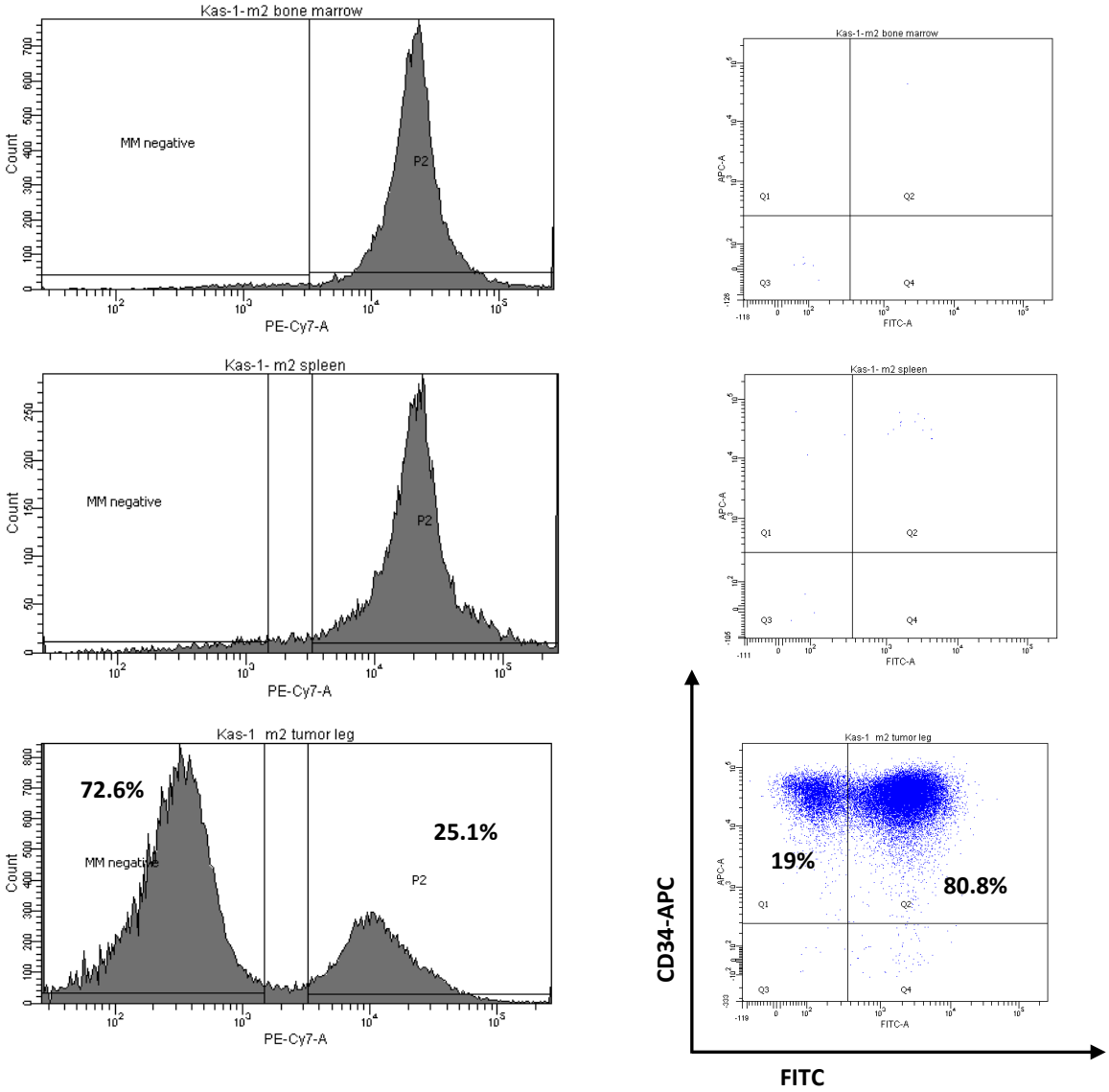

Figure 5.8 Flow cytometry analysis of samples collected from Kasumi-1$_{(gfp+luc+)}$ engrafted mouse 2 at the end-point on day 49. Bone marrow, spleen and leg tumour collected from the mouse were processed as described in the *Materials and Methods*. Cells were labelled with human antibody anti-CD34-APC combined with mouse antibodies anti-CD45- and anti-TER119-PE-Cy7. Top: histogram and dot plot graphs from bone marrow; Middle: histogram and dot plot graphs from spleen; Bottom: histogram and dot plot graphs from leg tumour. Figures on the graphs indicate percentage of Kasumi-1 (human) cells in the gates.

Analyses of cells collected from mouse 3 at terminal-point, three months post-transplantation, are shown in Figure 5.9. Although it was a long-term engraftment, the mouse spleen was at normal size measuring 1 cm in length. However the abdominal cavity was filled with two separate solid encapsulated tumours, a large tumour measuring 2 cm in diameter and a smaller tumour measuring 1 cm in diameter (Figure 5.9A). The spleen and tumours were processed as described in Materials and Methods Section 2.2.3.4. Flow cytometric analyses of the samples were as shown in Figure 5.9C. Although the spleen was a normal size, it was infiltrated with 29.4% of Kasumi-1 cells of which 86.4% were gfp-positive. However, in the bone marrow of the mouse there were only 6% of Kasumi-1 cells measured. The small abdominal tumour were consisted almost entirley of Kasumi-$1_{gfp+luc+}$ cells, 94% of the 95.3% positive Kasumi-1 cells were positive for gfp. Although only 66.3% cells in the large abdominal tumour were of Kasumi-1, 98.5% of these cells were gfp-positive. Therefore, these tumours corresponded with the two distinct luminescent masses seen in m3 at day 91.

For mouse 1, at terminal-point after 4.5 months post-implantation of Kasumi-$1_{gfp+luc+}$, the abdominal cavity of the mouse was found to be filled with fat-like, solid encapsulated, spongy spleen-attached and stomach-attached tumours as shown in photograph (A) in Figure 5.10. Flow analysis of the cells retrieved from bone marrow, spleen and the tumours were as shown in Figure 5.10B. As it was gated for human cells in the histogram, Kasumi-$1_{gfp+luc+}$ cells measured in the bone marrow and spleen were 11.8% and 18.2% respectively and 81% to 90% of those cells were positive for gfp. The tumours analyses isolated Kasumi-1 cells in fat-like, solid, spleen-attached and stomach-attached tumours as much as 70.8%, 93.3%, 89.7% and 79.6% respectively. All cells from these isolated populations were more than 99% gfp-positive. These results corresponded with the luminescent band on the abdomen of m1 seen on day 135 at the time the mouse was culled.

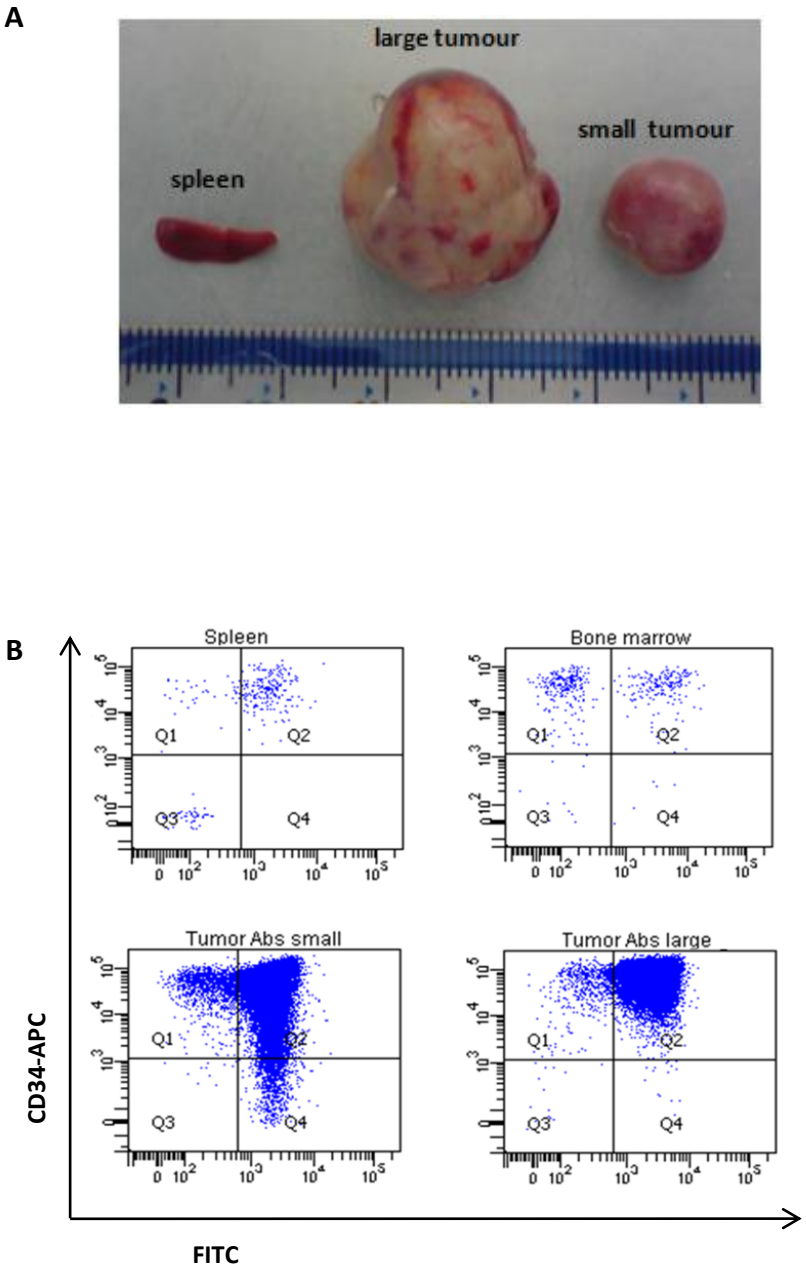

Figure 5.9 Flow cytometric analysis of Kasumi-1$_{gfp+luc+}$ engrafted mouse 3. Cells suspensions from bone marrow, spleen and two solid abdominal tumours (small and large) collected from mouse 3 at terminal day 91 post xenograft were labelled with human specific antibody anti-CD34-APC combined with mouse specific antibodies, anti-CD45 and anti-TER119 conjugated with PE-Cy7. The photograph on top, **A**, showed the normal spleen size of 1 cm length, with large solid tumour measuring 2 cm diameter and small solid tumour measuring 1 cm diameter. Analysis of the samples, **B**, showed dot plot data of spleen, bone marrow, small abdominal tumour and large abdominal tumour (as labelled on the graphs. Dot plot data was on channels FITC/CD34-APC. Abs=abdominal.

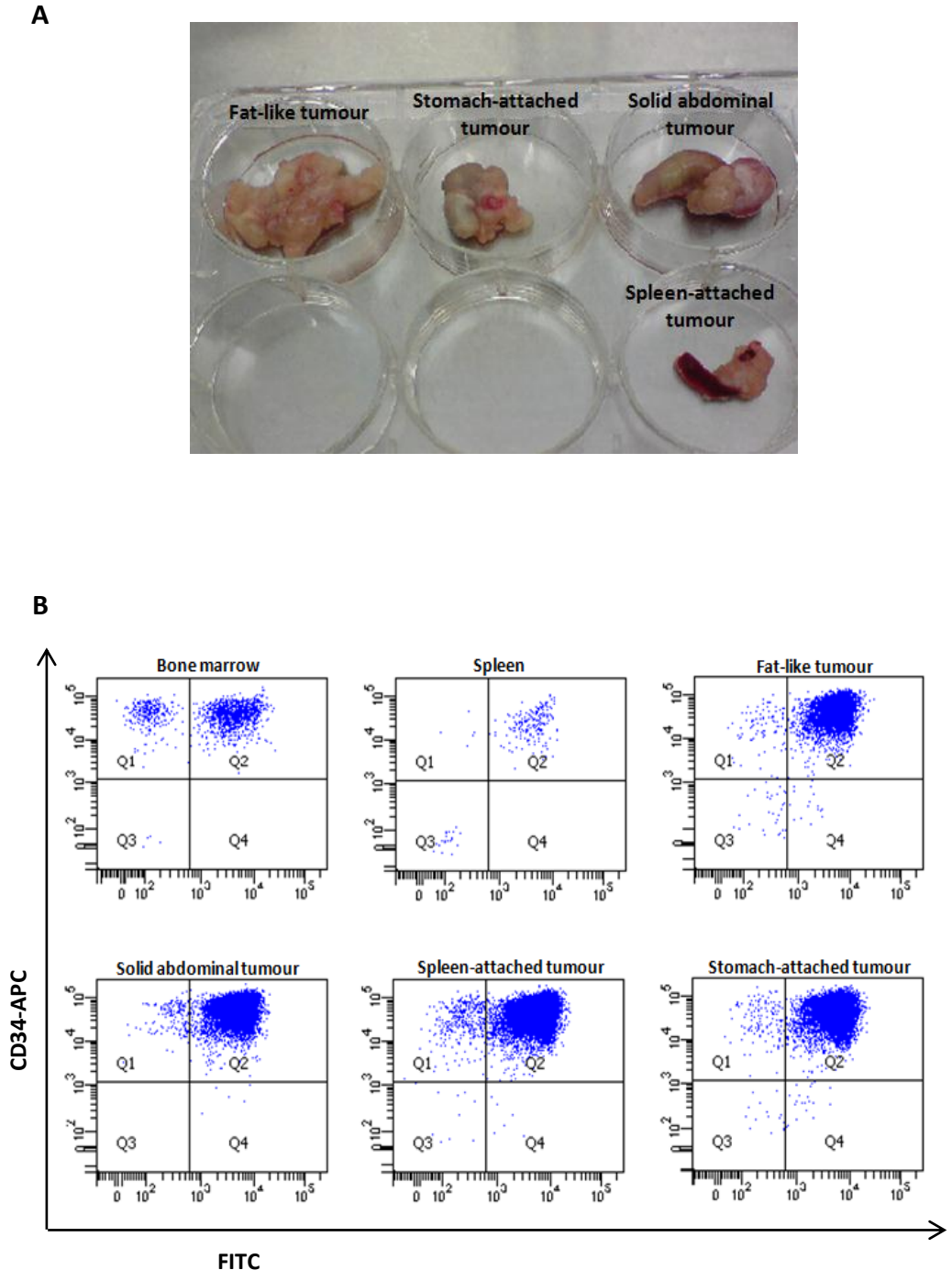

Figure 5.10 Flow cytometric analysis of Kasumi-1$_{gfp+luc+}$ engrafted mouse 1. Samples collected from mouse 1 at the terminal day 135 were processed and antibodies labelled were as described in *Materials and Methods*. Bone marrow, spleen and tumours suspension cells were labelled with human antibody anti-CD34-APC in combination with mouse antibodies anti-CD45- and anti-TER119-PE-cy7 to exclude mouse cells. **A**, Photograph showing various types of tumours isolated from the mouse abdominal cavity. **B**, Dot plot graphs showing analysis of samples collected from the mouse. FITC channel measured green fluorescent cells, CD34-APC channel measured human cells in samples.

5.2.2.3 SKNO-1$_{(gfp+luc+)}$ engraftment

Images showing progression of implanted SKNO-1gfp+luc+ cells in mice were as shown in Figure 5.11. On day 0, all three mice showed luminescent light emission from cells at the site of implantation. However, after one week of implantation, m1 showed a high intensity of luminescence light from the engrafted leg, which was low in m2. No visible light was detected in m3 even when the luminescence detection sensitivity was increased. On day 15, luminescent light was only detected in mouse 1. After three weeks post-implantation (d21), mouse 1 maintained the emission of luminescent light intensity, mouse 2 started to show emission of luminescence light suggesting the implanted cells in this mouse had started to expand, however, mouse 3 still did not show any sign of luminescent emission. Although the images from this week were 'contaminated' with false luminescent signal on the surface, the luminescence light emitted from the cells *in vivo* was still distinguishable. For the following two weeks at day 28 and day 35, images showed luminescent light detected in m1 and m2 but not m3. Unfortunately, all three mice did not regain consciousness and died after imaging on day 35. There was no sign of illness seen in animal up to the last day of luminescence imaging. Bone marrow and spleen from the mice were collected for flow cytometry analysis.

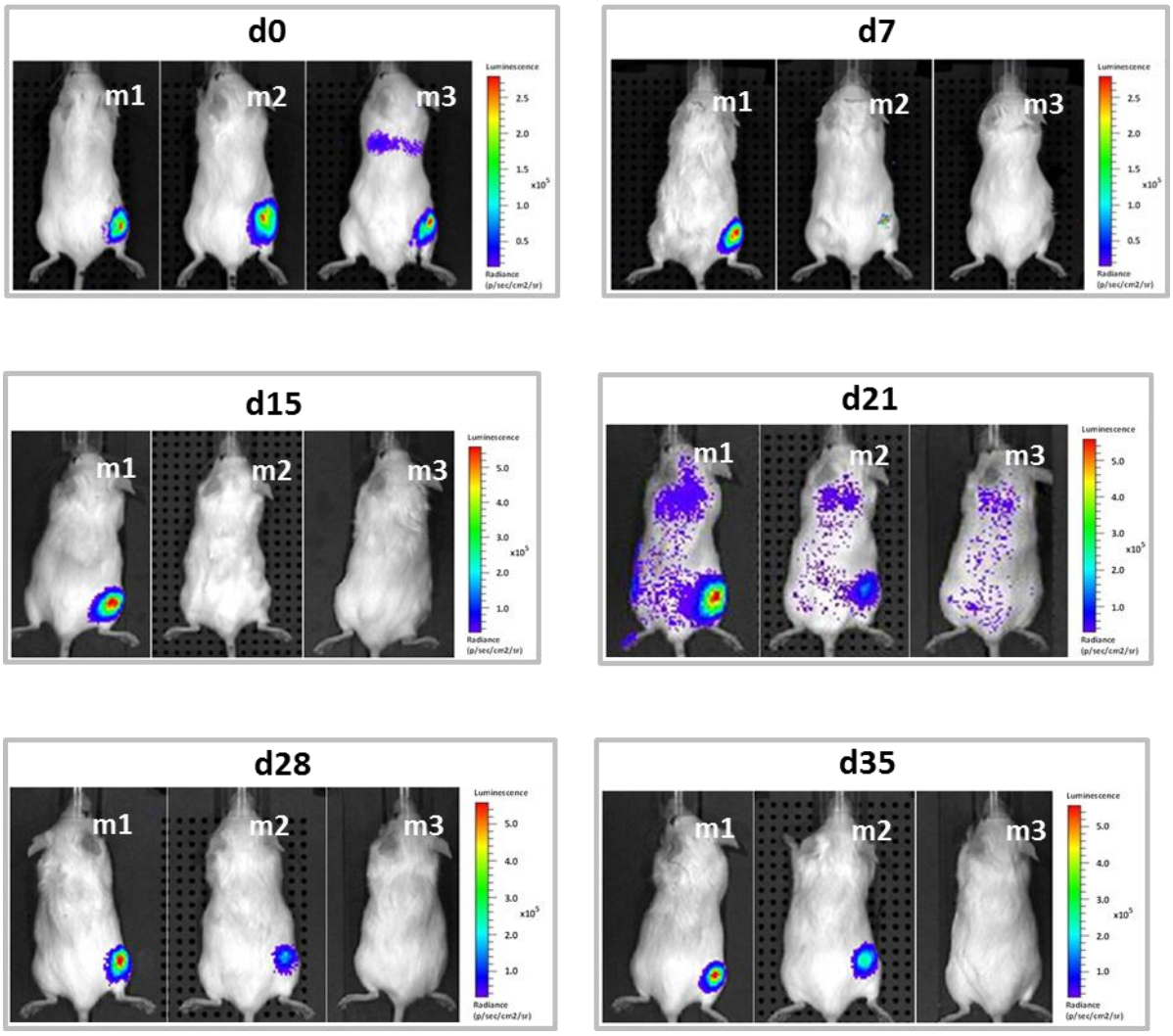

Figure 5.11 Bioluminescence imaging of mice engrafted with SKNO-1gfp+luc+ cells. Sedated mice were injected with 150 mg/kg body weight of Rediject D-Luciferin solution prior to luminescence imaging in dark chamber. Mice images were photographed and superimposed with the luminescence light emitted by the cells in vivo as detected by luminometer. Pseudocolor bars on the left of images indicate luminescence intensity measured. d=day; m=mouse

5.2.2.3.1 Flow cytometry analysis

Flow cytometry analysis of the cells retrieved from mice engrafted with SKNO-$1_{gfp+luc+}$ were performed as detailed in Materials and Methods Section 2.2.1.16 by labelling the cells with SKNO-1 markers anti-human CD38 conjugated with APC and exclusion of mouse cells by anti-mouse CD45 and TER119 conjugated with PE-Cy7.

Figure 5.12 shows the example of gating SKNO-1 cells in histogram (A) which shows the gated cells were of human cells. The gated SKNO-1 cells were purified from debris in dot plot (B). Figure 5.12C showed dot plot graphs for the negative control of non-transduced SKNO-1 cells on the left and the positive control of transduced SKNO-$1_{gfp+luc+}$ cells on the right.

For the bone marrow and spleen samples collected *post mortum* from all three mice engrafted with SKNO-$1_{gfp+luc+}$ cells, flow analyses of antibody labelled samples failed to demonstrate the presence of any luminescent SKNO-1 cell. All the dot plot results gave the same pattern as shown in Figure 5.13A for the analysis of the bone marrow (left) and spleen (right) samples from mouse 1. This is despite the presence of high SKNO-1 cells measured and gated in the histogram of the spleen and much lower percentage in bone marrow samples (Figure 5.13C). In all three mice, bone marrow samples were mouse cells in majority with less than 10% SKNO-1 cells detected. In the spleen samples analysis, histogram graphs distinguished two peaks, which were gated accordingly. Spleen in mouse 1 contained at least 39.4% SKNO-1 cells whereas 53.6% and 51.1% mouse 2 and mouse 3 spleens respectively were populated with SKNO-1 cells. Unfortunately peripheral blood of the mice was not collected for analysis.

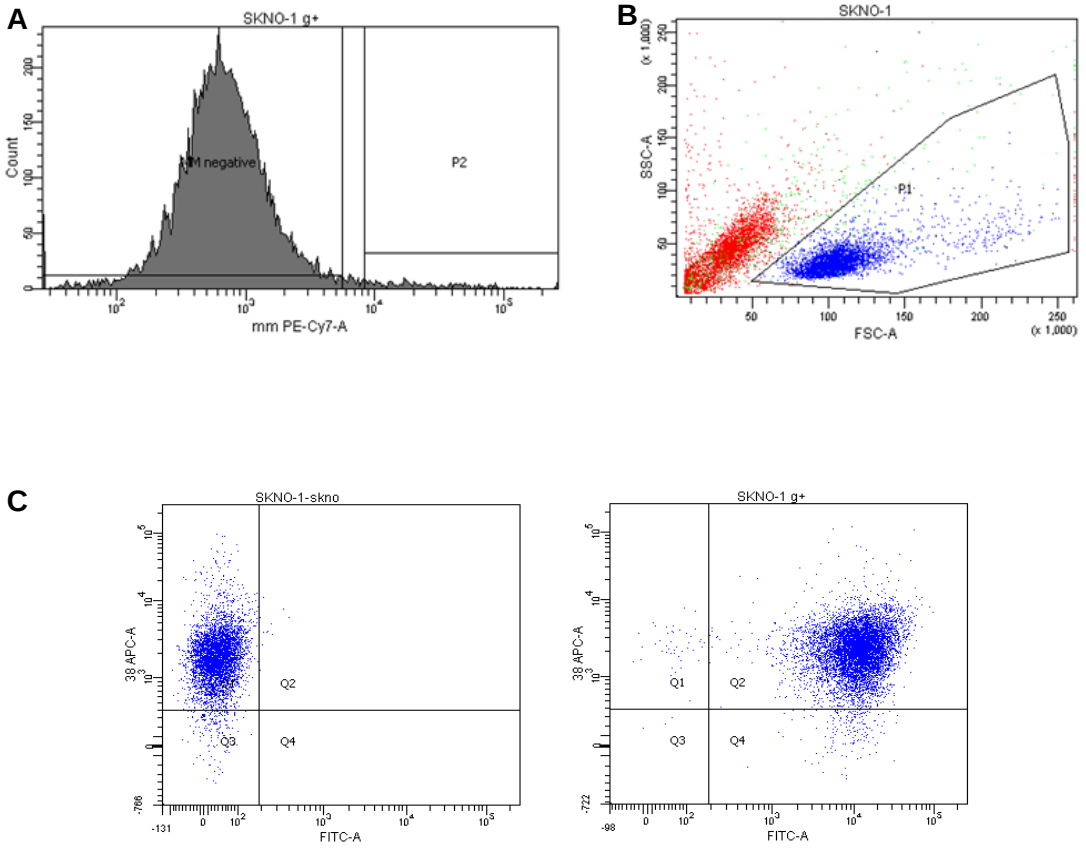

Figure 5.12 Gating of SKNO-1 cells in flow cytometric analysis. Single cell suspensions of cultured non-transduced SKNO-1 cells and unsorted gfp-positive transduced SKNO-1 cells in PBS were labelled with anti-human CD38-APC antibody in combination with anti-mouse CD45- and TER119-PE-Cy7 antibodies. **A**, Histogram showed the gating of human cells towards the right of the graph (marked as MM negative) on the mouse (mm) PE-Cy7 channel. **B**, Dot plot graph indicates further gating from MM negative to purify human cells from debris. **C**, Dot plot stained control negative (left) and control positive gfp (right) from ongoing culture showed SKNO-1 cells are CD38 positive. Negative control cells are negative for green fluorescence in FITC channel and positive control cells are positive green fluorescence cells.

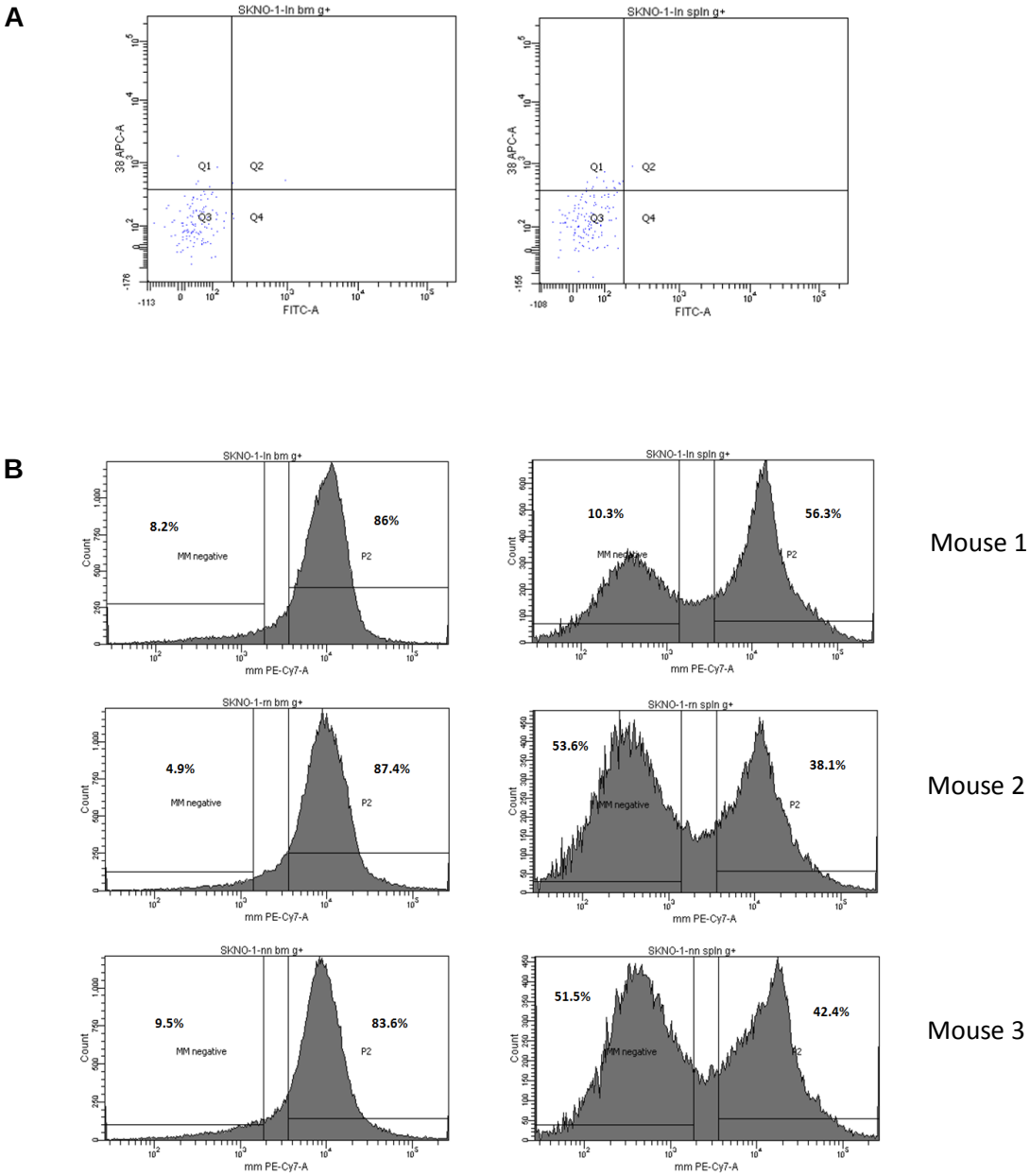

Figure 5.13 Flow cytometric analysis of SKNO-1$_{g+luc+}$ engrafted mice. Bone marrow and spleens were collected from all 3 dead mice and processed as described in *Materials and Methods*. Cells from bone marrow and spleen suspensions washed in PBS were labelled with human antibody CD38-APC in combination with mouse antibodies anti-CD45- and anti-TER119-PE-Cy7. **A**, Examples of dot plot results from bone marrow (left) and spleen (right) in FITC/CD38-APC channels. **B**, Histograms of bone marrow analysis (left panel) and spleen analysis (right panel) of mouse 1 (top), mouse 2 (middle) and mouse 3 (bottom). Histograms are in mmPE-Cy7/Count channel.

5.3 Discussion

The main aim of this chapter was to evaluate and track *in vivo* engraftment of different leukaemic cell lines transduced with lentivirus harbouring firefly (*Photinus sp.*) luciferase reporter gene (*luc*+) and green fluorescent protein (gfp+) sequence. *Luc*+ was utilized in the luminescence imaging whereas the gfp+ was used in the identification of the cells in flow cytometry analysis. In order to follow the expansion of the implanted cells and progression of the disease, a time course for bioluminescence imaging was performed.

Following implantation of the cells, all images of the engrafted mice showed luminescence at the site of implantation indicating the cells were successfully implanted into the femur cavity of the mice. This was based on the roughness felt during intrafemoral transplantation. However, the 26G needle used to 'drill' a hole on the tip of femur for insertion of the cells could possibly have minutely punctured the side wall of femur which could result in cells diffusing from the hole and accumulate in the surrounding muscle tissues, although this was never scientifically proven.

In the SEM implanted animals, dissemination of the cells was rapid. All mice presented with severe leukaemia conditions within 3-5 weeks post transplantation and mice were killed to prevent unnecessary suffering. Mice had loss of mobility of the hind limb, more severe in the first mouse to be affected, suggesting the cells had infiltrated the central nervous system of the animal. The engrafted mice seemed lethargic, which could be assumed due to heavy burden of the leukaemia. This was seen in the pattern of luminescence covering the entire body in one mouse and most body parts of the other two.

Isolated lymphocytes of mouse 2 however, were mistakenly labelled with CD38, which is not a surface marker for SEM cells. Thus, the SEM population could only be displayed as mouse negative cells; low in PE-Cy7 in the dot plot graphs. Nevertheless, the flow-analysis graphs confirmed the presence of SEM cells in the peripheral blood which proved the leukaemic cells were present in the circulation. It could be assumed, since all the mice had lost mobility of the hind leg towards the end-point, that the other two mice could have the same circulating leukaemic cells in the system, although the percentage of cells could be less. The bone marrow analysis showed the presence of the leukaemic cells indicating the leukaemic SEM cells were being generated in the compartment and the slightly enlarged spleens, measuring 1.2-1.5 cm in all mice, showed infiltration of

leukaemic cells as spleen also acts as a target for homing for lymphoid cells as well as the bone marrow.

In Kasumi-$1_{(gfp+luc+)}$ engraftment, none of the mice showed any effect of the disease on daily physical monitoring until the day the mice had to be terminated due to discomfort of the growing tumours. The luminescence images monitored throughout the study clearly indicated that the pattern of localized luminescence differed from those seen in SEM. The mice also survived longer despite the growing tumours. Compared to SEM engraftment, there was lower percentage of human cells populating the bone marrow cavity of Kasumi-1 engrafted mice.

There was a negligible percentage of cells measured by flow analysis of bone marrow and spleen in mice with leg tumours in the region of the initial site of implantation, which could probably mean that the implantation had missed the femoral compartment and implanted cells accumulated in the surrounding quadricep muscles. Hence, the Kasumi-$1_{(gfp+luc+)}$ cells implanted were trapped within the tissue and proliferated to form localized leg tumours. This phenomenon was occasionally seen in other xenograft studies in our group and may be because of fine, 27 or 30G, needle of the 0.5 ml insulin syringe used in intrafemoral injection is easily bent and could fail to penetrate the femoral cavity.

However, in the other two mice implanted with gfp+luc+ Kasumi-1 cells, localized tumours had also formed as seen in luminescence imaging. Flow analysis of bone marrow of these mice showed the bone marrow compartment contained only 6% to 11% human cells indicating the engrafted cells had migrated and expanded in different sites *in vivo*.

All Kasumi-1 transplanted mice develop localized tumours, although in different forms as shown by the photographs of the tumours. Interestingly, in all the tumours, more than 95% of the human cells gated out from mouse cells were gfp-positive cells. This phenomenon indicated that there was a possibility that the tumours retained the gfp+luc+ cells and the non-gfp+ cells spread elsewhere or did not survive in the engraftment.

The same behaviour of Kasumi-$1_{(gfp+luc+)}$ cells producing localized tumours and high percentage of these cells in the tumours were also seen in other experiments on intrahepatic transplantation of these cells into newborn Rag2 mice, not reported here. The Rag2 mice developed localized tumours in various sites, including the neck and abdominal cavity with no infiltration of the spleen or bone marrow after 8-9 weeks

engraftment (Elda Latif, Lars Buechler and Mike Batey). This indicates the Kasumi-$1_{(gfp+luc+)}$ cells tend to accumulate and form localized tumours.

Experiments using SKNO-1 engrafted mice failed to give conclusive results regarding the pattern of disease progression. The mice did not regain consciousness after the week 5 imaging procedure due to incorrect mixing oxygen and isoflurane in the anaesthesia. This experiment has not yet been repeated due to limitations in the numbers of NSG mice available for experimentation. In addition, the flow analysis of samples in the SKNO-1 mice did not show any gfp positive SKNO-1 cells although high percentages of gfp negative SKNO-1 cells were gated off from mice cells. The analysis was repeated twice at two separate times and the results were the same albeit the control positive SKNO-$1_{gfp+luc+}$ cells run at the same time gave high positive gfp cells population. The reasons for this are unclear.

In the growth curve study, all the cell lines used grew in suspension, but unlike the Kasumi-1 and SKNO-1 lines, the SEM cells tend to stick to flask surface and required a slight forced flushed with medium to detach the cells. This cell behaviour was a normal condition for SEM cells, as reported by other collaborating laboratories that used the same cell line (unpublished), although they were from different sources. The forced flushed was the reason causing the SEM cells to show a slower growth within 48 hours, a slightly longer lag phase time for the cells to recover before growing in its normal exponential phase, in which the doubling time of the SEM in the experiment is prolonged to between 48-72 hours instead of 30 hours as stated by the DSMZ database, the cell lines supplier. The growth curves for Kasumi-1 and SKNO-1 cells were as stated by the supplier. The growth curves study could explain the growth and expansion of the engrafted cell lines *in vivo* as mice transplanted with SEM cells developed leukaemic conditions earlier than SKNO-1 and Kasumi-1 engrafted mice.

In the luminescent imaging described in this chapter, SEM and Kasumi-1 images did not indicate the exact luminescent intensity. As the flow analysis indicated, there was also presence of gfp-negative cells in the culture which was used in the initial transplantation. This could give false negative images. For SKNO-1 it could be assumed that the luminescent light detected was totally from the cells since the SKNO-1 initially transplanted were from highly transduced cells (>98% cells transduced).

Several techniques have been improved since we first used IVIS System for bioluminescent imaging. Because luciferin can penetrate the cell membrane, luciferase in transduced cells in mice immediately reacted on the substrate producing luminescent light. In the beginning we measured the luminescent emission directly after injection of luciferin intraperitoneally, concomitant with anaesthesia. However, it has been reported that luminescent intensity produced is the highest 10 minutes after exogenous luciferin is administered.

After completion of the experiment in this chapter, it was decided that it was best to image mice individually rather than placing all three mice together in the chamber. This is due to different luminescence light intensity emitted by different mice depending on the expansion of the leukaemic cells in the individual mice. If a mouse with high engraftment of the lentiviral infected cells was viewed together with mouse with lower engraftment of the cells, the high luminescence intensity of the first mouse will obscure the luminescence intensity emitted by second mouse. Thus, the second mouse will appear to show no engraftment at the particular day of luminescence imaging.

It has been suggested that a comparison of luminescence intensity could be performed by serial dilution of transduced cells in plates viewed under the same conditions as the animal imaging to give an indication of cell expansion in transplanted mouse. A few studies of this type have been reported using the IVIS system. However, this method does not take into consideration diffraction of the light emitted by surrounding tissues.

In conclusion, mice engrafted with SEM cells succumbed to disease much earlier than Kasumi-1 and SKNO-1 engrafted mice, reflecting the rapid growth of this ALL cell line from a patient on relapse. The bioluminescence imaging was shown to provide a means of tracking progression of engrafted cells *in vivo*. Rapidly proliferating cells were shown to disseminate rapidly whereas slow proliferating cells were more likely to develop localize tumours in mice.

CHAPTER 6

GENERAL DISCUSSION

CHAPTER 6

GENERAL DISCUSSION

6.1 Overall Summary

Despite the many advances in understanding the development of acute lymphoblastic leukaemia, the ability to develop clinically effective therapies based on this knowledge is still of limited success. Although conventional therapies provide an overall favourable outcome for children with acute lymphoblastic leukaemia, up to 20% patients who include certain cytogenetic subgroups, suffer from a poor survival due to relapse. Re-treatment responses in these patients remain poor. There is therefore an urgent need for better targeted chemotherapy to improve event-free survival of these patients. Many advances have been made to understand the mechanisms which affect chemosensitivity. Various ALL cell lines or blasts from some ALL patients grown in specialized medium have been extensively used in drug response studies to relate the changes in drug uptake, metabolism or efflux on chemosensitivity. However, this does not reflect the clinical situation of the patients for several reasons. The majority of the cell lines are derived from relapse patients which are already chemoresistant. In addition, in most cell-line studies only a single therapeutic drug or one or two combinations of drugs are used while clinically patients are given more than 5 drugs in combination therapy for prolonged periods. Moreover, primary blast cells from patients do not divide in culture and the samples are time limited to work on extensively.

In order to overcome those limitations of in vitro work, this thesis have proposed an in vivo study utilizing humanized mice as a model for leukaemic blasts xenograft. The NOD-SCID IL2Rγ^{null} (NSG) mouse model was chosen as this model more accurately reflects the clinical situation. The NSG model is also suitable for highly efficient engraftment of malignant or normal hematopoietic cells as supported by other workers (Ishikawa, Yasukawa et al. 2005; Shultz, Ishikawa et al. 2007; Le Viseur, Hotfilder et al. 2008; Notta, Doulatov et al. 2008; Schmitz, Breithaupt et al 2011).

In Chapter 3, the xenografted match paired L707 presentation and relapse blast cells both were able to repopulate mouse bone marrow, disseminate in peripheral blood and infiltrate organs, particularly the spleen and ovaries, and occasionally at random, liver,

kidneys and gastric lining. The accumulation, distribution and localization of engrafted blasts were proven by the high percentage of human blasts measured in mouse bone marrow, spleens and ovaries, which is in agreement with other reported studies (Yan, Wieman et al. 2009; Cheung, Fung et al. 2010). Blast cells harvested from engrafted spleen of mice from primary and secondary transplantation of both L707 presentation and relapse showed similar morphology to that of the original patient biopsies, indicating high infiltration of human leukaemic cells, confirmed by the presence of ALL leukaemic markers. Importantly, the morphology and the immunophenotypes of xenografts were essentially unaltered from the original patient samples.

In primary transplantation of L707 blast cells and in the subsequent secondary transplantation, the ovaries of the mice were persistently infiltrated by engrafted relapse blasts but not the presentation blasts, marked by the high percentage of human leukaemic cells retrieved from the ovaries. Up to 99% of relapse blast cells were measured in the ovaries which is an interesting finding, although no similar findings have been reported. There were several studies reported on ovary infiltration in ALL patients who relapsed (Reid and Marsden 1980; Chu, Craddock et al. 1981; Kim, Cho et al. 2008) although the incidence is rare, and no indication of presentation cells localizing in the ovaries have been reported. However, Dolmans et al. in their study had reported that, although the histology of cryopreserved ovarian tissue from ALL patients did not show presence of leukaemic cells, 7 of 12 patients showed positive leukaemic markers in their ovarian tissues. In addition, 4 of the reimplanted ovarian tissues produced abdominal leukaemic masses in grafted mice (Dolmans, Marinescu et al. 2010). The claim from this paper indicates that there is a possibility of very minimal percentage of presentation cells residing in the ovary of engrafted mice without changing the morphology of the tissue. Unfortunately, this possibility was not taken into consideration in the L707 xenografts. Perhaps this parameter could be included in future experiments. Although the actual condition of the deceased L707 patient was not known, there is a high possiblility the disease could have affected the ovaries of the patient in similar manner after relapse. Infiltration of leukaemic blasts into other organs is an indicatation of widespread disease.

A study reported on an invasive pre-B-ALL relapse cell line and patient relapse cells that produced CNS leukaemia in engrafted NOD/SCID mice. The pre-B cell line uniquely expressed asparaginyl endopeptidase (AEP), intracellular adhesion molecule-1 (ICAM-1) and ras-related C3 botulinum toxin substrate 2 (RAC2), in which the latter was also

identified in the bone marrow aspirate obtained from the relapsed patient. These findings suggest that these proteins supported the engraftment of ALL blasts and the occurrence of CNS disease in the mice (Holland, Castro et al. 2011). Although the condition of the mice was not reported in their study, this evidence may perhaps explain the loss of hind leg mobility seen in the L707 presentation cell but not relapse cell engrafted mice (without treatment), which was persistently experienced by all primary and secondary xenografted mice. Flow cytometry analysis of the spinal cord (together with brain stem) of a few mice in this presentation group indicated the presence of human leukaemic blasts in the sample, which strongly supports the evidence for CNS infiltration of the presentation cells. Besides, the fundamental and essential mechanisms that control postural muscle tone and locomotion are located in the brain stem and spinal cord (Jahn, Deutschländer et al. 2008; Takakusaki and Matsuyama 2010). Thus, infiltration of leukaemic blasts in the brain stem and spinal cord could have caused the partial immobility condition, which was confirmed by the presence of blasts cells in these regions in flow cytometry analysis. Moreover, as mentioned in Chapter 3, the L707 presentation and relapse cells were positive for CD10 and CD19 fraction. These surface markers were also mentioned by Holland et al. as the fraction which contributed to infiltration of the relapse cells into the CNS (Holland, Castro et al. 2011). Contrary to the reported evidence, in the L707 case, there was no possible explanation for why the relapse cells did not invade the CNS compartment in the same way as presentation cells.

In the competitive repopulation of L707 discussed in Chapter 3, NSG mice were xenotransplanted with various proportions of presentation and relapse cells to investigate which clone has a greater advantage of repopulating and disseminating in the absence or presence of dexamethasone treatment. In the absence of treatment, following engraftment, mice engrafted with a higher proportion of presentation cells (90%-P+10%-R and 70%-P+30%-R) showed severe manifestation of the disease with loss of locomotion in the hind region, which was not observed in mice engrafted with lower presentation cell proportions (10%-P+90%-R, 30%-P+70%-R and 50%-P+50%-R). This condition shows that although in the presence of a small percentage of relapse cells, a higher percentage of presentation cells in the engrafted population manifested the disease. However, a higher proportion of relapse cells in the engrafted populations may combat the ability of presentation cells to manifest the disease by ‘crowding’ the in vivo environment, marginally lowering the presentation efficiency to manifest the disease condition. As a

lymphocytotoxic drug, dexamethasone presumedly killed most of the presentation cells, given that glucocorticoid receptors in this cell population are intact (unlike the affected GC-receptor in relapse cells).

Initially, it was thought that following relapse, leukaemic cells would divide more rapidly than presentation given the notion that in subpopulations of poor prognosis ALL, patients did not survive post relapse. However, this hypothesis proved to be wrong in the L707 case. The survival curve of the engrafted mice showed mice xenografted with L707 presentation cells had a shorter life span than those of relapse, indicating the presentation cells were more 'aggressive', proliferating rapidly, producing rapid fatality of engrafted mice. Mice engrafted with various proportions of presentation and relapse blasts had an intermediate level of survival. Meyer et al. in their study implied that the shorter the time that the diagnosis cells transplanted into NOD/SCID mice took to manifest leukaemia, the higher the risk that these patients would relapse (Meyer, Eckhoff et al. 2011). In the L707 case, mice engrafted with presentation cells succumbed to leukaemia in less than 8 weeks post transplantation, within the 10 weeks threshold of rapid time to leukemia. This result reflected the clinical condition where the L707 patient suffered from relapse 5 months after remission.

Introduction of dexamethasone prolonged the survival of mice engrafted with presentation blasts, and survival of mice engrafted with various proportions of the presentation blasts reached similarity to those of relapse. Relapse survival curves were not affected in the absence or presence of treatment. To date similar findings have not be reported elsewhere. One closely related study was reported by Kang et al., although in their study a combination of vincristine-dexamethasone-L-asparaginase (VXL) was used as treatment for engrafted mice. Event free survival (EFS) was quantified as the time taken from initiation of treatment until the mice were killed due to treatment-related toxicity during and 4 week post treatment. There was no difference in the EFS of vehicle-treated controls of both diagnostic and relapse engrafted mice. VXL treatment significantly delayed progression of diagnostic cells by 7-fold and relapse cells by 3.5-fold (Kang, Kang et al. 2007). It could be hypothesized that the treated presentation mice could have survived longer than relapse mice, due to elimination of presentation cells by dexamethasone. However, taking into consideration that not all presentation cells were killed during treatment, the remaining presentation cells would rapidly proliferate. With increasing tumour burden, the engrafted mice only survived 2 weeks longer than the non-

treated presentation mice. A study by Yan et al. derived pre-B ALL leukaemic blasts from the same patient at diagnosis and relapse, and subcutaneously inoculated the blasts into SCID mice. Based on the size of tumour growth subcutaneously, they reported that the diagnosis and first relapse blasts either did not grow or grew very slowly, while blasts at second relapse grew in an indolent manner, and blasts at third relapse displayed an aggressive growth pattern. They concluded that patients whose leukaemic cells grew aggressively either at diagnosis or relapsed had a worse clinical outcome than those with no tumour or indolent growth pattern (Yan, Wieman et al. 2009). This study is the closest possible comparison that showed a contrast of aggressiveness of leukaemic blasts to the findings from the L707 case. The prognosis of the patient is in agreement with their study. Interestingly, the duration of survival of mice engrafted with L707 relapse blasts correlated directly to the survival of the patient following relapse.

Further analysis was done in competitive repopulation with various proportions (mixed populations) of presentation and relapse blast cells to determine the proportion of cells populated in the engrafted mice. It was shown by FISH, in agreement with molecular analysis that without treatment, the percentages of presentation cells engrafted were higher than the initial proportions of the cells transplanted into mice, indicating the presentation cells outnumbered the relapse cells because of the aggressiveness and rapid proliferation of the cells. Dexamethasone administration successfully reduced the percentages of these presentation cells, allowing an advantage for relapse cells to populate more. Interestingly, in dexamethasone treated mice engrafted with presentation blasts, one of the mice had 16% of cells showing a single signal for the *NR3C1* gene which indicates a deletion of the *NR3C1* gene occurred in these cells. This heterozygous deletion is likely induced by dexamethasone treatment. In the whole population of leukaemia, leukaemic stem cells (LSCs) or leukaemic-initiating cells exist within the tumour and sustain the growth of the tumour by clonal proliferation. Perhaps following transplantation of the leukaemia cells intrafemorally into mice, the LSCs could have homed within the niche in the bone marrow. It has been mentioned elsewhere (Yamazaki, Iwama et al. 2009; van der Wath, Wilson et al 2009; Trumpp, Essers et al. 2010) that similar to hematopoietic stem cells, the leukaemic stem cells (LSCs) exist individually in their niches in the bone marrow in dormancy and quiescence stage. The dormant LSCs are awakened in response to hematopoietic stress to replenish hematopoietic system with a malignant clone (Trumpp, Essers et al. 2010). Dexamethasone treatment caused depletion in blood supply

when presentation cells (or other mice normal blood supply) were killed and in turn reduced the tumour burden. During the awakening from dormancy stage, LSCs could be targeted by continuous dexamethasone treatment which could have caused the heterozygous deletion. Following cessation of treatment, the affected LSCs would then proliferate to replenish the hematopoietic system with the new malignant clone. The proliferation capacity could be slower as the LSCs now are similar to the relapse cells. At the same time, probably the remaining presentation cell clones propagate to repopulate the system. Thus, a small percentage of heterozygous one allele deletion of *NR3C1* leukaemic cells and homozygous unaffected *NR3C1*leukaemic cells could have circulated in the engrafted mice, repopulate in the bone marrow, disseminate and infiltrate the spleen. This could be the possible explanation for the presence of heterozygous *NR3C1*allele.

Assessment of the repopulation of presentation and relapse blasts would be greatly facilitated if these cell populations could be physically tracked utilizing a real-time bioluminescence detector. For this purpose, lentiviruses carrying different reporter genes have been developed as a tool for transferring these genes into target cells. In Chapter 4, the generated lentiviruses pSLIEW and pSRLICW were proven fuctional. pSLIEW efficiently transduced AML (SKNO-1 and Kasumi-1), compared to ALL cells (SEM and RS4;11). By comparison to RS4;11 which yielded negligible transduction capacity, transduction efficiencies in SEM was 9-fold higher, Kasumi-1 was 15-fold higher and almost 20-fold higher in SKNO-1 cells. Several attemps were made to transduce L707 cells but patient primary cells were proven difficult to successfully tranduce. This work had to be abandoned due to limited supply of primary materials.

In Chapter 5, the transduced and sorted SEM and Kasumi-1 cells were engrafted into NSG mice and progression of disease was successfully monitored by luminescent imaging. Images from engrafted SEM cells showed a rapid progression of leukaemic disease in which the engrafted mice were short-lived; they succumbed to the disease after three to five weeks post xenotransplantation. These mice showed loss of locomotion in the hind region as seen in the L707 studies. Although SEM cells are cells from relapse, nonetheless, the imaging results and the physical condition may be the best way to correlate with the aggressiveness of the L707 presentation cells discussed in Chapter 3. It could be possible that similar images of disease progression were seen if the L707 were able to be transduced. The peripheral blood confirmed the presence of SEM cells which

explained the overall widespread luminescence detected. The luminescence image showed engraftment of the SEM cells through the blood system including the cranial region. This observation is in agreement with Xie et al. who demonstrated the first real time imaging on migration of HSC cells from bone marrow to the cranial region of mice (Xie, Yin et al. 2009). Moderate engraftments of blast cells were measured in the bone marrow and spleen of engrafted mice possibly because the cells were rapidly disseminating in the blood, without depositing to a great extent in the solid organs.

Contrasting observations were made in the Kasumi-1 engrafted mice. Kasumi-1 cells are slowly progressing cells which tend to produced solid tumours in xenografted mice. Luminescence images showed progression of tumour mass but not widespread disease. Mice were killed because of tumour mass burden, with no symptoms or signs of physical illness. At post mortem various types and sizes of tumours were discovered, particularly in the abdominal cavities of 2 of the engrafted mice. All tumours showed high percentages of Kasumi-1 cells. Low engraftment of Kasumi-1 cells was measured in the bone marrow and spleen of xenografted mice due to the accumulation of the cells in the tumours. Maris et al., in their anti-tumour drug testing study, used Kasumi-1 for the reason that the cell line produced solid tumours which was a suitable model for their experiment (Maris, Courtright et al. 2008).

6.2 Overview

L707 presentation and relapse cells repopulated and engrafted NSG mice and recapitulated human disease. Presentation cells persistently infiltrated the CNS whereas relapse cells persistently infiltrated the ovary. The presentation cells were more aggressive leading to rapid fatality; this proliferation was affected by dexamethasone.

The lentiviral-transduced cell lines SEM and Kasumi-1 xenografts have proved the in vivo monitoring capability by luminescence imaging. SEM lines showed rapid widespread disease whereas Kasumi-1 lines produced localized tumour masses.

6.3 Future Investigations

In future experiments, additional drug approaches such as treating mice with vincristine or methotrexate alone or in combination could be used to more closely mimic the clinical

situation and determine if the effect on therapy of GR deletion is restricted to dexamethasone.

In future work, a prospective study could be included to evaluate the molecular mechanism that may contribute to the different growth characteristics of the leukaemic blasts. Genes involved in proliferation and survival of the cells such as β-catenin could be of interest in future knockdown studies. β-catenin has been implicated as an integral component in Wnt signalling pathway which controls self-renewal of hematopoietic stem cells. Dysregulation of this pathway occurs in various malignancies including leukaemia. High expression and accumulation of β-catenin was detected in ALL blasts, which provide proliferation and survival advantage to leukaemic B-cell progenitors (Khan, Bradstock et al. 2007). It has been reported that by down-regulating β-catenin levels in AML cell lines and patient samples, engraftment in the bone marrow of xenografted mice was affected due to reduced adhesion to the endosteum. It was concluded that β-catenin plays a major role in proliferation, cell cycle progression, adhesion and influences disease establishment in vivo (Gandillet, Park et al. 2011; Siapati, Papadaki et al. 2011). In this way, targeting the Wnt signalling pathway might be a useful therapeutic strategy in treating pro-B ALL.

Very recently, Uchida et al. had perfected an optimized protocol by Millington et al. to improve the transduction efficiency of CD34+ cells by stimulating the cells for 24 hours in a serum-free media supplemented with SCF, FLT3 and thrombopoietin, and followed by 24 hours lentiviral transduction in the media (Millington, Arndt et al. 2009; Uchida, Hsieh et al. 2011). As a result, high transduction efficiency was achieved and the engraftment of cells in humanized xenograft mice was improved (Uchida, Hsieh et al. 2011). In future work, this technique could be adopted for improving transduction efficiency of cell lines. Importantly, the aim is to achieve high transduction efficiency for L707 blast cells for xenograft, and for tracking the cells as planned for the competitive repopulation study.

The disadvantage of the clonal evolution and competitive repopulation studies in this thesis is that the study is based only on a single case of matched paired presentation and relapsed t(17;19) cells. For comparison studies perhaps other matched paired patient primary materials of the same or different translocations could be obtained for the studies.

REFERENCES

REFERENCES

Ablett, S., C.R. Pinkerton, et al. (2003). "Recruiting children into cancer trials--role of the United Kingdom Children's Cancer Study Group (UKCCSG)." British journal of cancer. **88**(11): 1661-5.

Acute Lymphocytic Leukaemia (ALL): Leukaemias: Mercks Manual Home Edition." Retrieved 15/02/2011, from http://www.merckmanuals.com/home/sec13/ch159/ch159b. html.

Akahane, K., T. Inukai, et al. (2010). "Specific induction of CD33 expression by E2A–HLF: the first evidence for aberrant myeloid antigen expression in ALL by a fusion transcription factor." Leukaemia. **24**: 865-869.

al Yacoub N., M. Romanowska, et al. (2007). "Optimized production and concentration of lentiviral vectors containing large inserts." J Gene Med. **9**: 579–584.

Alcaraz-Perez, F., V. Mulero, et al. (2008). "Application of the dual-luciferase reporter assay to the analysis of promoter activity in Zebrafish embryos." BMC Biotechnology. **8**(1): 81.

Altura, R.A., T. Inukai, et al. (1998). "The chimeric E2A-HLF transcription factor abrogates p53-induced apoptosis in myeloid leukaemia cells." Blood. **92**(4): 1397-1405.

Anderson, K., C. Lutz, et al. (2011). "Genetic variegation of clonal architecture and propagating cells in leukaemia." Nature. **469**(7330): 356-361.

Appel, I.M., C. van Kessel-Bakvis, et al. (2007). "Influence of two different regimens of concomitant treatment with asparaginase and dexamethasone on hemostasis in childhood acute lymphoblastic leukaemia." Leukaemia. **21**: 2377-2380.

Arhel, N.J., S. Souquere-Besse, et al. (2007). "HIV-1 DNA Flap formation promotes uncoating of the pre-integration complex at the nuclear pore." Embo J. **26**: 3025-3037.

Armstrong, S.A. and A.T. Look. (2005). "Molecular genetics of acute lymphoblastic leukaemia." Journal of Clinical Oncology. **23**(26): 6306-6315.

Asou, H., S. Tashiro, et al. (1991). "Establishment of a human acute myeloid leukaemia cell line (kasumi-1) with 8;21 chromosome translocation." Blood. **77**(9): 2031-2036.

Auboeuf, D., A. Honig, et al. (2002). "Coordinated regulation of transcription and splicing by steroid receptor coregulators." Science. **298**(298): 416-419.

Bachmann, P.S., R. Gorman, et al. (2005). "Dexamethasone resistance in B-cell precursor childhood acute lymphoblastic leukaemia occurs downstream of ligand-induced nuclear translocation of the glucocorticoid receptor." Blood. **105**: 2519-252.

Bachmann, P.S., R. Gorman, et al. (2007). "Divergent mechanisms of glucocorticoid resistance in experimental models of paediatric acute lymphoblasttic leukaemia." Cancer Res. **67**: 4482-4490.

Bain, B.J. (1999). Leukaemia diagnosis. London: Blackwell Science.

Bain, G., E.C. Robanus-Maandag, et al. (1994). "E2A proteins are required for proper B-cell development and initiation of immunoglobulin gene rearrangements." Cell. **79**: 885-892.

Bain, G., E.C. Robanus-Maandag, et al. (1997). "Both E12 and E47 allow commitment to the B cell lineage." Immunity. **6**: 145–154.

Baird, S.D., M. Turcotte, et al. (2006). "Searching for IRES." RNA. **12**: 1755-1785.

Baltimore, D. (1970). "RNA-dependent DNA polymerase in virions of RNA tumor viruses." Nature. **266**: 1209-1211.

Baltimore, D. (2009). "Discovering NF-Kb." Cold Spring Harb Perspect Biol. **1**:a000026

Balvay, L., R. Soto Rifo, et al. (2009). "Structural and functional diversity of viral IRESs." Biochim Biophys Acta. **1789**: 542–557.

Bamberger, C.M., H.M. Schulte, et al. (1996). "Molecular determinants of glucocorticoid receptor function and tissue sensitivity to glucocorticoids." Endocr Rev. **17**(3): 245-261.

Benaron, D.A., P. Contag, et al. (1997). "Imaging brain structure and function, infection and gene expression in the body using light." Phil. Trans. R. Soc. Lond. **352**: 755-761.

Bhadri, V., M.J. Cowley, et al. (2010). "The NOD/SCID xenograft model provides clinically-relevant insights into glucocorticoid-induced gene expression in childhood B-cell precursor acute lymphoblastic leukemia (ALL)." Prosiding of the 53rd ASH Annual Meeting and Exposition.

Bhaumik, S. and S.S. Gambhir. (2002). "Optical imaging of Renilla luciferase reporter gene expression in mice." PNAS. **99**(1): 377-382.

Bomken, S., K. Fiser, et al. (2010). "Understanding the cancer stem cell." Br J Cancer. **103**(4): 439-445.

Bonapace, L., B.C. Bornhauser, et al. (2010). "Induction of autophagy-dependent necroptosis is required for childhood acute lymphoblastic leukaemia cells to overcome glucocorticoid resistance." The Journal of Clinical Investigation. **120**(4): 1310-1323.

Bonnet, D. (2005). "Leukemic stem cells show the way." Folia Histochemica et Cytobiologica. **43**(4): 183-186.

Bonnet, D. (2005). "Normal and leukaemic stem cells." British Journal of Hematology. **130**: 469-479.

Bonnet, D. and J.E. Dick. (1997). "Human acute myeloid leukemia is organized as a hierarchy that originates from a primitive hematopoietic cell." Nat Med. **3**: 730-737.

Bosma, G.C., R.P. Custer, et al. (1983). "A severe combined immunodeficiency mutation in the mouse." Nature. **301**: 527-530.

Bosma, M.J. and A.M. Carroll. (1991). "The SCID mouse mutant: definition, characterization, and potential uses." Annu Rev Immunol. **9**: 323-350.

Bostrom, B.C., M.R. Sensel, et al. (2003). "Dexamethasone versus prednisone and daily oral versus weekly intravenous mercaptopurine for patients with standard-risk acute lymphoblastic leukaemia: a report from the Children's Cancer Group." Blood. **101**: 3809-3817.

Brenner, S. and H.L. Malech. (2003). "Current developments in the design of onco-retrovirus and lentivirus vector systems for hematopoietic cell gene therapy." Biochemical et Biophysica Acta. 1-24.

Bronnegard, M. (1996). "Steroid receptor number: Individual variation and downregulation by treatment." Am. J. Respir. Crit. Care Med. **154**: S28-S33.

Bryder, D., D.J. Rossi, et al. (2006). "Hematopoietic Stem Cells: The Paradigmatic Tissue-Specific Stem Cell." Am J Pathol. **169**(2): 338-346.

Bukovsky, A.A., J.P. Song, et al. (1999). "Interaction of human immunodeficiency virus-derived vectors with wild-type virus in transduced cells." J Virol. **73**: 7087-7092.

Bukrinsky M.I., N. Sharova, et al. (1993). "Association of integrase, matrix, and reverse transcriptase antigens of human immunodeficiency virus type 1 with viral nucleic acids following acute infection." Proc Natl Acad Sci USA. **90**: 6125-6129.

Cai, S. H. Wang, et al. (2010). "Differential secondary reconstitution of in vivo-selected human SCID-repopulating cells in NOD/SCID versus NOD/SCID/γchain^{null} mice." Bone Marrow Research. **2011**: 1-11.

Campbell E.M., R. Nunez, et al. (2004). "Disruption of the actin cytoskeleton can complement the ability of Nef to enhance human immunodeficiency virus type 1 infectivity." J Virol. **78**: 5745-5755.

Carroll, W. L., D. Bhojwani, et al. (2003). "Pediatric Acute Lymphoblastic Leukaemia." Hematology. **2003**(1): 102-131.

Castor, A., L. Nilsson, et al. (2005). "Distinct patterns of hematopoietic stem cell involvement in acute lymphoblastic leukemia." Nat Med. **11**: 630-637.

Chang, J.S. (2008). "Parental smoking and childhood leukaemia." Methods in Molecular Biology. **472**: 103-137.

Charmandari, E., C. Tsigos, et al. (2005). "A novel point mutation in the ligand-binding domain (LBD) of the human glucocorticoid." J Clin Endocrinol. **67**: 259-284.

Charmandari, E., T. Kino, et al. (2004). "Molecular mechanisms of glucocorticoid action." Orphanet. 1-8.

Chessells, J.M., P. Veys, et al. (2003). "Long-term follow-up of relapsed childhood acute lymphoblastic leukaemia." British Journal of Haematology. **123**: 395-405.

Cheung AMS, TK Fung, et al. (2010). "Successful engraftment by leukaemia initiating cells in adult acute lymphoblastic leukaemia after direct intrahepatic injection into unconditioned newborn NOD/SCID mice." Experimental Hematology. **38**(1): 3-10.

Cheung, J. and D.F. Smith. (2000). "Molecular chaperone interactions with steroid receptors: an update." Mol Endocrinol. **14**: 939-946.

Chiu, P.P., E. Ivakine, et al. (2002). "Susceptibility to lymphoid neoplasia in immunodeficient strains of nonobese diabetic mice." Cancer Res. **62**: 5828-5834.

Chu, J.Y., T.V. Craddock, et al. (1981). "Ovarian tumor as manifestation of relapse in acute lymphoblastic leukaemia." Cancer. **48**(2): 377-379.

Chumsri, S., W. Matsui, et al**.** (2007). "Therapeutic implications of leukaemic stem cell pathways." Clinical Cancer Research. **13**(22): 6549-6554.

Clarke, M.F., J.E. Dick, et al. (2006). "Cancer stem cell - Perspectives on current status and future directions." Cancer Res. **66**: 9339-9344.

Clever, J., C. Sassetti, et al. (1995). "RNA secondary structure and binding sites for gag gene products in the 5' packaging signal of human immunodeficiency virus type 1." J Virol. **69**: 2101-2109.

Cobaleda, C., N. Gutierrez-Sianca, et al. (2000). "A primitive hematopoietic cell is the target for leukemic transformation in human Philadelphia-positive acute lymphoblastic leukemia." Blood. **95**: 1007-1013.

Coffin, J.M., S.H. Hughes, et al. (1997). Retroviruses. Cold Spring Harbor, NY: Cold Spring Harbor Laboratory Press.

Contag, C.H., and B.D. Ross. (2002). "It's not just about anatomy: In vivo bioluminescence imaging as an eyepiece into biology." Journal of Magnetic Resonance Imaging. **16**: 378-387.

Cox, C.V., R.S. Evely, et al. (2004). "Characterization of acute lymphoblastic leukaemia progenitor cells." Blood. **104**(9): 2919-2925.

Cox, C.V., P. Diamanti, et al. (2009). "Expression of CD133 on leukaemia-initiating cells in childhood ALL." Blood. **113**: 3287-3296.

Dang, J., T. Inukai, et al. (2001). "The E2A-HLF oncoprotein activates *Groucho*-related genes and suppresses *Runx1*." Molecular and Cellular Biology. **21**(17): 5935-5945.

Devaraj, P.E., L. Foroni, et al. (1994). "E2A/HLF fusion cDNAs and the use of RT-PCR for the detection of minimal residual disease in t(17;19)(q22;p13) acute lymphoblastic leukaemia." Leukaemia. **8**(7):1131-1138.

Dick, J.E. (2008). "Stem cell concepts renew cancer research." Blood. **112**(13): 4793-4807.

Dick, J.E., T. Lapidot, et al. (1991). "Transplantation of normal and leukemic human bone marrow into immune deficient mice: development of animal models for human haematopoiesis." Immunological Reviews. **124**(1): 25-43.

Dickinson, H.O. (2005). "The causes of childhood leukaemia." BMJ. **330**: 1279-1280.

Distelhorst, C.W. (2002). "Recent insights into the mechanism of glucocorticoid-induced apoptosis." Cell Death Differ. **9**: 6-19.

Dobrowsky T.M., Y. Zhou, et al. (2008) Monitoring early fusion dynamics of human immunodeficiency virus type 1 at single-molecule resolution. J Virol **82**: 7022–7033.

Dolmans, M.M, C. Marinescu, et al. (2010). "Reimplantation of cryopreserved ovarian tissue from patients with acute lymphoblastic leukemia is potentially unsafe." Blood. **116**: 2908-2914.

Dull, T., R. Zufferey, et al. (1998). "A third-generation lentivirus vector with a conditional packaging system." J Virol. **72**: 8463-8471.

Eden, O.B., G. Harrison, et al. (2000). "Long-term follow-up of the United Kingdom Medical Research Council protocols for childhood acute lymphoblastic leukaemia, 1980–1997." Leukaemia. **14**: 2307-2320.

Encio, I.J. and S.D. Detera-Wadleigh. (1991). "The genomic structure of the human glucocorticoid receptor." The Journal of Biological Chemistry. **266**(11): 7182-7188.

Essers, M.A.G. and A. Trumpp. (2010). "Targeting leukemic stem cells by breaking their dormancy." Molecular Oncology. **4**: 443-450.

Feng S. and E.C. Holland. (1988). "HIV-1 tat trans-activation requires the loop sequence within tar." Nature. **334**: 165–167.

Findley, H.W.Jr., M.D. Cooper, et al. (1982). "Two new acute lymphoblastic leukemia cell lines with early B-cell phenotypes." Blood. **60**: 1305-1309.

Fischer, A. and M. Cavazzana-Calvo. (2005). "Integration of Retroviruses: A Fine Balance between Efficiency and Danger." PLoS Med. **2**(1): e10.

Galili, U. (1983). "Glucocorticoid induced cytolysis of human normal and malignant lymphocytes." J Steroid Biochem. **19**: 483-490.

Gandillet, A., S Park, et al. (2011). "Heterogeneous sensitivity of human acute myeloid leukaemia to β-catenin down-modulation." Leukaemia. **25**: 770-780.

Gaynon, P.S. (2005). "Childhood acute lymphoblastic leukaemia and relapse." British Journal of Haematology. **131**: 579-587.

Gaynon, P.S. and A.L. Carrel. (1999). "Glucocorticoid therapy in childhood acute lymphoblastic leukemia." Adv Exp Med Biol. **457**: 593-605.

Geng, C-D. and V. Vedeckis. (2011). "A new lineage specific, autoup-regulation mechanism for human glucocorticoid receptor gene expression in 697 pre-B acute lymphoblastic leukemia cells." Molecular Endocrinology. **25**(1): 44-57.

Geng, C-D., K.B. Pedersen, et al. (2005). "Human glucocorticoid receptor α transcript splice variants with exon 2 deletions: evidence for tissue- and cell type-specific function." Biochemistry. **44**: 7395-7405.

Gibbs, J.S, D.A. Regier, et al. (1994). "Construction and in vitro properties of HIV-1 mutants with deletions in "nonessential" genes." AIDS Res Hum Retroviruses. **10**: 343-350.

Giguere, V., S.M. Hollenberg, et al. (1986). "Functional domains of the human glucorticoid receptor." Cell. **46**: 645-652.

Greaves, M. (1993). "A natural history for pediatric acute leukemia." Blood. **82**: 1043-1051.

Greaves, M. (1999). "Molecular genetics, natural history and the demise of childhood leukaemia." European Journal of Cancer. **3514**: 1941-1953.

Greaves, M. (2002). "Science, medicine and the future: Childhood leukaemia." BMJ. **324**: 283-287.

Greaves, M.F. (1993). "Stem cell origins of leukaemia and curability." British J Cancer. **67**: 413-423.

Greenstein, S., K. Ghias, et al. (2002). "Mechanism of glucocorticoid-mediated apoptosis in hematological malignancies." Clin Cancer Res. **8**: 1681-1694.

Greil, J., M. Gramatzki, et al. (1994). "The acute lymphoblastic leukaemia cell line SEM with t(4;11) chromosomal rearrangement is biphenotypic and responsive to interleukin-7." Br J Haematol. **86**(2): 275-283.

Greiner, D.L., R.A. Hesselton and L.D. Shultz. (1998). "SCID mouse models of human stem cell engraftment." Stem Cells. **16**: 166-177.

Hanahan, D. and R.A. Weinberg. (2000). "The hallmarks of cancer." Cell. **100**: 57-70.

Harrison, C.J. and L. Foroni. (2002). "Cytogenetics and molecular genetics of acute lymphoblastic leukaemia." Clinical and Experimental Hematology. **6**(2): 91-113.

Harvey, R.C., C.G. Mullighan, et al. (2010). "Identification of novel cluster groups in pediatric high-risk B-precursor acute lymphoblastic leukaemia with gene expression profiling: correlation with genome-wide DNAcopy number alterations, clinical characteristics, and outcome." Blood. **116**(23): 4874-4884.

Hastings, J.W. (1996). "Chemistries and colors of bioluminescent reactions: a review." Gene. **173**(1): 5-11.

Heerema, N.A., J.B. Nachman, et al. (1999). "Hypodiploidy with less than 45 chomosomes confers adverse risk in childhood acute lymphoblastic leukaemia: a report from the Children's Cancer Group." Blood. **94**(12): 4036-4045.

Hesselton, R.M., D.L. Greiner, et al. (1995). "High levels of human peripheral blood mononuclear cell engraftment and enhanced susceptibility to human immunodeficiency virus type 1 infection in NOD/LtSz-scid/scid mice." J Infect Dis. **172**:974-982.

Hilden, J.M., P.A. Dinndorf, et al. (2006). "Analysis of prognostic factors of acute lymphoblastic leukaemia in infants: report onCCG 1953 from the Children's Oncology Group." Blood. **108**: 441-451.

Hillmann, A.G., J. Ramdas, et al. (2000). "Glucocorticoid Receptor Gene Mutations in Leukemic Cells Acquired in Vitro and in Vivo." Cancer Research **60**(7): 2056-2062.

Hittleman, A.B., D. Burakov, et al. (1999). "Differential regulation of glucocorticoid receptor transcriptional activation via AF-1- associated proteins." EMBO J. **18**(19): 5380-5388.

Hjalgrim, L.L., K. Rostgaard et al. (2004). "Birth weight and risk for childhood leukaemia in Denmark, Sweden, Norway and Iceland." J Nat Cancer Inst. **96**: 1549-1556.

Hoffbrand, A.V., P.A.H. Moss, et al. (2006). Essential Hematology. Massachusetts, USA: Blacwell Publishing.

Holland, M., F.V. Castro, et al. (2011). "RAC2, AEP, and ICAM1 expression are associated with CNS disease in a mouse model of pre-B childhood acute lymphoblastic leukemia." Blood. **118**(3): 638-649.

Hollenberg, S.M. and R.M. Evans. (1988). "Multiple and cooperative trans-activation domains of the human glucocorticoid receptor." Cell. **55**(5): 899-906.

http://www.sciencedaily.com/releases/2008/05/080527091950.htm

Huggins, C.B. and K. **Uematsu.** (1976). "Induction of lymphatic leukaemia in non-inbred mice and its control with glucocorticoids." Cancer. **37**: 177-180.

Hudson, W.A., Q. Li, et al. (1998). "Xenotransplantation of human lymphoid malignancies is optimized in mice with multiple immunologic defects." Leukemia. **12**: 2029-2033.

Huggins, C.B. and K. **Uematsu.** (1976). "Induction of lymphatic leukaemia in non-inbred mice and its control with glucocorticoids." Cancer. **37**: 177-180.

Hunger, S.P., P.E. Devaraj, et al. (1994). "Two types of genomic rearrangements create alternative E2A-HLF fusion proteins in t(17;19)-ALL." Blood. **83**: 2970-2977.

Hunger, S.P., R. Brown, et al. (1994). "DNA-binding and transcriptional regulatory properties of hepatic leukaemia factor (HLF) and the t(17;19) acute lymphoblastic leukaemia chimera E2A-HLF." Molecular and Cellular Biology. **14**(9): 5986-5996.

Hystad, M.E., J.H. Myklebust, et al. (2007). "Characterization of Early Stages of Human B Cell Development by Gene Expression Profiling." The Journal of Immunology. **179**(6): 3662-3671.

Igarashi, H., K.L. Medina, et al. (2005). "Early lymphoid progenitors in mouse and man are highly sensitive to glucocorticoids." International Immunology. **17**(5): 501-511.

Ikushima S., T. Inukai, et al. (1997). "Pivotal role for the NFIL3/E4BP4 transcription factor in interleukin 3-mediated survival of pro-B lymphocytes." Proc. Natl. Acad. Sci. USA. **94**: 2609-2614.

Inaba, T., T. Inukai, et al. (1996). "Reversal of apoptosis by leukaemia-associated E2A-HLF chimaeric transcription factor." Nature. **382**: 541-544.

Inaba, T., W.M. Roberts, et al. (1992). "Fusion of the leucine zipper gene HLF to the E2A gene in human acute B-lineage leukaemia." Science. **25**: 531-534.

Inukai, T., K. Hirose, et. al. (2007). "Hypercalcemia in acute lymphoblastic leukaemia: frequent implication of parathyroid hormone-related peptide and E2A-HLF from translocation 17;19." Leukaemia. **21**: 288-296.

Inukai, T., T. Inaba, et al. (1997). "Cell transformation mediated by homodimeric E2A-HLF transcription factors." Molecular and Cellular Biology. **17**(3): 1417-1424.

Inukai, T., T. Inaba, et al. (1998). "The AD1 and AD2 transactivation domains of e2a are essential for the antiapoptotic activity of the chimeric oncoprotein in E2A-HLF." Molecular and Cellular Biology. **18**(10): 6035-6043.

Irving, J.A.E., L. Bloodworth, et al. (2005). "Loss of heterozygosity in childhood acute lymphoblastic leukaemia detected by genome-wide microarray single nucleotide polymorphism analysis." Cancer Research. **65**(8): 3053-3058.

Ishikawa, F., M. Yasukawa, et al. (2005). "Development of functional human blood and immune systems in NOD/SCID/IL2 receptor γ-chain^{null} mice." Blood. **106**: 1565-1573.

Ito, M., H. Hiramatsu, et al. (2002). "NOD/SCID/gamma(c)(null) mouse: an excellent recipient mouse model for engraftment of human cells." Blood. **100**(9): 3175-3182.

Jahn, K., A. Deutschländer, et al. (2008). "Supraspinal locomotor control in quadrupeds and humans." Prog Brain Res. **171**: 353-362.

Johnson, I. S., J. G. Armstrong, et al. (1963). "The vinca alkaloids: a new class of oncolytic agents." Cancer Research. **23**: 1390-1427.

Jonat, C., H.J. Rahmsdorf, et al. (1990). "Antitumor promotion and antiimflammation: down-modulation of AP-1(Fos/Jun) activity by glucocorticoid hormone." Cell. **62**(6): 1189-1204.

Kalwinsky, D.K., P. Roberson, et al. (1985). "Clinical relevance of lymphoblast biological features in children with acute lymphoblastic leukaemia." Journal of Clinical Oncology. **3**(4): 477-484.

Kamel-Reid, S. and J.E. Dick. (1988). "Engraftment of immunodeficient mice with human hematopoietic stem cells." Science. **242**: 1706-1709.

Kamel-Reid, S., M. Letarte, et al. (1989). "A model of human acute lymphoblastic leukaemia in immune-deficient SCID mice." Science. **246**: 1597-1600.

Kamel-Reid, S., M. Letarte, et al. (1991). "Bone marrow from children in relapse with pre-B acute lymphoblastic leukaemia proliferates and disseminates rapidly in scid mice." Blood. **78**(11): 2973-2981.

Kang, M.H., Y.H. Kang, et al. (2007). "Activity of vincristine, L-ASP, and dexamethasone against acute lymphoblastic leukaemia is enhanced by the BH3-mimetic ABT-737 in vitro and in vivo." Blood. **110**(6): 2057-2066.

Kasper, G.J., A.J. Veerman, et al. (1996). "Comparison of the antileukemic activity in vitro of dexamethasone and prednisolone in childhoodacute lymphoblastic leukemia." Med Pediatr Oncol. **27**: 114-121.

Khan, N.I., K.F. Bradstock, et al. (2007). "Activation of Wnt/beta-catenin pathway mediates growth and survival in B-cell progenitor acute lymphoblastic leukaemia." British Journal of Haematology. **138**(3): 338-348.

Kim, J.W., M.K. Cho, et al. (2008). "Ovarian and multiple lymph nodes recurrence of acute lymphoblastic leukaemia: a case report and review of literature." Pediatric Surgery International. **24**(11): 1269-1273.

Kim, V.N., K. Mitrophanous, et al. (1998). "Minimal requirement for a lentivirus vector based on human immunodeficiency virus type 1." J Virol. **72**: 811-816.

King, P.D. and M.C. Perry. (2001). "Hepatotoxicity of chemotherapy." The Oncologist. **6**: 162-176.

Kinlen, L.J. (2000). "Infection, childhood leukaemia and the Seascale cluster." Radiol Prot Bull. **226**: 9-18.

Kino, T., M.U. De Martino, et al. (2003). "Tissue glucocorticoid resistance/hypersensitivity syndromes." J. Steroid Biochem. Mol. Biol. **85**: 457-467.

Klerk, C.P.W., R.M. Overmeer, et al. (2007). "Validity of bioluminescence measurements for noninvasive in vivo imaging of tumor load in small animals." BioTechniques. **43**(1): 7-13.

Klumper, E., R. Pieters, et al. (1995). "In vitro cellular drug resistance in children with relapse/refractory acute lymphoblastic leukaemia." Blood. **86**: 3861-3868.

Kollet, O., A. Spiegel, et al. (2001). "Rapid and efficient homing of human CD34+CD38ΓêÆ/lowCXCR4+stem and progenitor cells to the bone marrow and spleen of NOD/SCID and NOD/SCID/B2m null mice." Blood. **97**(10): 3283-3291.

Kong, Y., S. Yoshida, et al. (2008). "CD34+CD38+CD19+ as well as CD34+CD38-CD19+ cells are leukemia-initiating cells with self-renewal capacity in human B-precursor ALL." Leukemia. **22**: 1207-1213.

Lambrou, G. I., S. Vlahopoulos, et al. (2009). "Prednisolone exerts late mitogenic and biphasic effects on resistant acute lymphoblastic leukaemia cells: Relation to early gene expression." Leukaemia Research. **33**(12): 1684-1695.

Lancaster, D.L., N. Patel, et al. (2001). "6-thioguanine in children with acute lymphoblastic leukaemia: influence of food on parent drug pharmacokinetics and 6-thioguanine nucleotide concentrations." Br J Clin Pharmacol. **51**: 531-539.

Landau, N.R., K.A. Page, et al. (1991). "Pseudotyping with human T-cell leukemia virus type I broadens the human immunodeficiency virus host range." J Virol. **65**: 162-169.

Landau N.R., M. Warton, et al. (1988) "The envelope glycoprotein of the human immunodeficiency virus binds to the immunoglobulin-like domain of CD4." Nature. **334**: 159-162.

Lapidot, T., C. Sirard, et al. (1994). "A cell initiating human acute myeloid leukaemia after transplantation into SCID mice." Nature. **367**: 645-648.

Lapidot, T., F. Pflumio, et al. (1992). "Cytokine stimulation of multilineage hematopoiesis from immature human cells engrafted in SCID mice." Science. **255**(5048): 1137-1141.

Le Viseur, C., M. Hotfilder, et al. (2008). "In childhood acute lymphoblastic leukaemia, blast at different stages of immunophenotypic maturation have stem cell properties." Cancer Cell. **14**: 47-58.

Lewinski M.K., M. Yamashita, et al. (2006). "Retroviral DNA integration: viral and cellular determinants of target-site selection." PLoS Pathog. **2**: e60.

Liem, N.L.M., R.A. Papa, et al. (2004). "Characterization of childhood acute lymphoblastic leukaemia xenograft models for the preclinical evaluation of new therapies." Blood. **103**: 3905-3914.

Lock, R.B., N. Liem, et al. (2002). "The non-obese diabetic/severe combined immunodeficient (NOD/SCID) mouse model of childhood acute lymphoblastic leukaemia reveals intrinsic differences in biological characteristics at diagnosis and relapse." Blood. **99**: 4100-4108.

Look, A.T. (1997). "Oncogenic transcription factors in the human acute leukaemias." Science. **278**: 1059-1064.

Lowry, P.A., L.D. Shultz, et al. (1996). "Improved engraftment of human cord blood stem cells in NOD/LtSz-scid/scid mice after irradiation or multiple-day injections into unirradiated recipients." Biol Blood Marrow Transplant. **2**: 15-23.

Lozzio, B.B., E.A. Machado, et al. (1976). "Hereditary asplenic-athymic mice: transplantation of human myelogenous leukemic cells." The Journal of Experimental Medicine. **143**(1): 225-231.

Lu, N.Z., S.E. Wardell, et al. (2006). "The pharmacology and classification of the nuclear receptor superfamily: glucocorticoid, mineralocorticoid, progesterone, and androgen receptors." Pharmacol Revl. **58** (4): 782-797.

Lustig, A. and A.J. Levine (1992). "One hundred years of virology." J Virol. **66**(8): 4629-4631.

Maekawa, A., T. Nagaoka, et al. (1990). "Two-year carcinogenicity study of 6-mercaptopurine in F344 rats." J Cancer Res Clin Oncol. **116**: 245-250.

Malynn, B.A., T.K. Blackwell, et al. (1988). "The scid defect affects the final step of the immunoglobulin VDJ recombinase mechanism." Cell. **54**: 453-460.

Maris J.M., J. Courtright, et al. (2008). "Initial testing (stage 1) of sunitinib by the pediatric preclinical testing program." Pediatr Blood Cancer. **51**(1): 42-48.

Masetti, R. and A. Pession. (2009). "First-line treatment of acute lymphoblastic leukaemia with pegasparaginase." Biologics Targets Therapy. **3**: 359-368.

Matozaki, S., T. Nakagawa, et al. (1995). "Establishment of a myeloid leukaemic cell line (SKNO-1) from a patient with t(8;21) who acquired monosomy 17 during disease progression." British Journal of Haematology. **89**(4): 805-811.

Matsuo, Y. and H.G. Drexler. (1998). "Establishment and characterization of human B cell precursor-leukaemia cell lines." Leukaemia Research. **22**: 567-579.

Mazurier, F., M. Doedens, et al. (2003). "Rapid myeloerythroid repopulation after intrafemoral transplantation of NOD-SCID mice reveals a new class of human stem cells." Nature Med. **9**: 959-963.

McCune, J.M., R. Namikawa, et al. (1988). "The SCID-hu mouse: murine model for the analysis of human hematolymphoid differentiation and function." Science. **241**(4873): 1632-1639.

McNally, R.J.Q. and T.O.B. Eden. (2004). "An infectious aetiology for childhood leukaemia." Br J Haematology. **127**: 243-263.

Melikyan G.B., R.M. Markosyan, et al. (2000). "Evidence that the transition of HIV-1 gp41 into a six-helix bundle, not the bundle configuration, induces membrane fusion." J Cell Biol. **151**: 413–423.

Millington, M., A. Arndt, et al. (2009). "Towards a clinically relevant lentiviral transduction protocol for primary human CD34+ hematopoietic stem/progenitor cells. PLoS One. **4**(7): 1-10 (e6461).

Mitta B., M. Rimann, et al. (2005). "Detailed design and comparative analysis of protocols or optimized production of high-performance HIV-1-derived lentiviral particles." Metab Eng. **7**: 426–436.

Mokrejs, C., V. Vopalensky, et al. (2006). "IRESite: the database of the experimentally verified IRES structures." Nucleic Acid Res. **34**(Database issue): D125-130.

Mochizuki, H., J.P. Schwartz, et al. (1998). "High-titer human immunodeficiency virus type1-based vector systems for gene delivery into nondividing cells." J Virol. **72**: 8873-8883.

Montini, E., D. Cesana, et al. (2009). "The genotoxic potential of retroviral vectors is strongly modulated by vector design and integration site selection in a mouse model of HSC gene therapy." J Clin Invest. **119**: 964-975.

Munker, R., E. Hiller, et al. (2000). Modern Hematology. New Jersey: Humana Press.

Naldini, L., U. Blomer, et al. (1996). "Efficient transfer, integration, and sustained long-term expression of the transgene in adult rat brains injected with a lentiviral vector." Proc Natl Acad Sci USA. **93**: 11382-11388.

Naldini, L., U. Blomer, et al. (1996). "In vivo gene delivery and stable transduction of nondividing cells by a lentiviral vector." Science. **272**: 263-267.

Ng, S.M., H.P. Lin, et al. (2000). "Age, sex, haemoglobin level, and white cell count at diagnosis are important prognostic factors in children with acute lymphoblastic leukaemia treated with BFM-type protocol." Journal of Tropical Pediatrics. **46**(6): 338-343.

Notta, F., C.G. Millighan, et al. (2011). "Evolution of human BCR-ABL1 lymphoblastic leukaemia-initiating cells." Nature. **469**: 362-368.

Notta, F., S. Doulatov, et al. (2010). "Engraftment of human hematopoietic stem cells is more efficient in female NOD/SCID/IL-2Rgcnull recipient." Blood. **115**(18): 3704-3707.

O'Brien, C.A., D. Jia, et al. (2004). "Glucocorticoids act directly on osteoblasts and osteocytes to induce their apoptosis and reduce bone formation and strength." Endocrinology. **145**: 1835-1841.

Ogbomo, H., M. Michaelis, et al. (2008). "Resistance of cytarabine induces the up-regulation of NKG2D ligands and enhances natural killer cell lysis of leukemic cells." Neoplasia. **10**(12): 1402-1410.

Oh, T., A. Bajwa, et al. (2007). "Lentiviral vector design using alternative RNA export elements." Retrovirology. **4**: 38.

Ohyashiki, K., H. Fujieda, et al. (1991). "Establishment of a novel heterotransplantable acute lymphoblastic leukaemia cell line with a t(17;19) chromosomal translocation the growth of which is inhibited by interleukin-3." Leukaemia. **5**(4): 322-331.

Page, K.A., N.R. Landau, et al.(1990). "Construction and use of a human immunodeficiency virus vectors for analysis of virus infectivity." J Virol. **64**: 5270-5276.

Passegué, E., C.H.M. Jamieson, et al. (2003). "Normal and leukaemic hematopoiesis: Are leukemias a stem cell disorder or a reacquisition of stem cell characteristics." **100**(1): 11842-11849.

Pedersen, F. S., M. Duch, et al. (2001). "Retroviral Replication." Encyclopedia of Life Sciences. 1-7.

Pluta, K. and M.M. Kacprzak. (2009). "Use of HIV as a gene transfer vector." Acta Biochimica Polonica. **56**(4): 531-595.

Pui, C.H., D. Campana, et al. (2009). "Treating childhood acute lymphoblastic leukaemia without cranial irradiation." The New England Journal of Medicine. **360**(26): 2730-41.

Pui, C.-H., L.L. Robison, et al. (2008). "Acute lymphoblastic leukaemia." The Lancet. **371**(9617): 1030-1043.

Pui, C-H and W.E. Evans. (2006). "Treatment of acute lymphoblastic leukaemia." NEJM. **354**: 166-178.

Pui, C-H, J. Mirro, et al. (2006). "Phagocytic activity and expression of myeloid-associated cell surface antigens by blast cells in acute lymphoblastic leukaemia." Medical and Pediatric Oncology. **4**(1): Article published online.

Pui, C-H. (1999). Childhood leukaemias. Cambridge, UK: Cambridge University Press.

Qweider, M., J.M. Gilsbach, et al. (2007). "Inadvertent intrathecal vincristine administration: a neurosurgical emergency." J Neurosurg Spine. **6**: 280-283.

Raimondi, S.C. (1993). "Current status of cytogenetic research in childhood acute lymphoblastic leukaemia." Blood. **81**: 2237.

Ramanujachar, R. (2009). "The molecular basis of E2A-HLF induced precursor-B cell acute lymphoblastic leukaemia in childhood." Doctoral thesis. University College London.

Rang, H.P., M.M. Dale, et al. (2010). Australian Medicines Handbook 2010. Adelaide: Australian Medicines Handbook Pty Ltd.

Ravandi, F. and Z. Estrov. (2006). "Eradication of Leukaemia Stem Cells as a New Goal of Therapy in Leukaemia." Clinical Cancer Research. **12**(2): 340-344.

Ray, P. and S.S. Gambhir. (2007). "Noninvasive imaging of molecular events with bioluminescent reporter genes in living subjects." Methods Mol Biol. **411**: 131-144.

Rehemtulla, A., L.D. Stegman, et al. (2000). "Rapid and quantitative assessment of cancer treatment response using in vivo bioluminescence imaging." Neoplasia. **2**(6): 491-495.

Reid, H. and H.B. Marsden. (1980). "Gonadal infiltration in children with leukaemia and lymphoma." J Clin Pathol. **33**: 722-729.

Reiser, J. (2000). "Production and concentration of pseudotyped HIV-1-based gene transfer vectors." Gene Ther. **7**: 910-913.

Reynolds, T. (1998). "Causes of childhood leukaemia beginning to emerge." J Nat Cancer Inst. **90**: 8-10.

Rhen, T. and J.A. Cidlowski. (2005). "Antiinflammatory action of glucocorticoids: new mechanisms for old drugs." N. Engl. J. Med. **353**(16): 1711-23.

Ricks, D.M., R. Kutner, et al. (2008). "Optimized lentiviral transduction of mouse bone marrow-derived mesenchymal stem cells." Stem Cells Dev. **17**: 441-450.

Rimsza, L.M., R.S. Larson, et al. (2000). "Benign hematogone-ich lymphoid proliferations can be distinguished from B-lineage acute lymphoblastic leukaemia by integration of morphology, immunophenotype, adhesion molecule expression, and architectural features." Am J Clin Pathol. **114**: 66-75.

Rooman, R, J-G Koster, et al. (1999). "The effect of dexamethasone on body and organ growth of normal and IGF-II-transgenic mice." Journal of Endocrinology. **163**: 543–552.

Rosenfeld, C., A. Goutner, et al. (1977). "An effect human leukaemic cell line: REH." Eur J Cancer. **13** :377-379.

Ruiz, M., U. Lind, et al. (2001). "Characterization of two novel mutations in the glucocorticoid receptor gene in patients with primary cortisol resistance." Clin Endocrinol. **55**: 363-371.

Sadikot, R. T. and T. S. Blackwell. (2005). Bioluminescence imaging." Proc Am Thorac Soc. **2**(6): 537-540.

Sala-Newby, G. B., C. M. Thomson, et al. (1996). "Sequence and biochemical similarities between the luciferases of the glow-worm Lampyris noctiluca and the firefly Photinus pyralis." Biochem J. **313**: 761-767.

Santoni, D.S.F. and L. Naldini. (2009). "Short-term culture of human CD34+ cells for lentiviral gene transfer." Methods Mol Biol. **506**: 59-70.

Scheinman, R.I., A. Gualberto, et al. (1995). "Characterization of mechanisms involved in transrepression of NK-kappa B by activated glucocorticoid receptors." Mol Cell Biol. **15**(2): 943-953.

Schmid M. and T.H. Jensen. (2008). "Quality control of mRNP in the nucleus." Chromosoma. **117**: 419-429.

Schmitz, M., P. Breithaupt, et al. (2011). "Xenografts of highly resistant leukaemia recapitulate the clonal composition of the leukemogenic compartment." Blood. Prepublished online. doi 10.1182/blood-2010-11-320309.

Shultz, L.D., B.L. Lyons, et al. (2005). "Human lymphoid and myeloid cell development in NOD/LtSz-scid IL2R gamma null mice engrafted with mobilized human hemopoietic stem cell." J Immunol. **174**(10): 6477-6489.

Shultz, L.D., F. Ishikawa, et al. (2007). "Humanized mice in translational biomedical research." Nat Rev Immunol. **7**:118-130.

Shultz, L.D., P.A. Schweitzer, et al. (1995). "Multiple defects in innate and adaptive immunologic function in NOD/LtSz-scid." J Immunol. **154**(1): 180-191.

Siapati E.K., M. Papadaki, et al. (2011). "Proliferation and bone marrow engraftment of AML blasts is dependent on β-catenin signalling." Br J Haematol. **152**(2):164-174.

Smith, K.S., J.W. Rhee, et al. (2002). "Transformation of bone marrow B-cell progenitors by E2A-HLF requires coexpression of of BCL-2." Molecular and Cellular Biology. **22**(21): 7678-7687.

Smith, M. (1997). "Consideration for a possible viral etiology for B precursor acute lymphoblastic leukaemia of childhood." Journal of Immunotherapy. **20**: 89-100.

Soneoka, Y., P.M. Cannon, et al. (2004). "A transient three-plasmid expression system for the production of high titer retroviral vectors." Nucleic Acid Res. **23**: 628-633.

Stankovic, T. and E. Marston. (2008). "Molecular mechanisms involved in chemoresistance in paediatric acute lymphoblastic leukaemia." Srpski arhiv za celokupno lekarstvo. **136**(3-4): 187-192.

Stiller, C.A. (2004). "Epidemiology and genetics of childhood cancer." Oncogene. **23**: 6429-6444.

Stong, R.S., S.J. Korsmeyer, et al. (1985). "Human acute leukemia cell line with the t(4;11) chromosomal rearrangement exhibits B lineage and monocytic characteristics." Blood. **65**(1): 21-31.

Szczepanski, T., V.H.J. van der Velden, et al. (2003). "Classification systems for acute and chronic leukaemias." Best Practice & Research Clinical Haematology. **16**(4): 561-582.

Takahashi, H., H. Goto, et al. (2001). "Expression of two types of E2A-HLF fusion protein in YCUB-2, a novel cell line established from B-lineage leukaemia with t(17;19)." Leukemia. 995-997.

Takakusaki, K. and K. Matsuyama. (2010). "Locomotor control by the braistem and spinal cord." Brain Nerve. **62**(11): 1117-1128.

Tissing, W.J.E., J.P.P. Meijerink, et al. (2003). "Molecular determinants of glucocorticoid sensitivity and resistance in acute lymphoblastic leukaemia." Leukemia. **17**: 17-25.

Trumpp, A., M. Essers, et al. (2010). "Awakening dormant hematopoietic stem cells." Nature Reviews. **10**: 201-209.

Turner, J.D. and C.P. Muller. (2005). "Structure of the glucocorticoid receptor (NR3C1) gene 5' untranslated region: identification, and tissue distribution of multiple new human exon 1." J Mol Endocrinol. **35**: 283-292.

Turner, J.D., A.B. Schote, et al. (2007). "A New Transcript Splice Variant of the Human Glucocorticoid Receptor." Annals of the New York Academy of Sciences. **1095**(1): 334-341.

Uchida, N, M.M. Hsieh, et al. (2011). "Optimal conditions for lentiviral transduction of engrafting human CD34+ cells." Gene Therapy. doi:10.1038/gt.2011.63.

Valente S.T. and S.P. Goff. (2009). "Somatic cell genetic analyses to identify HIV-1 host restriction factors." Methods Mol Biol. **485**: 235-255.

van der Wath, R.C., A. Wilson, et al. (2009). "Estimating dormant and active hematopoietic stem cell kinetics through extensive modelling of bromodeoxyuridine label-retaining cell dinamics." PLoS One. **4**(9): e6972 (1-12)

Vegiopoulos, A. and S. Herzig. (2007). "Glucocorticoids, metabolism and metabolic diseases." Molecular and Cellular Endocrinology. **275**(1-2): 43-61.

Vora, A. (2006). "t(17;19) (E2A-HLF): new high risk abnormality. Treatment recommendations." UKALL 2003.

Warner, J.K., J.C.Y. Wang, et al. (2004). "Concepts of human leukemic development." Oncogene. **23**: 7164-7177.

Weinstein, R.S. (2001). "Glucocorticoid-induced osteoporosis." Rev. Endocr. Metab. Disord. **2**: 65-73.

Wiemels, J. (2008). "Chromosomal translocations in childhood leukemia: natural history, mechanisms, and epidemiology." J Natl Cancer Inst Monogr. **39**:87-90.

Wright, A.P., J. Zilliacus, et al. (1993). "Structure and function of the glucocorticoid receptor." J Steroid Biochem Mol Biol. **47**(1-6): 11-19.

Xie, Y., T. Yin, et al. (2009). "Detection of functional haematopoietic stem cell niche using real time imaging." Nature. **457**(7225): 97-101.

Yamazaki, S., A. Iwama, et al. (2009). "TGF-β as a candidate bone marrow niche signal to induce hematopoietic stem cell hibernation." Blood. **113**: 1250-1256

Yan, Y., E.A. Wieman, et al. (2009). "Autonomous growth potential of leukaemia blast cells is associated with poor prognosis in human acute leukaemias." Journal of Hematology and Oncology. **2**: 51.

Yeung, J., H. Kempski, et al. (2006). "Characterization of the t(17;19) translocation by gene-specific fluorescent *in situ* hybridization-based cytogenetics and detection of the *E2A-HLF* fusion transcript and protein in patients' cells." Haematologica. **91**: 422-424.

Yoon, J.W. and H.S. Jun. (2005). "Autoimmune destruction of pancreatic β-cells." American Journal of Therapeutics. **12**: 580-591.

Yoshihara, T., T. Inaba, et al. (1995). "E2A-HLF-mediated cell transformation requires both the transactivation domain of E2A and the leucine zipper dimerization domain of HLF." Mol Cell Biol. **15**: 3247-3255.

Yudt, M.R. and J.A. Cidlowski. (2001). "Molecular identification and characterization of A and B forms of the glucocorticoid receptor." Molecular Endocrinology. **15**: 1093-1103.

Zinn, K.R., T.R. Chaudhuri, et al. (2008). "Noninvasive bioluminescence imaging in small animals." ILAR J. **49**(1): 103-115.

Zufferey, R., J.E. Donello, et al. (1999). "Woodchuck hepatitis virus posttranscriptional regulatory element enhances expression of transgenes delivered by retroviral vectors." J Virol. **73**: 2886-2892.

Zufferey, R., D. Nagy, et al. (1997). "Multiply attenuated lentiviral vector achieves efficient gene delivery in vivo." Nat Biotechnol. **15**: 871-875.

APPENDIX

APPENDIX 1

Percentage of leukaemic cells engrafted determined by immunophenotyping

Flow cytometry analysis - % of blasts in bm, spleen and ovaries

not tested or negligible value

ttd **time to death**

	% of cells tpln	ttd (days)	bm	spleen	ovaries
Primary transplant					
m1	100P	**44**	**80.1**	**86.5**	
m2		**51**	**88.2**	**92.1**	
m3		**43**	**86.4**	**91.9**	
m1	100R	**59**	**90.3**	**94.8**	**97.4**
m2		**59**	**94.2**	**85.1**	**98.9**
m3		**59**	**89.7**	**79.2**	**97.0**
Secondary transplant 1					
m1	100P	**33**	**86.2**	**93.3**	
m2		**70**	**90.6**	**98.3**	
m3		**51**	**80.8**	**86.0**	
m1	100R	**56**	**90.7**	**92.9**	**87.0**
m2		**56**	**82.9**	**89.1**	**96.3**
m3		**56**	**89.5**	**84.8**	**91.5**
Secondary transplant 2 - Untreated					
m1	100P	**38**	**82.8**	**89.8**	
m2		**31**	**92.8**	**94.5**	
m3		**38**			
m4		**35**	**88.9**	**67.8**	
m5		**38**	**72.9**	**81.4**	
m1	90P+10R	**34**	**62.4**	**86.9**	
m2		**35**	**87.9**	**90.5**	
m3		**31**		**84.6**	
m4		**45**	**92.5**	**79.6**	
m5		**31**	**89.5**	**89.3**	
m1	70P+30R	**48**	**65.4**	**89.7**	**71.6**
m2		**45**	**89.5**	**86.5**	
m3		**36**	**89.0**	**79.1**	**89.2**
m4		**35**			
m5		**42**	**73.4**	**95.8**	**78.0**
m1	50P+50R	**49**	**91.2**	**89.7**	**90.1**
m2		**45**	**89.6**	**93.8**	
m3		**41**	**88.2**	**91.9**	**95.4**
m4		**45**			
m5		**48**	**90.5**	**95.4**	**82.1**
m1	30P+70R	**38**	**89.1**	**87.7**	**48.2**
m2		**31**	**65.0**	**62.2**	**85.0**
m3		**44**			
m4		**45**	**89.9**	**90.7**	
m5		**62**	**82.1**	**93.2**	
m1	10P+90R	**41**			
m2		**35**	**79.2**		
m3		**34**	**82.7**	**84.5**	**86.2**
m4		**41**	**89.6**	**94.8**	**97.5**
m5		**49**	**97.6**	**86.4**	**87.9**

m1	100R	**48**			
m2		**62**	**88.1**	**92.8**	**99.2**
m3		**43**	**90.3**	**89.9**	**92.5**
m4		**58**	**79.8**	**94.3**	**95.9**
m5		**58**	**89.0**	**95.1**	**98.2**
Secondary transplant 3 - Dexamethasone treated					
m1	100P+dex	**42**			
m2		**64**	**55.0**	**53.6**	
m3		**64**	**87.6**	**41.2**	
m4		**59**	**69.5**	**61.2**	
m5		**55**	**71.5**	**24.6**	
m1	70P+30R+dex	**51**	**75.2**	**45.8**	**79.8**
m2		**55**	**57.5**	**59.4**	**66.1**
m3		**57**			
m4		**53**	**77.7**	**55.9**	**67.5**
m5		**48**			
m1	50P+50R+dex	**60**			
m2		**62**	**78.8**	**78.9**	**80.2**
m3		**64**	**87.5**	**63.1**	
m4		**62**	**90.7**	**83.8**	
m5		**51**	**88.8**	**87.0**	**94.7**
m1	30P+70R+dex	**60**	**88.0**	**74.2**	**95.4**
m2		**55**	**94.1**	**98.8**	**89.4**
m3		**51**	**80.6**	**93.2**	
m4		**62**			
m5		**51**	**74.1**	**89.2**	**75.3**
m1	100R+dex	**64**	**94.7**	**85.3**	
m2		**64**	**87.4**	**91.0**	**99.8**
m3		**55**			
m4		**62**	**79.5**	**62.7**	**99.3**
m5		**57**	**94.5**	**86.3**	**98.8**

APPENDIX 2

Cells scored in cytogenetic analysis by FISH technique

m#	Ratios of cells	2R2G	2R0G	2R1G
Non-treated				
m1	10P:0R	100	0	0
m2	10P:0R	100	0	0
m3	10P:0R	nc	nc	nc
m4	10P:0R	100	0	0
m5	10P:0R	100	0	0
m1	9P:1R	nc	nc	nc
m2	9P:1R	100	0	0
m3	9P:1R	99	1	0
m4	9P:1R	100	0	0
m5	9P:1R	97	3	0
m1	7P:3R	88	12	0
m2	7P:3R	82	18	0
m3	7P:3R	54	46	0
m4	7P:3R	nc	nc	nc
m5	7P:3R	89	11	0
m1	5P:5R	65	35	0
m2	5P:5R	81	19	0
m3	5P:5R	18	82	0
m4	5P:5R	nc	nc	nc
m5	5P:5R	100	0	0
m1	3P:7R	79	21	0
m2	3P:7R	96	4	0
m3	3P:7R			
m4	3P:7R	97	3	0
m5	3P:7R	15	85	0
m1	1P:9R	nc	nc	nc
m2	1P:9R	32	68	0
m3	1P:9R	66	34	0
m4	1P:9R	60	40	0
m5	1P:9R	35	65	0
m1	0P:10R	nc	nc	nc
m2	0P:10R	0	100	0
m3	0P:10R	0	100	0
m4	0P:10R	0	100	0
m5	0P:10R	0	100	0
Dexamethasone treated				
m1	10P:0R+ dex	nc	nc	nc
m2	10P:0R+ dex	177	1	35
m3	10P:0R+ dex	100	0	0
m4	10P:0R+ dex	100	0	0
m5	10P:0R+ dex	100	0	0
m1	7P:3R + dex	11	89	0
m2	7P:3R + dex	91	9	0
m3	7P:3R + dex	nc	nc	nc
m4	7P:3R + dex	45	55	0
m5	7P:3R + dex	nc	nc	nc
m1	5P:5R + dex	11	89	0
m2	5P:5R + dex	9	91	0
m3	5P:5R + dex	94	6	0
m4	5P:5R + dex	82	18	0
m5	5P:5R + dex	32	68	0
m1	3P:7R + dex	10	90	0
m2	3P:7R + dex	12	88	0
m3	3P:7R + dex	5	95	0
m4	3P:7R + dex	3	97	0
m5	3P:7R + dex	9	91	0
m1	0P:10R + dex	0	99	1
m2	0P:10R + dex	0	100	0
m3	0P:10R + dex	0	100	0
m4	0P:10R + dex	0	100	0
m5	0P:10R + dex	0	100	0

APPENDIX 3

EHA Abstract 1772

16th Congress of the European Hematology Association

June 8th – 12th 2011, Excel London, London, UK

FITNESS OF t(17;19) CHILDHOOD ACUTE LYMPHOBLASTIC LEUKAEMIA IN IMMUNODEFICIENT MICE

Elda Latif, Klaus Rehe, Mike Batey, Christine J. Harrison, Josef Vormoor, Andy Hall, Olaf Heidenreich

Northern Institute for Cancer Research, Paul O'Gorman Building, Medical School, Newcastle University and Sir James Spence Institute, Royal Victoria Infirmary, Newcastle upon Tyne.

Background

Survival rates in childhood ALL are now in the region of 90%, however treatment outcomes in certain cytogenetic subgroups remain poor. The translocation, t(17;19)(q22;p13), is a rare cytogenetic abnormality, which occurs in less than 1% of childhood acute lymphoblastic leukaemia (ALL) and is associated with a very poor prognosis and chemotherapy resistance. Understanding the mechanisms of resistance in these patients is therefore a priority.

Aims

It has been assumed that following relapse, ALL cells will divide more rapidly than at presentation. In order to test this hypothesis, we have developed an animal model of competitive repopulation using paired samples from presentation and relapse from a case of t(17;19) positive ALL.

Methods

Leukemic cells from a child with t(17;19) positive ALL obtained at presentation and at relapse were analysed for copy number variations using the Affymetrix Genome-Wide Human SNP Array 6.0 (SNP6.0) platform. Deletion of the NR3C1 gene (glucocorticoid

receptor) on chromosome 5 was detected at relapse but not at presentation. This was confirmed by fluorescence *in situ* hybridisation (FISH). Cells were separately transplanted via intrafemoral injection into immunocompromised NOD/scid IL2Rγnull (NSG) female mice. Human blasts recovered from primary transplantations were subsequently used for secondary transplantation in mixed populations with ratios of presentation to relapse cells of 10:0, 9:1, 7:3, 5:5, 3:7, 1:9 and 0:10. Engraftment and progression of disease were assessed by flow cytometry at the terminal time-point. The percentages of presentation and relapse cells which engrafted in these mice were determined using FISH for *NR3C1* deletion. The expression levels of glucocorticoid receptor (NR3C1) in the harvested leukemic cells were determined by real-time quantitative PCR.

Results

Microarray analysis identified a deleted region of chromosome 5 involving the NR3C1 gene in cells obtained at relapse but not at presentation. Without treatment, those mice transplanted with relapse cells survived significantly longer than those transplanted with presentation cells (p=0.005), while the survival rates of mixed cells fell between the two curves. All engrafted mice presented with an enlarged spleen indicating leukaemic infiltration. This was confirmed by flow cytometry, which identified t(17;19) cells with CD19+/CD10+/CD34- immunophenotype among those isolated from bone marrow (85-92%) and spleen (64-90%). FISH analysis showed that the percentages of presentation cells which engrafted in the mice with mixed populations were always higher than the ratios initially transplanted. Real-time PCR analysis confirmed that the levels of NR3C1 from all ratios of mixed cells represented the level of the presentation cells only. Repopulation experiments are currently being repeated with mice treated with Dexamethasone.

Conclusions

In this study we observed that in t(17;19) positive ALL, without treatment, presentation cells outgrew cells obtained at relapse regardless of the ratio of cells initially transplanted. It is anticipated that, on treatment, relapse cells will outgrow those obtained at presentation, due to deletion of the glucocorticoid receptor, which would render cells insensitive to steroid treatment.